2015

# CALCIUM PHOSPHATE CEMENTS AND FOAMS

## CHARACTERIZATION OF POROSITY AND USE AS LOCAL DRUG DELIVERY DEVICES

**David Pastorino**

Cristina Canal
Maria-Pau Ginebra

Materials Science and Engineering

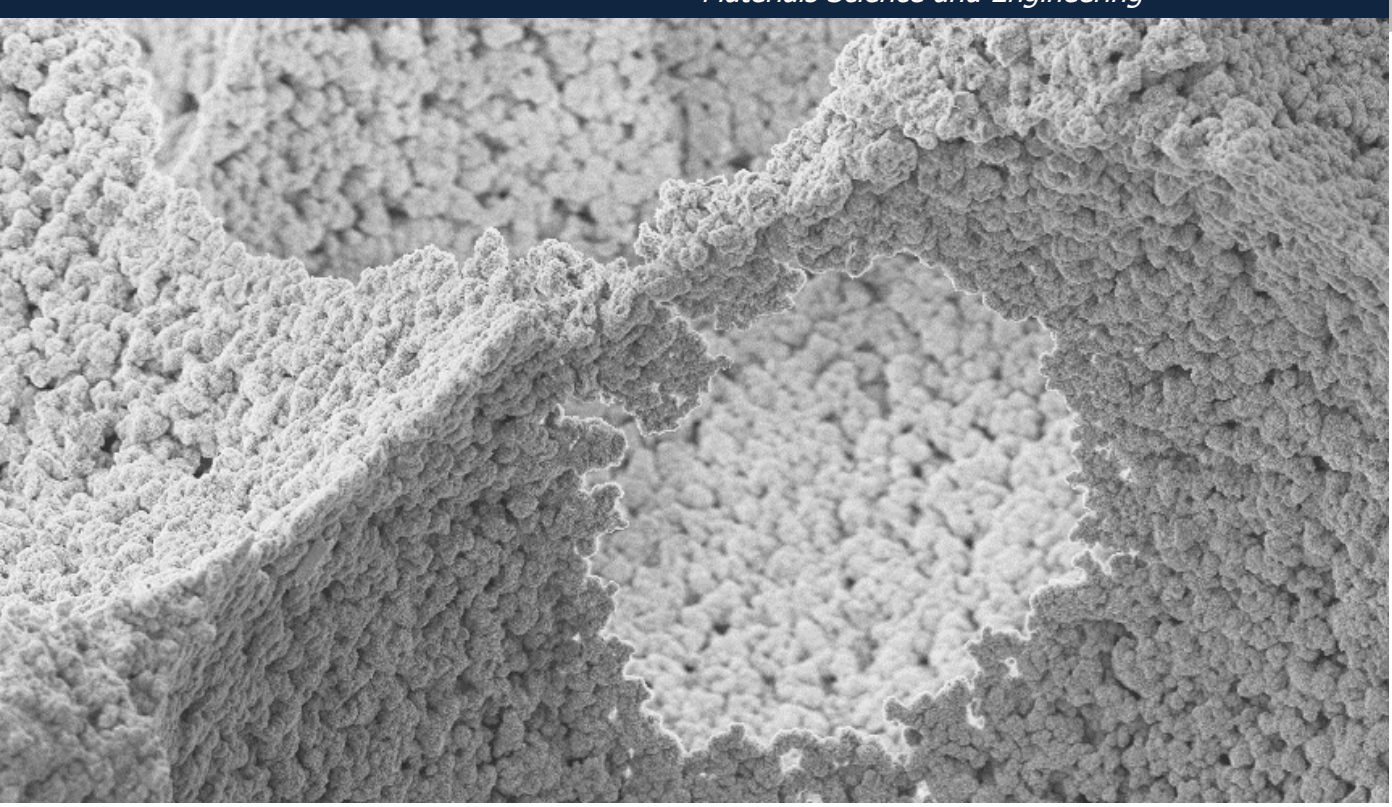

UNIVERSITAT POLITÈCNICA DE CATALUNYA
BARCELONATECH

Biomaterials, Biomechanics & Tissue Engineering

UNIVERSITAT POLITÈCNICA DE CATALUNYA BARCELONATECH

# *Calcium phosphate cements and foams characterization of porosity and use as local drug delivery devices*

**David Pastorino**

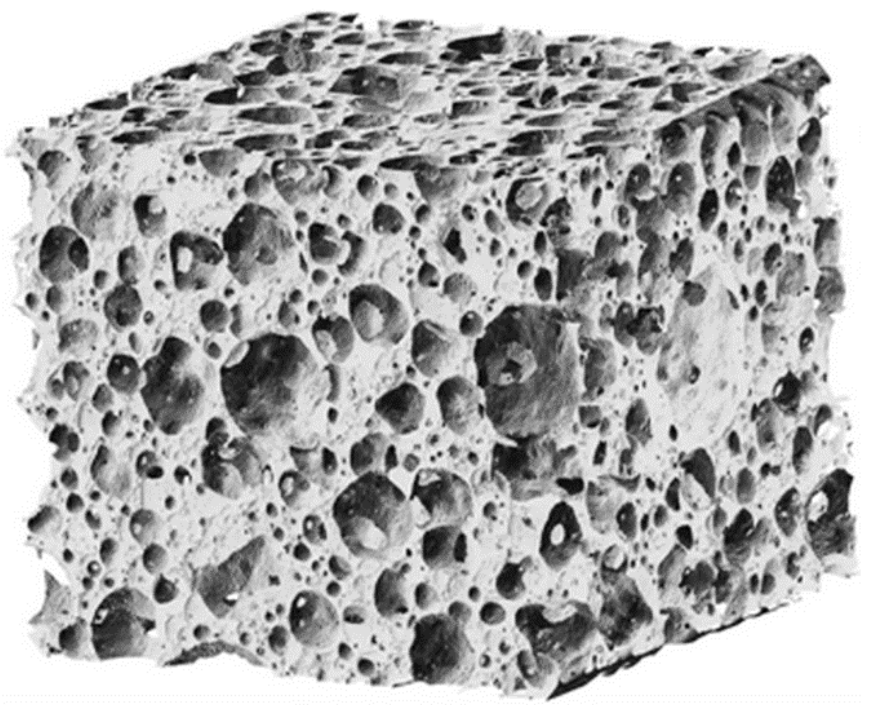

UNIVERSITAT POLITÈCNICA DE CATALUNYA
BARCELONATECH
Escola de Doctorat

**Curs acadèmic:**

## Acta de qualificació de tesi doctoral

Nom i cognoms

Programa de doctorat

Unitat estructural responsable del programa

## Resolució del Tribunal

Reunit el Tribunal designat a l'efecte, el doctorand / la doctoranda exposa el tema de la seva tesi doctoral titulada :

Acabada la lectura i després de donar resposta a les qüestions formulades pels membres titulars del tribunal, aquest atorga la qualificació:

☐ NO APTE ☐ APROVAT ☐ NOTABLE ☐ EXCEL·LENT

| | | |
|---|---|---|
| (Nom, cognoms i signatura)<br><br>President/a | | (Nom, cognoms i signatura)<br><br>Secretari/ària |
| (Nom, cognoms i signatura)<br><br>Vocal | (Nom, cognoms i signatura)<br><br>Vocal | (Nom, cognoms i signatura)<br><br>Vocal |

_____, _____ d'/de _____ de _____

El resultat de l'escrutini dels vots emesos pels membres titulars del tribunal, efectuat per l'Escola de Doctorat, a instància de la Comissió de Doctorat de la UPC, atorga la MENCIÓ CUM LAUDE:

☐ SÍ ☐ NO

| | |
|---|---|
| (Nom, cognoms i signatura)<br><br>President de la Comissió Permanent de l'Escola de Doctorat | (Nom, cognoms i signatura)<br><br>Secretari de la Comissió Permanent de l'Escola de Doctorat |

Barcelona, _____ d'/de _____ de _____

# Acknowledgments

It has been my privilege to work with you during the past years well spent and intensively dedicated to this PhD thesis. It has undoubtedly been a long journey learning, experimenting and investigating altogether. Way more than only science, I want to sincerely thank you. By *you*, I mean:

- *You*, Maria-Pau and Cristina, supervisors for your patience, commitment, guidance and support throughout this adventure. Thank you.

- *You*, Anna, Sara, Gemma, Montserrat, Marta, Meritxell, Javier, Mireia, Roberta, Maria-Isabel, María, Judit, Mònica, Nathalia, Noelia, Małgorzata, Joanna, Magdalena, Carolina, Marc, Marc, Lluis, Sergí, Bea, Daniel, Edgar, Zhitong, Cédric, Ramón, Raimon, Jose Maria, Romain, Miquel, Jordi, Carles, members of the BBT research group for your help, smiles, motivation and dedication in giving me a good reason to get up in the morning and not sleep at night.

- *You,* Ornella, Edgar, Lulah, Chlöé, Ferran, Nadège, Benoît, Laure, Romain, Guillaume, Helena, friends for supporting me during this process and understanding my absence at the end of it.

- *You,* my family for all the advices and encouragements that I received from you each moment of this PhD.

- *You,* Maria-Pau, Xavier, Yassine, Carlos, Jaume, members of *Subtilis Biomaterials* to allow this adventure to go on.

# 1. Summary

The topic of this Philosophy Doctor Thesis tallies with the national project MAT2012 of the BBT group of UPC: "Pore4Bone: Biomimetic calcium phosphates: tailoring porosity from the nano- to the macroscale for osteoinduction, drug delivery and bone tissue engineering".

Bone is one of the most transplanted tissues globally, with around one million surgical procedures each year. Ageing of the population worldwide requires intense effort in designing efficient, clinically applicable multifunctional biomaterials for bone regeneration. The need for a higher volume of bone graft, and advanced solutions make synthetic bone grafts an attractive alternative to auto- or xenografts.

Synthetic calcium phosphate cements (CPCs) provide a high freedom of processing and conformation, and excellent biomimicry to natural bone. Biocompatible and osteoconductive *per se*, CPCs support *in vivo* remodeling of bone. The intrinsic micro- and nano- porosity of CPCs resulting from the spaces between the entangled crystals and aggregates once set is a key property when considering bone regeneration and local release of drugs. It provides free space for drug diffusion and fluid penetration, both of which are essential elements for drug release. Thus, a comprehensive characterization of the porosity, especially at the microscopic and nanoscopic scale is of paramount interest to identify these mechanisms, so it has been tackled in detail in this work.

Focusing on bone infections, the combination of antibiotics with osteogenic matrices like CPCs is explored in the PhD Thesis. Indeed, while bone infections and bone disorders are generally treated post-operatively by systemic administration of the indicated antibiotic, achieving a therapeutically efficient local delivery of the active principles is a key challenge, as it allows reducing secondary unwanted effects, drug interactions and diminishing the required dose due to the enhanced local bioavailability.

In particular, the relationship between antibiotic addition, porosity and drug release in calcium phosphate cements (CPCs) is highlighted and studied in this PhD Thesis. Finally the introduction of macropores in CPCs is investigated to manufacture antibiotic-releasing calcium phosphate foams (CPFs) for bone regeneration, which present clear clinical benefits over CPCs as multifunctional biomaterials. Indeed, the clinical performance of CPCs as local drug delivery devices is restricted by the relatively low penetration of corporal fluids through their micro or nanopores, preventing a complete release of the drug. The slow release of the entrapped antibiotic during the degradation of the CPC may generate a local concentration below the minimum inhibitory concentration, with the risk to foster the development of antibiotic-resistant bacteria. The addition of a network of interconnected macropores in CPCs represents a major advance by enhancing fluid circulation, and the consequent increase of the release rate of the antibiotic. Thus, in addition to the injectability and biomimicry of CPCs, the interconnected macroporosity of CPFs endows these materials with clear advantages not only in terms of tuning the release kinetics of active principles, but also when considering their excellent osteogenic properties.

# 2. Resumen

La presente Tesis doctoral se enmarca dentro del proyecto MAT2012 del grupo de investigación BBT de la UPC: "Pore4Bone: Biomimetic calcium phosphates: tailoring porosity from the nano- to the macroscale for osteoinduction, drug delivery and bone tissue engineering" financiado por el Gobierno de España.

El hueso es uno de los tejidos más trasplantados mundialmente con hasta 1 millón de cirugías anuales. El envejecimiento de la población conlleva la necesidad de hacer grandes esfuerzos en el diseño de biomateriales multifuncionales, eficientes y clínicamente aplicables a la regeneración ósea. El aumento del número de injertos óseos necesarios y la necesidad de encontrar soluciones avanzadas hace que los biomateriales sintéticos sean una alternativa atractiva a los auto- o xeno-injertos actuales.

Los cementos de fosfato de calcio (CPCs) son materiales muy versátiles en cuanto a los procesos de conformado, y presentan propiedades muy similares a las del hueso natural. Siendo materiales biocompatibles y osteoconductivos, los CPCs actúan de soporte al proceso de remodelación ósea *in vivo*. Además, los CPCs presentan una micro- y nano- porosidad intrínseca, que tiene su origen en los espacios entre los cristales que se forman tras el fraguado. Dicha porosidad es de gran relevancia en la regeneración ósea y la liberación local de fármacos, al proporcionar espacios disponibles para la difusión de los fármacos y la circulación de fluidos corporales, ambos procesos esenciales para la liberación del principio activo. En esta Tesis Doctoral se ha abordado la caracterización de la porosidad de los CPCs en profundidad, especialmente a escala micro- y nanoscópica, por ser de gran interés en la identificación de los mecanismos de regeneración ósea y liberación controlada de fármacos.

En el caso de las infecciones óseas, en la presente Tesis Doctoral se explora la combinación de antibióticos con matrices bioactivas como los CPCs. Así, mientras las infecciones óseas se tratan habitualmente mediante la administración sistémica de antibióticos de forma post-operatoria, alcanzar una liberación local eficaz del principio activo es un reto clave, que permitiría reducir los efectos secundarios no deseados, minimizar las interacciones potenciales entre fármacos y disminuir la dosis necesaria, gracias a una mayor biodisponibilidad.

En este Trabajo, se ha estudiado en profundidad la relación entre la incorporación de antibiótico, la porosidad y la liberación de fármaco en cementos de fosfato de calcio (CPCs). Además, se ha investigado la introducción de macroporosidad en los CPCs con el objetivo de fabricar espumas de fosfato de calcio (CPFs) capaces de liberar fármacos para regeneración ósea a nivel local, con claras ventajas frente a los CPCs como biomateriales multifuncionales. En efecto, la eficacia clínica de los CPCs como dispositivos de liberación local de fármacos está limitada por la relativamente baja penetración y circulación de los fluidos corporales en los mismos, impidiendo una liberación completa del fármaco. El riesgo de que el antibiótico atrapado en el material se libere lentamente durante la degradación del mismo, dando lugar a concentraciones locales de antibiótico inferiores a la concentración mínima inhibitoria, puede llevar a la generación de resistencia bacteriana al antibiótico. La adición de una red de macroporos interconectados en los CPFs representa un avance importante, puesto que aumenta la circulación de fluidos corporales en el biomaterial, incrementa el control sobre la cinética de liberación de fármacos y permite colonización celular. Así pues, los

CPFs junto a la inyectabilidad y el biomimetismo de los CPCs, presentan a una macroporosidad interconectada que les confiere un elevado interés en vistas tanto a la regeneración ósea como a la liberación local de fármacos.

# 3. Objectives and innovations

**The main aim of this PhD Thesis is to study and characterize in depth the application of calcium phosphate cements (CPC) and calcium phosphate foams (CPF) as local drug delivery systems (DDS).**

Specifically, the following objectives have been set and constitute the different parts of this Thesis:

- Review thoroughly the existing literature on CPCs used as DDS (**Paper I**)

- Characterize in depth the micro- and nano- porosity of apatitic CPCs reviewing two techniques already used (MIP and $N_2$ Sorption) and adapting a novel technique (thermoporosimetry) for CPCs. (**Paper II**)

- Investigate the effect of the addition of doxycycline hyclate to CPCs on the microstructure, properties and antibiotic release kinetics of antibiotic and evaluate the effects of the setting on the release properties (**Paper III**).

- Adapt and characterize calcium phosphate foams (CPFs) for their use as DDS. Investigate the effects of doxycycline hyclate on CPFs' physical and chemical properties and drug release patterns (**Paper IV, Patent I**).

The following list details the different papers that constitute the core of this PhD Thesis:

**Paper I**

Ginebra M-P, Canal C, Espanol M, Pastorino D, Montufar EB. Calcium phosphate cements as drug delivery materials. Adv Drug Deliv Rev 2012; 64:1090–110.

**Paper II**

Pastorino D, Canal C, Ginebra M-P. Multiple characterization study on porosity and pore structure of calcium phosphate cements. Acta Biomater 2015. doi:10.1016/j.actbio.2015.09.017

**Paper III**

Canal C, Pastorino D, Mestres G, Schuler P, Ginebra M-P. Relevance of microstructure for the early antibiotic release of fresh and pre-set calcium phosphate cements. Acta Biomater 2013;9:8403–12.

**Paper IV**

Pastorino D, Canal C, Ginebra M-P. Drug delivery from injectable calcium phosphate foams by tailoring the macroporosity–drug interaction. Acta Biomater 2014; 12:250-59.

# 4. State-of-the-art

Bone tissue is a complex organ playing a key role in the metabolism of the human body, in addition to providing mechanical support. Its complex structure and specific composition are presented in the following sections in order to understand its regeneration mechanisms and the rationale behind the design of materials mimicking them.

Bone disorders have a major impact on the quality of life of an increasingly ageing population, especially in developed countries. The will to live a healthier and longer life emphasizes the importance of finding preventive techniques and therapies for the most common bone disorders: infections, fractures and cancers.

Strategies for bone regeneration are presented in the next sections, from the current standards of care, i.e. autografting, to synthetic materials, focusing especially on calcium phosphate based materials.

Finally, the local drug administration from calcium phosphate cements (CPCs) to enhance prevent or treat of bone infections, bone cancer or other pathologies, or to enhance bone ingrowth in particular compromised situations is reviewed.

## 3.1. Bone tissue

### 3.1.1. Function

Bone has a double function: biomechanical and metabolic. The skeleton serves as structural support system [1]. It can grow and change in shape and size to suit varying mechanical stimulus. It is also involved in tuning the calcium/phosphate balance of the body and in detoxification of heavy metals [2]. Moreover, bones protect internal organs and in conjunction with muscles facilitate movement [3].

### 3.1.2. Composition

Bone is a composite material consisting of extracellular matrix, cells and water. Its matrix is composed of an organic and an inorganic phase. The organic component represents around 40% of the dry bone weight. Called osteoid, it is composed of collagen, proteoglycans, glycoproteins, phospholipids and phosphoproteins. The remaining 60% of the dry weight is constituted by the inorganic phase and is primarily calcium-deficient hydroxyapatite (CDHA), considered as the key factor in determining bone mechanical properties, namely stiffness and strength, while collagen provides flexibility [4].

### 3.1.3. Structure

Different mechanisms during embryonic development allow the classification of bones in four families: long bones (i.e. femur, tibia), short bones, flat bones (i.e. sternum), and irregular shaped bones (i.e. vertebra). Long and flat bones have a recognizable structure: A hard and thin region of

dense compact bone called the cortical bone surrounding the marrow cavity known as spongy (or trabecular or cancellous) bone [2] (Figure 1).

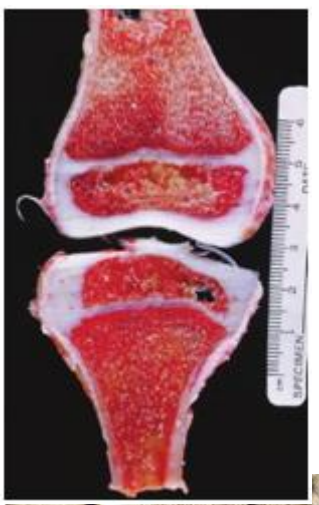

*Figure 1: Cut section of the knee joint, with femur above and tibia below. Facing the centrally located joint space is the white articular cartilage of both bones (lining the femoral condyle and tibial plateau). Adjacent to this is the red marrow and trabecular bone of the epiphysis seen in both bones* [2].

The cortical bone represents 80% of the total mass of the skeleton. One of the major microstructural parameters in cortical bone is its porosity, around 5-10%. This porosity is constituted by Haversian canals, Volkmann´s canals and resorption cavities [4] (Figure 2).

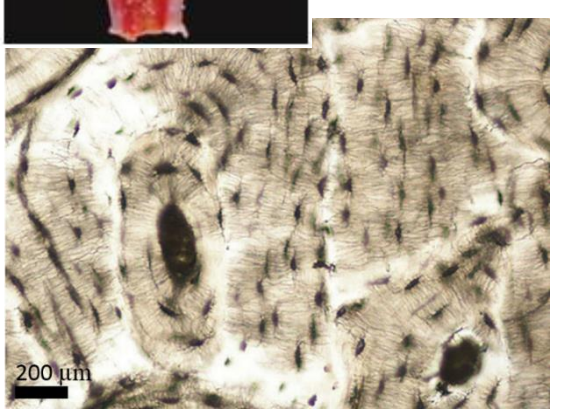


*Figure 2: Microstructure of a cross-section of cortical bone. Haversian canals are in the center of osteons. Interstitial tissues are the bone lamellae between osteons. Source: State University of New Mexico.*

Trabecular bone is a three-dimensional structure of interconnected plates and rods known as trabeculae of around 200µm thickness. The porosity of trabecular bone is between 75-95%. The pores in trabecular bone are interconnected and filled with bone marrow. This structure gives excellent mechanical properties to the bone: High compression resistance and important deformation before failure [2]. Microscopically, these two structures, cortical or spongy are consequences of a specific arrangement of the collagen fibers at lower scale: as woven bone or as lamellar bone.

### 3.1.4. Biology

Bone is a highly vascularized tissue, receiving 10-20% of the cardiac output. Bone tissues contain four important types of cells: osteoprogenitor cells, osteoblasts, osteocytes and osteoclasts. The major functions of the cells include matrix formation (osteogenesis), mineralization and degradation (resorption).

The osteoprogenitor cells are undifferentiated mesenchymal cells and thus have the potential for proliferation and capacity to differentiate (in this case into osteoblasts, chondroblasts, bone marrow stem cells or fibroblasts depending on the stimulus). Interestingly, these cells persist during postnatal life and are reactivated in adults during the repair of bone fractures and other injuries.

Derived from the osteoprogenitor cells, osteoblasts are responsible for the fabrication of bone extracellular matrix. They produce various substances (Collagen type I, glycosaminoglycans,

transforming growth factors or bone morphogenetic proteins) and control the mineralization of collagen. Osteoblasts and involved in new bone formation when an appropriate mechanical solicitation exists, a phenomenon called mechanotransduction. This allows bones to adapt in both size and shape to the mechanical stresses suffered. Osteocytes, also deriving from osteoprogenitor cells, are important in the translation of mechanical loads to cellular events such as bone formation. The fourth type of cells, osteoclasts, arise from monocyte/macrophage progenitor cells and are the primary bone resorbing cell type.

Bone tissue is continuously formed and remodeled during life. Initially, the bone increases size and adopts a shape by growth and modeling respectively. Further, during late childhood and adulthood, skeleton is continuously renewed through remodeling. Both periods require that two separate processes occur simultaneously to be effective, namely bone resorption and bone formation [2].

## 3.2. Bone disorders

Of all the existing bone disorders, bone cancer, osteoporosis and bone infections are by far the three diseases causing the major economic burden to the sanitary authorities as well as affecting more the patient's quality of life. Other bone diseases to be mentioned are Paget's disease, rickets, osteomalacia, acromegaly or Perthes' disease.

### 3.2.1. Bone Cancer

Bone cancer corresponds to the presence of a malignous tumor or metastases in the bone tissue and may be classified as: Osteosarcoma, Ewing's sarcoma, chondrosarcoma or spindle cell sarcoma [5]. In most cases, bone metastases are consequences of a primary tumor somewhere else, generally breast or prostate [6,7]. Bone is highly permissive for circulating cancerous cells to proliferate and accomplish metastases [7]. The major consequences of bone cancer is the loss of skeleton mechanical properties and cancer-induced bone pain [8], mainly due to neuropathy and inflammation.
Among the most studied treatments to fight bone cancer is the TGF-β regulation, identified to support tumor growth and bone resorption [9,10]. Surgically, the tumor removal may be performed by different techniques including high speed burring, cryotherapy, argon beam coagulation, or minimally invasive procedures [11] while the reconstruction of the bone volume may be performed with a bone graft substitute, although it is not always performed in order to allow for an additional surgical procedure if needed.

### 3.2.2. Osteoporosis

Osteoporosis is a bone disease consisting in a progressive reduction of the bone mineral density over time. Type 1 osteoporosis is very common among postmenopausal women and is caused by a decrease in estrogen production. Type 2 osteoporosis, also named senile osteoporosis, occurs to older patients and is mainly due to genetic predisposition.

Osteoporosis can lead to fragility fractures of long bones in the most critical cases [12]. As an indicative study, Tanriover et al. studied patients enrolled in the study with an osteoporotic fracture in a public Hospital in Turkey between 2003 and 2006 (50 patients) and revealed the age average was 74.2, and 72% of the patients were women. One third of the patients had no osteoporosis

documented prior to the study while the causes identified were vitamin D insufficiency and secondary hyperparathyroidism [13].

Both lack of estrogens [14] and deficiency in Vitamin D, calcium, vitamin K or phosphorus were identified as causes for osteoporosis [15] while indicators have been identified to indicate the stage of osteoporosis: osteopontin, osteocalcin, sclerostin or FGF-23 for instance [16,17]. Although some treatments are promising [18], this systemic disease is still nowadays an unsolved matter.

### 3.2.3. Bone infection

Osteomyelitis (*osteo-* derived from the Greek word *osteon*, meaning bone, *myelo-* meaning marrow, and *-itis* meaning inflammation) is the appellation used for bone infection. Different types of bone infection exist, depending on their causes [19]:

- **Trauma-related infection**: Osteomyelitis may originate from trauma or open wound fractures.

- **General infection**: Infection may come from damaged soft tissues or by accidental inoculation during surgery.

- **Implant associated infection**: Any foreign body is capable of retaining bacteria on its surface protected by a biofilm. In that case, incidence of bacterial infection is high and the success of the implantation will be based on the deletion of all the bacteria on the surface of the hardware.

Axford presented in 2010 a complete study of joint and bone infections with special focus on osteomyelitis [20] (Table 1). It highlights that the bacterium Staphylococcus aureus is the most common one in acute septic arthritis, acute haematogenous osteomyelitis and chronic osteomyelitis. Thompson and Townsend also published in 2011 a relevant paper on the drugs available providing guidelines for the treatment of soft and bone tissue infected by this bacterium [21]. A variety of antibiotics used to treat osteomyelitis were presented and the authors remark that the choice of the active principle must be based on the route of administration, predicted course length, side effect profile, toxicity, monitoring, bone tissue penetration and cost.

*Table 1: Bacteriological findings in joint and bone infection, adapted from Axford (Axford 2010).*

| | Acute Septic Arthritis | Acute haematogeneous osteomyelitis | Chronic Osteomyelitis |
|---|---|---|---|
| Staphylococcus Aureus | +++ | +++ | +++ |
| β-haemolytic Streptococcus | ++ | ++ | |
| Other streptococci | + | + | |
| Skin anaerobes | + | + | + |
| Gram-negative cocci | + | | |
| Haemophilus influenzae | + | + | |
| Gram-negative aerobes | + | + | + |
| Salmonella | + | + | + |
| Intestinal anaerobes | | | + |
| Mycobacteria | + | | + |

*+++, very common (>30%); ++, common (5-30%); +, occurs in some situations (age, underlying disease, foreign material).*

Depending on the principle of action, antibiotics used to treat osteomyelitis are classified into various families:

- **Penicillins** (family): Prevent the formation of peptidoglycan, the major component of the cell wall. Without this substance, internal pressure causes the bacterium to swell and burst.
- **Cephalosporins**: Prevent synthesis of bacterial cell walls. They are often used as substitutes for penicillin in penicillin-allergic patients.
- **Aminoglycosides**: Inhibit protein synthesis in bacteria (only gram-negative). They may be generated synthetically or semi synthetically although still presenting side effects.
- **Tetracyclines**: Inhibit the growth of bacteria (only gram-negative and certain gram-positive) by inhibiting protein synthesis. They present relatively mild side effects but are however known to destroy helpful bacteria in the body or interfere with calcium.

In general, the most common routes of administration are oral and intravenous and in both cases the presence of unwanted side effects, from generation of bacterial resistance to intense diarrhea affecting patient well-being and capacity of curing are described. The adequate local delivery of therapeutic agents presents various advantages (including reduction of side effects by not treating the whole body and increased availability of the active principle in the diseased area) which will be described in more detail in a following section (See Section 3.4).

## 3.3. Strategies for bone regeneration

Bone grafting is the replacement or augmentation of a fractured or diseased part of a bone. It is a surgical procedure generally done to reverse loss or resorption of bone due to trauma or disease, for instance. There are different approaches in bone grafting, as follows:

### 3.3.1. Autograft

This bone grafting procedure is performed using the patient's own bone harvested from another location. The usual places to harvest bone are the iliac crest, tibia, jaw or even the skull (cranium). This technique has been considered traditionally as the gold standard as the harvested bone is biologically active containing functional cells and tissues, thus providing an optimum substrate for osteogenesis.

The major drawbacks of this technique are the need of a second surgical procedure to harvest the bone, the limited bone volume available in the second site and the potential important and/or chronic pain depending on the patient's condition. Also, in case of osteoporotic patients, the drawbacks of harvesting bone may compensate the benefits of the primary bone regeneration.

### 3.3.2. Allogeneic graft

Also called allograft, this technique is based on the harvesting of bone from a genetically unrelated member of the same species. Typically, bone tissue is extracted from a cadaver, freeze dried in vacuum to extract water, subjected to a specific treatment in order to preserve the biological properties of the graft and implanted. As a result, it provides a good substrate for bone regeneration wherein the surrounding alive bone can grow by filling the voids and cavities. However, the graft is neither osteogenic (like an autograft) nor osteoinductive.

### 3.3.3. Xenograft

In parallel to the allograft, the xenograft is based on bone harvesting from other animal species, generally bovine, porcine or equine. Because of the high probability of immune rejection or contamination by viral proteins, the material extracted is treated either chemically or at high temperature to keep exclusively the mineral part of bone. The final result is equivalent to an allograft, meaning that it provides a framework for the bone to grow into without any osteogenic or osteoinductive property.
Allograft and xenograft may be preferred to autograft as it avoids a potentially painful harvesting procedure. However, bone regeneration is likely to take somewhat longer than in an autograft case due to the lack of osteogenic and osteoinductive properties. Moreover, implanting human- or animal-derived grafts may generate ethical or religious concerns depending on both culture and religion of the patients. Therefore, autografts remain the most efficient solutions when small amounts of graft are needed.

### 3.3.4. Synthetic bone grafts: Calcium phosphate cements

Although by nature lacking a biological part, synthetic materials present attractive features regarding bone grafting including unlimited amounts, avoidance of 2$^{nd}$ surgery, absence of risk of

disease transmission, injectability or freedom of conformation. Several types of synthetic materials are present in the research field and commercially, as for instance calcium sulfate materials, polymers or calcium phosphate based materials. The latter are by far the most accepted ones, due to their similarity to the mineral phase of bone in terms of composition. Compared to other biomaterials used as bone scaffolds, as for instance polymers, calcium phosphate (CaP) materials present some salient features when targeting at bone regeneration, namely their excellent bioactivity with the ability to form a direct bonding with bone, and osteoconductivity. In addition, they can be resorbable, with a resorption rate depending on their composition and microstructural features. A particular kind of CaPs, the calcium phosphate cements (CPCs) stand out away the rest of CaPs for their self-setting ability, potential injectability, and other features which are described in the following sections.

*Calcium Phosphate Cements (CPCs) are investigated in this PhD Thesis, due to their physico-chemical similarity with bone and their numerous salient features, such as low temperature self-setting ability or injectability.*

### a. Calcium Phosphate Cements:

Calcium phosphate cements (CPC) were discovered in the 1980s by Brown and Chow [22] and Legeros [23] while the first commercial CPC products were introduced in the 1990s for the treatment of maxillofacial defects [24–26]. Since then, new cement formulations have been developed that fulfill specific requirements for other applications, such as bone augmentation [27–31], reinforcement of osteoporotic bones [32–35], fixation of metallic implants in weakened bone [36–38], spinal fractures and vertebroplasty [39–41].

#### Composition

CPCs are cements made of one or more calcium orthophosphate powders, which upon mixing with a liquid phase, usually water or an aqueous solution, form a paste that is able to set and harden after being implanted within the body. The cement sets as a result of a dissolution and precipitation process from one calcium-phosphate phase to another more stable one. The entanglement of the precipitated crystals is responsible for cement hardening. Despite the large number of formulations, the CPCs developed up to now have only two different end products: calcium-deficient hydroxyapatite (CDHA) or brushite (DCPD). This situation is derived from the different pH stability of these two phases, being CDHA at pH > 4.2 and brushite at pH < 4.2.

The relevance of hydroxyapatite as a bone substitute arises from the fact that the mineral in bone is a poorly crystalline carbonate- and other substituent-containing analogue of geologic apatite. When set, CPCs consist of a network of calcium phosphate crystals, with a chemical composition and crystal size that may be tailored to closely resemble the biological calcium-deficient hydroxyapatite occurring in living bone [42,43]. The CPCs leading to the formation of CDHA can be classified in two main categories:

1) Monocomponent CPC, in which a single calcium phosphate compound, alpha tricalcium phosphate (α-TCP, $Ca_3(PO_4)_2$) hydrolyses to CDHA ($Ca_9(PO_4)_5(HPO_4)OH$) without varying the Ca/P ratio [44,45].

2) Multicomponent CPC, in which two or more calcium phosphates, some more acidic and the other basic, set following an acid–base reaction.

The setting reaction responsible of cement hardening may be decomposed into three stages: dissolution of the reactants, nucleation of the new phase and crystal growth. Therefore, the setting reaction is a dissolution-precipitation process [46]. During dissolution, the raw powders dissociate into calcium and phosphate ions, generating a supersaturated solution. Once the ionic concentration reaches a critical value, nucleation of the new phase occurs, generally surrounding the reactant particles, the latter acting as nucleation points. Afterwards, the new phase keeps growing as the dissolution of the reagents goes on. During the first hours the setting process is controlled by the dissolution kinetics of the raw materials, but once the new phase surrounds the reactants, the process is controlled by diffusion across the new phase [45].

*α-TCP based Calcium Phosphate Cements (CPCs) are used in this PhD Thesis due to biomimicry of the final phase, calcium-deficient hydroxyapatite, with natural human bone.*

Structure

CPCs are highly porous materials due to free spaces between precipitated crystals, with pore sizes in the nano/micrometric range [47]. While porosity can be a limitation for the use of these materials in high load-bearing applications, it is crucial for other aspects such as protein adsorption, cell behavior and colonization or drug delivery as aforementioned. Porosity is especially sought to enhance the material's resorbability and the extent of bioactivity by increasing the surface area available for reaction.

Total porosity, microporosity and specific surface area (SSA) vary with the processing conditions of the cements, such as the liquid to powder (L/P) ratio and the particle size of the starting powder. Thus, the total porosity increases when the L/P ratio is increased, and otherwise the particle size of the starting powder conditions the shape and size of the precipitated crystals. In this way, it has been shown that HA needle-like crystals with high specific surface area are obtained when fine α-TCP powder is used, whereas plate-like crystals with lower specific surface area are obtained using coarser powder [47,48]. It is therefore important to stress the need of a thorough characterization of these textural features of CPC in order to achieve a precise knowledge and control of the resorption and biological response of calcium phosphate cements, but especially the interactions with drugs and the release kinetics of the latter.

*In this PhD Thesis, a detailed characterization of the porosity of CPCs has been performed using multiple and complementary techniques, and critically assessing their advantages and limitations.*

### b. Preparation of macroporous calcium phosphate cements

As aforementioned, calcium phosphate cements present a relevant intrinsic porosity in the nano/micrometric range. In order to enhance corporal fluid circulation, cell colonization or nutrients circulation, the presence of an interconnected network of macropores is highly beneficial. Macropores and interconnections between these over 50 microns in diameter are generally reported to bring the benefits mentioned and some studies have dealt with this issue.

Macroporous calcium phosphates in general are sought for their osteoconductive architecture allowing cell colonization, nutrients circulation and enhanced resorption due to the higher area in contact with the human body. The benefits associated to the presence of an interconnected network of macropores are clear and frequently studied or reviewed in the literature [49–51]. Specifically, the size of the macropore, or macropore entry is of high interest for cell colonization [52,53] along with the mechanical properties of the macroporous materials taking into account that the size of the macropore greatly influences the compressive strength at constant porosity [54].

Different routes may be used for preparation of macroporous calcium phosphate cements. It should be highlighted that the approach used to introduce macropores should not affect the injectability or clinical use of CPCs. The macroporous CPC should still be injectable and able to set. Among all the protocols reported and published, various trends may be identified:

- Use of a polymeric sacrificial template such as fibers resorbing fast and thus generating macropores [55].

- Use of a leaking porogen [56], or for instance PLGA microspheres [57] dissolving once placed in the human body and generating macropores.

- Use of gas-generating porogens. For example, a mixture of sodium hydrogen carbonate and citric acid produces $CO_2$ and thus, macropores [58]. A major drawback of using porogens is that relevant interconnectivity between pores can be achieved only with high proportion of porogens [59] inducing an important change in the composition of the CPC, or increasing the risk of gas embolism.

- Foaming of the CPC paste [42,60,61]. Adding a surfactant in low concentration to the liquid phase of the cement allows the generation of stable foam by mechanical agitation. The foam acts then as a template and will keep all or part of its structure while mixing with the powder phase [59]. Macropores are the voids left by the initial bubbles of the foam. The set CPCs present high macroporosity and interconnections.

Preparation and generation of macroporous CPCs by the foaming technique described in the last bullet point presents major advantages, especially the fact that injectability is maintained, but still

needs further development to enhance its clinical and industrial applicability. Its potential for drug release is high as it covers expectations from others authors regarding the need for a combined approach between bone graft substitute and local sustained release of antibiotic [62] and presents attractive structural features when considering cell colonization.

Clinical use

Of all the processes used nowadays to generate macroporous calcium phosphate, none allows the preparation of an injectable macroporous material. The mechanical foaming of a surfactant solution allows the preparation of different Calcium Phosphate Foams based on a variety of natural or synthetic surfactants [42,60,59,61,63,64]. All the materials prepared with this technique are injectable and present a foam-like structure, high porosity, macroporosity and do not require a sintering process. The in-vivo behavior of some of them has already been evaluated and shows promising results concerning resorption [65]. However, the clinical applicability of the existing foaming protocols is still limited, due to the tools, equipment and know-how needed to prepare them.

*In this PhD Thesis, novel methods to produce macroporous biomaterials by foaming processes are proposed focusing on improving both the simplicity and clinical applicability of the process.*

## 3.4. Local delivery of antibiotics: potential of synthetic bone grafts

New therapeutic trends are leading, when possible, to a progressive replacement of systemic treatment by local drug administration providing a controlled release of the drug. A systemic treatment consists in the administration of a drug implying distribution of the active principle in the whole body. This includes for instance oral or intravenous administration routes to the organism. A local treatment is the administration of a substance at a precise site in the body. A drug delivery system (DDS) is defined as a formulation or a device that enables the introduction of a therapeutic substance in a specific site of within the body and improves its efficacy and safety by controlling the rate, time, and place of release of the active principle [66].

Focusing on the case of antibiotics, systemic treatment is the "default" treatment in bone surgery. In particular, it is estimated that 25% to 50% of the antibiotics prescribed for hospitalized patients are used for prevention, not for treatment of a declared or suspected infection [67].
In order for the antibiotic to prevent infection after surgery, its concentration in the surrounding tissues must be sufficient to prevent bacterial proliferation at the time of the anticipated contamination. Prophylactic antibiotic administration normally starts two hours before surgery and is continued for 12 to 24 hours post-surgery. The duration is short to avoid toxicity and prevent elimination of the patient´s natural bacterial flora which could lead to the development of antibiotic-resistant infection, but also to reduce costs. However, many antibiotics are less likely to cause side effects if administered slowly. In this case, rapid intravenous infusions should be avoided.

Side effects of antibiotics used for surgical prophylaxis appear after several doses and may vary depending on the antibiotic family:

- **Nephrotoxicity**: poisonous effect on the kidney.
- **Ototoxicity**: Damage to the ear by a toxin, generally derived from therapy with the aminoglycoside gentamicin.
- **Pseudomembranous colitis**: Antibiotic associated diarrhea, infection of the colon.
- **Bone marrow depression**: Decrease in cells responsible for providing immunity, carrying oxygen, and those responsible for normal blood clotting.
- **Coagulopathy**: Blood's ability to clot is impaired.

While the objective of systemic treatment is to prevent infection at the surgical location, the effects and side-effects of the antibiotic treatment are suffered by the whole body with potential severe consequences including interactions between prophylactic antibiotics and other substances used pre, intra or post-surgery.

Praveen and Rohaizak showed equivalence between local and intravenous antibiotics in a randomized trial [68]. They highlighted the reduction in side effects for the prevention of superficial wound infection. Schwach-Abdellaoui et al. presented the local delivery of antimicrobial agent as a necessary alternative when treating Periodontitis [69]. Describing unwanted side effects of the systemic antibiotic therapy such as hypersensitivity or gastrointestinal intolerance, they showed however, that an additional reason for choosing local delivery over systemic treatment was the impossibility to achieve an adequate concentration during the appropriate time of treatment. Authors concluded positively on the local treatment for some pathologies but remarked variability in effectiveness from site to site.

Management of chronic osteomyelitis by local delivery of antibiotics is a novel therapeutic modality as systemic treatment may not be able to provide sufficient concentrations at the infection site without supply of high doses potentially leading to toxicity or resistance [70]. In table 2, Nandi et al. compare various systems for treatment of osteomyelitis. The antibiotics used are very common antibiotics in clinical practice.

Nandi et al. [70]

*Table 2: Comparison of various systems for local treatment of osteomyelitis* [70].

| Study | System | Antibiotic release | Animal model | Duration of release (days) | Peak release (µg/g of bone cortex) | Day on which peak observed | Serum concentration at peak (mg/L) |
|---|---|---|---|---|---|---|---|
| **Koort et al.** | Poly (DL)-lactide | Ciprofloxacin | Rabbit | 42 | 12.6 | NA | 202 at 120 min |
| **Wei et al.** | DL-lactide acid oligomer | Dideoxy Kanamycin B | Rabbit | 63 | 48.7 | 1-2 weeks | 1.29 at 2 h |
| **Garvin et al.** | Polylactide/polyglycolide | Gentamicin | Canine | 42 | 20.1±21.5 | NA | 2.38 ±0.54 |
| **Korkusuz et al.** | Calcium hydroxyapatite | Gentamicin | Rat | 90 | 60±12 | 8 | 4.6±1.0 at 1 h |
| **Kanellakopoulou et al.** | Lactic acid polymer | Pefloxacin | Rabbit | 33 | 220.3±2.06 | 15 | NA |
| **Shinto et al.** | Calcium hydroxyapatite | Gentamicin | Rat | 90 | 60 | 8 | NA |
| **Itokazu et al.** | Hydrodyxapatite | Arbekacin | Rat | NA | NA | NA | 1.4 |
| **Tsourvakas et al.** | Fibrin clot | Ciprofloxacin | Rabbit | 15 | 32.5 | 2 | 0.8 |
| **Stemberger et al.** | Collagen sponge | Gentamicin | Rabbit | 56 | 13.2 | 7 | NA |
| **Nandi et al.** | Hydroxyapatite/ β-Tricalcium Phosphate | Cefuroxime<br>Cefuroxime | Rabbit<br>Rabbit | 42<br>42 | 37.65<br>10.45 | NA<br>NA | 13.72 mg/mL<br>9.42 mg/mL |

concluded that among different possible drug delivery materials, calcium phosphate cements present major advantages by degrading and mimicking bone composition. Considerable efforts and a large number of studies have been devoted in the last decades in order to combine the intrinsic bone regeneration potential of CPC with their ability to incorporate drugs or other active molecules relevant to different therapeutic needs. Most of the biomaterials/CPCs studied in the literature do the relevant property of injectability by loading the drug after setting. Additionally, the interaction between drug and material is a topic of interest but not always tackled.

*Doxycycline hyclate, a tetracycline antibiotic, is selected in this PhD Thesis in combination with Calcium Phosphate Cements and Foams to design, characterize and investigate dosage forms.*

The adequate composition of CPCs providing them with important regenerative properties once set, in parallel with its intrinsic porosity, non-thermal setting reaction and ease of preparation make them excellent drug carriers for bone and musculoskeletal regeneration[71]. A great variety of drugs may be loaded into the CPCs, aiming at different therapeutic effects related with the main bone pathologies. The most common molecules loaded are low molecular weight drugs such as antibiotics, anti inflammatories, anti-cancer, anti-osteoporotics; high molecular weight drugs such as proteins or growth factors; or even ions such as strontium, silicate, zinc or magnesium [72].

*Due to the focus of this PhD Thesis in DDS, the use of Calcium Phosphate Cements as local drug delivery systems is studied in depth including basic concepts regarding CPCs and a state-of-the-art of the methods to incorporate drugs, interactions between CPCs and drugs, and the kind of drugs and release kinetics associated.*

In addition to the studies reported in Paper I, recent papers were published since 2012 focusing on the release of simvastatin [73], vancomycin [74], growth factors [75,76], anesthetic [77] or bisphosphonates [78].

# 4. Results

## 4.1. Paper I: Calcium phosphate cements as drug delivery materials

This paper presents an overview of the literature regarding the use of calcium phosphate cements as local drug delivery devices. It includes different active principles and approaches to combine calcium phosphate cements with drugs, proteins or ions in order to design multifunctional biomaterials.

Advanced Drug Delivery Reviews 64 (2012) 1090–1110

Contents lists available at SciVerse ScienceDirect

Advanced Drug Delivery Reviews

journal homepage: www.elsevier.com/locate/addr

# Calcium phosphate cements as drug delivery materials ☆

Maria-Pau Ginebra [a,b,*], Cristina Canal [a,b], Montserrat Espanol [a,b], David Pastorino [a,b], Edgar B. Montufar [a,b,c]

[a] Biomaterials, Biomechanics and Tissue Engineering Group, Department of Materials Science and Metallurgical Engineering, Technical University of Catalonia (UPC), Av. Diagonal 647, 08028 Barcelona, Spain
[b] Biomedical Research Networking Center in Bioengineering, Biomaterials, and Nanomedicine (CIBER-BBN), Maria de Luna 11, Ed. CEEI, 50118 Zaragoza, Spain
[c] Institute for Bioengineering of Catalonia, Josep Samitier 1-5, 08028 Barcelona, Spain.

ARTICLE INFO

*Article history:*
Received 26 September 2011
Accepted 16 January 2012
Available online 25 January 2012

*Keywords:*
Biomaterial
Calcium phosphate cement
Ceramic matrix
Bioceramic
Hydroxyapatite
Bone regeneration
Protein
Growth factor
Ions
Antibiotic

ABSTRACT

Calcium phosphate cements are used as synthetic bone grafts, with several advantages, such as their osteoconductivity and injectability. Moreover, their low-temperature setting reaction and intrinsic porosity allow for the incorporation of drugs and active principles in the material. It is the aim of the present work to: a) provide an overview of the different approaches taken in the application of calcium phosphate cements for drug delivery in the skeletal system, and b) identify the most significant achievements. The drugs or active principles associated to calcium phosphate cements are classified in three groups, i) low molecular weight drugs; ii) high molecular weight biomolecules; and iii) ions.



**Contents**



*Abbreviations:* ACP, Amorphous Calcium Phosphate; AOM, anti-osteoporosis medications; BMP, bone morphogenetic protein; CDHA, calcium deficient hydroxyapatite; CMC, carboxymethylcellulose; BSA, bovine serum albumin; BMP, bone morphogenetic growth factor; CPC, calcium phosphate cement; DCPA, monetite, dicalcium phosphate anhydrous, $CaHPO_4$; DCPD, brushite, dicalcium phosphate dihydrate $CaHPO_4.2H_2O$; FGF, fibroblast growth factors; GF, growth factor; HA, hydroxyapatite, $Ca_{10}(PO_4)_6(OH)_2$; HPC, hydroxypropylcellulose; hLF1-11, lactoferrin; HRT, hormone replacement therapy; IGF, insulin growth factor; LMAP, low-methoxy amidated pectin; MCPA, monocalcium phosphate anhydrous $Ca(H_2PO_4)_2$; MCPM, monocalcium phosphate monohydrate $Ca(H_2PO_4)_2.H_2O$; MIC, minimum inhibitory concentration; MRSA, *Staphylococcus aureus* resistant to Meticilin-Cefem; NSAID, non-steroidal anti-inflammatories; PAA, polyacrylic acid; PBS, phosphate buffered saline; PDGF, platelet-derived growth factor; PLGA, poly(lactic-co-glycolic acid); PMMA, poly(methyl methacrylate); PRP, platelet rich plasma; RANKL, receptor activator of the nuclear factor κB ligand; rhBMP-2, human recombinant-bone morphogenetic protein-2; rhbFGF, human recombinant basic fibroblast growth factor; rhTGF-β1, human recombinant-transforming growth factor-β1; rhVEGF, human recombinant vascular endothelial growth factor; SBF, simulated body fluid; SDS, sodium dodecylsulfate; SS, Stationary Stage; α-TCP, alpha-tricalcium phosphate, $\alpha$-$Ca_3(PO_4)_2$; β-TCP, beta-tricaclium phosphate, β-$Ca_3(PO_4)_2$; TTCP, tetracalcium phosphate, $Ca_4(PO_4)_2O$; TGF, transforming growth factor; TGFβ-SF, superfamily of transforming growth factor-beta; VEGF, vascular endothelial growth factor.

☆ This review is part of the *Advanced Drug Delivery Reviews* theme issue on "Targeted delivery of therapeutics to bone and connective tissues".

* Corresponding author at: Biomaterials, Biomechanics and Tissue Engineering Group, Department of Materials Science and Metallurgical Engineering, Technical University of Catalonia (UPC), Av. Diagonal 647, 08028 Barcelona, Spain.
*E-mail address:* maria.pau.ginebra@upc.edu (M.-P. Ginebra).

0169-409X/$ – see front matter © 2012 Elsevier B.V. All rights reserved.
doi:10.1016/j.addr.2012.01.008

## 1. Introduction

Calcium phosphate cements (CPCs) were discovered in the 1980s by Brown and Chow [1] and LeGeros et al. [2]. The first commercial CPC products were introduced in the 1990s for treatment of maxillo-facial defects [3,4] as well as for treatment of fractures [5]. Since then, new cement formulations have been developed that fulfill specific requirements for other applications, such as bone augmentation [6–10], reinforcement of osteoporotic bones [11–14], fixation of metallic implants in weakened bone [15,16], and spinal fractures and vertebroplasty [17–19].

The main advantages of CPCs arise from their ability to harden in vivo, through a low-temperature setting reaction. After mixing, CPCs form a viscous moldable paste, which in some instances can be injected during surgery using minimally invasive procedures [20–23]. This provides significant benefits in several clinical situations, and represents a clear advantage with respect to conventional calcium phosphate ceramics. Moreover, unlike in acrylic bone cements, which are widely used in orthopedic surgery, especially for arthroplasty fixation and vertebroplasty [19,20], the setting reaction in CPCs is not exothermic, and therefore allows the incorporation of different drugs and biological molecules, making them good candidates for drug delivery applications [24].

Compared to acrylic bone cements and to other injectable biomaterials used as drug carriers, most of them polymers, CPCs have some salient features when targeting bone applications, namely their excellent bioactivity; their ability to form a direct bond with bone, and their osteoconductivity. In addition, they can be resorbable, with a resorption rate that depends on their composition and microstructural features. However, CPCs also have some drawbacks, related mainly to their poor mechanical performance, which has limited their applicability to non- or moderate-load-bearing situations [20,25]. Due to the intrinsic porosity of CPCs, their strength is lower than that of calcium phosphate ceramics. The lack of full injectability and in some cases their slow resorption rate are other limitations of CPCs that require further optimization.

In the last decades, considerable effort and large number of studies have been devoted to develop the combination of the intrinsic bone regeneration potential of CPCs with their ability to incorporate drugs or other active molecules which are relevant for different therapeutic needs.

It is the aim of the present work to provide an overview of the different approaches taken in the application of CPCs for drug delivery, and to identify the most significant achievements.

## 2. Calcium phosphate cements: basic concepts

### 2.1. Chemistry of calcium phosphate cements

CPCs are hydraulic cements. In general, all CPCs are formed by a combination of one or more calcium orthophosphate powders, which upon mixing with a liquid phase, usually water or an aqueous solution, form a paste that is able to set and harden after being implanted within the body. Unlike acrylic bone cements, which harden through a polymerization reaction, CPCs set as a result of a dissolution and precipitation process (see Fig. 1). The entanglement of the precipitated crystals is responsible for cement hardening. Despite the large number of possible formulations, the CPCs developed up to now have only two different end products, precipitated hydroxyapatite (HA) or brushite (DCPD). This in fact is a predictable situation since hydroxyapatite is the most stable calcium phosphate at pH > 4.2 and brushite the most stable one at pH < 4.2.

#### 2.1.1. Hydroxyapatite cements

The relevance of hydroxyapatite as a bone substitute arises from the fact that the mineral in bone is a poor crystalline carbonate- and other substituent -containing an analog of geologic apatite. Several substituents, both cations ($Mg^{2+}$, $Sr^{2+}$, $Fe^{2+}$, $Pb^{2+}$, $Na^{+}$, $K^{+}$) and anions ($CO_3^{2-}$, $F^{-}$, $HPO_4^{2-}$, $H_2PO_4^{-}$), are found within the lattice and on the surface of the bone's small mineral crystals (~20 × 40 × 200 Å) [26]. When set, CPCs consist of a network of calcium phosphate crystals, with a chemical composition and crystal size that can be tailored to

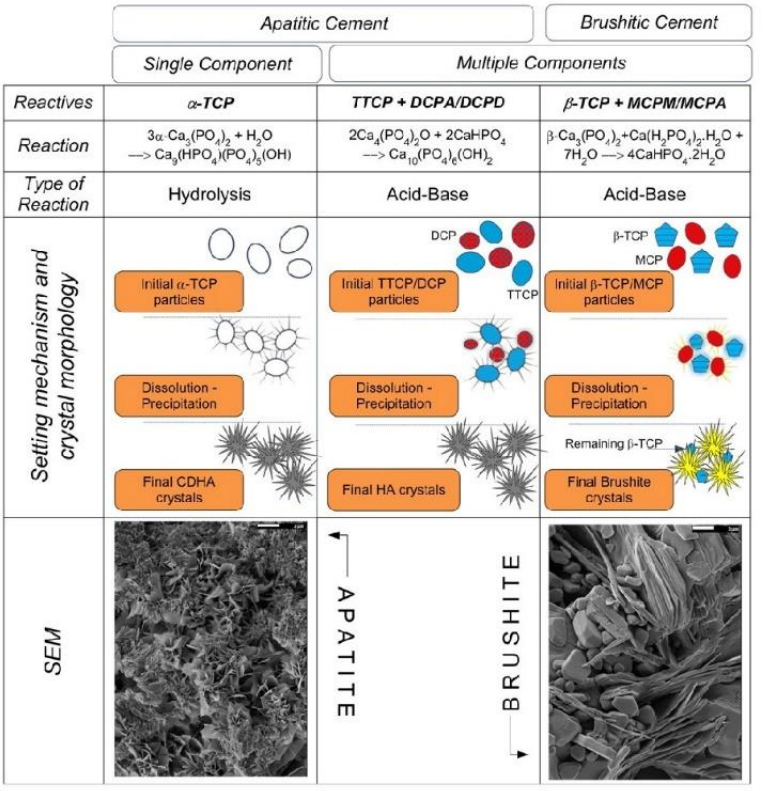


**Fig. 1.** Classification of calcium phosphate cements, with examples of the most common formulations. From top to bottom the cements are classified by the type of end-product (apatite or brushite), number of components in the solid phase (single or multiple), type of setting reaction (hydrolysis or acid–base reaction), setting mechanism and microstructure evolution during setting. Scanning electron micrographs of set apatite and brushite cements obtained by the hydrolysis of α tricalcium phosphate (α-TCP) and by reaction of β-TCP with MCPM (monocalcium phosphate monohydrate) respectively, are also shown.

closely resemble the biological hydroxyapatite occurring in living bone [27,28].

The CPCs leading to the formation of HA or calcium deficient HA (CDHA) can be classified in two main categories, which are summarized in Fig. 1: 1) Monocomponent CPCs, in which a single calcium phosphate compound, alpha tricalcium phosphate (α-TCP) hydrolyses to CDHA without varying the Ca/P ratio, according to the equation presented in Fig. 1 (left) [29,30]; 2) Multicomponent CPCs, in which two or more calcium phosphates, some more acidic and the other basic, set following an acid–base reaction (see Fig. 1 center). The basic component is normally tetracalcium phosphate (TTCP), and the most widely studied acidic reactants are either dicalcium phosphate anhydrous (DCPA) or dicalcium phosphate dihydrate (DCPD) [1,31,32]. The Ca/P ratio of the final HA depends on the ratio between TTCP and the acidic component.

### 2.1.2. Brushite cements

In contrast to hydroxyapatite, brushite is metastable under physiological conditions [33], and for this reason brushite CPCs resorb much faster than apatite CPCs [34], although it has been shown that in vivo DCPD tends to convert into HA [35]. All brushite CPCs are obtained as a result of an acid–base reaction. Several compositions have been proposed for brushite cements, most of them containing β-tricalcium phosphate (β-TCP) and an acidic component, namely monocalcium phosphate monohydrate (MCPM) or phosphoric acid (see Fig. 1 right) [36–38]. In excess of β-TCP, the final composition is in fact a mixture of brushite with unreacted β-TCP.

## 2.2. Hardening mechanism

The setting reaction that gives rise to the solid consists in three stages: dissolution of the reactants, nucleation of the new phase (either apatite or brushite) and crystal growth. Therefore, the setting reaction is a dissolution–precipitation process [39]. During dissolution, the raw powders release calcium and phosphate ions, generating a supersaturation in the solution. Once the ionic concentration reaches a critical value, the nucleation of the new phase occurs, generally surrounding the powder particles. Afterwards, the new phase keeps growing as the dissolution of the reagents goes on. During the first hours the setting process is controlled by the dissolution kinetics of the raw materials, but once the new phase surrounds the reactants, the process is controlled by diffusion across the new phase [30].

## 2.3. Cement microstructure and porosity

CPCs are highly porous materials due to free spaces between precipitated crystals, with pore size in the nano/micrometric range [40]. While porosity can be a limitation for the use of these materials in

high load-bearing applications, it is crucial for other applications. Thus, porosity is sought to enhance the material's resorbability and the extent of bioactivity by increasing the surface area available for reaction. In the same way, their inherent porosity makes these materials good carriers for controlled drug delivery systems.

Not only the total interconnected porosity is relevant for the loading and delivery of drugs, but also the pore dimensions and pore size distribution within the cement, as well as its specific surface area (SSA). These parameters vary with the processing conditions of the cements, such as the liquid to powder (L/P) ratio and the particle size of the starting powder, as shown in Fig. 2. Thus, the total porosity increases when the L/P ratio is increased, and otherwise the particle size of the starting powder conditions the shape and size of the precipitated crystals. In this way, it has been shown that HA needle-like crystals with high specific surface area are obtained when fine α-TCP powder is used, whereas plate-like crystals with lower specific surface area are obtained using coarser powder [40,41]. It is therefore important to stress the need of a thorough characterization of these textural features of CPCs in order to achieve a sound knowledge and control of the kinetics of drug elution, ensuring reproducibility and reliability of CPC based drug delivery systems.

### 2.4. Bioactivity and resorption of calcium phosphate cements

One of the most important properties of CPCs is bioactivity. When referring to bone substitutes, a bioactive material is one that is able to bind directly with the surrounding bone without the formation of fibrous tissue [42,43]. Bioactivity, together with the perfect adaptability of the cement paste during implantation, leads to a stable connection between defect and implant, speeding up bone healing process. Once implanted, CPCs can be resorbed by two different mechanisms. Active resorption regulated by living cells like macrophages or osteoclasts, and/or passive resorption via chemical dissolution or hydrolysis in the body fluids. Since brushite is soluble in body fluids, brushite cements are mainly resorbed by passive mechanism [44,45] while apatites being less soluble, cause apatite cements to be mostly resorbed by the active mechanism [46,47], i.e. macrophages and osteoclasts locally drop down the pH at values at which apatite becomes soluble. The incorporation of ionic substitutions is a method to control the degradation of CPCs. For example, incorporation of carbonates increases apatite lattice disorder favoring crystal dissolution [48,49]. Further factors that modulate CPC resorption are porosity and crystallinity among others. Besides, external factors like patient age, sex, metabolism, health, social habits, site of implantation, blood supply or mechanical loads, can affect resorption.

Ideally, when CPC is resorbed, it is progressively replaced by new bone in vivo. The replacement arises with the resorption of the cement surface in parallel with bone growth, thus avoiding gaps between implant and tissue, and guiding bone formation (osteoconduction) [50].

## 3. Calcium phosphate cements as drug carriers

### 3.1. Drug incorporation in calcium phosphate cements

The hardening of the CPC takes place at room or body temperature. This fact, together with their intrinsic porosity allows the incorporation of drugs, biologically active molecules or even cells, without thermal denaturalization or loss of activity during preparation or implantation.

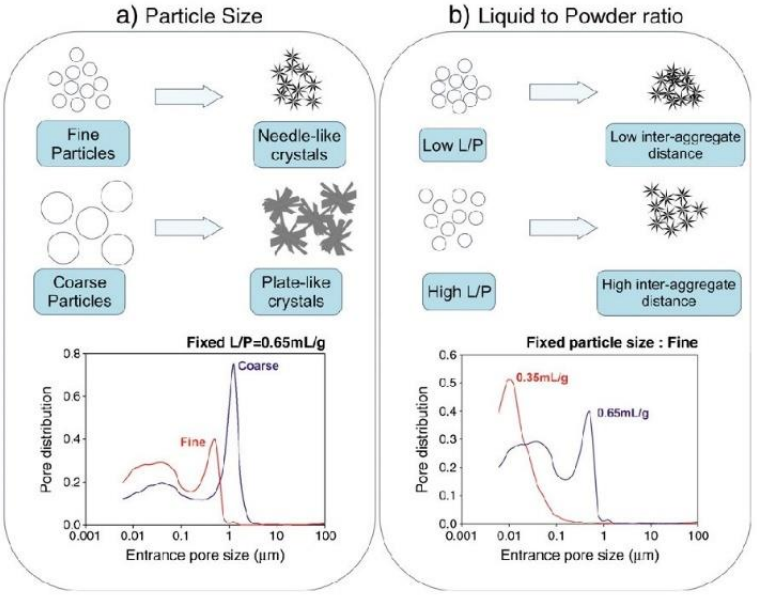


**Fig. 2.** The microstructure and porosity of CPCs can be tuned by adjusting some processing parameters, such as the particle size of the powder phase and the liquid to powder ratio (L/P). a) The reactivity of the powder increases when decreasing its particle size, due to an increase in its specific surface area. This results in a higher supersaturation degree achieved in the cement paste, which favors crystal nucleation and results in the precipitation of more numerous and smaller needle-like crystals, instead of the larger plate-like crystals formed when big particles are used. These different microstructures give rise to different pore size distributions in the set cements (bottom part of panel a). For the same L/P ratio and different powder size, the total porosity of the cement remains constant, but smaller pores are formed in the fine cement (i.e. using small particles); b) Another way of tuning the porosity and the pore size distribution of the CPCs is by varying the L/P ratio. At low L/P ratios the space between particles in the blend decreases. Considering that the precipitation of HA crystals takes place surrounding the initial powder particles, this leads to a more compact structure of crystal agglomerates. In contrast, when the L/P ratio increases, the total porosity of the cements increases and larger pores are formed due to the augmented separation between aggregates resulting from the larger distance between original α-TCP particles [40,183].

This offers the possibility of using CPCs not only as osteoconductive bone grafts, but also as local controlled drug delivery systems. The incorporation of active molecules can be used to increase the bone regeneration capacity of the material or to target specific skeletal disorders or pathologies.

The performance of any drug delivery device depends on different factors such as the microstructure (e.g. specific surface area, permeability, tortuosity and porosity), the potential degradation of the matrix, the drug solubility or the nature of the interactions between drug and matrix.

In the case of CPCs, a first issue that has to be considered and which will determine the drug distribution and its interaction with the matrix is the method of incorporation of the drug into the cement, as summarized in Fig. 3. Usually drugs are incorporated to CPCs by blending drug powder with the solid phase or by dissolving it within the liquid phase. In both cases the drug is incorporated throughout the whole volume of the material, although a more homogenous distribution will be achieved when incorporated in the liquid phase. A different approach is to incorporate the drug by impregnation of pre-set CPC solid blocks or granules with a drug solution. In this latter case, although injectability is compromised, some benefits are still retained when compared to conventional ceramic matrices. These advantages are mainly related to the fact that the consolidation of the material through a low-temperature dissolution-precipitation reaction allows obtaining hydrated compounds with high specific surface areas and particular microtextures that foster drug loading and release mechanisms.

The two strategies are very different in terms of the textural properties of the hosting matrix. On one hand, if the drug is incorporated to the cement reagents, it will be embedded in an evolving matrix. During the setting process the microstructure of the cement evolves in a lapse of hours or even days from a suspension of ceramic particles to a network of entangled crystals (see Fig. 1). On the other hand, if the drug is added to the pre-set cement, the microstructure will be stable throughout the release period, apart from potential degradation taking place, and therefore the results cannot be extrapolated to the previous situation. This stresses the need to conduct the drug release studies according to the real surgical conditions.

An alternative approach for drug loading is to incorporate the drug on polymeric microspheres before blending with the CPC. This strategy, when compared to the previous loading methods described, presents two additional benefits: on the one hand it allows modification of the release kinetics of the drug (for instance, by limiting burst release) and on the other, the degradation of the microspheres creates a porous matrix with enhanced resorption and remodeling capability.

### 3.2. Interactions between calcium phosphate cement and drugs

The setting reaction of the CPC can be influenced by the presence of the drug either in the liquid or in the powder phase, affecting the final features of the material. Thus, the addition of a drug can modify the setting kinetics, the rheological properties and the microstructural development of CPCs, all of them relevant for clinical performance. The impact of drug incorporation on the mechanical properties of CPCs is especially relevant, since it can limit their final applications. Nevertheless, there is no general rule for predicting the effect of drug incorporation in the physicochemical properties of CPCs and more particular in the mechanical properties, because the nature and extent of interaction will depend on the chemical nature of the drug molecule. For instance, some molecules interact with calcium and phosphate ions in solution, inducing a coprecipitation during setting [51], or complexing $Ca^{2+}$ [52,53], which results in a delay in the precipitation of the final product and modifies the viscosity of the paste, the setting time and the mechanical properties of the set cement. Moreover, crystallinity, crystal size and porosity can be modified, with a subsequent effect on the release kinetics. The effect of drug incorporation on CPC properties has been extensively studied in the case of antibiotics, as will be described in Section 5.1.

Finally, it must also be stressed the need to assess the stability of the drug or the bioactive molecule when incorporated in the CPC. Indeed, the dynamic nature of the dissolution–precipitation processes taking place in setting, leads to changes in local pH and ionic concentrations in solution that can have an effect on the drug functionality influencing in turn, its release. Therefore, drug release from CPCs should be studied from readily prepared cements. However, up to now most studies have been carried out on already set cements, so more studies need to be undertaken on that direction.

## 4. Drug release kinetics from calcium phosphate cements

CPCs can be ascribed to the category of non swellable monolithic systems. Moreover, in most cases they can be classified also as non-erodible or non-resorbable matrices, since, although some CPCs are resorbable, in most of them the rate of CPC degradation can be considered to be much lower than the rate of drug liberation. For these reasons it has been assumed that the drug release is mainly controlled by the process of diffusion through the cement matrix.

An important issue that will determine the kinetics of drug release is the distribution of the drug within the CPC. As previously mentioned, the drug can be incorporated either dissolved in the liquid phase or in the powder phase of the CPC. In this second case, partial dissolution of the drug particles will take place, depending on the solubility of the drug in the reactant liquid phase of the CPC. When liquid and powder are mixed, progressive dissolution of the ceramic particles takes place, and a new mineral phase precipitates. The drug dissolved in the liquid phase is not expected to be incorporated inside the crystalline lattice of the precipitated crystals (HA or brushite), or, if any, it would be in a very small amount. Most of the drug will remain trapped between the entangled crystals, in one of the following ways, as represented in Fig. 4: a) dissolved in the liquid phase within the existing pores between crystals, b) adsorbed or chemically bound

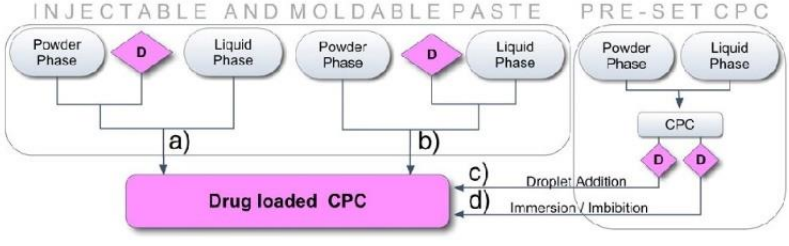


**Fig. 3.** Different options for the incorporation of drugs or biological active molecules (denoted as *D*) in the CPCs. Before cement preparation (i.e. prior to mixing the liquid and solid phase) the drug can either be mixed with the cement powder phase (a) or solubilized in the cement liquid phase (b). Drug loading can also be made after cement setting by droplet addition (c) or by imbibition (immersion) of the cement in the drug solution (d). The last procedures (c) and (d) do not allow cement injection since they require cement pre-setting, so the textural properties resulting from the low-temperature setting reaction are maintained.

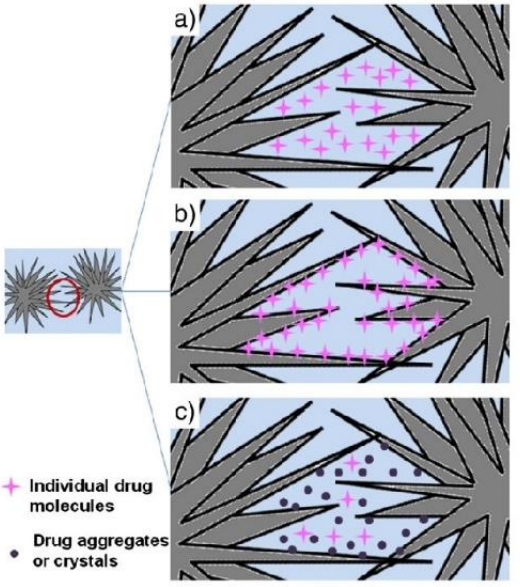


**Fig. 4.** Schematic presentation of the different ways a drug can be found in a CPC matrix: (a) as individual molecules dissolved in the liquid within the pores; (b) adsorbed or chemically bound to the crystals surface; (c) in a solid form, as drug crystals or aggregates.

on the surface of the newly formed inorganic crystals, or c) in a solid form, in the case that the concentration added was higher than the drug solubility in the aqueous phase of the cement. In this last scenario, dissolved drug molecules co-exist with amorphous aggregates and/or drug crystals. It has also to be considered that, due to dissolution of the reactants, significant changes can occur in the pH and ionic strength of the liquid phase, which can provoke the precipitation of the drug that was initially dissolved in the liquid phase of the CPC. In all these cases, the matrix possesses connecting pores that can be permeated by the surrounding physiological fluids, and the drug release can be assumed to be taking place predominantly by diffusion through the fluid filling the pores (see Fig. 5a). Since diffusion is intimately connected to the structure of the material through which diffusion takes place, the microstructure of the material must be accounted for in a successful model.

Numerous studies interpret the drug release from CPCs on the base of the Higuchi's model [54–65], which was initially developed for thin ointment films [66] and later on extended to other systems, particularly for release of solid drugs dispersed in solid granular matrices that were released by the leaching action of a penetrating solvent [66]. This model can be applied only if a) the initial drug concentration in the system is much higher than drug solubility, and therefore the drug is in solid state dispersed within the matrix; b) The size of the drug particles is much smaller than the release device; c) The carrier material does not swell or dissolve; and d) The diffusion coefficient of the drug is constant (not dependent on time or position).

For a flat geometry, where edge effects are negligible, the amount of drug released after time $t$ ($M_t$) can be calculated as:

$$M_t = A\left[\frac{D\,\varepsilon}{\tau}\,C_s\,(2\,C_0 - \varepsilon C_s)\,t\right]^{\frac{1}{2}} \quad (1)$$

Where $A$ is the surface area of the device exposed to the release medium; $D$ is the diffusion coefficient of the drug in the permeating fluid; $\varepsilon$ is the cement porosity; $\tau$ is the tortuosity of the cement; $C_s$ is the solubility of the drug in the permeating fluid and $C_0$ is the total amount of drug loaded in the cement.

This equation, meant only for one-dimensional systems, has often been used incorrectly to analyze drug transport from three dimensional configurations such as tablets [67]. However, in the case of monolithic devices, the system geometry significantly affects the resulting drug release kinetics. In fact, it should be recalled that Higuchi proposed also a mathematical model for a three dimensional leaching from a granular spherical pellet [66], following the same boundary conditions than in the one-dimensional model.

The validity of Higuchi's equation is restricted to drugs with an initial concentration above the drug solubility. When the opposite occurs, the drug becomes solubilized in the carrier and the pseudosteady state approach onto which the model is built is no longer valid. In these circumstances, drug release calculations can be made following Fick's second law if: a) the matrix remains stable throughout the release (e.g. there is no swelling and porosity is maintained), b) the drug permeability does not vary with time, c) working under sink conditions and, d) the mechanism that rules the delivery is mainly by diffusion control. Following these assumptions, early- and late-time release can be modeled using the following equations, respectively [68–70]:

$$\frac{M_t}{M_\infty} = 4\sqrt{\frac{Dt}{\pi L^2}} \text{ for } 0 \le \frac{M_t}{M_\infty} \le 0.6 \quad (2)$$

$$\frac{M_t}{M_\infty} = 1 - \frac{8}{\pi^2}\exp\left(\frac{-\pi^2 Dt}{L^2}\right) \text{ for } 0.4 \le \frac{M_t}{M_\infty} \le 1.0 \quad (3)$$

Where $M_\infty$ is the amount of drug released as time approaches infinite; $L$ is the thickness of the film, and the remaining symbols have the same meanings stated before.

It should be taken into consideration, however, that the porosity of CPCs may change in vivo. When cement resorption is relevant, mainly in brushite cements or carbonate-containing cements, an increment in porosity improves the mobility of the solubilized drug and increases the area in contact with the release medium speeding up drug release (see Fig. 5b) [71]. The reverse situation occurs when, as in most bioactive materials, an apatite layer is formed in vivo on the surface of the CPC, which may hinder drug release, inducing a membrane effect (see Fig. 5c) [72]. These contributions are not considered in Higuchi's law, meaning that if resorption or bioactivity are not negligible, this model cannot entirely describe or predict drug release.

In addition to the above mechanistic models, which are based on real phenomena and relate drug release with characteristics such as formulation, microstructure and processing parameters, there are also semi-empirical models that, although cannot unveil release mechanisms neither allow quantitative prediction of the formulation effects on the release profile, are very useful for comparison purposes.

Thus, the Peppas equation has become an easy model to apply for describing drug release [73]:

$$M_t/M_\infty = K\,t^n, \text{ for } M_t < 0.6\,M_\infty \quad (4)$$

Where $K$ is a constant that includes structural and geometric characteristics of the system; and $n$ is the release exponent, that might account for the mechanism of drug release.

In the particular case of thin film geometry, $n$ equal to 0.5 indicates Fick diffusion transport control being any other value indicative of non-Fickian transport. For different geometries, different values of the release exponent have been determined, being 0.45 and 0.43 for a cylinder and a sphere respectively when a Fickian diffusion is controlling the release. The classical Higuchi model (Eq. (1)), as well as the short time approximation of the exact solution of Fick's second

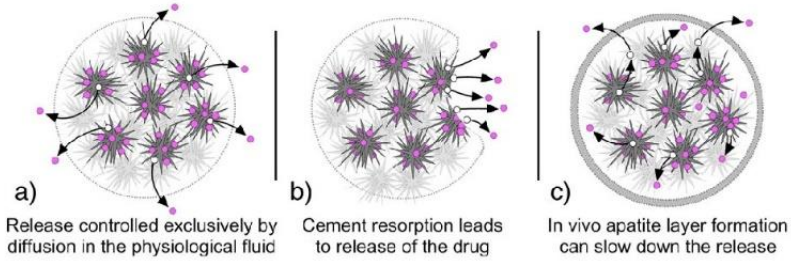


**Fig. 5.** Drug release from CPCs can encompass the following scenarios: (a) if the rate of CPC degradation is slower than drug diffusion, drug release is controlled by diffusion of the drug through the liquid permeating the cement, (b) if the rate of cement degradation is faster than drug diffusion, the former controls drug release, and (c) in some cases, namely in bioactive cements, an apatite layer can be formed on the surface of the cement after implantation, this hindering the diffusion of the drug to the surrounding tissue.

law (Eq. (2)), represent the special case of the Peppas equation where the release exponent is equal to 0.5. Therefore, even in the case that the cumulative amount released was proportional to the square root of time, this does not necessarily imply that it should follow Higuchi's model [74].

Concerning the experimental protocols used to determine the drug release kinetics in CPCs, the methods used have been diverse, including more often release to Phosphate Buffered Saline (PBS), Simulated Body Fluid (SBF) or water at 37 °C with or without stirring, and with or without periodic media change. To allow proper comparison, parameters such as the release media and the ratio between sample size or weight and media volume should be unified, for instance through Pharmacopoeia Standardised Methods. In this line, some recent studies have adapted the dynamic flow cell [75] or the paddle dissolution [76,77,250] test methods to evaluate drug release from CPCs. The relevance of the release method in the results obtained was put forward in the work from Suzuki [78], where the release of Nifedipine was evaluated by three release methods (Shaking method, Paddle method and Flow-through cell method). In that case, the flow test method showed the fastest dissolution profile, so authors considered it advantageous for rapid evaluation of dissolution characteristics of the active drug from slow-release preparations.

In the following sections, we present an overview of the use of CPCs as carriers of different types of drugs or active principles reported in the literature. They are classified in three groups, i) low molecular weight drugs; ii) high molecular weight biomolecules; and iii) ions.

## 5. Low molecular weight drugs

### 5.1. Antibiotics

Given the application of CPCs in bone replacement in traumatology or dentistry, treatment with antibiotics is indicated either prophilactically after surgical therapy [79,80], in the occurrence of infectious pathologies such as osteomyelitis and orthopedic infection [81–92], in periodontal diseases [56,93,94] or for treatment of the dentine caries cavity [95], in traumatologic therapy or in dentistry respectively. Thus, antibiotics have been the most extensively studied drugs for release from CPCs. As shown in Table 1, that summarizes the different CPC formulations evaluated for drug release of LMW therapeutic molecules, different kinds of antibiotics have been studied in CPCs, particularly of the families of aminoglicosides, cephalosporins, glycopeptides, quinolones and tetracyclines.

For prophylaxis, it is important that drug release from the CPC matrix is fast enough to reach concentrations above minimum inhibitory concentration (MIC) and avoiding subinhibitory concentrations for long times, which may lead to bacterial resistance. Besides, the treatment of infectious pathologies such as osteomyelitis or periodontitis requires longer and sustained release of the antibiotic.

#### 5.1.1. Effects of antibiotics on physico-chemical properties of CPCs

In general, addition of antibiotics alters the physicochemical properties of the cements; Regarding setting time, antibiotic incorporation usually increases this parameter [93,96–101]. To this regard, the interactions between the antibiotics and the cement particles do not usually interfere significantly with the phase transformation during setting [102,103], leading to apatite or brushite CPCs, in some cases, with traces of the initial reactants [93,99,104]. Of course, this is related to the interaction of the drug with the mineral phase of the cements in the dissolution-precipitation process taking place during setting. In particular, tetracyclines tend to chelate $Ca^{2+}$ ions which affect the primary nucleation, interfere with mineral precipitation and inhibit mineralization, delaying the setting reaction and leading to increased setting times [93,94,98,105]. The drug loading method to the CPC (Tables 1 and 2) plays a significant role in setting time, as in general, antibiotic incorporation from the liquid phase has greater influence on this parameter, usually by delaying it more markedly than when it is incorporated as a powder from the solid phase, as observed, for instance, in comparative studies for Kanamycin [89]. Additionally, in vitro release studies [89] comparing different routes of antibiotic incorporation into CPCs suggested better homogeneity of drug in the cement when added from the liquid phase. On the other hand, in general increasing antibiotic concentrations further increase setting times [106,107].

Although low antibiotic concentrations usually do not alter compressive strength [108,109], most usually the mechanical properties tend to decrease in the presence of the drugs, and further with increasing drug concentration [93,98,106,107]. This decrease of mechanical strength can be attributed to different factors, such as increased porosity or to some inhibition of the setting reaction [25].

CPC microstructure is also affected by the interactions with the antibiotic. For instance, Hesaraki et al. [80] found that the presence of Cephalexin inhibited crystal growth of HA, leading to smaller crystal size. This was attributed to the ability of carboxylic acid molecules to adsorb onto the surfaces of reactant and/or apatite nuclei of CPCs, inhibiting/retarding further growth of the precipitated phase [110]. Similarly, Bohner et al. [102] found that adding Gentamicin sulfate to a brushite cement led to thinner and smaller average crystal size. Contrarily, larger crystals with larger pores were observed within an apatite CPC with sodium alginate containing flomoxef sodium than its counterpart without antibiotic [111].

A relevant point is the possibility of partial denaturation of the antibiotic due to the pH changes during the setting reaction or to the interaction with the CPC components. In general, antimicrobial activity is maintained after setting [84,108]. For instance, no effects were observed on vancomycin with an apatite cement [90], while

**Table 1**
Low molecular weight drugs incorporated in Calcium Phosphate Cements. Cement composition, main in vitro drug release results and other studies.

| Solid phase | Liquid phase | Drug incorporation | Release method | In vitro release profile | In vitro release time | Other studies: microbial / celular / in vivo | Ref. |
|---|---|---|---|---|---|---|---|
| ***Antibiotics*** | | | | | | | |
| Aminoglicosides - **Gentamicin** | | | | | | | |
| Biobon (α-TCP) | NaCl 0.9% | S | 6 x 12 mm in 5 ml PBS, † | ☆ | 51 – 58% in 60 days SS not reached | In vivo efficacy towards S. Aureus bone infection | [108] |
| Equimolar DCPA + TTCP 1%wt $Na_2PO_4$ | $H_2O$ | PLGA microcapsules | 6 x 12 mm in 5ml PBS, 7.4, ● | No burst release 1 – 2% in 24h Nearly zero order | 16 – 17% in 96 days. SS not reached | In vitro fibroblast cell viability | [86] |
| β – TCP + MCPM | $H_2O$ or polymer | L | 12.5 x 18 mm, Paddle method, PBS, ● | ☆ 70% in 24h. Diffusion controlled release. | 100% in 80 h | – | [102] |
| β – TCP + MCPM | PAA | L | 12.5 x 10 mm, USP paddle method, PBS, ● | ☆ 40% – 100% in 24h. Diffusion controlled release. PAA did not modify release kinetics. | Reaching SS. Release between 100% and 50% depending on PAA contents. | – | [77] |
| Bone source | $H_2O$ | L | Cylinders, 5 ml PBS, 7.4, 15 cycles/min | ☆ 40% in 24h. | 50% in 30 days | Higher release than PMMA beads. Release above MIC for 30 days | [84] |
| 74.9% α-TCP, 5% DCP | Solution A | S blended with PLA | 6 x 6 mm, PBS, 7.4, † | ☆ | Sustained release for 2 months. SS not reached. | Release in bone marrow above MIC | [81] |
| 75% α-TCP, 20% TTCP, 5% DCPD | Solution A | S and/or PLA | 6 x 6 mm, 5 ml PBS, † | ☆ 70% in 24h | Release up to 60 days, SS not reached. | Implant in rabbit tibia. High [Drug] in bone marrow up to 8 weeks | [249] |
| $CaCO_3$, MCPM 7:3 | $Na_2HPO_4$ 1M | S | 5 ml PBS | ☆ 51 – 70% in 24h | 85 – 95% released. SS reached in 4 – 6 days. | Reduced COX-2 cell response.Good cell viability. | [103] |
| Biobon<br>Biofil<br>Bonesource<br>Calcibon<br>Chronos<br>Norian | Drug solution | L | 6 x 5 mm, 500 ml $H_20$, ●, †, ambient T°C | ☆ 40% in 24h<br>☆ 95% in 24h<br>☆ 70% in 24h<br>☆ 90% in 24h<br>☆ 95% in 24h<br>☆ 90% in 24h | All reach SS between 50 and 400h.<br>Initial release fits Higuchi | Antimicrobial activity vs. Staph Aureus. | [54] |
| Aminoglicosides - **Kanamycin** | | | | | | | |
| 74.9% α-TCP, 5% DCP, 18% TTCP, 2% HA, 0.1% MgP | Solution A | S or L | 7 x 14 mm in 10 ml SBF (7.4) † | ☆ 37 – 45% in 24h drug in liquid phase<br>37 – 42% in 24h drug in solid phase | Drug in L: SS reached at 57 – 64% after 30 days<br>Drug in S: 49 – 53% after 12 days | Elution above MIC in all cases during 36 days | [89] |
| Aminoglicosides - **Amikacin** | | | | | | | |
| BoneSource | $H_2O$ | L | Cylinders, 5 ml PBS, ● | ☆ 30 – 40% in 24h | 50 – 60% in 30 days | Elution above MIC for 30 days. | [84] |
| Cephalosporins - **Cephalexin** | | | | | | | |
| Equimolar DCPA + TTCP | 6% $Na_2HPO_4$ (+ SDS for macropores) | S | 5 x 3 mm discs. 25 ml SBF pH = 7.4, † | ☆ 42% in 10h | SS not reached 70% in 12 days (or 79% if macroporous) | – | [96] |
| Equimolar DCPA + TTCP | 6% $Na_2HPO_4$ (+ SDS for macropores) | S | 5 x 3 mm discs. 25 ml SBF pH = 7.4, † | ☆ Higuchi initially. Weibull for whole release | 70 – 90% released in 12 days | Released drug above MIC for S. Aureus and E.Coli | [55] |
| TTCP, CDPD, HA 3:3:2 | $H_3PO_4$ 20 mm | – | 9 x 20 mm, 50ml PBS, ● Rotating disk apparatus | ☆ 22% in 24h | 41% released in 100h. SS reached. | – | [250] |
| BoneSource | – | S | Cylinders, 5 ml PBS, ● | ☆ 9 – 20% | 10 – 30% in 30 days | Released drug above MIC for 7 days. | [84] |
| α-TCP | $H_2O$, NaCMC or acidic sol. | S(not pure active principle) | 10 x 1 mm, 50 ml $H_2O$, † | ☆ | SS reached between 5 and 30 days | | [95] |
| Cephalosporins - **Flomoxef** | | | | | | | |
| Equimolar TTCP + DCPA | $NaH_2PO_4$, $Na_2HPO_4$ Sodium alginate | L | 6 x 3 mm, 100 ml saline ● † | ☆ 29 – 35% in 24h Without sodium alginate: 31% in 24h & 55% in 72 | 54 – 57% in 72h. SS reached. | – | [79] |
| Equimolar TTCP + DCPA | 0,2MNa$H_2PO_4$, 0,2M$Na_2HPO4$ 0,5% Chitosan | L | 6x3mm, 100ml saline, ● | ☆ 26-34% in 24h | SS reached in 7h | - | [99] |
| Glycopeptides - **Vancomycin** | | | | | | | |
| Equimolar β-TCP + MCPM | 500 - 800 mM Citric acid | S | 6 x 12 mm in 50 ml PBS, ● | ☆ 60 – 80% in 24 h | SS reached for high L/P 4 days | – | [109] |
| Equimolar TTCP+DCPA | – | S | 6 x 12 mm, 15 ml TBS (7.4) ● † | ☆ 20% in 24 h | 70% in 7 days. SS not reached. | No bactericidal properties | [87] |
| β-TCP | 4 M $H_3PO_4$+ 1 mM Citric ac | S | 6 x 12 mm,15 ml TBS (7.4) ● † | ☆ 40% in 24 h | 60% SS not reached. | Bactericidal properties for 5 days | [87] |
| α-TCP, DCPA, $CaCO_3$, HA (Biopex) | Solution A | S | 10 mm beads of 2 g. 10 ml saline, † | | 5% in 13 days. | Successful treatment of MRSA osteomyelitis in 2 human patients | [114] |

*(continued on next page)*

**Table 1** (*continued*)

| Solid Phase | Liquid phase | Drug Incorporation | Release method | In vitro release profile | In vitro release time | Other studies: microbial / celular / in vivo | Ref. |
|---|---|---|---|---|---|---|---|
| ***Antibiotics*** | | | | | | | |
| Glycopeptides–**Vancomycin** | | | | | | | |
| α TCP, DCPA, $CaCO_3$, HA (Biopex) | Solution A | L | 10 ml PBS / g sample.. † | ☆ Stationary stage reached after 8 weeks. | Elution duration is greater and much longer in CPC than in PMMA | Antibacterial activity maintained after setting | [90] |
| TTCP, DCPD, HA | 20 mM $H_3PO_4$ | S | 8 x 3 mm / 4 x 2 mm, 5 ml PBS or SBF, †, ● | ☆ 60, 42, 30% in 24 h | 95% released in 60 days | Antibacterial activity above MIC between 17 and more than 40 days | [85] |
| Quinolones–**Ciprofloxacin** | | | | | | | |
| Equimolarβ–TCP + MCPM | 500–800 mM Citric acid | S | 6 x 12 mm in 50 ml PBS, ● | ☆ 30–60% in 24 h | SS reached for high L/P 14 days | | [109] |
| α – TCP | $H_2O$, NaCMC or acidic solution | S preformulated drug | 10 x 1 mm, 50 ml water, †. | ☆ | SS not reached | | [95] |
| Quinolones–**Norfloxacin** | | | | | | | |
| TTCP, DCPD, HA 3:3:2 | $H_3PO_4$ 20 mM | – | 9 x 20 mm, 50 mL PBS, ● Rotating disk apparatus | ☆ | SS reached after 450 h | – | [250] |
| Tetracyclines–**Tetracyclin** | | | | | | | |
| 49% TTCP, 38% α–TCP, 13% sodium glycerophosphate | 32% $Ca(OH)_2$, 68% $H_3PO_4$ | S | Flow cell apparatus 6 x 6 mm, $H_2O$, 0.5 ml/min | ☆ 22–30% release in 24 h. Then linear release. | 60% in 6 days. SS not reached. | | [93] |
| Tetracyclines–**Doxycycline hyclate** | | | | | | | |
| Sr–β–TCP + MCPM | $H_2O$ + 7.5 mg Doxy/simple | L | 10 x 5 mm, 8 ml PBS (pH7.4) ● † | ☆ | 100% in 25 days | Inhibition of P. Gingivalis | [94] |
| β–TCP + MCP + sodium pyrophosphate | 0.5M Citric acid | L | 10 x 5 mm, Variable volume PBS, ●, † | ☆ (50%) the first 10h fitting Higuchi. | 75% released in 4 days, SS not reached. | Bacterial growth inhibition of different bacteria. | [56] |
| Nitroimidazole–**Metronidazole** | | | | | | | |
| α–TCP | $H_2O$, NaCMC or acidic solution | S | 10 x 1 mm, 50 ml water, regular media change. | ☆ | Reaches SS between 1 and 5 days | – | [95] |
| ***Anti–inflammatory*** | | | | | | | |
| **Ibuprofen** | | | | | | | |
| 49% TTCP, 38% α–TCP, 13% sodium glycerophosphate | 32% $Ca(OH)_2$, 68% $H_3PO_4$ | 4% in LMAP microspheres | 15 ml SBF pH=7.25, ● 100 rpm 45 days | Higuchi No burst release (12–7% released in the first 24 h) | 31–69% in 45 days depending on initial concentration (2% or 6% microspheres in CPC) | – | [57] |
| **Indomethacin** | | | | | | | |
| TTCP, DCPD, Bovine collagen | 11 mM $H_3PO_4$ | S | 10 x 10 x 7.5 mm, 25 mL SBF, ● † | ☆ moderate, 4–10% in 24 h.Faster if macropores. Higuchi <30% | SS not reached in 325 h | – | [58] |
| TTCP, DCPD, 40% HA | 25 mM $H_3PO_4$ | S | 2 o 4 o 15 x 2 mm, 25 mL SBF, ● † | ☆46%, 29%, 5% in 24 h. Follows Higuchi initially | SS reached in 2.5–14 days. 92, 54, 18% release in 2 weeks | Subcutaneous in rats show higher $C_{max}$ when CPC is smaller, but total release is lower. 28, 58, 84% in 2 weeks | [59] |
| TTCP, DCPD, 40% HA | 25 mM $H_3PO_4$ | S | 25 mL SBF, ● † | ☆ Low 4–6% in 24 h. Diffusion controlled in initial stages | 32–45% in 21 days. SS reached for low concentrations | Subcutaneously implanted in rats showed continued release for 3 weeks | [72] |
| TTCP, DCPD, 40% HA | 25 mM $H_3PO_4$ | S | 25 mL SBF, ● † | ☆ 2–15% in 24 h (unsure) Higuchi fits up to 90% release | Release up to 5 weeks. SS not reached in most cases. | – | [60] |
| TTCP, DCPD, HA, NaHCO 3 | 20 mM $H_3PO_4$ | S | 16 x 2 mm, 25 mL SBF, ● † | ☆ 35–90% in 24 h. | 60–100% in 72h. SS reached for high concentrations between 24 and 40h. | – | [71] |
| ***Anticancer*** | | | | | | | |
| **Cisplatin** | | | | | | | |
| Cerapaste, Kobayashi Med. Japan | Aqueous solution | S | 7 x 14 mm, 10 mL PBS (7.4), † | ☆ 9% in 24 h | 13% released. SS reached after 3 weeks | Rat osteosarcoma cells proliferation inhibited with CPC+drug. Cell death when Cisplatin + Caffeine | [135] |
| 75% TCP, 20% TTCP, DCP | Solution A | S | 5 x 4 mm, 100 ml PBS (7.4) | ☆ 11% in 24 h | 24–60% in 4 weeks. SS reached for low drug concentrations | ↑[Drug] in bone marrow from implanted CPC than when systemic admin. | [133] |
| **Doxorubicin** | | | | | | | |
| TCP, TTCP, DCP | Solution A | S | 5 x 14 mm, 10 ml cell media, † | – | – | Inhibition of cell proliferation for 14 days. Higher survival in mice implanted with CPC+drug | [134] |

**Table 1** (*continued*)

| Solid phase | Liquid phase | Drug incorporation | Release method | In vitro release profile | In vitro release time | Other studies: microbial / celular / in vivo | Ref. |
|---|---|---|---|---|---|---|---|
| ***Anticancer*** | | | | | | | |
| **Methotrexate** | | | | | | | |
| TCP, DCPD, HA | 0.05% $H_3PO$ | S | 3 x 10 mm | – | – | In Rabbits CPC–Drug inhibited osteogenesis initially after implantation. | [137] |
| **6–Mercaptopurine** | | | | | | | |
| TTCP, DCPD, 40% HAP | 20 mM $H_3PO_4$ | S | 8.5 x 3 mm, 25 mL SBF, ● † | ☆ 7.5–13% in 24 h planar surface<br>☆ 20–30% in 24 h cylinder Higuchi | 15–25% in 92 h planar surface<br>38–55% in 92 h cylinder<br>SS not reached. | – | [132] |
| TTCP, DCPD, 40% HAP | 20 mM $H_3PO_4$ | S | 15 mm dia., 25 mL SBF, ● † | ☆ 14% in 24 h<br>Fits Higuchi up to 100 h | 65% in 600h<br>SS not reached | – | [61] |
| ***Anti-osteoporotic*** | | | | | | | |
| **Alendronate** | | | | | | | |
| 78% a –TCP, 10% CDHA, 5% DCPD, 5% MCPM, 2% HPMC | 5% $Na_2HPO_4$ | S–chemisorption | Column desorption was studied by passing 33 ml PBS. | – | – | – | [141] |
| β–TCP, TTCP, HA, DCPA | – | S | 6 x 12 mm, 2 mL PBS (7.25), ● † | ☆ 13–18% in 24h. | 33–21% released after 21 days. Release close to SS after 7 days. | No cytotoxicity for rat MSCs, thus, good biocompatibility in terms of cell proliferation. | [140] |
| **Estradiol** | | | | | | | |
| Equimolar TTCP + DCPD | 20 mM $H_3PO_4$ | S | SBF + $Ca^{2+}$, † | Higuchi | | In vivo in diseased rats. | [62] |
| TTCP, DCPD, 40% HAP | 20 mM $H_3PO_4$ | S | 155 mm dia., SBF + $Ca^{2+}$, ● † | Higuchi | SS not reached in 24 days | In vivo release in rats: ↑ $Ca^{2+}$, ↓ drug release | [63] |
| **Salmon-calcitonin** | | | | | | | |
| TTCP, DCPD, HA CHT/Collagen | – | – | 6x12 mm, SBF | 4–10% in 24 h. Sustained release 60 days: 50–70%. | SS not reached. | – | [144] |
| ***Other*** | | | | | | | |
| ***Vitamins*** **–Metatetrenone VIC2** | | | | | | | |
| TTCP, DCPD, bovine collagen | 11 mM $H_3PO_4$ | S | 10 x 10 x 7.5+holes. 25 ml SBF alternating with Acetate Buffer (4.5), ● † | Greater release in Acetate Buffer. | – | – | [150] |
| ***$Ca^{2+}$ Blocker*** **–Nifedipine** | | | | | | | |
| TTCP, DCPD, 40% HA | 25 mM $H_3PO_4$ | S | 15 x 2 mm SBF Shaking method Paddle method Flow through method | Faster release in flow through cell method. Higuchi. | SS not reached after 7 days. | – | [64] |
| **Caffeine** | | | | | | | |
| Cerapaste, Kobayashi Medical Japan | Aqueous solution | S | 7 x 14 mm, 10 mL PBS, † | ☆18% in 24h | Release for 8 weeks up to 90%. SS not reached. | Good rat osteosarcoma cell proliferation in CPC + caffeine. Cell death when caffeine + cysplatin. | [135] |
| **Clorhexidine** | | | | | | | |
| Equimolar β–TCP, MCPM | 800 mM citric acid | S | 8 x 1 mm, 10 ml $H_2O$ | ☆ 60% in 24h<br>Initially fits Higuchi | 100% released after 7 days | – | [65] |

□: apatite CPC. □: Brushite CPC. Unless otherwise indicated, release was performed at 37 °C. S: drug incorporated from solid phase. L: drug incorporated from liquid phase. ☆Burst release. ●Shaking or stirring. †Periodical media renewal. HPC: hydroxypropylcellulose, PAA: polyacrylic acid, CMC: carboxymethylcellulose, SDS: sodium dodecylsulfate, LMAP: Low methoxy-amidated pectin, PLGA: polylactide-co-glycolide, SS: Stationary Stage. Cylinder sample dimensions are indicated as diameter x height (in mm). Unless otherwise stated, pH media of PBS is 7.4 and of SBF is 7.25. Solution A: 5% sodium chondroitin sulfate, 12% sodium succinate, 0.3% $NaHSO_4$, 82.7% $H_2O$.

other authors [87] studying the same drug found that the concentration released also by an apatite cement exhibited no bactericidal properties, possibly due to pH fluctuations during setting, but when released by a brushite CPC it had bactericidal properties for 5 days.

As reflected in the previous paragraphs, antibiotic incorporation to CPCs (way of blending, concentration, chemistry of the antibiotic) may influence differently relevant properties such as setting times, mechanical properties, porosity, microstructure or the activity of the antibiotic. These have to be properly characterized given their relevance towards the antibiotic release profiles of the materials.

### 5.1.2. Antibiotic release from CPCs

Although it is known that brushite CPCs are more resorbable than apatite ones [112], the relatively short period of time evaluated in drug release studies (ranging from hours to a maximum of some weeks) allows not taking into account the effect of cement degradation towards the drug release mechanisms of antibiotics. Therefore, as observed experimentally [54–56,91,92] the mechanism of antibiotic release is in general governed by dissolution-diffusion processes, given the slower resorbability of the CPC compared to their rate of drug release.

**Table 2**
Low molecular weight drugs incorporated in Calcium Phosphate Cements by imbibition. Cement composition, main in vitro drug release results and other studies.

| Solid phase | Liquid phase | Incorporation | Release method | Release profile | Release time | Other | Ref. |
|---|---|---|---|---|---|---|---|
| ***Antibiotics*** | | | | | | | |
| Glycopeptides - **Vancomycin** | | | | | | | |
| β-TCP | 0.5M $Ca(H_2PO_4)_2$ in 10% $H_3PO_4$ | I + Vacuum | Static: 10 ml PBS, 37ºC, † Flow cell: 650 mg, 3 ml PBS, ↓flow | ☆ 60-80% released in 1-3 h. Fickian diffusion. | 100% release reached in 7-24 h depending o assay conditions. | Release was delayed up to 7-14 days by coating drug-CPC with PLA/PGA polymer layer. | [127] |
| **Tetracyclines-[Doxycycline hyclate]** | | | | | | | |
| Sr-β-TCP + MCPM | $H_2O$ | I 24 h (5; 24 mg/ml Doxy) | 10 x 5 cylinders in 8 ml PBS, ● † | Low [Doxy]: Fick High [Doxy]: anomalous transport mechanisms- ☆ Initial Burst n<0.45 Fickian diffusion model | 100% in 2 days | - | [94] |
| ***Anticancer*** | | | | | | | |
| **Paclitaxel** | | | | | | | |
| 85%wt αTCP + 10%wt DCPA + 5% pHA | 2%wt $Na_2HPO_4$ | I Droplet | disc , 3 ml DMEM | | Very low: In 24 h 26.5.E-5μg/ml | Avoids MDA cell proliferation. ↓OST cell number. | [136] |

I: drug incorporated by impregnation on set cement.

In general, antibiotic release from both apatite and brushite CPCs, shows a significant initial burst release, in some cases releasing even 100% of gentamicin in the first 24 h [92]. Apparently, brushite cements tend to have faster initial release than apatite ones (Table 1), as observed for gentamicin [91,92,249], vancomycin [109,113], ciprofloxacin [109] or doxycycline [56,94]. Considering that drug release in this case is mainly ruled by diffusion throughout the CPC pores, it would be interesting to investigate whether these differences are mainly due to compositional characteristics or to differences in porosity between apatite and brushite cements. However, very few studies have considered the effects of antibiotics on the porosity of CPCs, so up to now it is difficult to draw a conclusion in this regard.

In fact, several studies aim at correlating the drug release behavior with the textural properties of the unloaded CPC [87,94,109]. However this can be considered only as a first approximation, given the alterations in CPC microstructure, porosity and specific surface area due to the antibiotic addition reported in the previous section. Takechi et al. [79] found larger crystals and increasing porosity with higher Flomoxef sodium concentration in the cement (attributed to a higher effective L/P), as well as higher drug quantities released, although authors did not correlate both parameters.

Different studies [84,88,90,114] have evaluated incorporation and release of gentamicin and vancomycin from commercial CPCs. In particular, Stallmann et al. compared six commercial CPCs prepared with gentamicin as liquid phase. All of them presented burst release, in varying percentages in the first 24 h. For the authors, a discrete burst after implantation eradicating the contaminating bacteria in the surgical site could be sufficient for prophylactic therapy [54]. When compared to calcium phosphate granules impregnated with the gentamicin solution, more uniform distribution was found in the CPCs, which also showed more convenient release profiles, two of them continuously releasing up to 17 days, a point which could conform well to the treatment of osteomyelitis. As in most of the antibiotic-CPC literature, the initial release stages followed square root kinetics, and authors often claim diffusion release mechanism according to Higuchi model (Eq. (1)).

In the treatment of orthopedic infection, antibiotic-impregnated polymethylmethacrylate (PMMA) has been used in human patients for both prevention and treatment of such infections [115–122]. Because a second surgery to remove PMMA implants is often required [123], use of an absorbable material would eliminate the need for surgical removal [124]. Comparative studies between PMMA bone cements and CPCs revealed that elution of gentamicin, amikacin and ceftiofur from CPCs was greater than from PMMA cements, and that the two former released bactericidal concentrations of antibiotic for at least 30 days [84]. Vancomycin containing CPCs were able to maintain a higher antibiotic concentration and for longer periods than PMMA cements [90,114]. This, however, raises the concern of potentially having antibiotic concentration at subinhibitory levels which may allow mutational resistance to occur [125,126].

The relevance of the release method used experimentally was put forward by Gbureck et al. [127], who compared antibiotic release in static or dynamic conditions from vancomycin impregnated CPCs prepared by printing, and, as expected, found faster release in the flow through cell method. Another relevant experimental parameter is the solid or liquid introduction of the active principle in the cement. In particular, with identical concentrations of the liquid and powder form of kanamycin [89], a higher elution efficiency was obtained for the drug incorporated from the liquid phase, suggesting that when the drug is incorporated from the powder form, mixing is less even, and the drug takes longer to elute. Higher elution efficiency was achieved using smaller doses of the liquid antibiotic, with a reduction in the incidence of adverse reactions and medical costs in the clinical setting.

A strategy which has been investigated to delay antibiotic release has been the preparation of CPC-polymer (Polylactide-polyglycolide, alginate or chitosan) composites [79,86,91–93,127,128]. Polymer has been incorporated either during the preparation of the cement, as a polymer solution, as drug-containing microspheres, or by impregnation of the pre-set cement. Thus, when gentamicin is incorporated to brushite CPCs from the solid phase [91,92] it is usually completely released very fast (burst release). The addition of polymer solutions such as polyacrylamide during the preparation of CPCs decreases the percentage released without alteration of the release mechanism by diffusion, sometimes being able to delay this release efficiently. The encapsulation of the same drug in polymer microspheres [86] avoided burst release from the apatite CPC composite. Similar effects were obtained after dip-coating in a polymer a brushite CPC previously impregnated with vancomycin, [127]. Drug release was significantly delayed and it was controlled by diffusion and degradation of the coating. Ratier [93] also observed slower release (8% lower) during the first day when silicone was added to an apatite cement to improve its injectability. In this case they attributed it to the hydrophobic character of silicone, which made the CPC surface less wettable.

Different studies have evaluated the antibacterial properties of the antibiotic containing CPC, and as shown in Table 1, in most cases concentrations released showed performance above the MIC for relevant bacteria for periods of time ranging from one to several weeks. In vivo

animal studies in rabbits with induced osteomyelitis implanted with a gentamicin-loaded apatite CPC showed that only 3 weeks following treatment, no evidence of infection [88] or a significant reduction [83] was detectable in the animals which received the gentamicin-CPC, whereas in all other groups (including those treated systemically with gentamicin) infection was still present. The concentration of gentamicin in serum of the animals was much lower in those where gentamicin was provided from the CPC than those with parenteral administration. In two case studies with patients with osteomyelitis [114], CPC was efficient in the therapeutics of both cases. Additionally, the serum concentrations in both cases were low and under the safety limits of the manufacture (within 10 μg/ml).

Although several studies have been undertaken to evaluate antibiotic release from CPCs, work is still needed to be able of correlating the release kinetics with the CPC properties. This would allow designing the optimum material for each precise application.

### 5.2. Non-steroidal antiinflammatories

An important number of studies have also dealt with the incorporation of three different non-steroidal anti-inflammatories (NSAIDs) to CPCs to obtain sustained release. NSAIDs have analgesic, antipyretic and anti-inflammatory effects, and are usually indicated for the treatment of acute or chronic conditions where pain and inflammation are present. They are used for the symptomatic relief of conditions such as rheumatoid arthritis, osteoarthritis, or post-operative pain, among others. Indomethacin effects on apatite cements have been mainly studied by Otsuka et al. [58–60,71,72,129,130], and other well known NSAIDs blended on CPCs have been Ibuprofen [57] and Acetylsalicylic acid [53,131].

For the treatment of rheumathoid arthritis, indomethacin release was studied from TTCP-DCPD cements [60,72] and faster release was observed in PBS than in SBF media due to lower supersaturation of the media, following Higuchi model in both cases. In fact, SBF leads to precipitation of hydroxyapatite on the surface of CPCs, which reduces cement porosity and complicates the drug diffusion to the surrounding fluid. The in vitro drug release suggested that the release rate and thus final release, increased with higher drug concentrations in the cement [72]. The addition of Sodium Bicarbonate [71] increased the CPC resorption rate, and in this particular case, the release kinetics did not follow Higuchi's law. The effect of geometrical cement size on indomethacin release was also evaluated by Otsuka et al. [59] revealing that the rate of in vitro drug release decreased with the bigger geometrical size of the cement, ranging from 92% release in 2 mm diameter cylinders to 18% in 15 mm diameter cylinders of equal height. This was further investigated through the controlled introduction of holes in a collagen-containing TTCP-DCPD cement [58] in which the release rate increased with the number of macropores, consistently with the fact that more implant surface was exposed to the release media, and allowing a simplification of Higuchi's law, taking into account that the rate-determining step of indomethacin release is the diffusion in the liquid within the micropores of the matrices.

Good correlation was found between the in vitro and the in vivo indomethacin release from cements at the initial stages of drug release from planar CPC implants [72], while it was consistent at all stages when release was from the entire surface of the cements (cylindrical) and at a wider drug release range [59]. Subcutaneous implantation of indomethacin-containing cements [59,72] in rats suggested that the maximum released concentration depended on the drug concentration in the cements, and the half-life of the release were much longer than following subcutaneous administration, suggesting that indomethacin release from the cement continued for more than three weeks.

Girod-Fullana et al. [57] incorporated ibuprofen to hydroxyapatite cement pastes. CPCs released 100% ibuprofen within 48 h, clearly showing that there is no interaction between the cement and the drug. To diminish the release rate they encapsulated ibuprofen within low-methoxy amidated pectin (LMAP) microspheres, and both the CPC-microsphere and the microsphere release patterns presented the same shape and allowed controlled ibuprofen release from composites. The release data of CPC-LMAP microsphere composites correlated well with Higuchi's model. The release rate was inversely proportional to the quantity of microspheres in the composites.

For chronic articular rheumatism, Otsuka et al. [131] evaluated the eventual diffusion of aspirin compressed in an HA matrix through a CPC. The rate of drug liberation was found to increase with higher porosity of the cement, which was easily controlled by modifying L/P ratio. The authors confirmed drug release kinetics following a modified Fick's law, controlled by drug diffusion through the pores. Ginebra et al. studied the effect of the incorporation of an amino salicylic acid derived methacrylamide in an apatite α-TCP-based cement [53]. Possibly due to the calcium complexation ability of salicylic acid, strong effects were observed both in the rheological and mechanical properties. The injectability improved, but simultaneously a decrease in the reaction rate of the cement was observed. Smaller crystal size and lower porosity in the drug-containing CPCs led to improved mechanical strength, both in compression and in flexion.

NSAIDs release from CPCs has been intensively evaluated with different sample geometries, leading to interesting relationships which may possibly be extrapolated to other kinds of drugs blended in CPCs.

### 5.3. Anti-cancer drugs

In the treatment of malignant bone tumors, anticancer drugs are systemically administered simultaneously with surgical therapy. To avoid the severe side effects of oncologic chemotherapy on bone and other organs, studies [61,132–137] have aimed at designing new CPCs to deliver the drugs (cisplatin, doxorubicin, paclitaxel, methotrexate or mercaptopurine) locally while improving local structural defects after tumor resection.

The first work in this topic [61] compared the release between a homogeneously loaded mercaptopurine-CPC and the diffusion of the drug through an unloaded cement layer. The release kinetics of the drug-loaded CPC was faster, with burst release. Drug incorporation did not affect the setting reaction, and the release rate was clearly dependent on cement porosity, which could be easily controlled by modifying L/P ratio of the CPC paste [132].

Cisplatin is a strong, widely used chemotherapeutic drug which was blended in an apatite cement [133]. Between 20% and 60% was released in 4 weeks depending on the initial drug concentration. In vivo implantation in rabbits revealed higher concentration in the bone marrow with respect to systemic administration, higher body weight for the implanted group and bone formation up to 12 weeks. However, very high cisplatin concentrations (>20%) led to high concentrations in kidneys and liver, and impaired bone formation. As in studies with antibiotics, cisplatin release was higher from CPC than from acrylic bone cement [138]. Incorporation of caffeine in the cisplatin-CPC enhanced the release, and inhibited in vitro proliferation of SOSN2 cells.

Dropwise's incorporation of Paclitaxel to an α-TCP pre-set cement [136] resulted in good loading but very limited drug release. However, cell viability of osteosarcoma and metastatic breast cancer cells was lower with respect to the control. The addition of different concentrations of doxorubicin [134] to a commercial CPC did not alter the compressive strength of the cements, and the release medium suppressed RMT-1 E4 rat breast cancer cell proliferation in the first 14 days. Local administration of anticancer drugs may induce severe damage to the surrounding tissue including the skin due to extravasation. Nevertheless, the in vivo study carried out in rats did not reveal development of skin necrosis, even for subcutaneous injection.

In the case of anticancer drugs, the interest of targeting them at the diseased site through their blends with CPCs is even more appealing than in other kinds of drugs, given the undesirable side effects of oncologic chemotherapy. Relatively few works have been carried out in this area, with promising results in some cases, leaving the place for further studies.

### 5.4. Anti-osteoporotics

Orthopedists and oncologists often face the challenge of effectively reducing the risk of osteoporosis and other similar diseases. For osteoporosis, it is well known that the proliferation capability of osteoblasts is very low while the activity of osteoclasts is enhanced, so the bone mass is rapidly lost. Currently, the prescription patterns of hormone replacement therapy (HRT) and anti-osteoporosis medications (AOM) are changing, with a decrease in HRT and increases in bisphosphonates and raloxifene [139]. Accordingly, the most recent studies incorporating anti-osteoporotic drugs on CPCs have dealt with bisphosphonates such as alendronate or pamidronate [140–143] while previous ones studied estradiol [62,63] or calcitonin [144] release as HRT. The latter will be further discussed in Section 6.

Bishosphonates are the only non-hormonal agents used in the treatment of osteoporosis, and regarding calcium phosphates, it has to be taken into account that they have high affinity towards calcium owing to the strong cation chelating properties of calcium [145]. Panzavolta et al. [142,143] successfully added alendronate and pamidronate to a CPC, which included α-TCP, HA and DCPD. The incorporation of the bisphosphonates did not affect the rate of conversion of α-TCP into CDHA or the microstructure of the cement. Although its compressive strength was reduced, the cement still showed acceptable mechanical properties. Similarly, Jindong et al. [140] found longer setting times with increasing alendronate concentration, and decreased compressive strength. Burst release was observed, which was ascribed to surface-adsorbed drug particles dispersing rapidly from matrix into buffer, and the subsequent decline in release was related to the chelation between Ca and alendronate. With regards to cumulative release, Giocondi et al. [146] demonstrated that biphosphonate addition influenced the crystallization kinetics of CPCs, which was relevant to the bisphosphonate release profile in return. More recently, Schnitzler et al. explored interactions between alendronate and the CPC setting process, and discovered the role of bisphosphonates as a retarding agent for CPC setting [141]. The effect was found to be minimized when bisphosphonates were introduced by means of chemisorptions and alendronate release could be obtained constantly and not abruptly as predicted.

In the treatment of osteoporotic pathologies with small molecular weight drugs, bisphosphonates are the only ones which have been evaluated in CPCs. In this area, more release studies need to be carried out to obtain adequate information for further development of these cementitious biomaterials.

### 5.5. Other drugs/miscellaneous

As an alternative to antibiotics, Young et al. [65] incorporated clorhexidine, an antiseptic extensively used in dentistry, including treatment of periodontal infections or in antiseptic oral solutions, to a brushite CPC. Clorhexidine was released up to 7 days, with a release profile consistent with a single diffusion-controlled process. It seemed that interaction of clorhexidine with the brushite CPC is feebler than that with gentamicin [91].

A series of studies [147–149] have been carried out aiming at the local delivery of the traditional drug in Chinese medicine Danshen from CPCs. Danshen is an extract from *Salvia miltiorrhiza* which contains, among others diterpenes and phenolic acids and has been used in traditional Chinese medicine for promoting circulation and improving blood flow. Little details are given on the cement composition, except that Danshen is incorporated from the liquid phase. In vivo studies in human patients showed that the mechanical properties of the femoral head were reconstructed, cartilage collapse prevented, and the normal blood circulation and femoral bony structure was eventually restored.

Several studies have demonstrated that a poor vitamin K status is associated with an increased risk of osteoporotic bone fractures [150], and it was shown that its administration is paralleled by a moderate increase in the serum markers for bone formation (osteocalcin and alkaline phosphatase), among others. Otsuka [151] thus investigated the incorporation of menatetrenone (Vitamin K2) onto apatite CPC-collagen blocs, and the influence of alternating buffers (pH = 7.25 and pH = 4.5) on their release properties to simulate bone remodeling conditions. Lower pH led to dissolution of the CPC, therefore greatly enhancing drug release.

CPC possibilities are wide, so the door is open for evaluating new combinations of low molecular weight drugs with CPCs aiming at their local delivery.

## 6. High molecular weight molecules: growth factors and other proteins

Growth factors (GF) and proteins in general, are more complex structures than the preceding molecules used for the treatment of musculoskeletal disorders/infections. The complexity of proteins comes from the intricate folding and spatial arrangement of the long chain/s of amino acids, which govern the functionality of the molecule. Thus, delivering such molecules should be made taking special care at not damaging (denaturing) their structure in order to not to compromise their biological activity [152]. In general, the trouble of ensuring successful delivery of GF is compensated by their benefits. GF act as local regulators of cell function and some of them have long been recognized to have great potential for bone regeneration, e.g. bone morphogenetic proteins (BMPs), transforming growth factor beta (TGF-β), fibroblast growth factors (FGF), insulin growth factors (IGF), vascular endothelial growth factor (VEGF) and platelet-derived growth factor (PDGF) among others [153]. More specifically, BMPs are well known for their osteoinductive capacity, TGF-β by their role in stimulating migration of osteoprogenitor cells and as a potent regulator of cell proliferation, differentiation and extracellular matrix synthesis, FGF for regulating cell growth and wound healing, IGF by its role in bone metabolism, skeletal growth and maintenance of bone mass, VEGF as key regulator of angiogenesis during bone formation and PDGF as a general regulator of tissue repair [153]. All these signaling molecules, in an orchestrated manner, trigger the natural bone healing cascades responsible for bone restoration. But besides GF there are other proteins which endorse the material with additional functionality and influence bone repair [156–158]. That is the case for instance of the delivery of antimicrobial peptides like lactoferrin hLF1-11 and DHVAR-5 which can be used to prevent/fight infections [83,154,155], the protein RANKL (receptor activator of the nuclear factor κB ligand) a well known key stimulator of bone remodeling which enhances osteoclastic activity and is used to improve the resorption of materials [156,157], and hormones like estradiol and calcitonin which can be used to treat osteoporosis [62,63,144].

In spite of the innate capacity that bone has for self-reconstruction, in cases of severe pathological damage it cannot regenerate and the need for using materials to provide structural support becomes imperative. Hence, the application of any of the previously mentioned proteins in combination with CPCs appears as an excellent option to enhance bone repair. The CPC acts by controlling the dose and kinetics of the released protein but at the same time provides an osteoconductive platform onto which cells can migrate and eventually infiltrate (e.g. in macroporous CPCs) [159–161].

Since the advent of recombinant DNA technology, the synthesis of large amounts of pure proteins has led to an intense research in the delivery of these molecules using various types of carriers including CPCs. Unfortunately, despite the considerable amount of work published in the area, the large number of variables (cement composition,

type of protein, mode of protein incorporation, type of animal, bone and fracture model) and the lack of a systematic methodology make the comparison of results a difficult task. Nevertheless, we will attempt to summarize the general trends and most important achievements.

### 6.1. Protein loading and release behavior

Probably, one of the first aspects worth highlighting is the influence that protein loading has in the in vitro and in vivo release behavior from the CPC. Unlike calcium phosphate ceramics, cements offer the possibility of combining the protein in two manners: a) during cement preparation, resulting in the homogeneous distribution of the protein throughout the material, b) after cement setting, by soaking (seldom performed owing to prohibitive costs of proteins) or by droplet deposition (surface coating) (see Fig. 3). Contrarily to what one would expect, both incorporation modes (during and after) resulted in rather similar, yet very particular, in vitro release profile of GF [162–165]: an initial elution (burst release) followed by a stable stage or slow sustain release. Not even the introduction of macropores in the cement formulation could modify this trend [164]. In spite of what could seem an apparently hampered delivery system (a high content of the protein is retained by the material), the in vivo performance of the implant was not compromised [166,167]. Blom et al. ascribed the initial burst to the release of unbound proteins from the surface of the material [163], while the steady stage was attributed to the strong binding affinity of the proteins to the CPC. Thanks to the use of scintigraphic imaging of radiolabeled proteins, investigation of the protein release profile from CPCs has also become possible in in vivo situations [166,168–171]. Although the most obvious difference from in vitro studies was a faster protein clearance (nature of the biological milieu) independent of the protein loading method [166,170], the fact that in vivo the material is subjected to active degradation puts forward the differences in the loading of the protein. The homogeneous distribution of proteins in a matrix, as compared to protein surface coating, prolongs the release due to the liberation of bound proteins during resorption of the material by osteoclasts and multinucleated giant cells [172]. As will be shown later, there is one interesting strategy to modify the release kinetics from CPCs and this is by blending the cement with microspheres loaded with the protein of interest. The type and amount of microspheres and the protein loading method have been shown to affect the release behavior [169,187]. Nevertheless, it is worth bearing in mind that while is well accepted that direct delivery of proteins at the site is ineffective owing to the fast clearance by the tissue surroundings [170], up to date, the clinical relevance of a long term or short term retention is still unclear.

### 6.2. Growth factors

#### 6.2.1. Growth factor delivery from dense cements

Most of the experiments carried out with different GF on various types of dense cements have shown very promising results in terms of bone regeneration but they differed considerably in terms of cement resorption. In the study by Blom et al. on an α-TCP, DCPA, $CaCO_3$ and HA based cement, the incorporation of different amounts of rhTGF-β1 during cement preparation stimulated bone formation (rat calvarial bone defect) as was shown by a 50% increase of bone volume when compared to the control sample yet, less than 20% of the material was resorbed after two months. Both, bone formation and cement resorption were found to be dose-dependent [173]. The mixture of the rhTGF-β1 with the cement was shown to maintain both, the properties of the material and the activity of the protein upon release [162,174]. Similarly, in a series of experiments carried out by Li et al., Edward et al. and Seeherman et al. [165,175,176], a commercial α-BSM cement loaded with rhBMP-2 during cement preparation was implanted in different animals (rabbit, canine and monkey respectively) yielding impressive results with regards to bone formation and cement resorption. They found that the presence of rhBMP-2 accelerated resorption of the carrier when compared to the control sample (non loaded cement). That was believed to be caused by the ability of rhBMP-2 to stimulate accelerated osteoclast resorption [177]. However, this accelerated cement degradation was not found in other works that also use rhBMP-2 in combination with a cement carrier [178,179]. Ohura et al., unlike in the previous studies, deposited the rhBMP-2 on the surface of a set cement to investigate healing in segmental bone defects in rats and found rapid cement resorption and complete healing of the defect. They also found that this response was dose-dependent [180]. With regards to the incorporation of rhbFGF, studies by Niedhart et al. and Maus et al. showed that implantation of a mixture of the protein in a $CaSO_4$ β-TCP cement in the femur diaphysis of a rat and in the femur of an adult sheep did not show any healing improvement when compared to the control sample [181,182]. The presence of the protein was even shown to inhibit bone ingrowth during healing of the sheep defect. It was hypothesized that rhbFGF was released from the cement in small inhibitory doses.

One of the main drawbacks when working with most dense cements is their slow resorption rate which impairs bone ingrowth inside the materials and remodeling of the site, lengthening the healing process. This has triggered research moving towards the development of more open structures to facilitate both, cellular colonization but also the material resorption. At present, there are two main directions to solve this problem: 1) the use of cements with induced macroporosity and 2) to load cements with resorbable materials (e.g. microspheres) [183].

#### 6.2.2. Growth factor delivery from macroporous cements

Ruhe et al. performed a series of works using a macroporous cement based in α-TCP, DCPA, $CaCO_3$ and HA where porosity was created by $CO_2$ induction. A previous in vivo study proved that this formulation allowed bone ingrowth and favored resorption as compared to the dense formulation [184]. The incorporation of rhBMP-2 in this macroporous cement (done by deposition followed by lyophilization) and subsequent implantation either in a rabbit cranial defect or subcutaneously in the back of a rabbit showed that after 10 weeks bone had formed inside the pores but there were no signs of material degradation. In the same study, an in vitro release assay showed very limited protein release (less than 10% in 4 weeks) [167,185]. In order to assess if bone formation could be further enhanced by improving the release of rhBMP-2, the authors precoated the macroporous cement with BSA (bovine serum albumin) before rhBMP-2 loading. Their hypothesis was that adsorption of BSA would minimize the strong binding between rhBMP-2 and material enhancing the GF release. Although the in vitro results successfully proved this hypothesis, in vivo studies did not show any difference between BSA precoated samples and the controls. These findings underlined that in vitro study could only represent in vivo release kinetics to a limited degree [170]. Finally, in another experiment the macroporous material was loaded with rhTGF-β1 and implanted at the parietal calvaria of a rat. The addition of rhTGF-β1 did not show any additional effect on bone formation in the porous material nor a sign of degradation. It could not be unveiled if the wrong GF dose, carrier or animal model could have caused it [164].

#### 6.2.3. Growth factor delivery from microspheres/polymers in cements

Another way to increase macroporosity, as was mentioned before, is by introduction of biodegradable microspheres. Two different types of materials have been used for this purpose: poly(DL-lactic-co-glycolic acid) (PLGA) [168,169,171,186] and gelatine [165,187,188]. The common procedure to incorporate the GF was either by adsorption on the microspheres or by entrapment. The GF loaded microspheres were then mixed with the cement. One of the most significant findings was the possibility of controlling the in vitro and in vivo release kinetics by varying the molecular weight/isoelectric point of the microspheres as well as the mode of GF loading [169,187]. Comparison between high

and low molecular weight PLGA microspheres revealed that the higher solubility of the low molecular weight PLGA gave faster GF resorption and, 'GF entrapment' in contrast to 'GF adsorption', increased the protein release as the interaction with the CPC was minimized. The release profile was sustained throughout the experiment without any initial burst and the maximum amount released in 28 days varied from 25 to 50% [169]. With regards to the use of gelatin microspheres with different isoelectric point it was shown once again that the release could be controlled with the type of gelatin, the volume of microspheres and the loading method [187.The extent of bone ingrowth was also assessed in those materials. In the work of Bodde et al., PLGA microspheres were adsorbed with rhBMP-2 and embedded in cement were implanted in the skull of rats. Their results could not show bone ingrowth inside material and that was explained by a too slow degradation of the polymer [171]. Similar observations were made by Link et al. using gelatine microspheres loaded with rhTGF-β1 [188].

Several works have proved that blending the cement with other organic components could further improve the overall performance of the GF-cement in terms of mechanical properties (strength and toughness) [189,190], modulation of the growth factor release profile [191] and even enhancing the bioactivity of the material (e.g. by protecting the GF) [191,192]. More specifically Gu et al. could show the superior fusion capacity of an injectable cement/silk fibroin/rh-BMP-2 composite (CPC/SF/rhBMP-2) in an ovine interbody fusion model. They obtained similar stiffness values as the autograft but clearly superior to the CPC-SF and CPC-rhBMP-2 composites. Similarly, blending 15 wt.% of chitosan containing rhBMP-2 during cement preparation almost doubled the flexural strength and fracture toughness values of the CPC-rhBMP-2 material. The addition of heparin in a collagen-CPC composite during cement preparation proved a successful strategy to reduce, in a dose dependant manner, the initial burst of rhVEGF while the incorporation of collagen was found to improve the biological activity of GF.

### 6.3. Other proteins/miscellaneous

Up to now, all the above mentioned studies were carried out using GF synthesized by recombinant DNA technology making it a very expensive source of protein. In order to reduce cost, natural occurring GF such as platelet rich plasma (PRP) and Emdogain, are also being used in combination with a carrier. The former consists of an autologous cocktail of various GF such as TGF-b, VEGF, and PDGF and the later is an extract of porcine enamel matrix. Although the main drawback of such sources is the inherent variability from donor to donor, the results are promising but they require more investigation. The combination of these natural GF with CPCs was shown to affect differently the bioactivity of the material. While the presence of Emdogain in an Emdogain/PLGA-CPC composite failed to improve bone healing in the cranial defect of a rat [193], the deposition of PRP on a CPC previously seeded with human bone marrow stromal cells significantly promoted proliferation and differentiation of the cells in an in vitro assay proving its potential as mitogenic agent [194,195].

Aside from GF other proteins like lactoferrin hLF1-11 [83,155], RANKL [157], estradiol [62,63] and calcitonin [145] have also been incorporated in cements to endow the material with additional bioactivities. The antimicrobial properties of hLF1-11 when combined with a CPC were found to reduce bacterial infection of a previously inoculated femoral canal in rabbits. Similarly, combination of RANKL, a key stimulator of bone remodeling process, in a CPC proved to induce osteoclast formation in an in vitro study. The effects of estradiol, a hormone known to regulate bone mineral resorption/desorption, when incorporated in a CPC showed that was able to regulate the hormone liberation as a function of the calcium concentration in solution. Thus, in vivo studies showed that the rate of estradiol release in healthy rats was much lower than in diseased rats [62], and that in diseased animals fed with a low calcium supplement diet, the estradiol delivered increased the bone mass density [63]. In vitro release studies using calcitonin hormone showed that blending the CPC with different contents of collagen/chitosan it was possible to modulate the release of the hormone. An almost linear release up to 60 days was achieved [144].

### 6.4. Remarks

One important aspect worth considering and not explicitly addressed in many of the previous works, was the assessment of protein stability upon being loaded in the material. Any protein incorporation, if made during cement preparation, should take into account the aggressive milieu of the cement components. In most of the above mentioned cases the protein was first dissolved in the cement liquid phase and subsequently mixed with the solid phase to form the cement. While the mixture did not significantly modify the properties of the CPC, both, the pH and ionic strength of the cement paste, depending on the particular composition of the cement of work, can potentially damage the protein structure compromising its biological activity. Although in some works the activity of the protein was assessed upon delivery from the cement, these studies could not guarantee full activity of the whole protein fraction.

A very interesting scenario when dealing with the delivery of naturally occurring proteins appears when considering that the protein/s of interest is already present in the body or, in its absence, can be expressed during bone healing. This consideration is the central concept in the development of carriers that, rather than deliver 'loaded' proteins, are capable of entrapping the proteins of interest from the patient's own body. It has already been proved that the particular architecture in some materials can endorse additional osteoinductive properties to the material by means of concentrating relevant proteins from the body [196]. Thus, the grounds of a new generation of carriers have already been paved.

## 7. Calcium phosphate cements as ion release materials

The relevance of ions in the human body is readily observed in the many functions where they are involved: iron for instance, is essential for oxygen transport in the blood [197], while calcium ions are responsible for signaling and activating specific responses such as bone resorption or bone formation [198,199]. The ability of ions to trigger bone tissue responses opens a new avenue in the bone regeneration field. Thus, the implantation of materials with the capacity of locally deliver specific ions can have as big impact in bone tissue healing as the use of GF, with the additional advantages of safety and low cost. Two main axes in the delivery of ions can be differentiated: ions targeting bone remodeling processes (calcium, phosphate, strontium, silicate, zinc and magnesium) and ions with antimicrobial activity (silver) to treat and prevent infections. Although it is a relatively recent field of research, this section will review the delivery of ions from CPCs.

### 7.1. Ions influencing bone modeling and remodeling processes

#### 7.1.1. Calcium and phosphate

Calcium and phosphate ions are of especial interest not just because they are the principal components of mineral bone but also of CPCs. While it is well established from cell culture studies that the level of calcium and phosphate ions have significant effects on the activity of bone cells and mesenchymal stem cells [200–202], it is also well acknowledged that calcium phosphate materials react in aqueous environments. Thus, they can suffer from dissolution, hydrolysis, precipitation and ionic substitutions [203–208]. All these reactions make it difficult to draw a line between calcium phosphates intended for local drug delivery or aimed as substrates for bone healing [209].

Gustavsson et al. assessed the reactivity of a CDHA cement obtained by hydrolysis of α-TCP in different culture media and observed a constant and sustained sorption of calcium up to 21 days in contact with Dulbecco's Modified Eagle's Medium (DMEM) and McCoy's 5A Modified Medium (McCoy), followed by pseudo-first-order and pseudo-second-order sorption models. In contrast, the sorption of phosphorous from McCoy decreased over time, while in DMEM, phosphorous was slowly released from CDHA [210]. This study clearly emphasizes the relevance of the composition of the local environment on the reactivity of apatite cements.

#### 7.1.2. Strontium

The interest of incorporating strontium lies in the fact that it can stimulate osteoblast differentiation and inhibit osteoclastogenesis and osteoclast activity [211] in a dose dependent manner [212–214], making it a very valuable ion in the treatment of osteoporosis. Although there are many studies that investigate the effect of strontium incorporation in various cement formulations at different levels, i.e. physicochemical characterization [215–218], in vitro [216,219] and in vivo testing [220], only one study reported on the release kinetics of strontium from the material [221]. Overall, the incorporation of strontium affects the reactivity of the cement but can also modify the final composition of the material. In the work of Alkhraisat et al., monetite instead of brushite was formed which rendered the material with a more reliable degradability. Release experiments under dynamic conditions for up to 15 days revealed the release of strontium ions at dose ranges of 12-30 ppm with zero order release kinetic [221]. Ectopic and orthotopic implantation of a strontium substituted HA cement in a rabbit model showed increased bioactivity, biocompatibility and biodegradation than the strontium free cement. In addition, the presence of strontium in the new bone interface suggested that strontium competed with calcium during bone mineralization [220].

#### 7.1.3. Silicate

The presence of silicon in areas of calcification suggests that it is involved in bone development [222]. For this reason, several researchers are working on silicate substituted calcium phosphate ceramics and cements for bone regeneration [223–227]. When silicate substituted phosphate in the crystal lattice of calcium phosphates, the material showed increased bone formation [225] but it could not be proved that it was caused by the release of silicate, as the 'bound' ion could have also affected bioactivity [228]. Silicate incorporation in α-TCP cement was shown to increase its reactivity due to the lower stability of the doped crystalline structure [224].

#### 7.1.4. Zinc

The relevant role of zinc in several physiological processes, from DNA and RNA replication to development of the skeleton system [229,230], turns it into an essential element in the human body. Zinc promotes osteoblast activity, inhibits osteoclast differentiation and controls the crystal size of biological apatites [231–234]. However, as for many other ions, effects of zinc are dose dependent [235] and a high dose of zinc provokes inflammation and subsequent bone resorption [236]. The effects of zinc on bone formation have been tested in both brushite and apatite CPCs. Zinc was either introduced in the lattice of β-TCP for the brushite cement or in the α-TPC lattice for the apatite one. Release studies in SBF showed a slow release of zinc from the brushite cement while cell culture proved the superior adhesion, proliferation, higher collagen I secretion and alkaline phosphatase activity of the zinc containing cement [219,237,238]. In a pilot study in pigs, this cement showed a more extended bone formation than the zinc-free one. This beneficial effect was further improved combining strontium with zinc [238]. With regards to the zinc apatite cements, similar positive results were also observed but were shown to be dependant of the zinc dose [236,239].

#### 7.1.5. Magnesium

Besides influencing osteoblast and osteoclast activity [240], magnesium plays a key role in HA nucleation and growth [205,241]. It has also been proposed to balance phosphate/diphosphate anions via activation of alkaline phosphatase, thus promoting mineralization and preventing the inhibitory nucleation effect of diphosphate [209,242]. Recently, magnesium containing apatite cement was developed by incorporating magnesium oxide and MCP into TTCP/DCPA cement [243]. The composition upon setting was a mixture of calcium apatite and magnesium substituted apatite, with a higher solubility than the free magnesium cement. Ion release studies in SBF showed magnesium release and cell culture revealed an improvement in proliferation and alkaline phosphatase expression. There was, however, no evidence whether these effects were caused by the release of magnesium or by degradation of the material. This latter issue puts forward the need of isolating both phenomena in order to discern the role of each effect.

In summary, it can be concluded that in numerous cases the incorporation of selected ions in CPCs has shown beneficial effects on bone development. However, very few true ion release studies have been undertaken and it is difficult to correlate the in vivo results with the activity of the specific ion. Moreover, the fact that ionic incorporation further affects the physicochemical characteristics of the cement, e.g. solubility, leads to the question of identifying if the benefits are caused by the ionic release or by e.g. the increased solubility of the material.

### 7.2. Ions with antimicrobial activity

One of the major complications after orthopedic or oral surgical procedures is bacterial infection [244,245] and ions can be used as an alternative to antibiotics to fight infection. There are two approaches in the delivery of antimicrobial ions: the design of cement formulations that give rise to high pH values (e.g. a brushite or apatite cement containing alkali phosphates of hydroxides) [246] or the addition of antimicrobial cations like silver to the cement formulation [247].

Both, apatite and brushite cements doped with silver have been developed by incorporating silver ions in the α and β TCP phase respectively. Among both, the silver doped brushite cement showed a higher antibacterial activity than the silver doped apatite one due to the higher solubility of brushite which yielded increased silver release [248].

## 8. Conclusions

In the quest of the ideal biomaterial for bone repair, CPCs have raised great awareness due to their bioactivity, mouldability and capacity of self-setting in vivo, allowing minimally invasive surgical techniques. In this context, different drawbacks associated with musculoskeletal disorders or infections highlight the interest of developing new CPC-based drug delivery systems. Therefore, several works have dealt with the incorporation of different active principles with the aim of achieving local and controlled delivery to bone or dental sites.

Three main kinds of active principles have been identified as relevant in the potential therapy with CPCs, being LMW drugs, high molecular weight biomolecules and ions. Given the nature of CPC reactants (a powder and a liquid), drugs can be incorporated to the solid or the liquid phase during the preparation of the biomaterial, or after its setting by drug loading or impregnation with a drug solution.

Within LMW drugs, antibiotics are by far the most studied group, while osteoporotic, anticancer and other drugs have also been evaluated, showing in most cases profiles with burst release initially fitting Higuchi model. It has been shown that these drugs remain active after their incorporation into the cements. However, given the dynamic nature of the setting process, and to approach the reality of the

surgical room, it would be of interest to increase the number of release studies from unset drug-containing cements.

In high molecular weight biomolecules (GF and other proteins) the concern is how to load the molecule without compromising its bioactivity. It has yet to be proven that setting does not partly denature the protein. Furthermore, the high affinity of proteins towards CPCs raises also the question up to which extent the molecule acts from a bound or release state. Understanding these aspects would not just help elucidating fundamental aspects but would also allow the design of more specific carriers for the successful delivery of proteins.

Ion substitution in calcium phosphate cement has focused either on ions influencing the bone remodeling process (strontium, silicate, zinc and magnesium) or on those with antimicrobial properties (i.e. silver). Of special interest is to discriminate if the improvement comes from the active role of the ions released or by the modification of the physicochemical and textural properties of the cement. Thus ion release kinetics should be quantified and correlated with bone healing.

Apart from in vitro release studies in simulated body fluids or in contact with cellular lines, many in vivo studies have yielded promising results. However, to allow a more systematic study, it is still necessary to improve homogeneity of the methods evaluating release, and a more in-depth study of the release mechanisms would be desirable, as up to now a significant number of studies are mainly experimental. In any case, the path has been set for the development of new dosage forms for local delivery to bone sites, and given the increasing relevance of the topic there is still a long and interesting way to go.

## Acknowledgements

Authors acknowledge the financial support of the Spanish Ministry of Science and Innovation in the MAT 2009-13547 project and for the Juan de la Cierva fellowship of CC. Support for the research of MPG was received through the prize "ICREA Academia" for excellence in research, funded by the Generalitat de Catalunya.

## References

[1] W.E. Brown, L.C. Chow, A new calcium phosphate setting cement, J. Dent. Res. 62 (1983) 672.
[2] R.Z. LeGeros, A. Chohayeb, A. Shulman, Apatitic calcium phosphates: possible dental restorative materials, J. Dent. Res. 61 (1982) 343.
[3] C.D. Friedman, P.D. Costantino, S. Takagi, L.C. Chow, BoneSource hydroxyapatite cement: a novel biomaterial for craniofacial skeletal tissue engineering and reconstruction, J. Biomed. Mater. Res. 43 (1998) 428–432.
[4] D.B. Kamerer, B.E. Hirsch, C.H. Snyderman, P. Costantino, C.D. Friedman, Hydroxyapatite cement: a new method for achieving watertight closure in transtemporal surgery, Am. J. Otol. 15 (1994) 47–49.
[5] B.R. Constantz, I.C. Ison, M.T. Fulmer, R.D. Poser, S.T. Smith, M. VanWagoner, et al., Skeletal repair by in situ formation of the mineral phase of bone, Science 267 (1995) 1796–1799.
[6] \W.G. Horstmann, C.C.P.M. Verheyen, R. Leemans, An injectable calcium phosphate cement as a bone-graft substitute in the treatment of displaced lateral tibial plateau fractures, Injury 34 (2003) 141–144.
[7] E.J. Strauss, K.A. Egol, The management of ankle fractures in the elderly, Injury 38 (Suppl. 3) (2007) S2–S9.
[8] P.A. Livermeaux, Osteoporotic distal radius curettage—filling with an injectable calcium phosphate cement. A cadaveric study, Eur. J. Orthop. Surg. Traumatol. 15 (2004) 1–6.
[9] R.D. Welch, H. Zhang, D.G. Bronson, Experimental tibial plateau fractures augmented with calcium phosphate cement or autologous bone graft, J. Bone Joint Surg. 85 (2003) 222.
[10] A. Aral, S. Yalçin, Z.C. Karabuda, A. Anil, J.A. Jansen, Z. Mutlu, Injectable calcium phosphate cement as a graft material for maxillary sinus augmentation: an experimental pilot study, Clin. Oral Implants Res. 19 (2008) 612–617.
[11] B. Bai, L.M. Jazrawi, F.J. Kummer, J.M. Spivak, The use of an injectable, biodegradable calcium phosphate bone substitute for the prophylactic augmentation of osteoporotic vertebrae and the management of vertebral compression fractures, Spine 24 (1999) 1521–1526.
[12] T. Schildhauer, A. Bennett, T. Wright, J. Lane, P. O'Leary, Intravertebral body reconstruction with an injectable in situ-setting carbonated apatite: biomechanical evaluation of a minimally invasive technique, J. Orthop. Res. 17 (1999) 67–72.
[13] G. Maestretti, C. Cremer, P. Otten, R.P. Jakob, Prospective study of standalone balloon kyphoplasty with calcium phosphate cement augmentation in traumatic fractures, Eur. Spine J. 16 (2007) 601–610.
[14] M. Libicher, J. Hillmeier, U. Liegibel, U. Sommer, W. Pyerin, M. Vetter, et al., Osseous integration of calcium phosphate in osteoporotic vertebral fractures after kyphoplasty: initial results from a clinical and experimental pilot study, Osteoporos. Int. 17 (2006) 1208–1215.
[15] L.E. Mermelstein, L.C. Chow, C.D. Friedman, J.J. Crisco, The reinforcement of cancellous bone screws with calcium phosphate cement, J. Orthop. Trauma 10 (1996) 15–20.
[16] E. Ooms, J. Wolke, J. Van der Waerden, J. Jansen, Use of injectable calcium-phosphate cement for the fixation of titanium implants: an experimental study in goats, J. Biomed. Mater. Res. B Appl. Biomater. 66 (2003) 447–456.
[17] R. Takemasa, K. Kiyasu, T. Tani, S. Inoue, Validity of calcium phosphate cement vertebroplasty for vertebral non-union after osteoporotic fracture with middle column involvement, Spine J. 7 (2007) 148S.
[18] S. Tomita, A. Kin, M. Yazu, M. Abe, Biomechanical evaluation of kyphoplasty and vertebroplasty with calcium phosphate cement in a simulated osteoporotic compression fracture, J. Orthop. Sci. 8 (2003) 192–197.
[19] G. Lewis, Injectable bone cements for use in vertebroplasty and kyphoplasty: state-of-the-art review, J. Biomed. Mater. Res. B Appl. Biomater. 76 (2006) 456–468.
[20] M.P. Ginebra, Cements as bone repair materials, in: J.A. Planell (Ed.), Bone repair biomaterials, Woodhead Publishing Limited, Cambridge, England, 2009, pp. 271–308.
[21] I. Khairoun, M. Boltong, F.C.M. Driessens, J. Planell, Some factors controlling the injectability of calcium phosphate bone cements, J. Mater. Sci. Mater. Med. 9 (1998) 425–428.
[22] M. Bohner, G. Baroud, Injectability of calcium phosphate pastes, Biomaterials 26 (2005) 1553–1563.
[23] K. Ishikawa, S. Karashima, A. Takeuchi, S. Matsuya, Apatite foam fabrication based on hydrothermal reaction of α-tricalcium phosphate foam, Key Eng. Mater. 361–363 (2008) 319–322.
[24] M.P. Ginebra, T. Traykova, J.A. Planell, Calcium phosphate cements: competitive drug carriers for the musculoskeletal system? Biomaterials 27 (2006) 2171–2177.
[25] C. Canal, M.P. Ginebra, Fibre-reinforced calcium phosphate cements: a review, J. Mech. Behav. Biomed. 4 (2011) 1658–1671.
[26] A.L. Boskey, Bone mineralization, CRC Press, 2001.
[27] E. Morgan, D. Yetkinler, B. Constantz, R. Dauskardt, Mechanical properties of carbonated apatite bone mineral substitute: strength, fracture and fatigue behaviour, J. Mater. Sci. Mater. Med. 8 (1997) 559–570.
[28] E.B. Montufar, T. Traykova, E. Schacht, L. Ambrosio, M. Santin, J.A. Planell, et al., Self-hardening calcium deficient hydroxyapatite/gelatine foams for bone regeneration, J. Mater. Sci. Mater. Med. 21 (2010) 863–869.
[29] M.P. Ginebra, E. Fernandez, E.A. De Maeyer, R.M. Verbeeck, M.G. Boltong, J. Ginebra, et al., Setting reaction and hardening of an apatitic calcium phosphate cement, J. Dent. Res. 76 (1997) 905–912.
[30] M.P. Ginebra, E. Fernandez, F.C.M. Driessens, J.A. Planell, Modeling of the hydrolysis of alpha-tricalcium phosphate, J. Am. Ceram. Soc. 82 (1999) 2808–2812.
[31] W.E. Brown, L.C. Chow, Dental restorative cement pastes, US Patent RE33,221. (1985).
[32] W.E. Brown, A new calcium phosphate setting cement, J. Dent. Res. 62 (1983) 672.
[33] W.E. Brown, M. Fulmer, Kinetics of hydroxyapatite formation at low temperature, J. Am. Ceram. Soc. 74 (1991) 934–940.
[34] D. Apelt, F. Theiss, A.O. El-Warrak, K. Zlinszky, R. Bettschart-Wolfisberger, M. Bohner, et al., In vivo behavior of three different injectable hydraulic calcium phosphate cements, Biomaterials 25 (2004) 1439–1451.
[35] B.R. Constantz, B.M. Barr, I.C. Ison, M.T. Fulmer, J. Baker, L. McKinney, et al., Histological, chemical, and crystallographic analysis of four calcium phosphate cements in different rabbit osseous sites, J. Biomed. Mater. Res. 43 (1998) 451–461.
[36] J. Lemaitre, A. Mirtchi, A. Mortier, Calcium phosphate cements for medical use: state of the art and perspectives of development, Silic. Ind. 52 (1987) 141–146.
[37] A.A. Mirtchi, J. Lemaitre, N. Terao, Calcium phosphate cements: study of the [beta]-tricalcium phosphate–monocalcium phosphate system, Biomaterials 10 (1989) 475–480.
[38] P. Bajpai, C. Fuchs, D.E. McCullum, Development of tricalcium phosphate ceramic cements, in: J. Lemons (Ed.), ASTM International, 1987, pp. 377–388.
[39] W.C. Chen, J.H.C. Lin, C.P. Ju, Transmission electron microscopic study on setting mechanism of tetracalcium phosphate/dicalcium phosphate anhydrous-based calcium phosphate cement, J. Biomed. Mater. Res. A 64 (2003) 664–671.
[40] M. Espanol, R.A. Perez, E.B. Montufar, C. Marichal, A. Sacco, M.P. Ginebra, Intrinsic porosity of calcium phosphate cements and its significance for drug delivery and tissue engineering applications. Acta Biomater. 5 (2009) 2752–2762.
[41] M.P. Ginebra, F. Driessens, J.A. Planell, Effect of the particle size on the micro and nanostructural features of a calcium phosphate cement: a kinetic analysis, Biomaterials 25 (2004) 3453–3462.
[42] L.L. Hench, R. Splinter, W. Allen, T. Greenlee, Bonding mechanisms at the interface of ceramic prosthetic materials, J. Biomed. Mater. Res. 5 (1971) 117–141.
[43] W. Cao, L.L. Hench, Bioactive materials, Ceram. Int. 22 (1996) 493–507.
[44] L. Grover, J. Knowles, G. Fleming, J. Barralet, In vitro ageing of brushite calcium phosphate cement, Biomaterials 24 (2003) 4133–4141.
[45] F. Theiss, D. Apelt, B. Brand, A. Kutter, K. Zlinszky, M. Bohner, et al., Biocompatibility and resorption of a brushite calcium phosphate cement, Biomaterials 26 (2005) 4383–4394.
[46] E.P. Frankenburg, S.A. Goldstein, T.W. Bauer, S.A. Harris, R.D. Poser, Biomechanical and histological evaluation of a calcium phosphate cement, J. Bone Joint Surg. 80 (1998) 1112–1124.

[47] S. Wenisch, J.P. Stahl, U. Horas, C. Heiss, O. Kilian, K. Trinkaus, et al., In vivo mechanisms of hydroxyapatite ceramic degradation by osteoclasts: fine structural microscopy, J. Biomed. Mater. Res. A 67 (2003) 713–718.
[48] I. Khairoun, M. Boltong, F. Driessens, J. Planell, Effect of calcium carbonate on clinical compliance of apatitic calcium phosphate bone cement, J. Biomed. Mater. Res. 38 (1997) 356–360.
[49] E. Fernandez, J.A. Planell, S. Best, Precipitation of carbonated apatite in the cement system α-$Ca_3$ $(PO_4)_2$-$Ca(H_2PO_4)_2$-$CaCO_3$, J. Biomed. Mater. Res. 47 (1999) 466–471.
[50] F. Driessens, J.A. Planell, M.G. Boltong, I. Khairoun, M.P. Ginebra, Osteotransductive bone cements, Proc. Inst. Mech. Eng. H 212 (1998) 427–435.
[51] A. Bigi, B. Bracci, S. Panzavolta, Effect of added gelatin on the properties of calcium phosphate cement, Biomaterials 25 (2004) 2893–2899.
[52] A. Ratier, S. Best, M. Freche, J. Lacout, F. Rodriguez, Behaviour of a calcium phosphate bone cement containing tetracycline hydrochloride or tetracycline complexed with calcium ions, Biomaterials 22 (2001) 897–901.
[53] M.P. Ginebra, A. Rilliard, E. Fernández, C. Elvira, J. San Román, J.A. Planell, Mechanical and rheological improvement of a calcium phosphate cement by the addition of a polymeric drug, J. Biomed. Mater. Res. 57 (2001) 113–118.
[54] H.P. Stallmann, C. Faber, A.L.J.J. Bronckers, A.V. Nieuw Amerongen, P.I.J.M. Wuisman, In vitro gentamicin release from commercially available calcium-phosphate bone substitutes influence of carrier type on duration of the release profile, BMC Musculoskelet. Disord. 7 (2006) 18.
[55] S. Hesaraki, R. Nemati, Cephalexin-loaded injectable macroporous calcium phosphate bone cement, J. Biomed. Mater. Res. B Appl. Biomater. 89 (2009) 342–352.
[56] F. Tamimi, J. Torres, R. Bettini, F. Ruggera, C. Rueda, M. López-Ponce, et al., Doxycycline sustained release from brushite cements for the treatment of periodontal diseases, J. Biomed. Mater. Res. A 85 (2008) 707–714.
[57] S. Girod Fullana, H. Ternet, M. Freche, J.L. Lacout, F. Rodriguez, Controlled release properties and final macroporosity of a pectin microspheres-calcium phosphate composite bone cement, Acta Biomater. 6 (2010) 2294–2300.
[58] M. Otsuka, H. Nakagawa, A. Ito, W.I. Higuchi, Effect of geometrical structure on drug release rate of a three-dimensionally perforated porous apatite/collagen composite cement, J. Pharm. Sci. 99 (2010) 286–292.
[59] M. Otsuka, Y. Nakahigashi, Y. Matsuda, J.L. Fox, W.I. Higuchi, Y. Sugiyama, Effect of geometrical cement size on in vitro and in vivo indomethacin release from self-setting apatite cement, J. Control. Release 52 (1998) 281–289.
[60] M. Otsuka, Y. Nakahigashi, Y. Matsuda, J.L. Fox, W.I. Higuchi, A novel skeletal drug delivery system using self-setting calcium phosphate cement. 7. Effect of biological factors on indomethacin release from the cement loaded on bovine bone, J. Pharm. Sci. 83 (1994) 1569–1573.
[61] M. Otsuka, Y. Matsuda, Y. Suwa, J.L. Fox, W.I. Higuchi, A novel skeletal drug delivery system using a self-setting calcium phosphate cement. 5. Drug release behavior from a heterogeneous drug-loaded cement containing an anticancer drug, J. Pharm. Sci. 83 (1994) 1565–1568.
[62] M. Otsuka, Y. Matsuda, A.A. Baig, A. Chhettry, W.I. Higuchi, Calcium-level responsive controlled drug delivery from implant dosage forms to treat osteoporosis in an animal model, Adv. Drug Deliv. Rev. 42 (2000) 249–258.
[63] M. Otsuka, K. Yoneoka, Y. Matsuda, J.L. Fox, W.I. Higuchi, Y. Sugiyama, Oestradiol release from self-setting apatitic bone cement responsive to plasma-calcium level in ovariectomized rats, and its physicochemical mechanism, J. Pharm. Pharmacol. 49 (1997) 1182–1188.
[64] T. Suzuki, K. Arai, H. Goto, M. Hanano, J. Watanabe, K. Tomono, Dissolution tests for self-setting calcium phosphate cement-containing nifedipine, Chem. Pharm. Bull. 50 (2002) 741–743.
[65] A.M. Young, P.Y.J. Ng, U. Gbureck, S.N. Nazhat, J.E. Barralet, M.P. Hofmann, Characterization of chlorhexidine-releasing, fast-setting, brushite bone cements, Acta Biomater. 4 (2008) 1081–1088.
[66] T. Higuchi, Mechanism of sustained-action medication. Theoretical analysis of rate of release of solid drugs dispersed in solid matrices, J. Pharm. Sci. 52 (1963) 1145–1149.
[67] J. Siepmann, N.A. Peppas, Higuchi equation: derivation, applications, use and misuse, Int. J. Pharm. 418 (2011) 6–12.
[68] J. Crank, The mathematics of diffusion, Oxford University Press, USA, 1979.
[69] R.W. Baker, Controlled release of biologically active agents, John Wiley & Sons, 1987.
[70] J.M. Vergnaud, Controlled drug release of oral dosage forms, CRC, 1993.
[71] M. Otsuka, Y. Matsuda, Z. Wang, J.L. Fox, W.I. Higuchi, Effect of sodium bicarbonate amount on in vitro indomethacin release from self-setting carbonated-apatite cement, Pharm. Res. 14 (1997) 444–449.
[72] M. Otsuka, Y. Nakahigashi, Y. Matsuda, J. Fox, W.I. Higuchi, Y. Sugiyama, A novel skeletal drug delivery system using self-setting calcium phosphate cement VIII: the relationship between in vitro and in vivo drug release from indomethacin-containing cement, J. Control. Release 43 (1997) 115–122.
[73] N.A. Peppas, Analysis of Fickian and non-Fickian drug release from polymers, Pharm. Acta Helv. 60 (1985) 110–111.
[74] F. Siepmann, S. Herrmann, G. Winter, J. Siepmann, A novel mathematical model quantifying drug release from lipid implants, J. Control. Release 128 (2008) 233–240.
[75] U. Gbureck, E. Vorndran, J.E. Barralet, Modeling vancomycin release kinetics from microporous calcium phosphate ceramics comparing static and dynamic immersion conditions, Acta Biomater. 4 (2008) 1480–1486.
[76] M. Bohner, J. Lemaître, P. Van Landuyt, P.Y. Zambelli, H.P. Merkle, B. Gander, Gentamicin-loaded hydraulic calcium phosphate bone cement as antibiotic delivery system, J. Pharm. Sci. 86 (1997) 565–572.
[77] M. Bohner, J. Lemaître, H.P. Merkle, B. Gander, Control of gentamicin release from a calcium phosphate cement by admixed poly(acrylic acid), J. Pharm. Sci. 89 (2000) 1262–1270.
[78] T. Suzuki, K. Arai, H. Goto, M. Hanano, J. Watanabe, K. Tomono, Dissolution tests for self-setting calcium phosphate cement-containing nifedipine, Chem. Pharm. Bull. 50 (2002) 741–743.
[79] M. Takechi, Y. Miyamoto, K. Ishikawa, M. Nagayama, M. Kon, K. Asaoka, et al., Effects of added antibiotics on the basic properties of anti-washout- type fast-setting calcium phosphate cement, J. Biomed. Mater. Res. 39 (1998) 308–316.
[80] S. Hesaraki, F. Moztarzadeh, N. Nezafati, Evaluation of a bioceramic-based nanocomposite material for controlled delivery of a non-steroidal anti-inflammatory drug, Med. Eng. Phys. 31 (2009) 1205–1213.
[81] S. Sasaki, Y. Ishii, Apatite cement containing antibiotics: efficacy in treating experimental osteomyelitis, J. Orthop. Sci. 4 (1999) 361–369.
[82] T. Sasaki, Y. Ishibashi, H. Katano, A. Nagumo, S. Toh, In vitro elution of vancomycin from calcium phosphate cement, J. Arthroplasty 20 (2005) 1055–1059.
[83] H.P. Stallmann, C. Faber, A.L.J.J. Bronckers, A.V. Nieuw Amerongen, P.I.J.M. Wuisman, Osteomyelitis prevention in rabbits using antimicrobial peptide hLF1-11- or gentamicin-containing calcium phosphate cement, J. Antimicrob. Chemother. 54 (2004) 472–476.
[84] M.T. Ethell, R.A. Bennett, M.P. Brown, K. Merritt, J.S. Davidson, T. Tran, In vitro elution of gentamicin, amikacin, and ceftiofur from polymethylmethacrylate and hydroxyapatite cement, Vet. Surg. 29 (2000) 375–382.
[85] C. Hamanishi, K. Kitamoto, S. Tanaka, M. Otsuka, Y. Doi, T. Kitahashi, A self-setting TTCP-DCPD apatite cement for release of vancomycin, J. Biomed. Mater. Res. 33 (1996) 139–143.
[86] J. Schnieders, U. Gbureck, R. Thull, T. Kissel, Controlled release of gentamicin from calcium phosphate-poly(lactic acid-co-glycolic acid) composite bone cement, Biomaterials 27 (2006) 4239–4249.
[87] P.J. Jiang, S. Patel, U. Gbureck, R. Caley, L.M. Grover, Comparing the efficacy of three bioceramic matrices for the release of vancomycin hydrochloride, J. Biomed. Mater. Res. B Appl. Biomater. 93 (2010) 51–58.
[88] U. Joosten, A. Joist, T. Frebel, B. Brandt, S. Diederichs, C. von Eiff, Evaluation of an in situ setting injectable calcium phosphate as a new carrier material for gentamicin in the treatment of chronic osteomyelitis: studies in vitro and in vivo. Biomaterials 25 (2004) 4287–4295.
[89] O. Kisanuki, H. Yajima, T. Umeda, Y. Takakura, Experimental study of calcium phosphate cement impregnated with dideoxy-kanamycin B, J. Orthop. Sci. 12 (2007) 281–288.
[90] K. Urabe, K. Naruse, H. Hattori, M. Hirano, K. Uchida, K. Onuma, et al., In vitro comparison of elution characteristics of vancomycin from calcium phosphate cement and polymethylmethacrylate, J. Orthop. Sci. 14 (2009) 784–793.
[91] M. Bohner, J. Lemaître, P. Van Landuyt, P.Y. Zambelli, H.P. Merkle, B. Gander, Gentamicin-loaded hydraulic calcium phosphate bone cement as antibiotic delivery system, J. Pharm. Sci. 86 (1997) 565–572.
[92] M. Bohner, J. Lemaître, H.P. Merkle, B. Gander, Control of gentamicin release from a calcium phosphate cement by admixed poly(acrylic acid), J. Pharm. Sci. 89 (2000) 1262–1270.
[93] A. Ratier, M. Freche, J.L. Lacout, F. Rodriguez, Behaviour of an injectable calcium phosphate cement with added tetracycline, Int. J. Pharm. 274 (2004) 261–268.
[94] M.H. Alkhraisat, C. Rueda, J. Cabrejos-Azama, J. Lucas-Aparicio, F.T. Mariño, J. Torres García-Denche, et al., Loading and release of doxycycline hyclate from strontium-substituted calcium phosphate cement, Acta Biomater. 6 (2010) 1522–1528.
[95] A. Akashi, Y. Matsuya, M. Unemori, A. Akamine, Release profile of antimicrobial agents from [alpha]-tricalcium phosphate cement, Biomaterials 22 (2001) 2713–2717.
[96] S. Hesaraki, R. Nemati, N. Nosoudi, Preparation and characterisation of porous calcium phosphate bone cement as antibiotic carrier, Adv. Appl. Ceram. 108 (2009) 231–240.
[97] K. Ishikawa, Y. Miyamoto, M. Takechi, T. Toh, M. Kon, M. Nagayama, et al., Non-decay type fast-setting calcium phosphate cement: hydroxyapatite putty containing an increased amount of sodium, J. Biomed. Mater. Res. 36 (1997) 393–399.
[98] A. Ratier, I. Gibson, S. Best, M. Freche, J. Lacout, Setting characteristics and mechanical behaviour of a calcium phosphate bone cement containing tetracycline, Biomaterials 22 (2001) 897–901.
[99] M. Takechi, Y. Miyamoto, Y. Momota, T. Yuasa, S. Tatehara, M. Nagayama, et al., The in vitro antibiotic release from anti-washout apatite cement using chitosan, J. Mater. Sci. Mater. Med. 13 (2002) 973–978.
[100] F. Tamimi, J. Torres, I. Tresguerres, L. Blanco Jerez, E. López Cabarcos, Vertical bone augmentation with granulated brushite cement set in glycolic acid, J. Biomed. Mater. Res. 81 A (2007) 93–102.
[101] C.-J. Wang, T.-Y. Chen, J. Zhang, C.-S. Liu, An in vivo study of tobramycin-impregnated calcium phosphate cement as an artificial bone material repairing bone defect, Fudan Univ. J. Med. Sci. 28 (2001) 473–475.
[102] M. Bohner, J. Lemaître, P. Van Landuyt, P.Y. Zambelli, H.P. Merkle, B. Gander, Gentamicin-loaded hydraulic calcium phosphate bone cement as antibiotic delivery system, J. Pharm. Sci. 86 (1997) 565–572.
[103] C.-H. David Chen, C.-C. Chen, M.-Y. Shie, C.-H. Huang, S.-J. Ding, Controlled release of gentamicin from calcium phosphate/alginate bone cement, Mater. Sci. Eng. C 31 (2011) 334–341.
[104] M. Takechi, Y. Miyamoto, K. Ishikawa, M. Nagayama, M. Kon, K. Asaoka, et al., Effects of added antibiotics on the basic properties of anti-washout-type fast-setting calcium phosphate cement, J. Biomed. Mater. Res. 39 (1998) 308–316.
[105] F. Tamimi, J. Torres, R. Bettini, F. Ruggera, C. Rueda, M. López-Ponce, et al., Doxycycline sustained release from brushite cements for the treatment of periodontal diseases, J. Biomed. Mater. Res. A 85 (2008) 707–714.

[106] O. Kisanuki, H. Yajima, T. Umeda, Y. Takakura, Experimental study of calcium phosphate cement impregnated with dideoxy-kanamycin B, J. Orthop. Sci. 12 (2007) 281–288.
[107] M.H. Alkhraisat, C. Rueda, J. Cabrejos-Azama, J. Lucas-Aparicio, F.T. Mariño, J. Torres García-Denche, et al., Loading and release of doxycycline hyclate from strontium-substituted calcium phosphate cement, Acta Biomater. 6 (2010) 1522–1528.
[108] U. Joosten, A. Joist, T. Frebel, B. Brandt, S. Diederichs, C. von Eiff, Evaluation of an in situ setting injectable calcium phosphate as a new carrier material for gentamicin in the treatment of chronic osteomyelitis: studies in vitro and in vivo, Biomaterials 25 (2004) 4287–4295.
[109] M.P. Hofmann, A.R. Mohammed, Y. Perrie, U. Gbureck, J.E. Barralet, High-strength resorbable brushite bone cement with controlled drug-releasing capabilities. Acta Biomater. 5 (2009) 43–49.
[110] S. Hesaraki, A. Zamanian, F. Moztarzadeh, The influence of the acidic component of the gas-foaming porogen used in preparing an injectable porous calcium phosphate cement on its properties: Acetic acid versus citric acid, J. Biomed. Mater. Res. B Appl. Biomater. 86 (2008) 208–216.
[111] K. Ishikawa, Y. Miyamoto, M. Takechi, T. Toh, M. Kon, M. Nagayama, et al., Non-decay type fast-setting calcium phosphate cement: hydroxyapatite putty containing an increased amount of sodium alginate, J. Biomed. Mater. Res. 36 (1997) 393–399.
[112] D. Apelt, F. Theiss, A.O. El Warrak, K. Zlinszky, R. Bettschart-Wolfisberger, M. Bohner, et al., In vivo behavior of three different injectable hydraulic calcium phosphate cements, Biomaterials 25 (2004) 1439–1451.
[113] W. Liu, J. Chang, In vitro evaluation of gentamicin release from a bioactive tricalcium silicate bone cement, Mater. Sci. Eng. C 29 (2009) 2486–2492.
[114] T. Sasaki, Y. Ishibashi, H. Katano, A. Nagumo, S. Toh, In vitro elution of vancomycin from calcium phosphate cement, J. Arthroplasty 20 (2005) 1055–1059.
[115] H. Buchholz, R. Elson, K. Heinert, Antibiotic-loaded acrylic cement: current concepts, Clin. Orthop. Relat. Res. 190 (1984) 96.
[116] J.H. Calhoun, J.T. Mader, Antibiotic beads in the management of surgical infections, Am. J. Surg. 157 (1989) 443–449.
[117] W.W. Brien, E.A. Salvati, R. Klein, B. Brause, S. Stern, Antibiotic impregnated bone cement in total hip arthroplasty. An in vivo comparison of the elution properties of tobramycin and vancomycin, Clin. Orthop. Relat. Res. (1993) 242–248.
[118] J.H. Calhoun, S.L. Henry, D.M. Anger, J.A. Cobos, J.T. Mader, The treatment of infected nonunions with gentamicin-polymethylmethacrylate antibiotic beads, Clin. Orthop. Relat. Res. 295 (1993) 23–27.
[119] S.L. Henry, P.A.W. Ostermann, D. Seligson, The antibiotic bead pouch technique: the management of severe compound fractures, Clin. Orthop. Relat. Res. 295 (1993) 54–62.
[120] M.A. McNally, J.O. Small, H.G. Tofighi, R.A. Mollan, Two-stage management of chronic osteomyelitis of the long bones. The Belfast technique, J. Bone Joint Surg. Br. 75 (1993) 375–380.
[121] P.A.W. Ostermann, S.L. Henry, D. Seligson, The role of local antibiotic therapy in the management of compound fractures, Clin. Orthop. Relat. Res. 295 (1993) 102–111.
[122] P.A. Ostermann, D. Seligson, S.L. Henry, Local antibiotic therapy for severe open fractures. A review of 1085 consecutive cases, J. Bone Joint Surg. Br. 77 (1995) 93–97.
[123] S.S. Trostle, D.A. Hendrickson, W.C. Stone, A.A. Klohnen, Use of antimicrobial-impregnated polymethyl methacrylate beads for treatment of chronic, refractory septic arthritis and osteomyelitis of the digit in a bull, J. Am. Vet. Med. Assoc. 208 (1996) 404–407.
[124] T. Miclau, L.E. Dahners, R.W. Lindsey, In vitro pharmacokinetics of antibiotic release from locally implantable materials, J. Orthop. Res. 11 (1993) 627–632.
[125] R.W. Kendall, C.P. Duncan, J.A. Smith, J.H. Ngui-Yen, Persistence of bacteria on antibiotic loaded acrylic depots. A reason for caution, Clin. Orthop. Relat. Res. (1996) 273–280.
[126] B. Thomes, P. Murray, D. Bouchier-Hayes, Development of resistant strains of Staphylococcus epidermidis on gentamicin-loaded bone cement in vivo, J. Bone Joint Surg. Br. 84 (2002) 758–760.
[127] U. Gbureck, E. Vorndran, J.E. Barralet, Modeling vancomycin release kinetics from microporous calcium phosphate ceramics comparing static and dynamic immersion conditions, Acta Biomater. 4 (2008) 1480–1486.
[128] B. Zhou, J. Maao, Y. Liu, L. Yao, The effect of premixed schedule on the crystal formation of calcium phosphate cement-chitosan composite with added tetracycline, J. Hauzhong Univ. Sci.-Med. 28 (2008) 483–486.
[129] M. Otsuka, Y. Matsuda, Y. Suwa, J.L. Fox, W.I. Higuchi, A novel skeletal drug delivery system using self-setting calcium phosphate cement. 2. Physicochemical properties and drug release rate of the cement-containing indomethacin, J. Pharm. Sci. 83 (1994) 611–615.
[130] C. Hamanishi, K. Kitamoto, S. Tanaka, M. Otsuka, Y. Doi, T. Kitahashi, A self-setting TTCP-DCPD apatite cement for release of vancomycin, J. Biomed. Mater. Res. 33 (1996) 139–143.
[131] M. Otsuka, Y. Matsuda, Y. Suwa, J.L. Fox, W.I. Higuchi, A novel skeletal drug delivery system using a self-setting calcium phosphate cement. 4. Effects of the mixing solution volume on the drug-release rate of heterogeneous aspirin-loaded cement, J. Pharm. Sci. 83 (1994) 259–263.
[132] M. Otsuka, Y. Matsuda, J.L. Fox, W.I. Higuchi, A novel skeletal drug delivery system using self-setting calcium phosphate cement. 9: effects of the mixing solution volume on anticancer drug release from homogeneous drug-loaded cement, J. Pharm. Sci. 84 (1995) 733–736.
[133] Y. Tahara, Y. Ishii, Apatite cement containing cis-diamminedichloroplatinum implanted in rabbit femur for sustained release of the anticancer drug and bone formation, J. Orthop. Sci. 6 (2001) 556–565.
[134] T. Tani, K. Okada, S. Takahashi, N. Suzuki, Y. Shimada, E. Itoi, Doxorubicin-loaded calcium phosphate cement in the management of bone and soft tissue tumors, In Vivo 20 (2006) 55–60.
[135] Y. Tanzawa, H. Tsuchiya, T. Shirai, H. Nishida, K. Hayashi, A. Takeuchi, et al., Potentiation of the antitumor effect of calcium phosphate cement containing anticancer drug and caffeine on rat osteosarcoma, J. Orthop. Sci. 16 (2011) 77–84.
[136] M.A. Lopez-Heredia, G.J.B. Kamphuis, P.C. Thüne, F.C. Öner, J.A. Jansen, X.F. Walboomers, An injectable calcium phosphate cement for the local delivery of paclitaxel to bone, Biomaterials 32 (2011) 5411–5416.
[137] D. Li, Z. Yang, X. Li, Z. Li, J. Li, J. Yang, A histological evaluation on osteogenesis and resorption of methotrexate-loaded calcium phosphate cement in vivo, Biomed. Mater. 5 (2010) 25007.
[138] Y. Tanzawa, H. Tsuchiya, T. Shirai, H. Nishida, K. Hayashi, A. Takeuchi, et al., Potentiation of the antitumor effect of calcium phosphate cement containing anticancer drug and caffeine on rat osteosarcoma, J. Orthop. Sci. 16 (2011) 77–84.
[139] L. Huot, C. Couris, V. Tainturier, S. Jaglal, C. Colin, A.M. Schott, Trends in HRT and anti-osteoporosis medication prescribing in a European population after the WHI study, Osteoporos. Int. 19 (2008) 1047–1054.
[140] Z. Jindong, T. Hai, G. Junchao, W. Bo, B. Li, W. Qiang, Evaluation of a novel osteoporotic drug delivery system in vitro: alendronate-loaded calcium phosphate cement, Orthopedics 33 (2010) 561.
[141] V. Schnitzler, F. Fayon, C. Despas, I. Khairoun, C. Mellier, T. Rouillon, et al., Investigation of alendronate-doped apatitic cements as a potential technology for the prevention of osteoporotic hip fractures: critical influence of the drug introduction mode on the in vitro cement properties, Acta Biomater. 7 (2011) 759–770.
[142] S. Panzavolta, P. Torricelli, B. Bracci, M. Fini, A. Bigi, Alendronate and pamidronate calcium phosphate bone cements: setting properties and in vitro response of osteoblast and osteoclast cells, J. Inorg. Biochem. 103 (2009) 101–106.
[143] S. Panzavolta, P. Torricelli, B. Bracci, M. Fini, A. Bigi, Functionalization of biomimetic calcium phosphate bone cements with alendronate, J. Inorg. Biochem. 104 (2010) 1099–1106.
[144] D.X. Li, H.S. Fan, X.D. Zhu, Y.F. Tan, W.Q. Xiao, J. Lu, et al., Controllable release of salmon-calcitonin in injectable calcium phosphate cement modified by chitosan oligosaccharide and collagen polypeptide, J. Mater. Sci. Mater. Med. 18 (2007) 2225–2231.
[145] K. Su, X. Shi, R.R. Varshney, D.A. Wang, Transplantable delivery systems for in situ controlled release of bisphosphonate in orthopedic therapy, Expert Opin. Drug Deliv. 8 (2011) 113–126.
[146] J.L. Giocondi, B.S. El-Dasher, G.H. Nancollas, C.A. Orme, Molecular mechanisms of crystallization impacting calcium phosphate cements, Philos. Trans. R. Soc. A 368 (2010) 1937–1961.
[147] H. Jiang, X.-J. Huang, Y.-C. Tan, D.-Z. Liu, L. Wang, Core decompression and implantation of calcium phosphate cement/Danshen drug delivery system for treating ischemic necrosis of femoral head at Stages I, II and III of antigen reactive cell opsonization, Chin. J. Traumatol. 12 (2009) 285–290.
[148] H. Jiang, X. Huang, Y. Tan, Physicochemical properties and drug release rate of calcium phosphate cement containing Danshen composite injection, Chin. J. Reparative Reconstr. Surg. 21 (2007) 1113–1117.
[149] X. Huang, H. Jiang, D. Liu, Z. Zhou, L. Wang, Implantation of calcium phosphate cement/Danshen drug delivery system for avascular necrosis of femoral head, Chin. J. Reparative Reconstr. Surg. 22 (2008) 307–310.
[150] C. Vermeer, K.S. Jie, M.H. Knapen, Role of vitamin K in bone metabolism, Annu. Rev. Nutr. 15 (1995) 1–22.
[151] M. Otsuka, R. Hirano, Bone cell activity responsive drug release from biodegradable apatite/collagen nano-composite cements—in vitro dissolution medium responsive vitamin K2 release, Colloid Surf. B 85 (2011) 338–342.
[152] W. Wang, Instability, stabilization, and formulation of liquid protein pharmaceuticals, Int. J. Pharm. 185 (1999) 129–188.
[153] D.H.R. Kempen, L.B. Creemers, J. Alblas, L. Lu, A.J. Verbout, M.J. Yaszemski, et al., Growth factor interactions in bone regeneration, Tissue Eng. Part B Rev. 16 (2010) 551–566.
[154] H.P. Stallmann, C. Faber, E.T. Slotema, D.M. Lyaruu, A.L.J.J. Bronckers, A.V.N. Amerongen, et al., Continuous-release or burst-release of the antimicrobial peptide human lactoferrin 1-11 (hLF1-11) from calcium phosphate bone substitutes, J. Antimicrob. Chemother. 52 (2003) 853–855.
[155] H.P. Stallmann, R. Roo, C. Faber, A.V. Amerongen, P.I.J.M. Wuisman, In vivo release of the antimicrobial peptide hLF1-11 from calcium phosphate cement, J. Orthop. Res. 26 (2008) 531–538.
[156] D. Le Nihouannen, S.V. Komarova, U. Gbureck, J.E. Barralet, Bioactivity of bone resorptive factor loaded on osteoconductive matrices: stability post-dehydration, Eur. J. Pharm. Biopharm. 70 (2008) 813–818.
[157] D. Le Nihouannen, S.A. Hacking, U. Gbureck, S.V. Komarova, J.E. Barralet, The use of RANKL-coated brushite cement to stimulate bone remodelling, Biomaterials 29 (2008) 3253–3259.
[158] X. Yu, M. Wei, Preparation and evaluation of parathyroid hormone incorporated CaP coating via a biomimetic method, J. Biomed. Mater. Res. B Appl. Biomater. 97 (2011) 345–354.
[159] A. Almirall, G. Larrecq, J.A. Delgado, S. Martinez, J.A. Planell, M.P. Ginebra, Fabrication of low temperature macroporous hydroxyapatite scaffolds by foaming and hydrolysis of an alpha-TCP paste, Biomaterials 25 (2004) 3671–3680.
[160] E.B. Montufar, T. Traykova, C. Gil, I. Harr, A. Almirall, A. Aguirre, E. Engel, J.A. Planell, M.P. Ginebra, Foamed surfactant solution as a template for self-setting injectable hydroxyapatite scaffolds for bone regeneration, Acta Biomater. 6 (2010) 876–885.

[161] S. del Valle, N. Mino, F. Munoz, A. Gonzalez, J.A. Planell, M.P. Ginebra, In vivo evaluation of an injectable Macroporous Calcium Phosphate Cement, J. Mater. Sci. Mater. Med. (2007) 353–361.
[162] E. Blom, E. Burger, J. Klein-Nulend, M. van Waas, J. Wolke, F. Driessens, Physico-chemical properties and release characteristics of growth factor-modified calcium phosphate bone cement, Materialwiss. Werkstofftech. 32 (2001) 962–969.
[163] E.J. Blom, J. Klein-Nulend, J.G.C. Wolke, M.A.J. van Waas, F. Driessens, E.H. Burger, Transforming growth factor-beta1 incorporation in a calcium phosphate bone cement: material properties and release characteristics, J. Biomed. Mater. Res. 59 (2002) 265–272.
[164] R.O. Huse, P. Quinten Ruhe, J.G.C. Wolke, J.A. Jansen, The use of porous calcium phosphate scaffolds with transforming growth factor beta 1 as an onlay bone graft substitute, Clin. Oral Implants Res. 15 (2004) 741–749.
[165] M. Li, X. Liu, X. Liu, B. Ge, Calcium phosphate cement with BMP-2-loaded gelatin microspheres enhances bone healing in osteoporosis: a pilot study, Clin. Orthop. Relat. Res. 468 (2010) 1978–1985.
[166] M. Li, X. Liu, X. Liu, B. Ge, Calcium phosphate cement with BMP-2-loaded gelatin microspheres enhances bone healing in osteoporosis: a pilot study, Clin. Orthop. Relat. Res. 468 (2010) 1978–1985.
[167] P. Ruhé, H. Kroese-Deutman, J. Wolke, Bone inductive properties of rhBMP-2 loaded porous calcium phosphate cement implants in cranial defects in rabbits, Biomaterials 25 (2004) 2123–2132.
[168] P. Ruhé, E.L. Hedberg, N.T. Padron, P.H.M. Spauwen, J.A. Jansen, A.G. Mikos, rhBMP-2 release from injectable poly(DL-lactic-co-glycolic acid)/calcium-phosphate cement composites, J. Bone Joint Surg. 85-A (2003) 75–81 Suppl.
[169] P. Ruhé, O. Boerman, F. Russel, Controlled release of rhBMP-2 loaded poly (dl-lactic-co-glycolic acid)/calcium phosphate cement composites in vivo, J. Control. Release 106 (2005) 161–171.
[170] P.Q. Ruhé, O.C. Boerman, F.G.M. Russel, A.G. Mikos, P.H.M. Spauwen, J.A. Jansen, In vivo release of rhBMP-2 loaded porous calcium phosphate cement pretreated with albumin, J. Mater. Sci. Mater. Med. 17 (2006) 919–927.
[171] E. Bodde, O. Boerman, The kinetic and biological activity of different loaded rhBMP2 calcium phosphate cement implants in rats, J. Biomed. Mater. Res. 87A (2008) 780–791.
[172] H. Seeherman, J.M. Wozney, Delivery of bone morphogenetic proteins for orthopedic tissue regeneration, Cytokine Growth Factor Rev. 16 (2005) 329–345.
[173] E.J. Blom, J. Klein-Nulend, L. Yin, M.A. van Waas, E.H. Burger, Transforming growth factor-beta1 incorporated in calcium phosphate cement stimulates osteotransductivity in rat calvarial bone defects, Clin. Oral Implants Res. 12 (2001) 609–616.
[174] E.J. Blom, J. Klein-Nulend, C.P. Klein, K. Kurashina, M.A. van Waas, E.H. Burger, Transforming growth factor-beta1 incorporated during setting in calcium phosphate cement stimulates bone cell differentiation in vitro, J. Biomed. Mater. Res. 50 (2000) 67–74.
[175] R.B. Edwards, H.J. Seeherman, J.J. Bogdanske, J. Devitt, R. Vanderby, M.D. Markel, Percutaneous injection of recombinant human bone morphogenetic protein-2 in a calcium phosphate paste accelerates healing of a canine tibial osteotomy, J. Bone Joint Surg. 86-A (2004) 1425–1438.
[176] H.J. Seeherman, M. Bouxsein, H. Kim, R. Li, X.J. Li, M. Aiolova, et al., Recombinant human bone morphogenetic protein-2 delivered in an injectable calcium phosphate paste accelerates osteotomy-site healing in a nonhuman primate model, J. Bone Joint Surg. 86-A (2004) 1961–1972.
[177] H. Kaneko, T. Arakawa, H. Mano, T. Kaneda, A. Ogasawara, M. Nakagawa, et al., Direct stimulation of osteoclastic bone resorption by bone morphogenetic protein (BMP)-2 and expression of BMP receptors in mature osteoclasts, Bone 27 (2000) 479–486.
[178] W. Pan, Y. Wei, L. Zhou, D. Li, Comparative in vivo study of injectable biomaterials combined with BMP for enhancing tendon graft osteointegration for anterior cruciate ligament reconstruction, J. Orthop. Res. 29 (2011) 1015–1021.
[179] R.G. Sorensen, U.M.E. Wikesjö, A. Kinoshita, J.M. Wozney, Periodontal repair in dogs: evaluation of a bioresorbable calcium phosphate cement (CeredexTM) as a carrier for rhBMP-2, J. Clin. Periodontol. 31 (2004) 796–804.
[180] K. Ohura, C. Hamanishi, S. Tanaka, N. Matsuda, Healing of segmental bone defects in rats induced by a beta-TCP-MCPM cement combined with rhBMP-2, J. Biomed. Mater. Res. 44 (1999) 168–175.
[181] U. Maus, S. Andereya, J.A.K. Ohnsorge, S. Gravius, C.H. Siebert, C. Niedhart, A bFGF/TCP-composite inhibits bone formation in a sheep model, J. Biomed. Mater. Res. B Appl. Biomater. 85 (2008) 87–92.
[182] C. Niedhart, U. Maus, O. Miltner, H.G. Gräber, F.U. Niethard, C.H. Siebert, The effect of basic fibroblast growth factor on bone regeneration when released from a novel in situ setting tricalcium phosphate cement, J. Biomed. Mater. Res. A 69 (2004) 680–685.
[183] M.P. Ginebra, M. Espanol, E.B. Montufar, R.A. Perez, G. Mestres, New processing approaches in calcium phosphate cements and their applications in regenerative medicine. Acta Biomater. 6 (2010) 2863–2873.
[184] R. Del Real, E. Ooms, J. Wolke, M. Vallet-Regi, J. Jansen, In vivo bone response to porous calcium phosphate cement, J. Biomed. Mater. Res. A 65 (2003) 30–36.
[185] H.C. Kroese-Deutman, P.Q. Ruhé, P.H.M. Spauwen, J.A. Jansen, Bone inductive properties of rhBMP-2 loaded porous calcium phosphate cement implants inserted at an ectopic site in rabbits, Biomaterials 26 (2005) 1131–1138.
[186] Z. Fei, Y. Hu, D. Wu, H. Wu, R. Lu, J. Bai, et al., Preparation and property of a novel bone graft composite consisting of rhBMP-2 loaded PLGA microspheres and calcium phosphate cement, J. Mater. Sci. Mater. Med. 19 (2008) 1109–1116.
[187] W. Habraken, O. Boerman, J. Wolke, A. Mikos, J. Jansen, In vitro growth factor release from injectable calcium phosphate cements containing gelatin microspheres, J. Biomed. Mater. Res. A 91 (2009) 614–622.
[188] D.P. Link, J. van den Dolder, J.J. van den Beucken, J.G. Wolke, A.G. Mikos, J.A. Jansen, Bone response and mechanical strength of rabbit femoral defects filled with injectable CaP cements containing TGF-[beta] 1 loaded gelatin microparticles, Biomaterials 29 (2008) 675–682.
[189] Y. Gu, L. Chen, H.-L. Yang, Z.-P. Luo, T.-S. Tang, Evaluation of an injectable silk fibroin enhanced calcium phosphate cement loaded with human recombinant bone morphogenetic protein-2 in ovine lumbar interbody fusion, J. Biomed. Mater. Res. A 97 (2011) 177–185.
[190] M.D. Weir, H.H.K. Xu, Human bone marrow stem cell-encapsulating calcium phosphate scaffolds for bone repair, Acta Biomater. 6 (2010) 4118–4126.
[191] A. Lode, A. Reinstorf, A. Bernhardt, C. Wolf-Brandstetter, U. König, M. Gelinsky, Heparin modification of calcium phosphate bone cements for VEGF functionalization, J. Biomed. Mater. Res. A 86 (2008) 749–759.
[192] A. Lode, C. Wolf-Brandstetter, A. Reinstorf, A. Bernhardt, U. König, W. Pompe, et al., Calcium phosphate bone cements, functionalized with VEGF: release kinetics and biological activity, J. Biomed. Mater. Res. A 81 (2007) 474–483.
[193] A. Plachokova, J. Van Den Dolder, J. Jansen, The bone-regenerative properties of Emdogain adsorbed onto poly (d, l-lactic-coglycolic acid)/calcium phosphate composites in an ectopic and an orthotopic rat model, J. Periodontal Res. 43 (2008) 55–63.
[194] P. Kasten, J. Vogel, R. Luginbühl, P. Niemeyer, S. Weiss, S. Schneider, et al., Influence of platelet-rich plasma on osteogenic differentiation of mesenchymal stem cells and ectopic bone formation in calcium phosphate ceramics, Cells Tissues Organs 183 (2006) 68–79.
[195] P. Kasten, J. Vogel, I. Beyen, S. Weiss, P. Niemeyer, A. Leo, et al., Effect of platelet-rich plasma on the in vitro proliferation and osteogenic differentiation of human mesenchymal stem cells on distinct calcium phosphate scaffolds: the specific surface area makes a difference, J. Biomater. Appl. 23 (2008) 169–188.
[196] R.Z. LeGeros, Calcium phosphate-based osteoinductive materials, Chem. Rev. 108 (2008) 4742–4753.
[197] F.B. Jensen, The dual roles of red blood cells in tissue oxygen delivery: oxygen carriers and regulators of local blood flow, J. Exp. Biol. 212 (2009) 3387.
[198] W.F. Boron, E.L. Boulpaep, Medical physiology: a cellular and molecular approach, Elsevier Saunders, St Louis, 2004.
[199] P.J. Marie, The calcium-sensing receptor in bone cells: a potential therapeutic target in osteoporosis, Bone 46 (2010) 571–576.
[200] G.R. Beck Jr., Inorganic phosphate as a signaling molecule in osteoblast differentiation, J. Cell. Biochem. 90 (2003) 234–243.
[201] M.M. Dvorak, A. Siddiqua, D.T. Ward, D.H. Carter, S.L. Dallas, E.F. Nemeth, et al., Physiological changes in extracellular calcium concentration directly control osteoblast function in the absence of calciotropic hormones, Proc. Natl. Acad. Sci. U. S. A. 101 (2004) 5140.
[202] Y.K. Liu, Q.Z. Lu, R. Pei, H.J. Ji, G.S. Zhou, X.L. Zhao, et al., The effect of extracellular calcium and inorganic phosphate on the growth and osteogenic differentiation of mesenchymal stem cells in vitro: implication for bone tissue engineering, Biomed. Mater. 4 (2009) 025004.
[203] J. Lu, M. Descamps, J. Dejou, G. Koubi, P. Hardouin, J. Lemaitre, et al., The biodegradation mechanism of calcium phosphate biomaterials in bone, J. Biomed. Mater. Res. 63 (2002) 408–412.
[204] S. Cazalbou, D. Eichert, X. Ranz, C. Drouet, C. Combes, M.F. Harmand, et al., Ion exchanges in apatites for biomedical application, J. Mater. Sci. Mater. Med. 16 (2005) 405–409.
[205] L. Wang, G.H. Nancollas, Calcium orthophosphates: crystallization and dissolution, Chem. Rev. 108 (2008) 4628–4669.
[206] E. Boanini, M. Gazzano, A. Bigi, Ionic substitutions in calcium phosphates synthesized at low temperature, Acta Biomater. 6 (2010) 1882–1894.
[207] W.F. Neuman, M.W. Neuman, The chemical dynamics of bone mineral, University of Chicago Press, 1958.
[208] S. Cazalbou, C. Combes, D. Eichert, C. Rey, Adaptative physico-chemistry of bio-related calcium phosphates, J. Mater. Chem. 14 (2004) 2148–2153.
[209] P. Habibovic, J.E. Barralet, Bioinorganics and biomaterials: bone repair, Acta Biomater. 7 (2011) 3013–3026.
[210] J. Gustavsson, M. Ginebra, E. Engel, J.A. Planell, Ion reactivity of calcium-deficient hydroxyapatite in standard cell culture media, Acta Biomater. 8 (2012) 386–393.
[211] E. Bonnelye, A. Chabadel, F. Saltel, P. Jurdic, Dual effect of strontium ranelate: stimulation of osteoblast differentiation and inhibition of osteoclast formation and resorption in vitro, Bone 42 (2008) 129–138.
[212] S.C. Verberckmoes, M.E. De Broe, P.C. D'Haese, Dose-dependent effects of strontium on osteoblast function and mineralization, Kidney Int. 64 (2003) 534–543.
[213] M. Grynpas, P. Marie, Effects of low doses of strontium on bone quality and quantity in rats, Bone 11 (1990) 313–319.
[214] P.J. Marie, M.T. Garba, M. Hott, L. Miravet, Effect of low doses of stable strontium on bone metabolism in rats, Miner. Electrolyte Metab. 11 (1985) 5–13.
[215] S.J. Saint-Jean, C.L. Camiré, P. Nevsten, S. Hansen, M.P. Ginebra, Study of the reactivity and in vitro bioactivity of Sr-substituted alpha-TCP cements, J. Mater. Sci. Mater. Med. 16 (2005) 993–1001.
[216] S. Panzavolta, P. Torricelli, L. Sturba, B. Bracci, R. Giardino, A. Bigi, Setting properties and in vitro bioactivity of strontium-enriched gelatin–calcium phosphate bone cements, J. Biomed. Mater. Res. A 84 (2008) 965–972.
[217] L. Leroux, J.L. Lacout, Preparation of calcium strontium hydroxyapatites by a new route involving calcium phosphate cements, J. Mater. Res. 16 (2001) 171–178.
[218] D. Guo, K. Xu, X. Zhao, Y. Han, Development of a strontium-containing hydroxyapatite bone cement, Biomaterials 26 (2005) 4073–4083.

[219] S. Pina, P.M. Torres, F. Goetz-Neunhoeffer, J. Neubauer, J.M.F. Ferreira, Newly developed Sr-substituted alpha-TCP bone cements, Acta Biomater. 6 (2010) 928–935.
[220] G. Dagang, X. Kewei, H. Yong, The influence of Sr doses on the in vitro biocompatibility and in vivo degradability of single-phase Sr-incorporated HAP cement, J. Biomed. Mater. Res. A 86 (2008) 947–958.
[221] M. Hamdan Alkhraisat, C. Moseke, L. Blanco, J.E. Barralet, E. Lopez-Carbacos, U. Gbureck, Strontium modified biocements with zero order release kinetics, Biomaterials 29 (2008) 4691–4697.
[222] E.M. Carlisle, Silicon: a possible factor in bone calcification, Science 167 (1970) 279–280.
[223] G. Mestres, C. Le Van, M.P. Ginebra, Silicon-stabilized α-tricalcium phosphate and its use in a calcium phosphate cement: characterization and cell response, Acta Biomater. 8 (2012) 1169–1179.
[224] C.L. Camiré, S.J. Saint-Jean, C. Mochales, P. Nevsten, J.-S. Wang, L. Lidgren, et al., Material characterization and in vivo behavior of silicon substituted alpha-tricalcium phosphate cement, J. Biomed. Mater. Res. B Appl. Biomater. 76 (2006) 424–431.
[225] A.M. Pietak, J.W. Reid, M.J. Stott, M. Sayer, Silicon substitution in the calcium phosphate bioceramics, Biomaterials 28 (2007) 4023–4032.
[226] M. Vallet-Regí, D. Arcos, Silicon substituted hydroxyapatites. A method to upgrade calcium phosphate based implants, J. Mater. Chem. 15 (2005) 1509–1516.
[227] N. Patel, S. Best, W. Bonfield, I. Gibson, K. Hing, E. Damien, et al., A comparative study on the in vivo behavior of hydroxyapatite and silicon substituted hydroxyapatite granules, J. Mater. Sci. Mater. Med. 13 (2002) 1199–1206.
[228] M. Bohner, Silicon-substituted calcium phosphates — a critical view, Biomaterials 30 (2009) 6403–6406.
[229] A.S. Prasad, Zinc: an overview, Nutrition 11 (1995) 93–99.
[230] M. Yamaguchi, Role of zinc in bone formation and bone resorption, J. Trace Elem. Exp. Med. 11 (1998) 119–135.
[231] B.S. Moonga, D.W. Dempster, Zinc is a potent inhibitor of osteoclastic bone resorption in vitro, J. Bone Miner. Res. 10 (1995) 453–457.
[232] S. Mann, J. Webb, R.J.P. Williams, Biomineralization: chemical and biochemical perspectives, John Wiley & Sons, 1989.
[233] M. Yamaguchi, Role of nutritional zinc in the prevention of osteoporosis, Mol. Cell. Biochem. 338 (2010) 241–254.
[234] N.M. Lowe, W.D. Fraser, M.J. Jackson, Is there a potential therapeutic value of copper and zinc for osteoporosis? Proceedings-nutrition Society of London, Cambridge Univ Press, 2002, pp. 181–185.
[235] A. Cerovic, I. Miletic, S. Sobajic, D. Blagojevic, M. Radusinovic, A. El-Sohemy, Effects of zinc on the mineralization of bone nodules from human osteoblast-like cells, Biol. Trace Elem. Res. 116 (2007) 61–71.
[236] X. Li, Y. Sogo, A. Ito, H. Mutsuzaki, N. Ochiai, T. Kobayashi, et al., The optimum zinc content in set calcium phosphate cement for promoting bone formation in vivo, Mater. Sci. Eng. C Mater. Biol. Appl. 29 (2009) 969–975.
[237] S. Pina, P.M.C. Torres, J.M.F. Ferreira, Injectability of brushite-forming Mg-substituted and Sr-substituted α-TCP bone cements, J. Mater. Sci. Mater. Med. 21 (2010) 431–438.
[238] S. Pina, S.I. Vieira, P. Rego, P.M.C. Torres, O.A.B. da Cruz e Silva, E.F. da Cruz e Silva, et al., Biological responses of brushite-forming Zn- and ZnSr- substituted beta-tricalcium phosphate bone cements, Eur. Cells Mater. 20 (2010) 162–177.
[239] Y. Sogo, A. Ito, M. Kamo, T. Sakurai, K. Onuma, N. Ichinose, et al., Hydrolysis and cytocompatibility of zinc-containing [alpha]-tricalcium phosphate powder, Mater. Sci. Eng. C 24 (2004) 709–715.
[240] G. Qi, S. Zhang, K.A. Khor, S.W. Lye, X. Zeng, W. Weng, C. Liu, S.S. Venkatraman, L.L. Ma, Osteoblastic cell response on magnesium-incorporated apatite coatings, Appl. Surf. Sci. 255 (2008) 304–307.
[241] I. Fadeev, L. Shvorneva, S. Barinov, Synthesis and structure of magnesium-substituted hydroxyapatite, Inorg. Mater. 39 (2003) 947–950.
[242] H. Zreiqat, C. Howlett, A. Zannettino, P. Evans, G. Schulze-Tanzil, C. Knabe, et al., Mechanisms of magnesium-stimulated adhesion of osteoblastic cells to commonly used orthopaedic implants, J. Biomed. Mater. Res. 62 (2002) 175–184.
[243] J. Lu, J. Wei, Y. Yan, H. Li, J. Jia, S. Wei, et al., Preparation and preliminary cytocompatibility of magnesium doped apatite cement with degradability for bone regeneration, J. Mater. Sci. 22 (2011) 607–615.
[244] D.J.F. Moojen, S.N.M. Spijkers, C.S. Schot, M.W. Nijhof, H.C. Vogely, A. Fleer, et al., Identification of orthopaedic infections using broad-range polymerase chain reaction and reverse line blot hybridization, J. Bone Joint Surg. 89 (2007) 1298–1305.
[245] W.P. Saunders, E.M. Saunders, Coronal leakage as a cause of failure in root-canal therapy: a review, Endod. Dent. Traumatol. 10 (1994) 105–108.
[246] U. Gbureck, O. Knappe, L.M. Grover, J.E. Barralet, Antimicrobial potency of alkali ion substituted calcium phosphate cements, Biomaterials 26 (2005) 6880–6886.
[247] J.L. Clement, P.S. Jarrett, Antibacterial silver, Met.-Based Drugs 1 (1994) 467–482.
[248] A. Ewald, D. Hösel, S. Patel, L.M. Grover, J.E. Barralet, U. Gbureck, Silver-doped 2007 calcium phosphate cements with antimicrobial activity, Acta Biomater. 7 (2011) 4064–4070.
[249] I. Takano, Y. Ishii, Experimental study of apatite cement containing antibiotics, J. Orthop. Sci. 2 (1997) 98–105.
[250] I.C. Tung, In vitro drug release of antibiotic-loaded porous hydroxyapatite cement, Artif. Cells Blood Substit. Immobil. Biotechnol. 23 (1995) 81–88.

## 4.2. Paper II: Multiple characterization study on porosity and pore structure of calcium phosphate cements

Calcium phosphate materials are highly micro- and nano- porous biomaterials. An in-depth characterization and understanding of their porosity is highly relevant when considering biological interactions and drug release properties, among others. This paper presents a comparative study between three different techniques used for the characterization of the porosity and pore size distribution in different size ranges, highlighting their advantages and limitations, together with the particular features of calcium phosphate cements.

# Multiple characterization study on porosity and pore structure of calcium phosphate cements

David Pastorino[1,2], Cristina Canal[1,2], Maria-Pau Ginebra[1,2 *]

[1] Biomaterials, Biomechanics and Tissue Engineering Group, Department of Materials Science and Metallurgy, Universitat Politècnica de Catalunya. BarcelonaTech (UPC), Av. Diagonal 647, 08028 Barcelona, Spain

[2] Centre for Research in Nanoengineering, Technical University of Catalonia (UPC) c/Pascual i Vila 15, 08028 Barcelona, Spain

david.pastorino@upc.edu; cristina.canal@upc.edu ; maria.pau.ginebra@upc.edu

*Corresponding author:

Maria-Pau Ginebra

Biomaterials, Biomechanics and Tissue Engineering Group

Department of Materials Science and Metallurgical Engineering

Universitat Politècnica de Catalunya. BarcelonaTech (UPC)

Av. Diagonal 647, 08028 Barcelona, Spain

Telephone: +34 934017706, Fax: +34 934016706

E-mail: maria.pau.ginebra@upc.edu

**Abstract**

Characterization of the intricate pore structure of calcium phosphate cements is a key step to successfully link the structural properties of these synthetic bone grafts with their most relevant properties, such as *in vitro* or *in vivo* behaviour, drug loading and release properties, or degradation over time. This is a challenging task due to the wide range of pore sizes in calcium phosphate cements, compared to most other ceramic biomaterials. This work provides a critical assessment of three different techniques based on different physical phenomena, namely Mercury Intrusion Porosimetry (MIP), Nitrogen sorption, and Thermoporometry (TPM) for the detailed characterization of four calcium phosphate cements with different textural properties in terms of total porosity, Pore Size Distribution (PSD), and Pore Entrance Size Distribution (PESD). MIP covers a much wider size range than TPM and Nitrogen sorption, offering more comprehensive information at the micrometer level. TPM, and especially Nitrogen sorption, are non-destructive techniques and, although they cover a limited size range, provide complementary information regarding pore structure associated with crystal shape at the nanoscale, recording both PSD and PESD in a single experiment. MIP tended to register smaller sizes, especially at low L/P ratios, due to the network effect, which has a strong influence on the outcome of this technique.

## 1. Introduction

Porosity has become a key feature in the design of biomaterials for bone regeneration. Some crucial aspects, like the rate of resorption and the extent of tissue colonization, depend not only on the intrinsic properties of the material but also on the amount, size, and shape of the pores of the biomaterial [1,2]; the relevance of porosity is even higher when the material is designed to act, in addition, as a substrate for the local and controlled delivery of drugs or cells, since its performance will depend on some physical phenomena like permeability or diffusion, which are directly linked to porosity [3]. The physical and biological behaviours of a porous material are strongly affected by the way in which the pores of various sizes are distributed within the solid, in addition to the effects of total porosity. Hence, it is important to characterize the porosity and textural properties of the material through the full-scale range. Whereas this can be relatively straightforward in the case of high-temperature sintered ceramics, the situation becomes more complex in biomimetic calcium phosphate materials, where nanometer-sized crystals are obtained, with intricate microstructures and high specific surface areas [4].

Calcium phosphate cements (CPCs) are good examples of nanostructured calcium phosphates [4,5]. These synthetic bone substitutes present attractive properties, such as similarity to the mineral phase of bone, the capacity to harden within the body, and injectability. Once hardened, the material consists of a network of nanometric and micrometric precipitated crystals, which generates a high intrinsic micro/nano porosity with a very wide pore size range, from 1 nm to 1 mm, i.e., six orders of magnitude [6,7]. This allows the design of materials inspired by the nanostructured nature of native bone [4,7], with distinct advantages in terms of bioactivity, resorbability, permeability, and

the adsorption and release of active compounds [3,4,5,8,9]. Despite this, their intrinsic complexity makes the detailed evaluation of the porosity of CPCs a challenging task; therefore, the selection of the most adequate method for its characterization is not trivial.

Pycnometry, based on the Archimedes principle, can be used to determine the total pore volume but provides only limited or no information on pore structure parameters, like pore size distribution and specific surface area.

Mercury intrusion porosimetry (MIP) has proven to be a powerful technique to characterize porous materials with pore sizes ranging in several orders of magnitude [10]. MIP is based on the intrusion of a non-wetting liquid, mercury, into a material, and the possibility of relating the pressure needed to force mercury into the specimen with the equivalent pore sizes [11]. MIP is the most widely used method for determining the pore size distribution of hardened cement pastes for civil engineering applications, and it has also been successfully applied to the characterization of CPCs [5]; however, some concerns have been raised recently [12–14] related to the ink-bottle effect [15] and the high pressures applied there, which are speculated to be potentially harmful for the material. Moreover, a drying step is required prior to the experiment, which might affect its outcome. Other drawbacks are related to the toxicity of mercury and that MIP is a destructive method, since the sample cannot be reused after part of the mercury remains irreversibly trapped in the pores.

An alternative technique is gas adsorption, which is one of the most popular methods for the study of pore structure in materials that contain micropores (< 2nm) and mesopores (between 2 and 50 nm). In the field of CPCs, however, gas adsorption has generally been limited to the characterization of the specific surface area [1,16–18]

using the Brunauer-Emmet-Teller (BET) theory [19], which involves a model for the adsorption of a monolayer of gas onto the surface of a material. However, capillary condensation measurements allow also the correlation of vapour pressure with pore dimensions, providing information on the pore size distribution in the material.

Thermoporometry (TPM), also called thermoporosimetry, is based on the decrease in freezing point of a probe liquid confined in the pores of the material tested. The method, first described by Brun and Lallemand, allows correlation of the shifts of the freezing and melting points with the pore size distribution of the material [21]. One of the main advantages of TPM is that, unlike most other techniques, it allows the characterisation of wet samples and there is no need for specialized instruments, since a differential scanning calorimeter can be used to perform the measurements. TPM has already been applied in Portland cements with success [23]. Many probe liquids may be used, such as water [23], cyclohexane [24], or acetonitrile [25]; the only requirement is that the liquid must present a solid-liquid phase transition, while the methods used to track the phase change are many [22]. In this study, water was chosen as probe liquid and the phase transition (solid-liquid) was recorded by a micro calorimeter; the advantages and drawbacks of that choice will be discussed.

The three methods described, i.e., MIP, $N_2$ adsorption, and TPM, have access only to open pores and are applicable to different ranges of pore sizes, as presented in Fig. 1, together with the IUPAC classification of pore sizes [22,26]. However, not only are the ranges of pore sizes different, the specific structural features measured by each technique vary. Thus, MIP evaluates the pore entrance size [12], the gas adsorption technique allows one to measure both the pore size and pore entrance size, using the adsorption and desorption curves, respectively [20,27], and TPM allows the

determination of the size of the cavity of the pore during the melting cycle and the pore entrance size during the freezing cycle [21,27].

The objective of this work is to perform a critical assessment of the suitability of the different techniques described, i.e., gas sorption, mercury intrusion, and TPM, for the characterization of the porosity and pore structure of apatitic CPCs obtained by hydrolysis of α-tricalcium phosphate (α-TCP) [28–30]. Four cements with a range of different porosities were compared to evaluate the information that can be obtained from them and the advantages and limitations of each technique.

## 2. Materials and Methods

### *2.1. Materials*

α-TCP was used for the preparation of the cement's solid phase and was obtained by heating in a furnace (Hobersal CNR-58) in air at a 2:1 molar ratio a mixture of calcium hydrogen phosphate ($CaHPO_4$, Sigma Aldrich) and calcium carbonate ($CaCO_3$, Sigma Aldrich) at 1400 ºC for 15 h, followed by quenching in air. Four cements with different microstructures and porosities were prepared by varying the initial particle size and liquid-to-powder ratio (L/P), as described in a previous paper [5] (Fig. 2). To this end, the α-TCP obtained was milled in a planetary mill (Pulverisette 6, Fritsch GmbH) using an agate bowl (10 cm diameter) and balls, following two different protocols to prepare two different granulometries: i) a coarse (C) powder, obtained by milling with 10 balls (d = 30 mm) for 15 min at 450 rpm; and ii) a fine (F) powder, obtained by milling in three steps: first with 10 balls (d = 30 mm) for 60 min at 450 rpm, followed by 40 min at 500 rpm, and a last step with 100 balls (d = 10 mm) for 60 min at 500 rpm. 2 wt % of precipitated hydroxyapatite (Merck, US) was added as a seed to the powder.

Cements were prepared with two L/P ratios, 0.35 and 0.65 mL/g, using both F and C α-TCP powders. The powder phase was mixed with water in a mortar for about 1 min and then transferred into 6 mm diameter x 12 mm height cylindrical Teflon moulds. The samples were allowed to set at 100% relative humidity for 7 days at 37 ºC. CPCs obtained were coded as C35, C65, F35, and F65, where C or F stands for coarse or fine powder, respectively, and 35 or 65 corresponds to the L/P.

*2.2. Phase composition and microstructure characterization*

The hardened CPC samples were dried at 60 ºC for 24 h and the phase composition was assessed by X-ray diffraction (XRD) using a PAN-Alytical X'Pert powder X-Ray diffractometer. Scanning was performed in the Bragg-Brentano geometry using CuKα radiation with the following conditions: 2θ scan between 20 and 70 degrees, with a scan step of 0.016 degrees, and a counting time of 50 s per step at 45 kV and 40 mA. To observe the inner microstructure of the material, the specimens were fractured and the fracture surfaces were observed using a Field Emission Scanning Electron Microscope (SEM, JEOL JSM-7001F). Prior to observation, the samples were AuV-sputter coated (Emitech K950X, US).

2.3. Sequence of analysis

The techniques selected have been described as highly reproducible [23,31-34] and precise [35]. Therefore, the same 4 cylinders of each composition were tested in the different techniques according to the following sequence:

CPC preparation & setting → TPM → drying → $N_2$ sorption → MIP

*2.4. Total porosity*

The value of the total porosity ($P_{TOT}$) was calculated following Eq. 1:

$$P_{TOT}(\%) = \left(1 - \frac{\rho_{app}\,(g/cm^3)}{\rho_{skel}\,(g/cm^3)}\right).100 \qquad \text{Equation 1}$$

The apparent density $\rho_{app}$ was determined by MIP (Autopore IV 9500 porosimeter, Micromeritics, USA) using the envelope volume measured at 0.54 psia, and the skeletal density of the samples ($\rho_{skel}$) was determined by Helium pycnometry (AccuPyc 1330, Micromeritics, USA) [36].

*2.5. Nitrogen Sorption*

The gas sorption experiments were performed in an ASAP 2020 (Micromeritics, USA), using $N_2$ as the adsorbate. Four cylinders of each composition were degassed at 10 mm Hg at 90ºC for 1 h, followed by 2 h at 100 ºC. The adsorption and desorption isotherms were recorded. The specific surface area (SSA) for each composition was reported using the 8 points Brunauer–Emmett–Teller (BET) theory. The Barrett-Joyner-Halenda (BJH) theory was applied for the treatment of the data to determine the pore size distribution (PSD), using the adsorption branch and the pore entrance size distribution (PESD) from the desorption branch of the curve, based on the Kelvin equation (Eq. 2).

$$\ln(P_v/P_{sat}) = \quad 2.H.\gamma.V_l/R.T \qquad \text{Equation 2,}$$

where $P_v$ is the equilibrium vapor pressure, $P_{sat}$ the saturation vapor pressure, H the mean curvature of meniscus, $\gamma$ the liquid/vapor surface tension, $V_l$ the liquid molar volume, R the ideal gas constant, and T the temperature. Different models can be applied to convert the data in pore size distribution, one of the most common being the BJH method [16], which makes use of the combined effect of capillary condensation in the inner pore volume and physical adsorption on the pore walls, and assumes that pores are cylindrical. It provides the pore size distribution at the nanometer range [20].

The total porosity ($P_{N2}$) was calculated using the total volume of pores per gram, $V_p$, and the skeletal density of the materials ($\rho_{skel}$) obtained by He pycnometry, following Eq. 3:

$$P_{N2}(\%) = \frac{V_p(cm^3/g)}{V_p(cm^3/g) + 1/\rho_{skel}(g/cm^3)} \cdot 100 \qquad \text{Equation 3}$$

*2.6. Mercury Intrusion Porosimetry (MIP)*

MIP experiments were performed, in the same specimens previously analysed by $N_2$ sorption, using an Autopore IV 9500 porosimeter (Micromeritics, USA), with tri-distilled mercury. Four cylinders were used for each measurement. The intrusion and extrusion curves were recorded, and the PESD was obtained from the intrusion curve. The porosity ($P_{MIP}$) was calculated as the integral of the curve obtained. The pressure needed to force mercury into the specimen can be converted to equivalent pore sizes, using the equation derived by Washburn (Eq. 4):

$$P = -2.\gamma\cos\theta/r \qquad \text{Equation 4,}$$

where P is the pressure causing the intrusion, r is the radius of the cylindrical pore being intruded, $\gamma$ is the surface tension of mercury, and $\theta$ is the contact angle between the mercury and the pore wall.

*2.7. Thermoporometry (TPM)*

TPM was performed using a differential scanning calorimeter microDSC III (DSC, Setaram, France). CPC samples were saturated with distilled water by immersing them at 40 mbar for 24 h. Two wet cylindrical samples (6 mm diameter, 4 mm height) were placed in the chamber, allowing a thin layer of water around the samples. The thermal cycle applied was:

- Tempering to -20 ºC and isotherm for 15 min;
- Heating (melting cycle) until -0.01 ºC, at a rate of 0.2 ºC/min;
- Freezing until -20 ºC, at a rate of 0.2 ºC/min (cooling cycle).

The initial temper to -20 ºC allowed all the water in the DSC capsule to freeze. The heating step up to -0.01 ºC was slow to reduce any thermal lag and led to the melting of all ice confined in the pores, but not the bulk ice (the ice between the capsule and the sample). The bulk ice provided nucleation sites for the water confined in the samples to convert into ice during the following cooling step to prevent metastability of water [23]. The total porosity ($P_{TPM}$) was determined by the total amount of water absorbed by direct weighing of the samples. The PSD and the PESD were evaluated using the heating and cooling cycles, respectively, based on the Gibbs-Thompson equation that relates the depression of the freezing or melting temperature with curvature of the liquid-solid interface (Eq. 5):

$$\Delta T = T - T_0 = -\frac{\gamma_{ls} \cdot T_0}{\rho \cdot \Delta H} \frac{dA}{dV} \qquad \text{Equation 5,}$$

where $\Delta T$ is the melting point depression, $T_0$ is the bulk melting temperature, $\gamma_{ls}$ is the surface tension of the liquid-solid interface, $\rho$ is the density, $\Delta H$ is the specific enthalpy of melting, and $dA/dV$ is the curvature of the solid-liquid interface, which is 1/r for a cylinder and 2/r for a sphere, where r is the radius of the curvature [22].

*2.8. Pore Size Distribution (PSD) and Pore Entrance Size Distribution (PESD) Representation*

The size distribution curves were all represented using the logarithm of the differential volume of pores as a function of the pore (entrance) size diameter using a logarithmic scale to facilitate visual interpretation of the curves [37]. By using this distribution, a

square of given area placed at a random position under the curve represents a constant volume [38].

## 3. Results

### *3.1. Phase composition and microstructure*

According to the XRD studies, the hardened cement specimens, after 7 days of reaction, consisted of a single-phase calcium-deficient hydroxyapatite (data not shown). No residual α-TCP was found, indicating that the hydrolysis reaction was completed. The morphologies of the fracture surfaces of the four different compositions studied are shown in Fig. 3.

In the case of cements prepared with a low L/P (C35 and F35), a highly packed network of entangled crystals was observed. At high L/P (C65 and F65), aggregates of entangled crystals were present, generating a more open structure. The fracture took place between the aggregates, revealing an irregular morphology. As expected, cements prepared from coarse particles presented mainly plate-like crystals, while fine initial particles mostly led to the formation of needle-like crystals.

The specific surface area for each composition, as measured by $N_2$ adsorption using the BET technique, is reported in Table 1. A major influence of the initial particle size was observed, the SSA increasing with decreasing initial particle size, from 18.13 to 31.46 $m^2/g$ for L/P=0.35 mL/g and from 22.60 to 39.69 $m^2/g$ for L/P= 0.65 mL/g. Moreover, the specific surface area was higher when a higher L/P ratio was used, regardless of the initial particle size used.

### *3.2. Total porosity*

The skeletal density of the specimens ($\rho_{skel}$), determined by He pycnometry, was 2.74 ± 0.02 g/cm$^3$, which was used afterwards in the calculations of total porosity. The total porosity ($P_{TOT}$), as well as the porosities measured by MIP ($P_{MIP}$), nitrogen sorption ($P_{N2}$), and TPM ($P_{TPM}$), are presented in Fig. 4. $P_{TOT}$ was larger than the porosities determined by the other techniques in all series, followed as a general rule by $P_{MIP}$ and $P_{TPM}$; the porosity determined by $N_2$ sorption tended to provide the smallest value. In general, porosity was logically mainly influenced by the L/P used, while the powder particle size had only a minor effect.

*3.3. MIP*

The Hg intrusion and extrusion curves for the cumulative volume as a function of the pore entrance diameter obtained by MIP are shown in Fig. 5. The intruded volume was significantly higher for high L/P ratios. Moreover, the mismatch between the intrusion and extrusion curves highlights the presence of a particular type of porosity, consisting of large cavities connected by small openings. Hysteresis was higher when using a low L/P ratio, regardless of the initial particle size used.

Two different distributions were found for the pore entrance diameter, regardless of the initial particle size used. At low L/P (0.35 mL/g), a unimodal distribution, centred at 8 and 11 nm for C35 and F35, respectively, was recorded. At high L/P (0.65 mL/g), the PESD was bimodal. For both C65 and F65, the first and second peaks were observed at 30 nm and 700 nm, respectively.

*3.4. Nitrogen Sorption*

The isotherms of $N_2$ adsorption and desorption for each sample are reported in Fig. 6. All isotherms were identified to be type IIb and displayed a H3 hysteresis loop. According to the literature, type IIb isotherms are typical of adsorbents having

mesopores and macropores [20]. The amount of $N_2$ adsorbed at maximum pressure was higher in the samples prepared with a higher L/P ratio, while the use of a coarse initial particle size led to larger hysteresis loops, irrespective of the L/P used.

The PSD and PESD are also shown in Fig. 6. The curves of PESD, obtained from the desorption isotherm, were corrected by accounting for the tensile strength effect. This correction is associated with the forced closure of the hysteresis loop that is produced around $p/p_0 = 0.45$. The direct application of the BJH model to this segment of the curve would lead to misinterpretation of the PESD, erroneously attributing it to a narrow distribution of pores centred around 4 nm, which is actually an artefact [39]. In the case of the material prepared with coarse initial powder, C65 presented a higher volume of slightly bigger pores than C35, with pore diameters centred at 100 and 80 nm, respectively. In contrast, the pore entrance size was bimodal for C65, with peaks at 10 and 70 nm, as compared to the unimodal PESD of C35, showing a lower volume centred at 7 nm. F35 and F65 had similar unimodal PSD and PESD at 100 and 40 nm, respectively, and F65 displayed a higher volume than F35, due to its high L/P ratio.

*3.5. Thermoporometry*

The cooling and heating cycles obtained by TPM are reported in Fig. 7. Both C35 and C65 presented a freezing exothermic peak at lower temperature than the corresponding endothermic melting peak. F35 and F65 presented a bimodal freezing exothermic profile and unimodal endothermic melting peak.

Cements prepared with coarse initial powder size, C35 and C65, presented a unimodal PSD centred at 30 nm and 35 nm, respectively. A higher volume of pores was recorded for C65 than C35. The PESD of C65 was bimodal with a peak at 80 nm and a shoulder

at 15 nm, while C35 showed two peaks at 10 nm and 80 nm. The PESD volume recorded was higher for C65.

Materials prepared with fine initial particle size, F35 and F65, had very similar PSDs both centred at 30 nm. The PESD of F65 was shifted to slightly higher values than that of F35 (35 and 20 nm, respectively). In all cases, F65 presented a slightly higher volume than F35.

## 4. Discussion

### *4.1. Microstructure and total porosity*

The SEM observations (Fig. 3) revealed that CPCs prepared with coarse initial particle size (C35 and C65) presented plate-like crystals, while the ones prepared with fine initial particle size (F35 and F65) led to the formation of needle-like crystals with higher SSA values (Table 1), in accordance with previous studies [5,6]. The materials prepared with a low L/P also showed a denser structure than those prepared with a high L/P. This trend was consistent with the higher total porosity measured for the cements with high L/Ps (Fig. 4); however, clear differences were observed between the porosity quantified using the different techniques. In fact, it must be considered that the total porosity measured by pycnometry ($P_{TOT}$) includes both open and closed pores and covers the entire range of sizes. In contrast, the other three techniques used, i.e., MIP, $N_2$ sorption, and TPM, account only for the open pores that are accessible to a liquid (either Hg or water) or a gas ($N_2$) and cover a limited range of sizes, determined by the underlying physical principles (Fig. 1). Taking this into account, a good correlation was found between the values of porosity and the size range covered by each technique, as the general trend was $P_{TOT}>P_{MIP}>P_{TPM}>P_{N2}$.

Specifically, in the MIP measurement, the pores smaller than 6 nm were not accounted for. Thus, assuming that the samples did not contain non-interconnected pores, the comparison between $P_{TOT}$ and $P_{MIP}$ (Fig. 4) allowed calculation of the porosity that can be ascribed to pores smaller than 6 nm, obtaining the values of 9.5, 2.7, 5.3, and 3.5 % for C35, C65, F35, and F65, respectively. This indicates that the samples prepared with a low L/P ratio exhibited a greater number of pores with entrance diameters smaller than 6 nm, which can be associated with a more compact structure and smaller spaces between crystals.

*4.2. Pore structure assessed by MIP*

MIP provides information on the pore size distribution over a larger size range than TPM and N2 sorption. It must be emphasized, however, that MIP measures the diameter of the pore entrance, rather than the pore diameter itself. Thus, large cavities connected by smaller necks are registered as porosity having the diameter of the necks (bottle-neck effect) [12, 40]. The high amount of Hg retained inside the structure after extrusion (Fig. 5, Top), especially for the samples with low L/P, is indicative of the intricate micro/nanostructure of the CPCs, with bottle-neck-shaped pores.

As revealed in the SEM images, the cements studied, especially those with low L/P (C35 and F35), contained pores of different sizes, but most of them could be reached by mercury only through a long percolative chain of very small pores. Thus, all the pore volume was attributed to the small-size pores that surrounded bigger cavities, and a unimodal pore size distribution was registered. In contrast, the samples prepared with a higher L/P ratio (C65 and F65) not only presented a higher porosity, but also a drastically different pore structure with a bimodal size distribution. A second peak was

detected around 700 nm, which Espanol *et al.* [5] attributed to the separation between the crystal aggregates that originated from the initial α-TCP particles of the starting powder. The situation represented in Figure 8 illustrates what is known as the network effect, which is different from the bottle-neck effect of individual pores and must be accounted for when interpreting the pore size distribution curves obtained by MIP. Thus, rather than providing an actual distribution of pore entrance sizes, MIP gives an indication of the threshold diameter that allows mercury penetration into the pore network [12,40]. This network effect can explain why a few large pores seen in the SEM micrographs (Fig. 3) were not reflected in the MIP measurements (Fig. 5), which registered only submicrometric pores. Although this could be interpreted as a limitation of the technique, the possibility to determine this "accessibility" diameter is very relevant, since it is related to permeability and diffusion processes taking place in the material, i.e., in the release of active substances from the material in drug delivery applications [9, 41] or in the absorption and entrapment of biomolecules or ions from the physiological environment [5, 42], which in turn influence cell response [43] and the *in vivo* performance of the materials [1,2,4].

The strong network effect present in MIP measurements was the reason why, in all cases, a higher volume of pores at smaller sizes was detected by MIP, as compared to other techniques. This effect was less pronounced in the CPCs prepared with high L/P (C65 and F65), where mercury was able to intrude into some pores of the sample at smaller pressures, although some shift between the MIP peak and the TPM or $N_2$ sorption peaks was still present at small pores.

*4.3. Porosity at the nanoscale: characterization by Nitrogen Sorption and TPM*

$N_2$ sorption and TPM provided information on both pore size and pore entrance size, although limited to diameters smaller than 200 -400 nm. In this size range, according to the model proposed by Espanol *et al.* [5], the inter-aggregate porosity would not be detected and only the pores between individual crystals would be recorded.

Concerning $N_2$ sorption, the hysteresis loops for all isotherms obtained (Fig. 6, Top) were of type H3, according to the IUPAC classification [20]. Since there was no indication of plateau at high $P/P_0$, the isotherms should not be classified as Type IV but as Type IIb [20,44]. This kind of isotherm is the result of interparticle capillary condensation, suggesting materials composed of aggregates of particles, giving rise to slit-shaped pores [20,45], which cope well with the morphology of our materials, as shown in Fig. 3. However, two kinds of isotherm shapes could be easily distinguished (Fig. 6, Top). The cements prepared with coarse powder (C35 and C65) exhibited a larger width of the hysteresis loop than those prepared with fine powders (F35 and F65). This narrower loop accounts for an easier desorption for the F samples, as the desorption branch followed a path closer to the adsorption branch, suggesting that less narrow constrictions were present in these samples at the nanometric scale. Moreover, the more pronounced forced closure of the hysteresis loop near $P/P_0$= 0.45 for the coarse cements (C35 and C65) was indicative of pore network effects, when interconnected larger pores had to empty through pores with smaller diameters that connected the larger pores to the outer surface of the sample. This was consistent with the different morphologies of the crystals in the coarse and fine samples (Fig. 3). Whereas the coarse cements consisted mostly of plate-like crystals, the fine cements contained rather acicular crystals, the latter giving rise to a more open structure. This was evidenced also by the fact that, even if in all cases pore entrance sizes were smaller than pore sizes (Fig. 6), closer PSD and PESD curves were found in the fine cements, compared to the

coarse ones, suggesting a smaller difference between pore size and pore neck size. It is interesting to note that, even if it covered only a fraction of the porosity, $N_2$ sorption was able to detect, with more detail, the differences arising from the morphology of this type of material at the nanoscale, which were not easily derived from the MIP results.

Similarly, TPM also registered different behaviours for the F and C cements (Fig. 7). As happened with $N_2$ sorption (Fig. 6), the shape of the PESD curves obtained by TPM for the F35 and F65 cements were similar, although in this case the former (F35) was slightly displaced to smaller pore diameters. In contrast, coarse cements exhibited different PESD curves, as happened with the $N_2$ sorption curves.

In the light of these results, after comparing the MIP and $N_2$ adsorption data, it cannot be concluded that the drying step required for $N_2$ adsorption measurements significantly modified the pore structure of the CPCs. While it is true that the drying step can affect pore structure in some cementitious materials that contain a gel-like phase, like Portland cement [44], the situation is expected to be rather different in the CPCs analysed in this work, where the drying step at 100ºC is expected to cause only the loss of the surface-bound water in the calcium-deficient hydroxyapatite obtained as the reaction product [46, 47].

*4.4. Comparison between the different techniques*

The PESD and PSD obtained with the different techniques are represented together in a single diagram for comparison (Fig. 9). When analysing the PESD curves obtained by MIP, $N_2$ sorption, and TPM in the overlapping range, a shift towards lower values was observed for MIP in the samples with low L/P ratio, C35 and F35 (refer also to Fig. 6 to better appreciate the shape of the $N_2$ sorption PESD curve at a higher magnification). These results suggest that there is no disruption of the microstructure induced by the

high-pressure values during MIP measurements and that MIP is more sensitive to the network effect than the other two techniques (Fig. 8). Indeed, during $N_2$ sorption, $N_2$ circulates through the sample in a gaseous state and condenses in the smaller pores at lower relative pressure, followed by bigger pores at higher relative pressure. Thus, in the case of having a big cavity surrounded by small pores (Fig. 8, left), this process would not suffer from a network effect as MIP does, since the gas would condense in the small pores first and in the big cavity later, registering a bimodal pore size distribution. In the case of TPM, the measurement is based on the freezing/melting of a confined liquid and performed in wet samples. Therefore, TPM is expected to be less sensitive to the network effect also in this case.

According to MIP and N2 sorption, for a given L/P ratio, the pore entrance size was smaller for coarse than for fine cements (Fig. 9, left column), which can be ascribed to the different morphologies of the pores created: plate-like or needle-like crystals. This highlights the relevance of crystal morphology, in addition to crystal size, on pore size. Thus, it is interesting to note that samples produced with fine initial particle size (F35 and F65) did have a higher SSA, which did not result in a smaller pore entrance size than their coarse counterparts, but rather they had larger pore entrance sizes due to the more open spaces between acicular crystals. This trend was not observed in the TPM measurements, which showed discordant results, particularly for the coarse cements, where larger pore entrance sizes were recorded. In contrast, when considering the PSD (Fig. 9, right column), TPM generally recorded smaller pore sizes than $N_2$ sorption, except for C35 cement. However, these results, which appear contradictory, must be interpreted with caution; different factors must be considered. On one hand, some studies have shown that the BJH theory tends to underestimate pore sizes [48]. On the other hand, it cannot be ruled out that some bias could be introduced by the interaction

between the probe liquid used in TPM, in this case water, and the material, which could lead to a shift in the freezing point and the consequent miscalculation of the pore size. Indeed, it is known that the presence of ions in solution, e.g., calcium, produces a shift in the freezing point to a lower temperature, compared to pure water, at equal confinement. The use of other probe liquids, such as cyclohexane or decane, as non-reactive solvents and the tracking of a solid-solid phase transition could allow the evaluation of a wider range of pores, with a higher sensitivity of the experiment [27,49].

*4.5. Methodological considerations*

Finally, the preparation protocols and the risk of sample damage should be considered. $N_2$ sorption and TPM techniques include a soft preparation step of the sample, consisting of degassing for 24 h or water filling at 40 mbar (0.004 MPa) for 24 h which can be assumed to provoke limited or no damage to the samples. Importantly, TPM is one of the few available methods to characterize wet samples. During measurement, the $N_2$ sorption is non-destructive, considering that the maximum pressure applied is 0.101 MPa. During TPM measurements, the stress applied by the freezing of water and its associated volume augmentation inside the voids of the CPC is not easily evaluated. On the other hand, high pressures are applied to the samples during MIP measurements to force Hg penetration into the smallest pores, ranging from 6 to 3 nm. Although it has been hypothesized that this high isostatic pressure, representing up to 414 MPa [10], might lead to sample cracking and possible penetration of mercury into previously non-interconnected volumes of the sample and/or partial destruction of the sample's microstructure [50], no damage was observed in the samples analysed in this study.

Our results allow exploration of the potential of the different techniques for the characterization of specific features of the pore structure of CPCs. The data were compared with SEM micrographs as a qualitative control, since the complexity of the

microstructure made it difficult to extract quantitative information from the two-dimensional SEM images. In this respect, it is expected that recent advances in high-resolution tomography will allow obtainment of reliable quantitative information on pore structure and pore size distribution, even at the nanoscale, in the near future. This will yield new insights in the characterization of the pore structure of this kind of material and will provide a good quantitative control against which the reported techniques will have to be validated.

## 5. Conclusions

CPCs' intrinsic porosity covers a wide range of pore sizes with intricate microstructures, and its characterization is a challenging task. The three techniques analysed have different advantages and limitations. MIP provides the unique benefit of covering a wide range of pore entrance sizes, but it is a destructive technique. Moreover, MIP results must be interpreted with caution, as MIP is strongly affected by the network effect. This, rather than being a limitation, can be understood as a very useful source of information, as it provides insights into the real accessibility of the pore network by external elements, e.g., cells, bacteria, drugs, or nutrients. $N_2$ sorption and TPM are non-destructive techniques, and although covering a limited size range, were complementary to MIP and allowed new insights into the pore size morphology related to the crystal shape at the nanoscale, recording both PSD and PESD in a single experiment. The comparison between these techniques showed, that for low L/P ratios, the pore entrance size detected by MIP was shifted to smaller values due to the network effect. PSD measured by TPM showed also a shift towards smaller values compared to $N_2$ sorption, the reason for which should be further explored.

**Acknowledgements**

Authors acknowledge the Spanish Government for financial support through Project MAT2012-38438-C03-01, co-funded by the EU through European Regional Development Funds, and Ramon y Cajal fellowship of CC. Support for the research of MPG was received through the "ICREA Academia" Award for excellence in research, funded by the Generalitat de Catalunya. The authors acknowledge technical support by T. Trifonov in SEM imaging.

**References**

[1] M.C. Von Doernberg, B. Von Rechenberg, M. Bohner, S. Grünenfelder, G.H. Van Lenthe, R. Müller, B. Gasser, R. Mathys, G. Baroud, J. Auer, In vivo behavior of calcium phosphate scaffolds with four different pore sizes, Biomaterials 27 (2006) 5186–98.

[2] J. Zhang, X. Luo, D. Barbieri, A.M.C. Barradas, J.D. de Bruijn, C.A. Van Blitterswij, H. Yuan, The size of surface microstructures as an osteogenic factor in calcium phosphate ceramics, Acta Biomater. 10 (2014) 3254–63.

[3] M.P. Ginebra, C. Canal, M. Espanol, D. Pastorino, E.B. Montufar, Calcium phosphate cements as drug delivery materials, Adv. Drug Deliv. Rev. 64 (2012) 1090–110.

[4] P. Wang, L. Zhao, J. Liu, M.D. Weir, X. Zhou, H.H.K. Xu, Bone tissue engineering via nanostructured calcium phosphate biomaterials and stem cells, Bone Research 2 (2014) 14017.

[5] M. Espanol, R.A. Perez, E.B. Montufar, C. Marichal, A. Sacco, M.P. Ginebra, Intrinsic porosity of calcium phosphate cements and its significance for drug delivery and tissue engineering applications, Acta Biomater. 5 (2009) 2752–62.

[6] M.P. Ginebra, F.C.M. Driessens, J.A. Planell, Effect of the particle size on the micro and nanostructural features of a calcium phosphate cement: A kinetic analysis, Biomaterials 25 (2004) 3453–62.

[7] M.P. Ginebra, M. Espanol, E.B. Montufar, R.A. Perez, G. Mestres, New processing approaches in calcium phosphate cements and their applications in regenerative medicine, Acta Biomater. 6 (2010) 2863–73.

[8] M.P. Ginebra, T. Traykova, J.A. Planell, Calcium phosphate cements: Competitive drug carriers for the musculoskeletal system? Biomaterials 27 (2006) 2171–7.

[9] D. Pastorino, C. Canal, M.P. Ginebra, Drug delivery from injectable calcium phosphate foams by tailoring the macroporosity-drug interaction, Acta Biomater. 12 (2015) 250–59.

[10] H. Giesche, Mercury Porosimetry: A General (Practical) Overview, Part. Part. Syst. Charact. 23 (2006) 9–19.

[11] E.W. Washburn, Note on a Method of Determining the Distribution of Pore Sizes in a Porous Material, Proc. Natl. Acad. Sci. U S A 7 (1921) 115–6.

[12] S. Diamond, Mercury porosimetry An inappropriate method for the measurement of pore size distributions in cement-based materials, Cem. Concr. Res. 30 (2000) 1517–25.

[13] S. Chatterji, A discussion of the paper "Mercury porosimetry — an inappropriate method for the measurement of pore size distributions in cement-based materials" by S . Diamond. Mercury 31 (2001) 1657–8.

[14] C. Galle, Reply to the discussion by S . Diamond of the paper "Effect of drying on cement-based materials pore structure as identified by mercury intrusion porosimetry: a comparative study between oven, vacuum- and freeze-drying", Cem. Concr. Res. 33 (2003) 171–2.

[15] F. Moro, H. Böhni, Ink-bottle effect in mercury intrusion porosimetry of cement-based materials, J. Colloid Interface Sci. 246 (2002) 135–49.

[16] J. Schnieders, U. Gbureck, E. Vorndran, M. Schossig, T. Kissel, The effect of porosity on drug release kinetics from vancomycin microsphere/calcium phosphate cement composites, J. Biomed. Mater. Res. - Part B Appl. Biomater. 99 B (2011) 391–8.

[17] M.H. Alkhraisat, C. Rueda, J. Cabrejos-Azama, J. Lucas-Aparicio, F.T. Mariño, J. Torres García-Denche, L.B Jerez, U. Gbureck, E.L. Cabarcos, Loading and release of doxycycline hyclate from strontium-substituted calcium phosphate cement, Acta Biomater. 6 (2010) 1522–8.

[18] J.J. Thomas, H.M. Jennings, A.J. Allen, The Surface Area of Hardened Cement Paste as Measured by Various Techniques, Concr. Sc. Eng. 1 (1999) 45–64.

[19] G. Fagerlund, Determination of specific surface by the BET method, Mat. 22 (1973) 233–45.

[20] J. Rouquerol, F. Rouquerol, K.S.W. Sing, P. Llewellyn, G. Maurin, Adsorption by Powders and Porous Solids: Principles, Methodology and Applications, second ed., Academic Press, Waltham 2014

[21] M. Brun, A. Lallemand, J.F. Quinson, C. Eyraud, A new method for the simultaneous determination of the size and shape of pores: the thermoporometry, Thermochim. Acta 21 (1977) 59–88.

[22] J. Riikonen, J. Salonen, V.P. Lehto, Utilising thermoporometry to obtain new insights into nanostructured materials, J. Therm. Anal. Calorim. 105 (2010) 811–21.

[23] M. Landry, Thermoporometry by differential scanning calorimetry: experimental considerations and applications, Thermochim. Acta 433 (2005) 27–50.

[24] M. Baba, Calibration of cyclohexane solid–solid phase transition thermoporosimetry and application to the study of crosslinking of elastomers upon aging, J. Non Cryst. Solids 315 (2003) 228–38.

[25] M. Wulff, Pore size determination by thermoporometry using acetonitrile, Thermochim. Acta 419 (2004) 291–4.

[26] K.H. Aligizaki, Pore structure of cement-based materials, Taylor & Francis, London, 2006.

[27] Z. Sun, G. Scherer, Cement and Concrete Research Pore size and shape in mortar by thermoporometry, Cem. Concr. Res. 40 (2010) 740–51.

[28] Y. Li, X. Zhang, K. de Groot, Hydrolysis and phase transition of alpha-tricalcium phosphate, Biomaterials 18 (1997) 737–41.

[29] M. Espanol, J. Portillo, J.M. Manero, M.P. Ginebra, Investigation of the hydroxyapatite obtained as hydrolysis product of α-tricalcium phosphate by transmission electron microscopy, Cryst. Eng. Comm. 12 (2010) 3318.

[30] M.P. Ginebra, E. Fernandez, E.A.P. De Maeyer, R.M.H. Verbeeck, M.G. Boltong, J. Ginebra, F.C. Driessens, J.A. Planell, Setting Reaction and Hardening of an Apatitic Calcium Phosphate Cement, J. Dent. Res. 76 (1997) 905–12.

[31] R.A. Siegel, Characterization of porous solids II, J Control Release 23 (1993) 183–4.

[32] Ö.Z.Cebeci, Mercury intrusion porosimetry theory and its application to air-entrained cement pastes and mortars, Iowa State University (1977) 1-85.

[33] M.F. De Lange, T.J.H. Vlugt, J. Gascon, F. Kapteijn, Adsorptive characterization of porous solids: Error analysis guides the way, Microporous Mesoporous Mater 200 (2014) 199–215.

[34] M. Sliwinska-Bartkowiak, J. Gras, R. Sikorski, R. Radhakrishnan, L. Gelb, K.E. Gubbins, Phase transitions in pores: experimental and simulation studies of melting and freezing, Langmuir 15 (1999) 6060–9.

[35] F. Rodriguez-Reinoso, B. McEnaney, J. Rouquerol, K. Unger, Characterization of Porous Solids VI, Elsevier, Amsterdam, 2002.

[36] A. Almirall, G. Larrecq, J.A. Delgado, S. Martínez, J.A. Planell, M.P. Ginebra. Fabrication of low temperature macroporous hydroxyapatite scaffolds by foaming and hydrolysis of an α-TCP paste, Biomaterials 25 (2004) 3671–80.

[37] P.PA. Webb, C. Orr, Analytical methods in fine particle technology, Micromeritic Instrument Corporation, Norcross, 1997.

[38] K. Meyer, P. Klobes, Comparison between different presentations of pore size distribution in porous materials, Fresenius J. Anal. Chem. 363 (1999) 174–8.

[39] J.C. Groen, A.A. Louk, L.A.A. Peffer, J. Perez-Ramirez, Pore size determination in modified micro- and mesoporous materials. Pitfalls and limitations in gas adsorption data analysis, Microporous Mesoporous Mater. 60 (2003) 1–17.

[40] C.A. León y Leon, New perspectives in mercury porosimetry, Adv. Colloid Interface Sci. 76-77 (1998) 341-72.

[41] C. Canal, D. Pastorino, G. Mestres, P. Schuler, M.P. Ginebra, Relevance of microstructure for the early antibiotic release of fresh and pre-set calcium phosphate cements. Acta Biomater. 9 (2013) 8403–8412.

[42] M. Espanol, I. Casals, S. Lamtahri, M.T. Valderas, M.P.Ginebra, Assessment of protein entrapment in hydroxyapatite scaffolds by size exclusion chromatography. Biointerphases 7: 37 (2012), DOI 10.1007/s13758-012-0037-7

[43] E. Engel, S. Del Valle, C. Aparicio, G. Altankov, L. Asin, J.A Planell, M.P Ginebra. Discerning the role of topography and ion exchange in cell response of bioactive tissue engineering scaffolds. Tissue Engineering A (2008), 14(8), 1341-1351.

[44] A. Korpa, R. Trettin, The influence of different drying methods on cement paste microstructures as reflected by gas adsorption: Comparing between freeze-drying (F-drying), D-drying, P-drying and oven-drying methods, Cem. Concr. Res. 36 (2006) 634-49.

[45] K.S.W. Sing, Reporting physisorption data for gas/solid systems with special reference to the determination of surface area and porosity (Recommendations 1984), Pure Appl. Chem. 57 (1985) 603–19.

[46] G.Mestres, C. Le Van, M.P. Ginebra. Silicon-stabilized α-tricalcium phosphate and its use in a calcium phosphate cement: characterization and cell response, Acta Biomater. 8 (2012) 1169-79.

[47] J.C. Elliott. Structure and chemistry of the apatites and other calcium orthophosphates. Amsterdam: Elsevier; 1994

[48] G.S. Armatas, The possible use of Γ-functions for the determination of microporosity–mesoporosity and the pore size in materials with ordered (MCM) and quasi-ordered pore structure, Microporous Mesoporous Mater. 67 (2004) 167–74.

[49] R. Mu, V. Malhotra, Effects of surface and physical confinement on the phase transitions of cyclohexane in porous silica, Phys. Rev. B 44 (1991) 4296–303.

[50] M.A.I. LaskarRakesh, B. Bhattacharjee, Some aspects of evaluation of concrete through mercury intrusion porosimetry, Cem. Concr. Res. 27 (1997) 93–105.

**Figure Captions**

Figure 1. Range of pore sizes potentially measurable by different techniques of applicability for calcium phosphate cements. Pore size nomenclature according to IUPAC.

Figure 2. Effect of the particle size and L/P ratio on the morphology of CPCs, adapted from [3].

Figure 3. Scanning Electron Micrographs of fracture cross-sections of C35, C65, F35 and F65 at low magnification (left) and high magnification (right). Top insert shows high-magnification micrograph of plate-like crystals corresponding to C CPCs. Bottom insert shows high-magnification micrograph of needle-like crystals of F CPCs.

Figure 4. Total porosity and porosity evaluated by three different techniques: MIP, TPM and $N_2$ sorption of four different CPCs.

Figure 5. MIP Intrusion/Extrusion curves (Top) and Pore Entrance Size Distributions (Bottom) for the cements prepared with coarse initial particle size (C35 and C65, left) and fine initial particle size (F35 and F65, right).

Figure 6. $N_2$ Adsorption/Desorption Isotherms (Top) and Pore Size Distributions (PSD) and Pore Entrance Size Distribution (PESD) obtained applying the BJH theory to the adsorption and desorption branch respectively (Bottom) for materials prepared with coarse initial particle size (C35 and C65, left) and fine initial particle size (F35 and F65, right).

Figure 7. TPM Solidification/Melting curves (Top) and Pore Size Distributions (PSD) and Pore Entrance Size Distribution (PESD) obtained from the melting and freezing curves respectively (Bottom) for cements prepared with coarse initial particle size (C35 and C65, left) and fine initial particle size (F35 and F65, right).

Figure 8. Schematic representation of the network effect and its influence on pore entrance size distribution recorded by mercury intrusion porosimetry (MIP). On the left, a material with large (3) and medium-sized (2) pores embedded in a network of small (1) pores, and its corresponding pore entrance size distribution MIP diagram. Mercury is able to enter the large and medium-size pores only when the pressure overcomes the threshold allowing to enter the pore network connecting the material with the exterior (Blue). On the right, a material with large (3) and small (1) pores embedded in a network of medium-sized (2) pores, and its corresponding pore entrance size distribution MIP diagram. When pressure is high enough to enter the medium-sized pores (2) it can also enter the large pores (3), (Blue). To enter the small pores (1) pressure has to increase to higher values (Red).

Figure 9. Pore entrance size distribution, PESD (left) and Pore size distribution, PSD (right) recorded using different techniques for the four different cements.

Table 1: Specific Surface Area (SSA) as evaluated by $N_2$ adsorption for C35, C65, F35 and F65.

| **Composition** | **SSA ($m^2/g$)** |
|---|---|
| C35 | 18.1 ± 0.2 |
| C65 | 22.6 ± 0.2 |
| F35 | 31.5 ± 0.3 |
| F65 | 39.7 ± 0.4 |

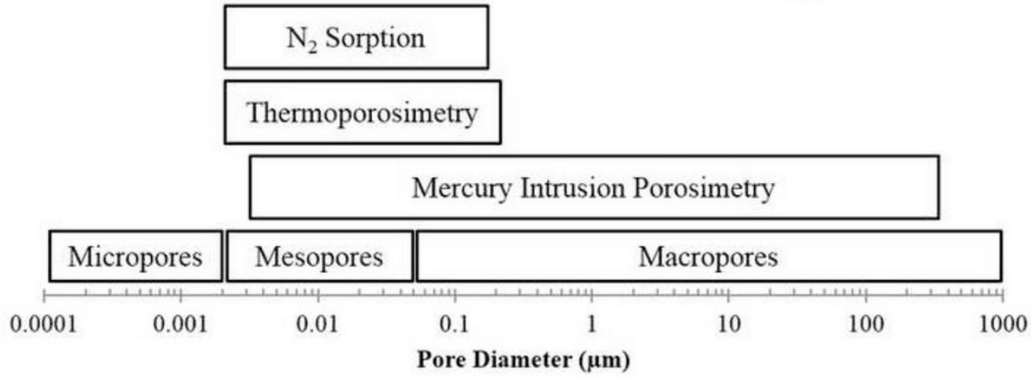




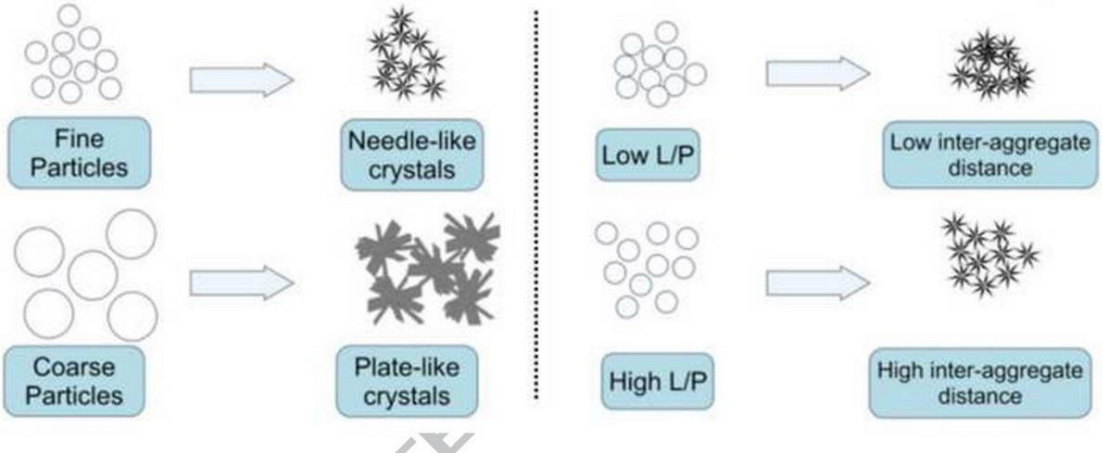

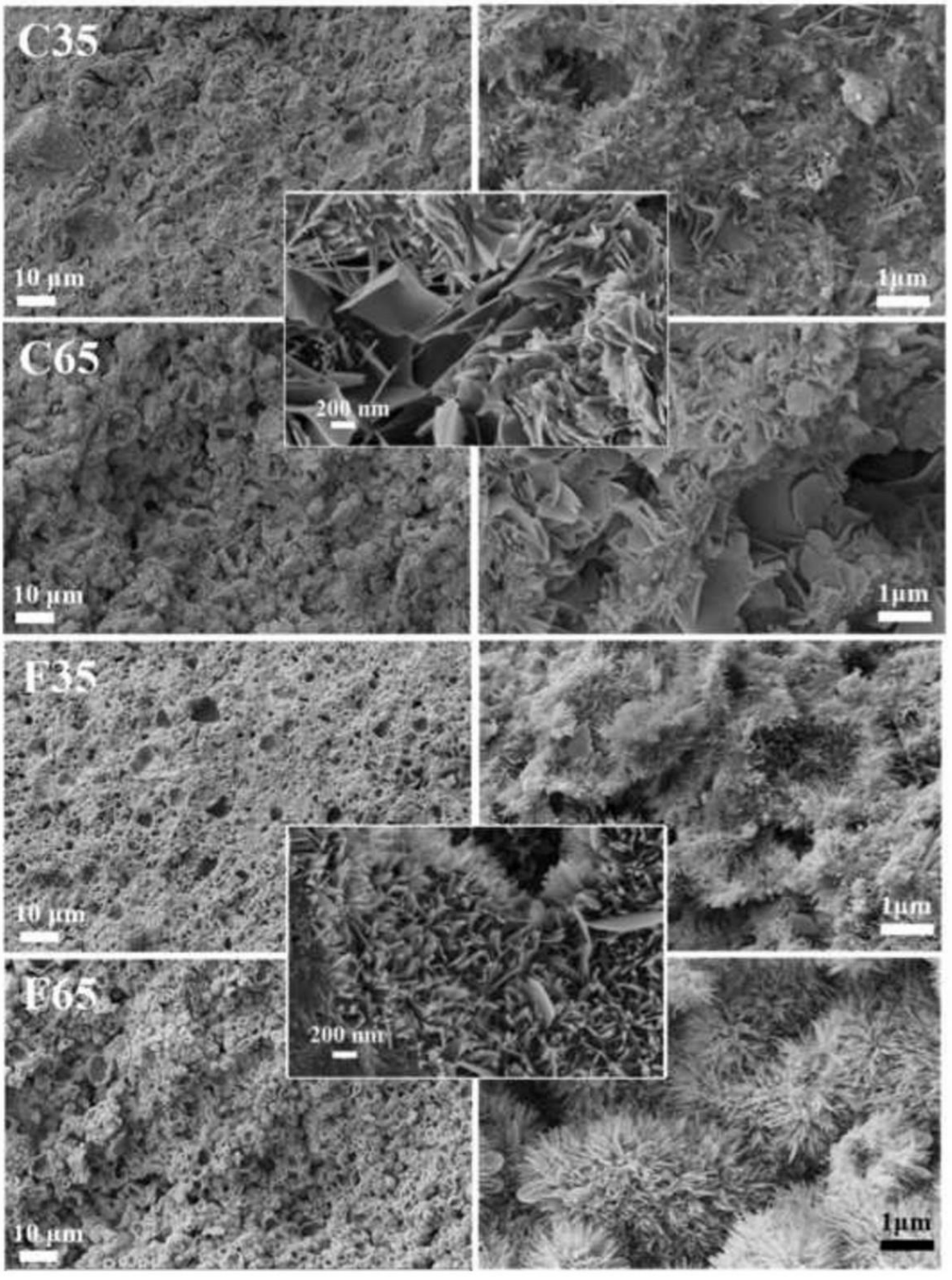

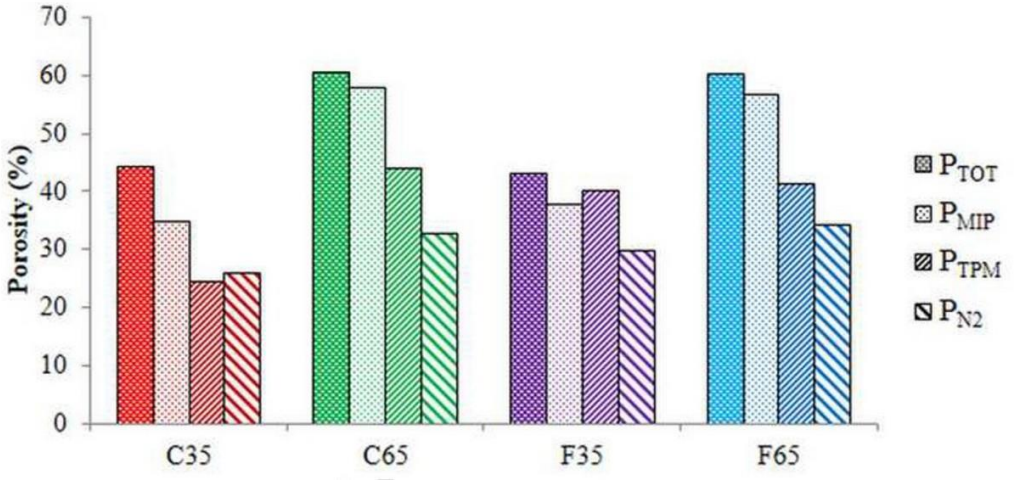


ACCEPTED MANUSCRIPT

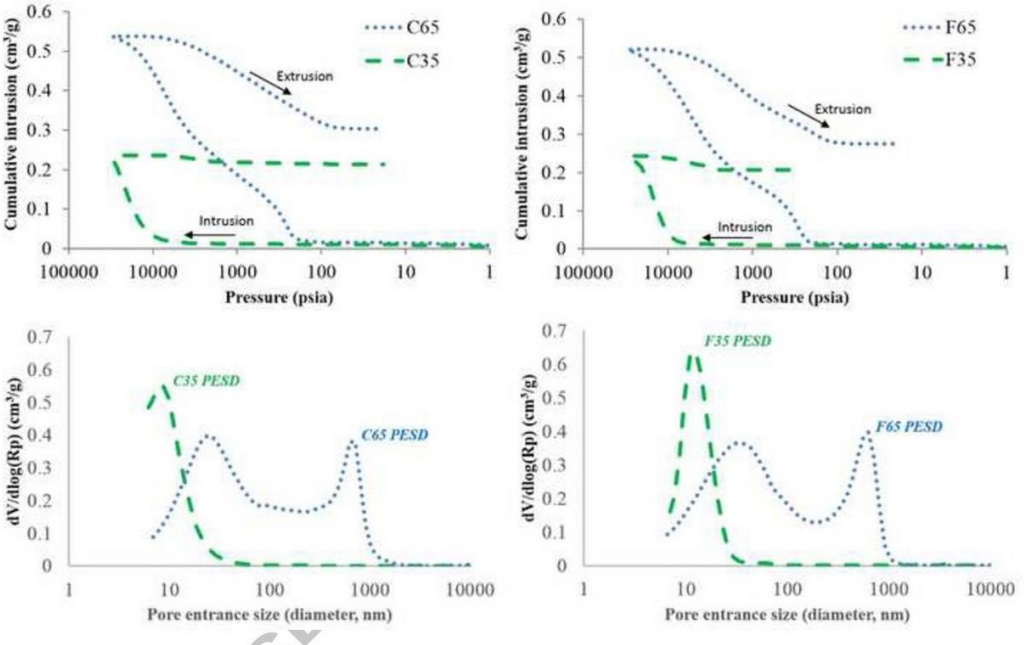

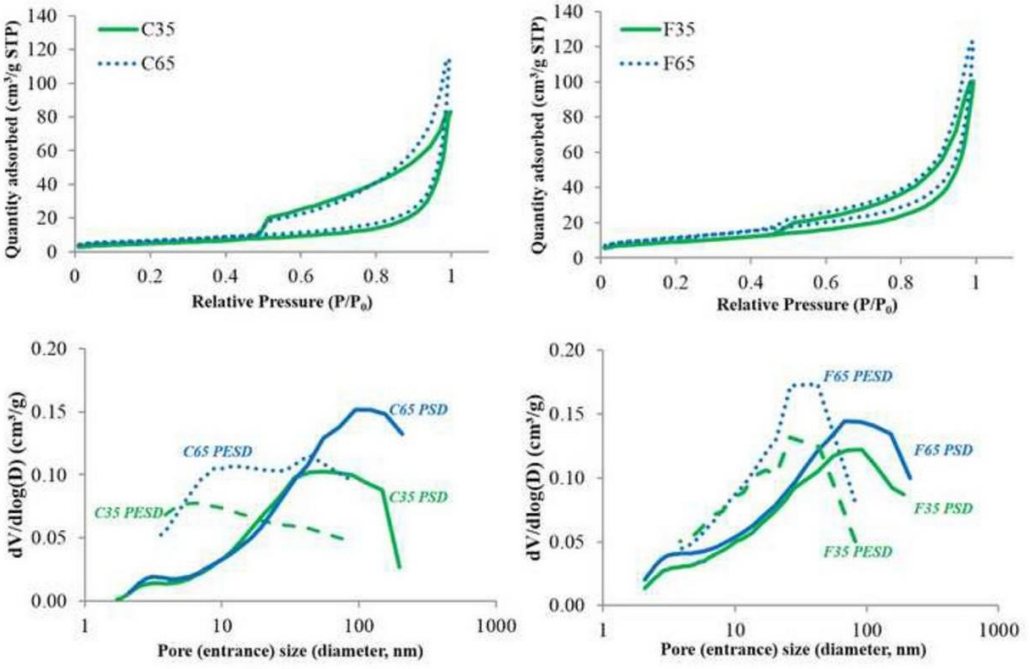




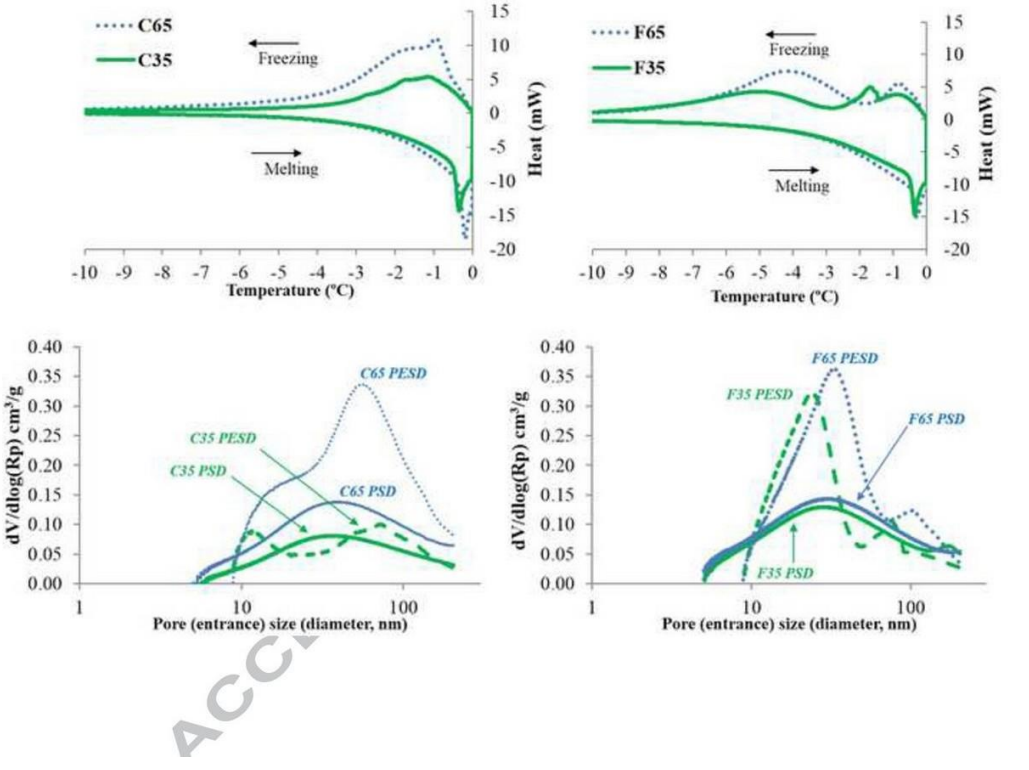

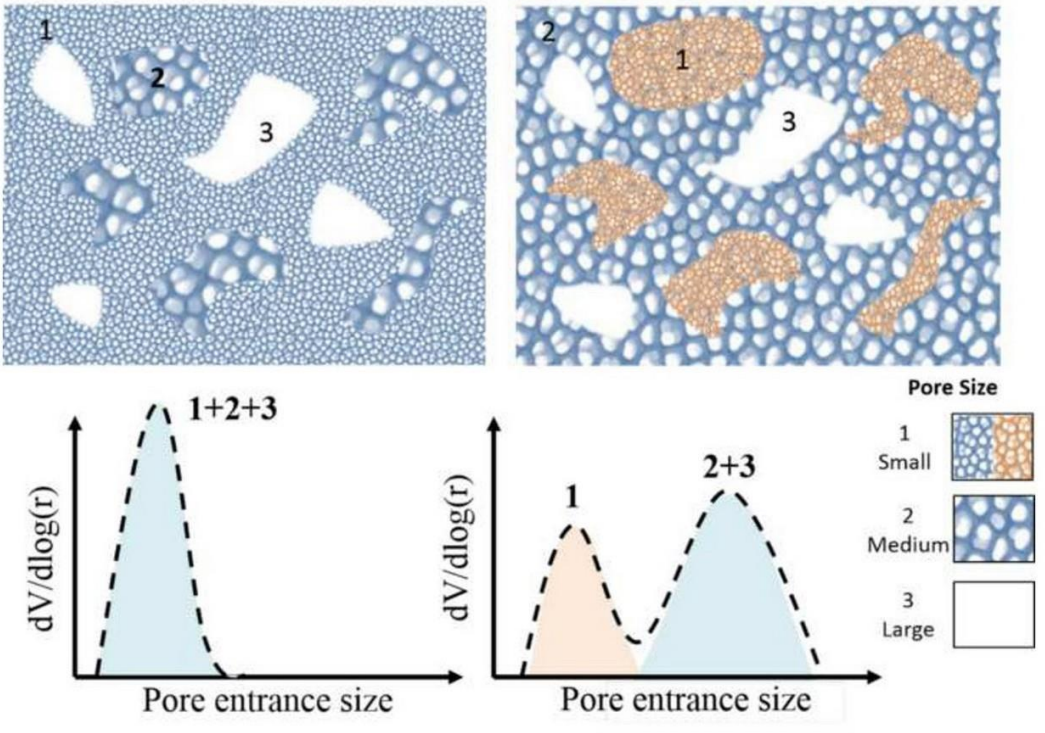

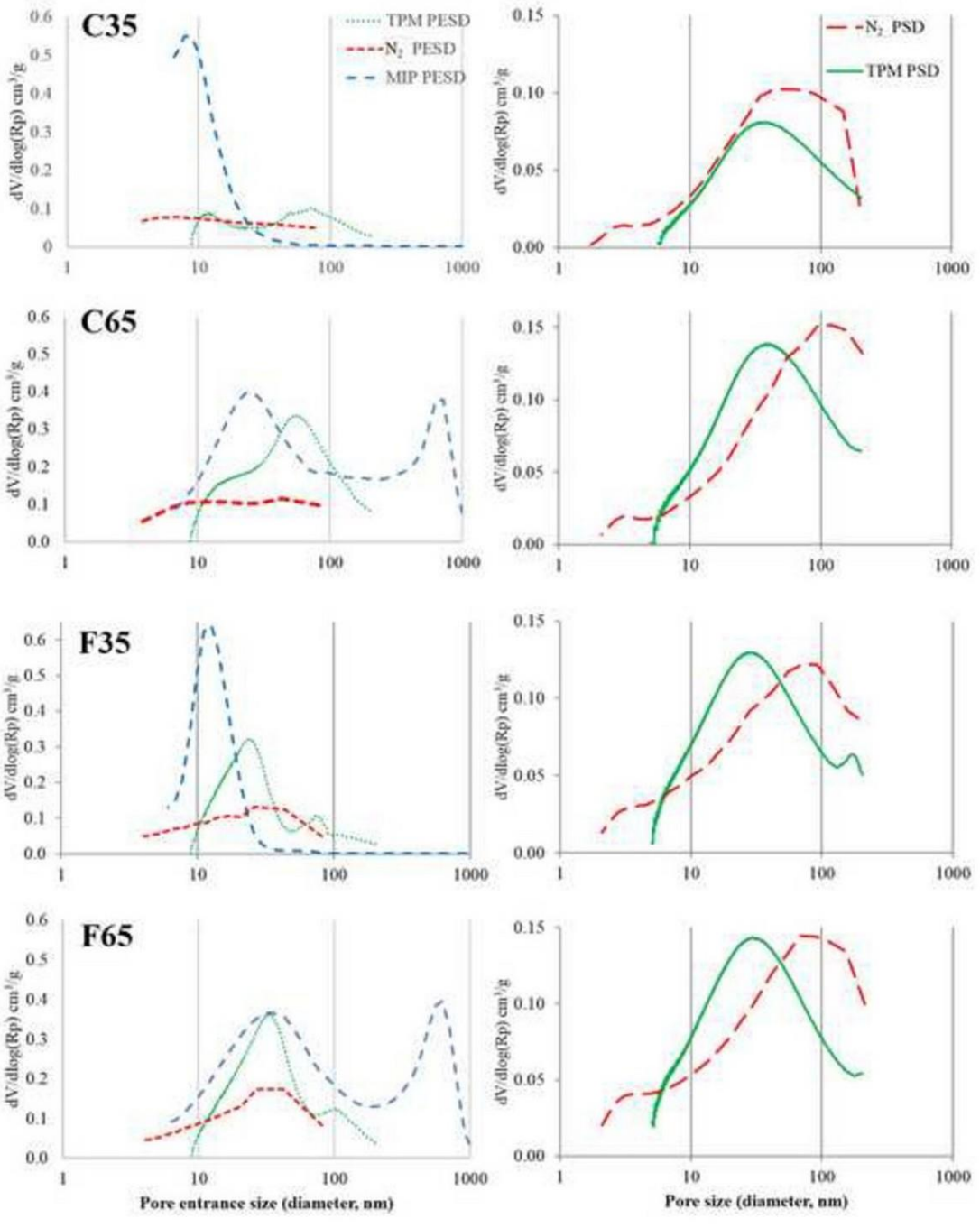

## 4.3. Paper III: Relevance of microstructure for the early antibiotic release of fresh and pre-set calcium phosphate cements

As detailed in the state-of-the-art section, Calcium Phosphate Cements (CPCs) are materials able to self-set at physiological temperature. The micro- and nano- porosity evolves during the setting, while α–TCP particles dissolve in water and precipitate into an entangled network of crystals of calcium-deficient hydroxyapatite. The following publication investigates the effect of the addition of an antibiotic on the physic-chemical and structural properties of CPCs, and the drug release profiles of freshly prepared and pre-set CPCs loaded with Doxycycline hyclate.

Acta Biomaterialia 9 (2013) 8403–8412

Contents lists available at SciVerse ScienceDirect

Acta Biomaterialia

journal homepage: www.elsevier.com/locate/actabiomat

# Relevance of microstructure for the early antibiotic release of fresh and pre-set calcium phosphate cements

Cristina Canal [a,b,c,1], David Pastorino [a,b,c,1], Gemma Mestres [a,b,c], Philipp Schuler [a], Maria-Pau Ginebra [a,b,c,*]

[a] Biomaterials, Biomechanics and Tissue Engineering Group, Department of Materials Science and Metallurgy, Technical University of Catalonia (UPC), Av. Diagonal 647, 08028 Barcelona, Spain
[b] Centre for Research in Nanoengineering, Technical University of Catalonia (UPC), C/Pascual i Vila 15, 08028 Barcelona, Spain
[c] Biomedical Research Networking Center in Bioengineering, Biomaterials, and Nanomedicine (CIBER-BBN), Maria de Luna 11, Ed. CEEI, 50118 Zaragoza, Spain

ARTICLE INFO

*Article history:*
Received 27 February 2013
Received in revised form 14 May 2013
Accepted 15 May 2013
Available online 23 May 2013

*Keywords:*
Calcium phosphate cement
Drug release
Hydroxyapatite
Antibiotic
Doxycycline

ABSTRACT

Calcium phosphate cements (CPCs) have great potential as carriers for controlled release and vectoring of drugs in the skeletal system. However, a lot of work still has to be done in order to obtain reproducible and predictable release kinetics. A particular aspect that adds complexity to these materials is that they cannot be considered as stable matrices, since their microstructure evolves during the setting reaction. The aims of the present work were to analyze the effect of the microstructural evolution of the CPC during the setting reaction on the release kinetics of the antibiotic doxycycline hyclate and to assess the effect of the antibiotic on the microstructural development of the CPC. The incorporation of the drug in the CPC modified the textural and microstructural properties of the cements by acting as a nucleating agent for the heterogeneous precipitation of hydroxyapatite crystals, but did not affect its antibacterial activity. In vitro release experiments were carried out on readily prepared cements (fresh CPCs), and compared to those of pre-set CPCs. No burst release was found in any formulation. A marked difference in release kinetics was found at the initial stages; the evolving microstructure of fresh CPCs led to a two-step release. Initially, when the carrier was merely a suspension of α-TCP particles in water, a faster release was recorded, which rapidly evolved to a zero-order release. In contrast, pre-set CPCs released doxycycline following non-Fickian diffusion. The final release percentage was related to the total porosity and entrance pore size of each biomaterial.



## 1. Introduction

Bone infections, like osteomyelitis or periodontitis, are associated with bone loss. Often, a bone grafting procedure is needed after infection elimination. The local adminstration of antibiotics in combination with a delivery matrix with osteoconductive or osteoinductive properties may allow combating the infection while simultaneously promoting bone regeneration. In this approach, it is essential not only to ensure drug access to the specific bone site, but also to maintain the drug concentration released within the therapeutic range for long periods of time. Therefore, the drug elution kinetics must be carefully controlled.

Calcium phosphate cements (CPCs) have great potential as carriers for controlled release and vectoring of drugs in the skeletal system due to their composition close to bone mineral, excellent bioactivity and possible use as injectable and degradable grafting materials [1,2]. Their cold self-hardening process mimics the processes taking place in the biomineralization phenomena. Moreover, their microstructure can be tuned by modifying different processing parameters, such as the chemical composition of reactants, particle size or presence of nucleating agents [3]. This has allowed the fabrication of pre-set solid scaffolds or granules with controlled textural properties, with porosities ranging from the nano- to the macroscale, using new CPC-based fabrication routes [4].

Despite the abundant literature generated in the last decades on CPCs as drug delivery matrices [1], there is still a need for more reproducible and predictable CPC delivery systems, and this requires a better understanding of the parameters governing the release process. In their role as drug-eluting systems, CPCs can be classified as non-swellable monolithic systems. Although some CPCs are resorbable, their degradation rate can be considered to be much lower than the rate of drug liberation, and it can be assumed that the drug release is mainly controlled by diffusion through the cement matrix, the microstructural features of the CPCs playing a

* Corresponding author at: Biomaterials, Biomechanics and Tissue Engineering Group, Department of Materials Science and Metallurgy, Technical University of Catalonia (UPC), Av. Diagonal 647, 08028 Barcelona, Spain. Tel.: +34 934017706; fax: +34 934016706.
*E-mail address:* maria.pau.ginebra@upc.edu (M.-P. Ginebra).
[1] These authors contributed equally to this work.

1742-7061/$ - see front matter © 2013 Acta Materialia Inc. Published by Elsevier Ltd. All rights reserved.
http://dx.doi.org/10.1016/j.actbio.2013.05.016

crucial role in the drug eluting process. However, there are two facts that add complexity to the CPCs as drug delivery systems, and which are often overlooked when designing drug-eluting CPCs [5–7]: (1) the setting reaction of the CPC will be influenced by the presence of the drug, not only in terms of the setting kinetics and the rheological properties, but also in terms of the microstructural development and therefore the final textural features of the material, which must therefore be carefully characterized; and (2) the microstructure of the CPC, which is the drug eluting matrix, will be evolving during the setting process, in a lapse of hours or even days, from a suspension of ceramic particles in a liquid phase to a network of entangled crystals, which will affect the drug eluting kinetics. This is critical when the material is intended to be readily injected in the host tissue [8]. In this case the drug eluting process starts immediately after mixing the two phases, and takes place simultaneously to the setting process of the cement paste. In contrast, the situation is completely different when drug-loaded pre-set CPC matrices are fabricated in the form of scaffolds, implants or microspheres [9–13]. Recently different techniques have been reported that utilize the calcium phosphate setting reaction to fabricate bioceramic implants at low temperature, compatible with the introduction of bioactive molecules of drugs, including cement casting [9], emulsion [10] and low temperature three-dimensional (3-D) printing [11–13]. This last technique is especially promising since it allows the production of drug-releasing scaffolds with a precise control of the geometry and localized deposition of biologically active molecules [12,13]. In these approaches the material is not intended to be implanted in a paste form, but as a pre-set construct, and therefore the drug release process is independent of the setting reaction of the cement.

This study aims at elucidating the relevance of these two phenomena in a doxycycline-hyclate-containing CPC. Doxycycline hyclate (Doxy), of the family of tetracyclines, is an antibiotic commonly used in the treatment of bone infections, especially in periodontitis, due to its strong activity against periodontal pathogens and its broad-spectrum antibiotic effects [14]. It was the primary objective of this work to characterize the effect of Doxy on the microstructural and textural properties at the micro- and nano-scale of an apatitic CPC, and correlate them with the release properties. Also, the influence of the setting process on the release of the antibiotic and subsequent antimicrobial activity was assessed, by comparing the in vitro drug release from either fresh or pre-set CPCs, in order to identify the effect of the microstructural evolution during the first hours of setting on the release kinetics.

## 2. Material and methods

### 2.1. Liquid and solid phase preparation

α-TCP was used as the cement's solid phase, and was obtained by heating an equimolar mixture of calcium hydrogen phosphate ($CaHPO_4$, Sigma-Aldrich) and calcium carbonate ($CaCO_3$, Sigma-Aldrich) in a furnace (Hobersal CNR-58) in air at 1400 °C for 15 h followed by quenching in air. The α-TCP obtained was milled in a planetary mill (Pulverisette 6, Fritsch GmbH) using an agate bowl and ten agate balls ($d$ = 30 mm) for 15 min at 450 rpm. 2 wt.% of precipitated hydroxyapatite (Merck, Germany) was added in the powder as a seed. The particle size distribution of the powders was analyzed by laser diffraction (LS 13 320 Beckman Coulter), after dispersing the samples in ethanol in an ultrasonic bath to minimize aggregation during the measurement. The specific surface area (SSA) of the powders was analyzed by $N_2$ adsorption following the Brunauer–Emmet–Teller (BET) method (ASAP 2020 Micromeritics). The properties of the powder used are summarized in Table 1.

The drug loading method of the CPC plays a significant role in different parameters [1,15], such as setting time or drug distribution within the CPC matrix. Preliminary studies conducted here reflected better homogeneity when Doxy, an antibiotic freely soluble in water [14], was incorporated into the CPC from the liquid phase than when it was added as a powder to the solid phase, where antibiotic aggregates were observed in the set cement (results not shown). Therefore, the liquid phase employed consisted of either MilliQ water for pristine CPCs or 50 mg ml$^{-1}$ aqueous solutions of doxycycline hyclate (Sigma-Aldrich, doxycycline hydrochloride hemiethanolate hemihydrate, $C_{22}H_{24}N_2O_8\cdots HCl\cdots 0.5H_2O\cdots 0.5C_2H_6O$; MW: 1025.89).

### 2.2. Cement preparation and characterization

Cements were prepared with two different liquid-to-powder (L/P) ratios of 0.35 and 0.65 ml g$^{-1}$. The powder phase was mixed with the liquid phase (either MilliQ water or drug solution) in a mortar for ~1 min. The cements set due to the dissolution of α-TCP followed by the precipitation of calcium-deficient hydroxyapatite (CDHA) according to the following reaction [3,16]:

$$3Ca_3(PO_4)_{2(s)} + H_2O_{(l)} \rightarrow Ca_9(HPO_4)(PO_4)_5(OH)_{(s)} \quad (1)$$

Initial and final setting times were measured with the standard Gillmore needles method (ASTM C266–08). Cement samples were fabricated by introducing the paste with a spatula in 6 mm diameter × 12 mm height cylindrical Teflon molds. CPCs obtained were named C35 or C65 after the L/P ratio used, being 0.35 or 0.65 ml g$^{-1}$, respectively, and referred to as "water" or "Doxy" depending on the liquid phase employed. The samples were allowed to set in Ringer's solution (0.15 M sodium chloride solution) for 7 days at 37 °C.

The evolution of the pH during the setting reaction was measured in an α-TCP aqueous slurry at an L/P ratio of 200 with a Crison pHmeter connected to data acquisition software. The setting reaction was followed by X-ray diffraction analysis (XRD) in a PANalytical X'Pert powder X-ray diffractometer. The XRD measurements were obtained by scanning in Bragg–Brentano geometry using CuKα radiation. The experimental conditions were: 2 h scan step 0.016 between 4 and 100, counting time 50 s per point, voltage 45 kV and intensity 40 mA. The diffraction patterns were compared with the Joint Committee on Powder Diffraction Standards for α-TCP (JCPDS No. 9–348) and HA (JCPDS No. 9–432). The textural properties of the set cements were determined by $N_2$ adsorption–desorption by using a Micromeritics ASAP 2020. The samples were previously degassed under vacuum for 24 h, at 100 °C. The surface area was determined using the BET method. Total porosity and entrance pore size distribution were measured by mercury intrusion porosimetry (MIP, Autopore IV 9500, Micromeritics). BET and MIP measurements were done in duplicate for each formulation. The cross-section microstructure was imaged by Field emission scanning electron microscopy (SEM, JEOL JSM-7001F). The compressive strength was measured in wet samples ($n$ = 6) in a universal testing machine (Bionix 858, MTS Systems) at a cross-head speed of 1 mm min$^{-1}$.

### 2.3. Drug release from the cements

Firstly, the stability of doxycycline in the release media was assessed by preparing dissolutions of different concentrations (from 1 to 100 μg ml$^{-1}$) in phosphate buffered saline (PBS), which were stored in the dark at 37 °C. Its stability was also studied for several hours at different pHs found in the setting reaction of cements by preparing NaOH solutions in PBS at pH 7.5, 8.5 and 9.5. UV-vis spectroscopy (Infinite M200 Pro Microplate reader TECAN,

Switzerland, λ = 351 nm) was used to follow changes for a period of 1 week. The solubility of doxycycline hyclate in PBS at pH = 7.4, as used in this study, was 168.75 mg $ml^{-1}$.

Drug release studies were carried out with either fresh or pre-set CPCs. The cements were prepared as described in the previous section, and placed at 37 °C in 100% relative humidity (RH) to avoid drug loss in the setting media, either for 1 h (fresh CPCs) or for 7 days to achieve complete setting (herein pre-set CPCs). 100% RH was achieved by a closed recipient half-filled with water, with the samples contained in another recipient, uncovered, and floating in the water. Fresh CPCs were allowed to set for 1 h to be close to the longest initial setting time and avoid washout of the samples in the release media. After the specified times, the drug release tests were performed according to the USP pharmacopoeia dissolution test in a paddle dissolution tester (Pharma Alliance, USA) with eight amber vessels of 250 ml with 150 ml PBS. Pristine cements were used as control. Stirring conditions were 150 rpm, temperature was set to 37 °C and 1 ml aliquots were withdrawn at predetermined times from the receptor compartment for spectroscopy analysis at λ = 351 nm (TECAN, Infinite M200 Pro Microplate Reader). After each sample withdrawal, the same volume of fresh PBS was added to the receptor medium. The concentration of Doxy in the receptor solution was below 20% of the saturation concentration (sink conditions) during the experiment [17]. Four replicates were studied of each sample ($n = 4$). To precisely determine the doxycycline concentration at each time point, three corrections were taken into account: (1) a total volume correction due to evaporation; (2) a correction to take into account the drug quantity withdrawn at each sampling; (3) a correction due to the antibiotic degradation in the experiment conditions.

Mathematical modeling was carried out using MatLab software (The Mathworks Inc., USA). Drug release kinetics was analyzed by plotting the mean release data vs. time. The MatLab program was used to fit the mathematical models to the experimental kinetics.

### 2.4. Antibacterial activity of the cements

To evaluate an eventual denaturation of the antibiotic due to the pH changes occurring during the setting reaction or to the interaction with the CPC components, the antibacterial activity of the cement formulations was tested against two bacterial strains commonly found in buccal flora: *Streptococcus sanguinis* (CECT 480) and *Lactobacillus salivarius* (CECT 4063), provided by the Colección Española de Cultivos Tipo (University of Valencia, Valencia, Spain). The culture media were prepared by dissolving 3.6 wt.% of Todd–Hewitt broth (Scharlau, Reference No. 02-191) for the *S. sanguinis* or 5.2 wt.% of MRS (Scharlau, Reference No. 02-135) for the *L. salivarius* in distilled water, which were sterilized by autoclaving. To determine the antibacterial activity of the antibiotic containing CPCs, the agar diffusion test was used. This test allows us to qualitatively determine the effectiveness of a diffusible antimicrobial agent to inhibit the bacterial growth, being a relatively quick and easy assay. The test was performed by plating $10^7$ colony forming units (CFU) on agar plates, previously prepared with the appropriate culture media for each bacteria tested. Cement disks (6 mm diameter) consolidated for 1 h (fresh) or set for 7 days (pre-set), prepared in the conditions described above, were gently placed on the surface of the agar plate. After incubation at 37 °C for 24 h, the diameter of inhibition for each sample was measured using images of the plates taken with a digital camera. The inhibition zone was calculated from the diameter of the inhibition zone ($\phi_{iz}$) and the diameter of the cement ($\phi_c$), according to Eq. (2) [18]. Four replicates of each formulation were studied ($n = 4$):

$$\text{Inhibition zone size (mm)} = \frac{\phi_{iz} - \phi_c}{2} \quad (2)$$

**Table 1**
Properties of the α-TCP powder used.

| D10 (μm)[a] | Median particle diameter D50 (μm) | D90 (μm)[b] | Specific surface area SSA ($m^2 g^{-1}$) |
|---|---|---|---|
| 0.781 | 4.517 | 16.410 | 0.98 ± 0.01 |

[a] D10: 10% in volume of the powder particles are smaller than this value.
[b] D90: 90% in volume of the powder particles are smaller than this value.

### 2.5. Statistics

Statistical differences were determined using one-way ANOVA with Tukey's post-hoc tests using Minitab 16 software (Minitab, Inc., USA). Statistical significance was considered when $p < 0.05$. Data are presented as mean ± standard deviation.

## 3. Results

### 3.1. Effect of doxycycline incorporation on the physico-chemical properties of CPCs

The influence of incorporating Doxy in the liquid phase of the CPCs on their setting times is shown in Table 2. In general the addition of Doxy led to longer setting times, except in the case of C65, where the initial setting time was reduced. After 7 days, the CPCs had transformed to CDHA, even in presence of the drug, as shown by the sample X-ray diffractograms. However, in the Doxy-CPCs, the presence of small peaks that could be ascribed to traces of unreacted α-TCP was detected (Fig. 1a). Fig. 1b shows the compressive strength of the different cement formulations, prepared with MilliQ water or a Doxy solution as a liquid phase. Increasing the L/P ratio of pristine CPCs led to a significant decrease in strength ($p = 0.00$). Although the introduction of Doxy tended to reduce the compressive strength for each sample, in general the differences were not statistically significant. These results were in good agreement with the higher total porosity in the samples with high L/P ratio, as measured by Hg porosimetry (Fig. 1c). The addition of the antibiotic reduced slightly the porosity, especially at low L/P ratios. Microstructural modifications were also revealed by the SSA of each formulation. Antibiotic addition significantly increased the SSA of the set cements (Fig. 1d) ($p = 0.033$). This increase was consistent with the SEM images of the fracture surfaces of the cements (Fig. 2), where the formation of smaller crystals in the presence of the drug suggests that Doxy may be acting as a nucleating agent. This was confirmed by SEM images at lower magnification (Fig. 2, left column), where different microstructures were clearly observed. Whereas in the pristine cements the CDHA crystals precipitated in aggregates surrounding the initial α-TCP particles, the addition of Doxy resulted in a more homogeneous distribution of the crystals and no inter-aggregate spaces. These results are consistent with the MIP pore size distribution shown in Fig. 3a and b. The pore entrance size distribution was clearly modified by the presence of the drug, with the disappearance of the pores above 0.1 μm. The $N_2$ adsorption–desorption isotherms shown in Fig. 3c and d confirmed this trend. All the curves were identified

**Table 2**
Initial and final setting times of the cements with and without Doxy in the liquid phase.

| Liquid phase | $t_{setting}^{initial}$ (min) | | $t_{setting}^{final}$ (min) | |
|---|---|---|---|---|
| | $H_2O$ | Doxy | $H_2O$ | Doxy |
| C35 | 5.7 ± 0.6 | 11.0 ± 0.5 | 34.6 ± 2.3 | 69.3 ± 1.5 |
| C65 | 143.0 ± 3.6 | 71.5 ± 2.1 | 193.0 ± 4.4 | 243.0 ± 4.2 |

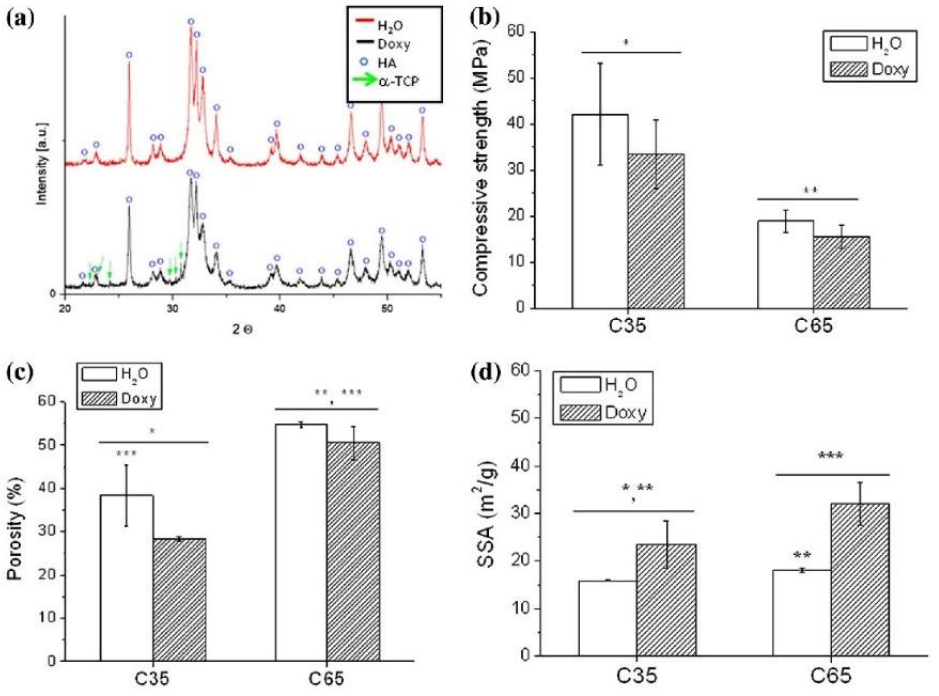


**Fig. 1.** CPCs prepared with liquid phase being either water or Doxy, after immersion in Ringer's solution for 7 days. (a) X-ray diffractograms of cements at an L/P ratio of 0.65. (b) Compressive strength of cements with L/P ratios of 0.35 and 0.65, with liquid phase being water or Doxy, $p = 0.00$, $n = 6$. (c) Open porosity of the same formulations, as determined by MIP, $p = 0.010$, $n = 8$. (d) Specific surface area (SSA), $p = 0.033$, $n = 8$. Different symbols (*, **) indicate groups with statistically significant differences.

as type IV isotherms, and the hysteresis loops were identified as type H3 [19]. The presence of antibiotic in the CPCs did not modify the shape of the hysteresis loops. The only difference observed was that the antibiotic-containing CPCs showed higher volumes of $N_2$ in the high $p/p^0$ range, indicating that these samples have a higher volume of mesopores. This can also be observed in the pore size distribution curves obtained applying the Barrett, Joyner & Halenda (BJH) method on the desorption isotherms (Fig. 3e and f); incorporation of Doxy did not alter the pore diameters but increased the volume of pores in this region in both L/P ratios studied.

The evolution of the pH during the setting reaction is displayed in Fig. 4a. When α-TCP was dissolved in water, the pH increased up to values slightly above 9.5, and then it progressively decreased in the subsequent hours to ~pH 7. The effect of a range of pHs between 7.5 and 9.5 on the stability of the drug is shown in Fig. 4b. Considering the timeframe when the drug would be exposed to alkaline pHs (up to 10 h at a pH above 8.5 and up to 20 h at pH above 7.5), it can be assumed that Doxy was not degraded during the setting reaction. Subsequently, the stability of Doxy in the receptor medium (PBS) at 37 °C was assessed, showing a concentration decrease as a function of time (Fig. 4c), which, according to the UV-vis spectra of Doxy solutions right after preparation and after storage, suggest that it is due to degradation of the drug (Fig. 4d). This degradation was conveniently taken into account in the calculations of the release experiments by incorporating an exponential decrease function (obtained from fitting the drug degradation profile, Fig. 4a, to calculate the quantity of drug degraded at each time point.

In the evaluation of the drug release properties of the materials, two situations were taken into account, as shown in Fig. 5: (i) the use of fresh Doxy-CPCs readily prepared, to mimic as much as possible the real surgical scenario when the CPC setting reaction takes place after implantation, and (ii) the use of Doxy-CPCs pre-set for 7 days. In both cases the samples presented a progressive release without any major burst (a sudden, quick release of drug at very short time), and only a small fraction of the drug, below 10%, was released in 5 days, with potential for longer and sustained release, given the positive release rate. However, the behavior was markedly different in the fresh or pre-set CPCs, especially in the early stages, as revealed in Fig. 5c and d. In general, initially the release was faster in the fresh CPCs than in the pre-set counterparts. Moreover, whereas in the pre-set CPCs a continuous evolution was found, in the fresh CPCs two different regions were clearly distinguished: in the first 2–4 h there was a fast release, which then slowed down, giving rise to a second stage of linear release. As summarized in Table 3, both fresh and pre-set CPCs with high L/P ratios reached higher release percentages after 5 days than their low L/P ratio homologues, although the difference was smaller in the fresh CPCs.

### 3.2. Antibacterial activity of the CPCs

The antibacterial activity of the doxycycline diffused from the CPC disks against *S. sanguinis* and *L. salivarius* is shown in Table 4. All formulations displayed antibacterial properties. In the case of *L. salivarius*, larger inhibition zones were found in the formulations prepared with a higher L/P ratio, which in fact contained a larger amount of Doxy, as shown in Table 3. Although larger inhibition zones were consistently found for the fresh compared with the pre-set cements, the differences were not statistically

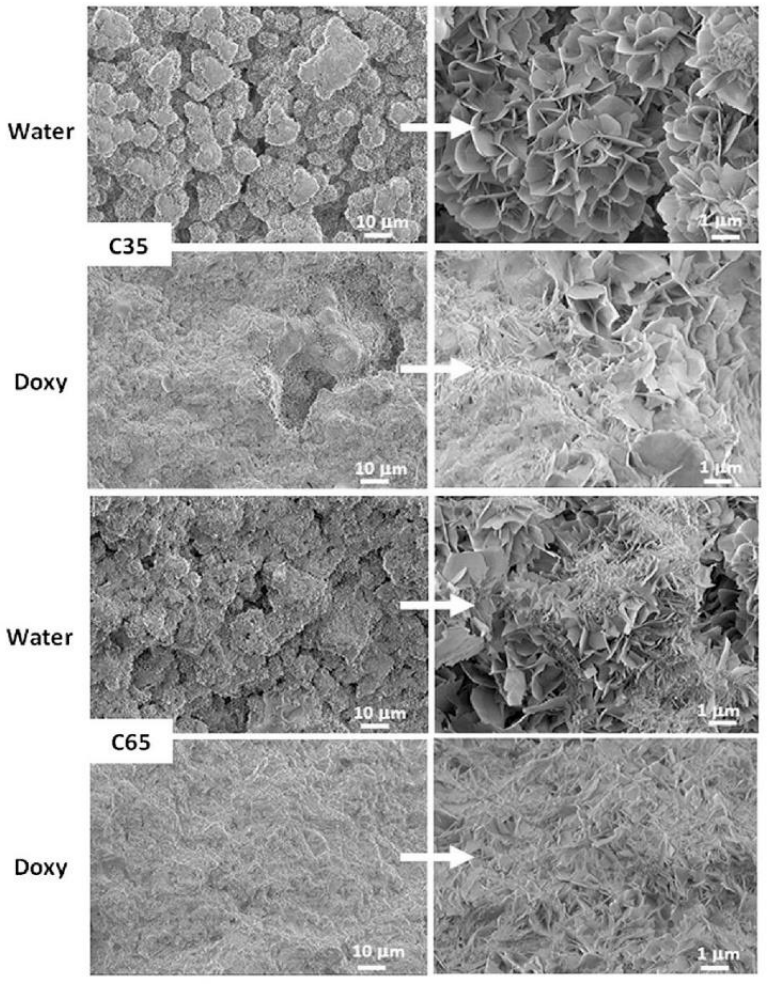


**Fig. 2.** FESEM micrographs of the fracture surfaces of cements prepared with different liquid-to-powder ratios (C35 or C65), using either water or a Doxy solution as liquid phase. Low magnification in the left column and higher magnification in the right one.

significant ($p > 0.05$). The inhibition zones were smaller for *S. Sanguinis* than for *L. salivarius*, fresh CPCs showing higher antibacterial activity than their set homologues, although no significant differences ($p > 0.05$) were observed between formulations.

## 4. Discussion

### *4.1. Effect of doxycycline incorporation on the physico-chemical properties of CPCs*

The release behavior of CPCs can be understood only if a thorough characterization of the drug-loaded cements is performed. In fact, the results obtained showed that the addition of the antibiotic in the liquid phase of the CPCs had clear effects on their setting kinetics and on the microstructural development, textural properties and porosity.

As expected, in the pristine cements low L/P ratios resulted in shorter setting times (Table 2). As a general trend, the addition of Doxy in the liquid phase tended to increase the setting times of the cements (Table 2). This was in agreement with other authors, who claimed that low concentrations of tetracyclines can give rise to calcium chelates that affect the primary nucleation, interfering with mineral precipitation and delaying the setting reaction both in apatite [20,21] and in brushite cements [6,22]. However, according to the X-ray diffraction studies, this initial deceleration of the setting reaction produced by the addition of Doxy did not avoid the hydrolysis of α-TCP to CDHA, as only some traces of remnant α-TCP were observed in the Doxy-containing cements after 7 days, regardless of the L/P ratio (Fig. 1a). This indicated that Doxy slightly delayed the reaction. Similarly, previous works also observed that the interactions between antibiotics and cement particles did not interfere considerably with the phase transformation during setting [23], leading to apatite, and also traces of the initial reactants were observed in some cases [20,24,25].

The setting reaction of CPC is based on the dissolution of α-TCP and the precipitation of CDHA according to Eq. (1). Interestingly,

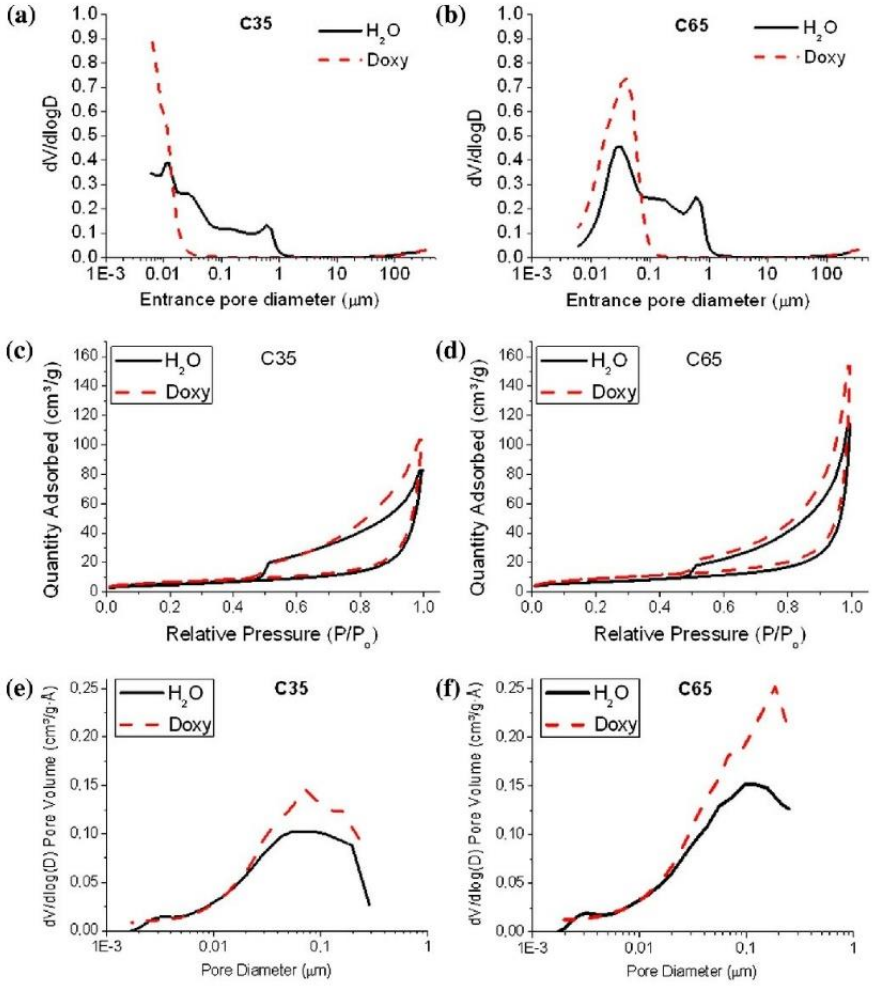


**Fig. 3.** Pore entrance size distribution curves obtained by MIP for CPCs prepared with water or Doxy as liquid phase at an L/P ratio of: (a) 0.35 and (b) 0.65. $N_2$ adsorption–desorption isotherms at an L/P ratio of: (c) 0.35 and (d) 0.65. Pore size distribution obtained from the desorption isotherms using the BJH model at an L/P ratio of: (e) 0.35 and (f) 0.65.

the addition of the antibiotic significantly modified the final microstructure, SSA and pore size distribution of the cements, as consistently revealed by the SEM, $N_2$ adsorption and MIP results (Figs. 1–3). Thus SSA was nearly doubled due to the presence of Doxy. This, according to SEM images, was due to the formation of smaller crystals in the presence of the drug, which may indicate that Doxy may be acting as a nucleating agent. This is confirmed when the FESEM micrographs of the fracture surface of a CPC with and without Doxy are compared (Fig. 2). In the pristine CPC prepared with water as liquid phase, it can be clearly seen that CDHA aggregates were formed surrounding the initial α-TCP particles, giving rise to a shell-like structure [3,16,26]. On the other hand, the presence of Doxy led to a more homogeneous distribution of the precipitated crystals, suggesting that crystals did not necessarily grow from the α-TCP particles as in pristine cements, and support the hypothesis that Doxy may act as a heterogeneous nucleating agent (Fig. 2). Thinner and smaller average crystal size was also observed due to the addition of gentamicin to the liquid phase of brushite CPCs [27]. A direct consequence of the more homogeneous distribution of the precipitated crystals was the important change in the pore size distribution (Fig. 3). The entrance pore diameter was shifted to lower values due to the elimination of inter-aggregate porosity [3]. Thus, whereas the pristine CPCs presented a multimodal pore size distribution, ranging from 0.006 μm (lower detection limit of the porosimeter) to 1 μm, in the antibiotic-containing CPCs a monomodal porosity distribution was found, centered around 0.03 μm for the C65 formulation, and smaller for the C35. According to the adsorption–desorption isotherm profiles (Fig. 3c and d) Type H3 hysteresis loops were found in both pristine and antibiotic-containing CPCs, which are characteristic of aggregates of plate-like particles containing slit-shaped pores [19], which is in agreement with the images obtained by SEM. The hysteresis loops

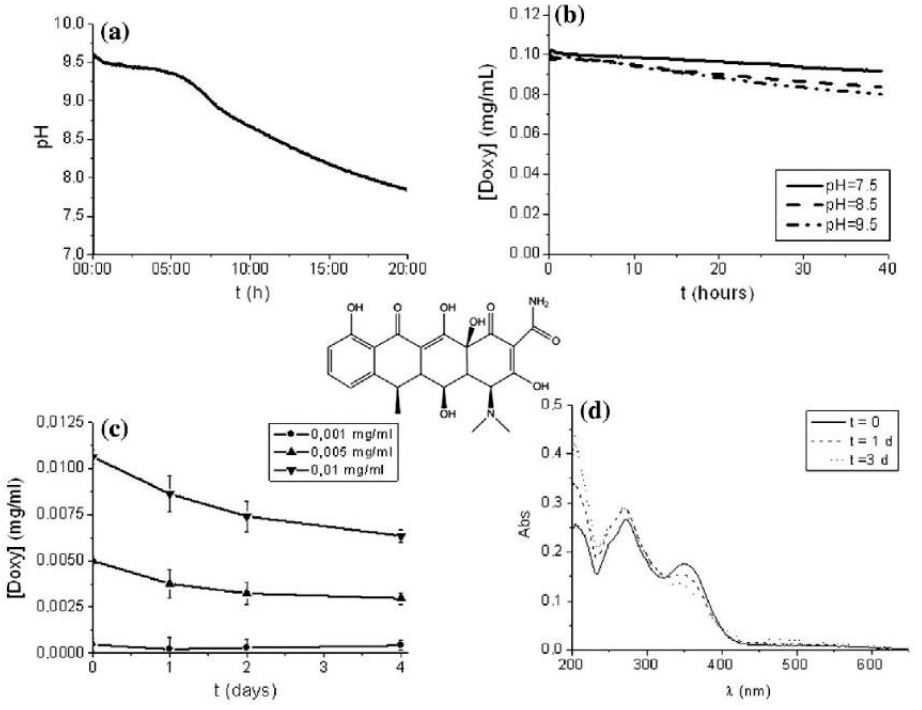


**Fig. 4.** Evolution of the setting pH of α-TCP (a), doxycycline hyclate stability assessment at different pHs at 37 °C (b) and degradation profile (c) and spectra (d) of the drug in PBS stored in the dark at 37 °C, with details of its chemical structure.

confirmed the presence of pores in the mesopore range (2–50 nm), in higher volume in the case of antibiotic-containing CPCs, consistently with the MIP measurements.

The total porosity of the set pristine cements (Fig. 1c) was closely related to the L/P ratio, varying between 42 and 55%, and increasing with the higher L/P ratio. By increasing the L/P ratio, the strength decreased significantly, by 55%, as a consequence of the porosity increase [3]. The addition of Doxy in the liquid phase slightly decreased the total porosity (Fig. 1c). This reduction in porosity did not result in an increase of the compressive strength of the cements, since the Doxy-containing cements presented slightly lower values of this parameter, although the differences were not statistically significant. These results agree with those found in the literature; in general, the mechanical properties of CPCs tend to decrease in the presence of antibiotics, especially in those with high Ca-chelation ability [20,21], this effect being dependent on antibiotic concentration [6,15]. In our particular case, in spite of the low affinity of Doxy with Ca compared to other tetracyclines, the slight decrease in mechanical strength could be associated to the incomplete hydrolysis of the α-TCP reflected in the X-ray diffractograms (Fig. 1a).

### 4.2. Doxycycline release from fresh and pre-set CPCs

One of the main objectives of the current study was to correlate the drug release kinetics with the different evolving microstructures of the CPCs. As a first step, the stability of the drug in the receptor media was tested (Fig. 4). The concentration–time curves for solutions containing different initial amounts of Doxy in PBS, recorded in the conditions of the release experiments (pH = 7.4 and 37 °C), showed a concentration decrease with time (Fig. 4a), suggesting antibiotic degradation. At all concentrations tested, the concentration of Doxy followed an exponential decreasing function of the form ($C = C_0 \cdot e^{-\lambda t}$). The results obtained are consistent with previous works [28] where degradation of doxycycline occurred at nearly physiological conditions. However, the mentioned degradation was not taken into account in previous research evaluating drug release of Doxy from CPCs [6,22], even though it is relevant, as in fact Doxy available for therapeutic activity is higher than that directly measured in in vitro testing due to its degradation. Thus, due to the degradation of the drug in assay conditions, a correction step was included in the calculation of Doxy released in the delivery experiments.

As mentioned previously, CPCs can be ascribed to the category of non-swellable, non-resorbable monolithic systems and it can be assumed that the drug release is mainly controlled by the drug diffusion through the cement matrix. Therefore, it must be expected that the microstructure of the cement matrix plays a major role in the drug release kinetics. To evaluate the effect of the evolving microstructure on the drug diffusion mechanisms, release experiments were carried out with: (a) freshly prepared CPCs, which would mimic more closely a real surgical situation where the cement is readily injected inside the body, and (b) CPCs previously set for 7 days, which would mimic the situation where pre-set granules, scaffolds or microcarriers are used. The freshly prepared Doxy-containing CPCs were placed in the release media after 1 h. This is slightly below the initial setting time of C65 but to our understanding this does not affect the comparison of the drug released from both cements. In fact, the setting time as determined by the Gilmore needles is just a comparative measurement,

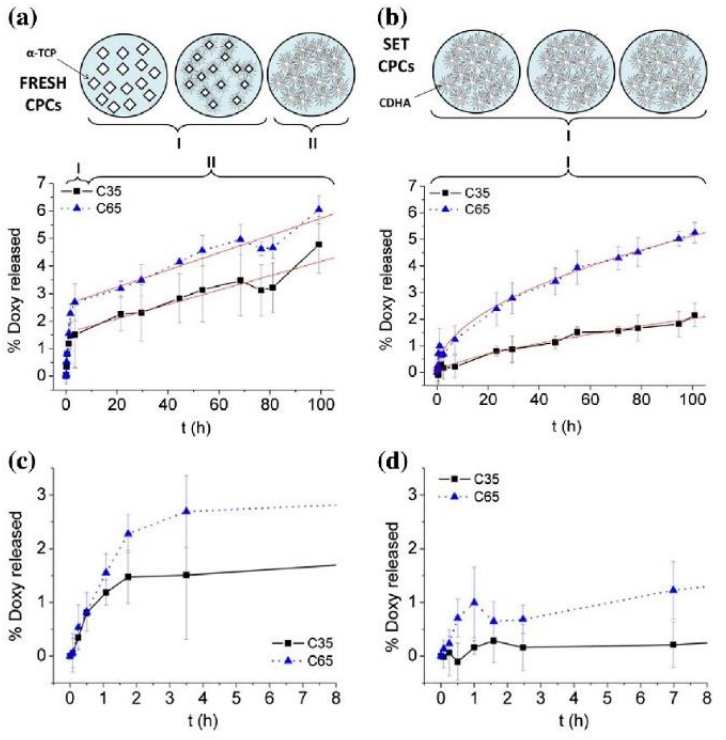


**Fig. 5.** Accumulated doxycycline release (%) from CPCs prepared with liquid phase containing antibiotic at L/P ratios of 0.35 and 0.65. Release curves of the (a) fresh CPCs, (b) pre-set CPCs with the corresponding fitting (red lines) and zoom of the first 8 h for (c) fresh and (d) pre-set CPCs. A schematic representation of the evolution of the microstructure of fresh and pre-set CPCs with time is included.

**Table 3**
Initial dose of doxycycline loaded in each cement specimen, quantity and accumulated percentage of antibiotic released after 100 h.

| | Loaded amount per sample | Release after 100 h | | Fitting parameters | |
|---|---|---|---|---|---|
| Fresh CPCs | $Q^{Doxy}_{loaded}$ (mg) | $Q^{Doxy}_{released}$ (mg) | % release | Zero-order release | |
| | | | | Rate of release (% $h^{-1}$) | $R^2$ |
| C35 | 8.28 ± 0.03 | 0.37 ± 0.09 | 4.49 ± 1.07 | 0.027 | 0.868 |
| C65 | 10.28 ± 0.14 | 0.62 ± 0.06 | 6.05 ± 0.51 | 0.031 | 0.922 |
| Pre-set CPCs | $Q^{Doxy}_{loaded}$ (mg) | $Q^{Doxy}_{released}$ (mg) | % release | Korsmeyer–Peppas | |
| | | | | $n$ | $R^2$ |
| C35 | 8.40 ± 0.03 | 0.17 ± 0.04 | 2.03 ± 0.43 | 0.676 | 0.984 |
| C65 | 10.99 ± 0.22 | 0.58 ± 0.03 | 5.25 ± 0.29 | 0.492 | 0.992 |

Fitting parameters for the release curves of doxycycline, assuming: (a) a zero-order release for the fresh CPCs after the initial stage of fast release (after 4 h); (b) Korsmeyer–Peppas model fitting for pre-set cements.

**Table 4**
Inhibition zone size (cm) of the Doxy-containing cements either readily prepared (fresh) or pre-set for 7 days.

| Bacterial strain | Inhibition zone (cm) | | | |
|---|---|---|---|---|
| | *L. salivarius* | | *S. sanguinis* | |
| | Fresh CPC | Pre-set CPC | Fresh CPC | Pre-set CPC |
| C35 | 1.14 ± 0.03 | 0.75 ± 0.07 | 1.23 ± 0.07 | 0.85 ± 0.05 |
| C65 | 1.19 ± 0.06 | 0.97 ± 0.03 | 1.10 ± 0.26 | 0.85 ± 0.04 |

No statistical differences were observed among the different formulations (for $p > 0.05$; $n = 4$).

which does not correspond to any particular stage of the setting reaction. In these apatite cements the setting reaction is a continuous process that takes several days and implies an evolution of the microstructure until complete transformation to CDHA [26,29].

As shown in Fig. 5, no burst release was observed from any of the formulations of either fresh CPCs (Fig. 5a and c) or pre-set ones (Fig. 5b and d). In contrast, previous works evaluating drug release from CPC matrices did register burst release [6,20,25,27,30–32]. In other tetracycline-containing cements also prepared by blending the drug with the CPC reactants, either in the solid or liquid phase, the high initial release (22–30% in 24 h in apatite cements [20] or 25–60% in 24 h in brushite cements) [6,22] was attributed to the dissolution of drug adsorbed on the external surface. In our case,

the absence of significant burst release and the slow release rate could be associated to the very small pore size in the Doxy-containing CPCs.

The release kinetics was different in the fresh and pre-set CPCs. The simplest scenario corresponded to the release from pre-set CPCs, where the microstructure remained mostly unaltered throughout the release period. As observed in Fig. 5b and d, the release profiles clearly depended on the porosity and pore size distribution of the materials (Fig. 3). For instance, pre-set C35 had both the lowest release rate and final release percentage, which matches with its lowest porosity and smallest entrance pore size, so the flow of release media within the sample was more impaired. Taking into account that the stationary stage was not reached during the release period studied in any of the cement formulations, it can be assumed that diffusion of the active principle may continue, although longer-term studies should be performed.

The Korsmeyer–Peppas (KP) model (Eq. (3)) was applied to identify the underlying controlling mechanisms of the drug release:

$$\frac{M_t}{M_\infty} = k \cdot t^n \tag{3}$$

where $M_t/M_\infty$ is the fractional solute release, $t$ is the release time, $k$ is a constant accounting for the properties of the matrix and the diffusing drug such as the effective diffusion coefficient and $n$ is the diffusional exponent characteristic of the release mechanism. Fickian diffusion is defined by $n = 0.45$ for release from cylinders, and non-Fickian diffusion by $n$ greater than 0.45. The equation is valid only during the first 60% of the fraction released [33,34]. The fitting parameters of the release curves with the KP model are displayed in Table 3. The values obtained for the exponent $n$ indicated non-Fickian release.

The release from the fresh CPCs followed a different pattern (Fig. 5a and c) than for pre-set CPCs. In fact, two different regions were clearly distinguished (Fig. 5a), as compared to a more continuous behavior in the pre-set specimens (Fig. 5b). Thus, after an initial stage where the release was faster than in the pre-set cements, the amount of eluted drug leveled off, resulting in a zero-order release, with a similar rate of release for the two formulations, as shown in Table 3. The initial release rate was higher for the cement with a higher L/P ratio, and this fast release stage was longer for the cement with higher a L/P ratio (C65, 3.5 h) than for the cement with a low L/P ratio (C35, ~1.5 h). Interestingly, a correlation was found between the time when the elution kinetics changed and the final setting times of the cements, which were 243 and 69 min for C65 and C35, respectively, as reported in Table 2. This supports the hypothesis that the evolving microstructure during the cement setting is responsible for the change in the elution regime (Fig. 5). Initially, the cement paste is just a suspension of ceramic α-TCP particles in water. As the setting reaction proceeds, the precipitation of a network of CDHA nanocrystals [26,29] in the space between particles previously occupied by the antibiotic-containing liquid results in a progressive increase of tortuosity, hindering the drug diffusion and reducing the release rate.

Oral doses of Doxy are established at 200 mg in the first day followed by 100 mg per day [35], so local bioavailability should be much lower. Even though the quantities of Doxy released (Table 3) were relatively low, it can be expected that after adjusting the doses and sample size, adequate local therapeutic activity is achieved in future formulations. Moreover, since the stationary stage was not reached, a potential for continued release is envisaged, with maintained antibacterial activity, which also needs to be carefully tuned to avoid bacterial resistance due to too low daily doses.

### 4.3. Antibacterial activity of the CPCs

A relevant issue that has to be taken into account is the possibility of partial denaturation of the antibiotic due to the pH changes during the setting reaction or to the interaction with the CPC components [1]. It has been shown (Fig. 4b) that the concentration of Doxy does not greatly vary due to different pHs, in the setting timeframe at each pH. In general it has been reported that antimicrobial activity is maintained after setting of apatitic cements with different antibiotics (gentamicin, cephalexin or vancomycin) [31,36,37], although in some particular cases vancomycin in apatitic CPC did not exhibit any bactericidal properties [5], possibly due to pH fluctuations during setting. Doxycycline has shown antibacterial activity towards different bacteria when incorporated in brushite cements [22].

In the current study, the antibacterial diffusion activity of fresh and pre-set Doxy-containing CPCs was tested against two gram positive bacteria commonly found in the normal bacterial flora of the oral cavity (*S. sanguinis* and *L. salivarius*, Table 4). All Doxy-CPC formulations set for 7 days showed antibacterial activity against both strains, being more effective (bigger inhibition diameter) against *L. salivarius*. Freshly prepared CPCs were also evaluated, and it was observed that in this case the inhibition diameter was greater for each fresh formulation with respect to the pre-set ones, in agreement with the faster elution of the antibiotic, as assessed in the release studies. The effects of higher diffusion with higher water content were also observed in the tests with *L. salivarius* with fresh cements, where a significantly higher inhibition was observed in the CPCs prepared with a higher L/P ratio of 0.65 ml $g^{-1}$ with respect to those prepared at 0.35 ml $g^{-1}$. This is a further confirmation that Doxy was not significantly degraded by the setting reaction, as also shown by the stability tests in the different setting pH (Fig. 4b), and within the adequate timeframe.

## 5. Conclusions

This work highlights the interactions between an antibiotic, doxycycline hyclate, and the microstructural development of the CPC during setting. The microstructural evolution of the cement is strongly altered by the presence of the antibiotic, especially in terms of SSA, micro- and nanoporosity, causing a decrease in pore size of more than one order of magnitude. Moreover, the evolving microstructure during cement setting affects the release kinetics in the early stages. Distinct release kinetics are identified when the drug is released from fresh or pre-set CPCs, which must be taken into account when either pre-set materials or injectable CPCs are used as drug delivery systems.

## Acknowledgements

The authors acknowledge the MICINN, the financial support in the MAT 2009-13547 project and the Juan de la Cierva fellowship of CC. Support for the research of MPG was received through the prize "ICREA Academia" for excellence in research, funded by the Generalitat de Catalunya. The authors are grateful to M. Molmeneu and M. Fernández for their help with SSA and MIP tests.

## Appendix Figures. with essential colour discrimination

Certain figures in this article, particularly Figs. 1, 3, and 5, are difficult to interpret in black and white. The full colour images can be found in the on-line version, at doi:http://dx.doi.org/10.1016/j.actbio.2013.05.016.

## References

[1] Ginebra MP, Canal C, Espanol M, Pastorino D, Montúfar EB. Calcium phosphate cements as drug delivery materials. Adv Drug Deliv Rev 2012;64:1090–110.
[2] Ginebra MP, Traykova T, Planell JA. Calcium phosphate cements: competitive drug carriers for the musculoskeletal system? Biomaterials 2006;27:2171–7.

[3] Espanol M, Perez RA, Montufar EB, Marichal C, Sacco A, Ginebra MP. Intrinsic porosity of calcium phosphate cements and its significance for drug delivery and tissue engineering applications. Acta Biomater 2009;5:2752–62.
[4] Montufar EB, Traykova T, Gil C, Harr I, Almirall A, Aguirrre A, et al. Foamed surfactant solution as a template for self-setting injectable hydroxyapatite scaffolds for bone regeneration. Acta Biomater 2010;6:876–85.
[5] Jiang PJ, Patel S, Gbureck U, Caley R, Grover LM. Comparing the efficacy of three bioceramic matrices for the release of vancomycin hydrochloride. J Biomed Mater Res B Appl Biomater 2010;93:51–8.
[6] Alkhraisat MH, Rueda C, Cabrejos-Azama J, Lucas-Aparicio J, Mariño FT, Torres García-Denche J, et al. Loading and release of doxycycline hyclate from strontium-substituted calcium phosphate cement. Acta Biomater 2010;6:1522–8.
[7] Hofmann MP, Mohammed R, Perrie Y, Gbureck U, Barralet JE. High-strength resorbable brushite bone cement with controlled drug-releasing capabilities. Acta Biomater 2009;5:43–9.
[8] Montufar EB, Mazzouz Y, Ginebra MP. Relevance of the setting reaction to the injectability of TCP pastes. Acta Biomater 2013;9:6188–98.
[9] Le Nihouannen D, Komarova SV, Gbureck U, Barralet JE. Bioactivity of bone resorptive factor loaded on osteoconductive matrices: stability postdehydration. Eur J Pharm Biopharm 2008;70:813–8.
[10] Perez RA, Del Valle S, Altankov G, Ginebra MP. Porous hydroxyapatite and gelatin/hydroxyapatite microspheres obtained by calcium phosphate cement emulsion. J Biomed Mater Res B Appl Biomater 2011;97(1):156–66.
[11] Gbureck U, Vorndran E, Muller FA, Barralet JE. Low temperature direct 3D printed bioceramics and biocomposites as drug release matrices. J Controlled Release 2007;122:173–80.
[12] Gbureck U, Holzel T, Doillon CJ, Muller FA, Barralet JE. Direct printing of bioceramic implants with spatially localized angiogenic factors. Adv Mater 2007;19:795–800.
[13] Vorndran E, Klammert U, Ewald A, Barralet JE, Gbureck U. Simultaneous immobilization of bioactives during 3D powder printing of bioceramic drug release matrices. Adv Funct Mater 2010;20:1585–91.
[14] Parfitt K, Martindale W. The complete drug reference. London: Pharmaceutical Press; 1999. pp. 203, 260.
[15] Kisanuki O, Yajima H, Umeda T, Takakura Y. Experimental study of calcium phosphate cement impregnated with dideoxy-kanamycin B. J Orthop Sci 2007;12:281–8.
[16] Ginebra MP, Driessens F, Planell JA. Effect of the particle size on the micro and nanostructural features of a calcium phosphate cement: a kinetic analysis. Biomaterials 2004;25:3453–62.
[17] Gibaldi M, Feldman S. Establishment of sink conditions in dissolution rate determinations. Theoretical considerations and application to nondisintegrating dosage forms. J Pharm Sci 1967;56:1238–42.
[18] Bauer AW, Kirby WM, Sherris JC, Turck M. Antibiotic susceptibility testing by a single disk method. Am J Clin Pathol 1966;45(4):493–6.
[19] Sing KSW, Everett DH, Haul RAW, Moscou L, Pierotti RA, Rouquérol J, et al. Reporting physisorption data for gas/solid systems with special reference to the determination of surface area and porosity. Pure Appl Chem 1985;57(4):603–19.
[20] Ratier A, Freche M, Lacout JL, Rodriguez F. Behaviour of an injectable calcium phosphate cement with added tetracycline. Int J Pharm 2004;274:261–8.
[21] Ratier A, Gibson I, Best S, Freche M, Lacout J. Setting characteristics and mechanical behaviour of a calcium phosphate bone cement containing tetracycline. Biomaterials 2001;22:897–901.
[22] Tamimi F, Torres J, Bettini R, Ruggera F, Rueda C, López-Ponce M, et al. Doxycycline sustained release from brushite cements for the treatment of periodontal diseases. J Biomed Mater Res A 2008;85:707–14.
[23] David Chen CH, Chen CC, Shie MY, Huang CH, Ding SJ. Controlled release of gentamicin from calcium phosphate/alginate bone cement. Mater Sci Eng C 2011;31:334–41.
[24] Takechi M, Miyamoto Y, Momota Y, Yuasa T, Tatehara S, Nagayama M, et al. The in vitro antibiotic release from anti-washout apatite cement using chitosan. J Mater Sci Mater M 2002;13:973–8.
[25] Takechi M, Miyamoto Y, Ishikawa K, Nagayama M, Kon M, Asaoka K, et al. Effects of added antibiotics on the basic properties of anti-washout-type fast-setting calcium phosphate cement. J Biomed Mater Res 1998;39:308–16.
[26] Ginebra MP, Fernandez E, Driessens FCM, Planell JA. Modeling of the hydrolysis of alpha-tricalcium phosphate. J Am Ceram Soc 1999;82:2808–12.
[27] Bohner M, Lemaître J, Van Landuyt P, Zambelli PY, Merkle HP, Gander B. Gentamicin-loaded hydraulic calcium phosphate bone cement as antibiotic delivery system. J Pharm Sci 1997;86:565–72.
[28] Sunaric SM, Mitic SS, Miletic GZ, Pavlovic AN, Naskovic-Djokic D. Determination of doxycycline in pharmaceuticals based on its degradation by $Cu(II)/H_2O_2$ reagent in aqueous solution. J Anal Chem 2009;64:231–7.
[29] Ginebra MP, Fernandez E, DeMaeyer EA, Verbeeck RM, Boltong MG, Ginebra J, et al. Setting reaction and hardening of an apatitic calcium phosphate cement. J Dent Res 1997;76:905–12.
[30] Bohner M, Lemaître J, Merkle HP, Gander B. Control of gentamicin release from a calcium phosphate cement by admixed poly(acrylic acid). J Pharm Sci 2000;89:1262–70.
[31] Ethell MT, Bennett RA, Brown MP, Merritt K, Davidson JS, Tran T. In vitro elution of gentamicin, amikacin, and ceftiofur from polymethylmethacrylate and hydroxyapatite cement. Vet Surg 2000;29:375–82.
[32] Stallmann HP, Faber C, Bronckers ALJJ, Nieuw Amerongen AV, Wuisman PIJM. In vitro gentamicin release from commercially available calcium-phosphate bone substitutes influence of carrier type on duration of the release profile. BMC Musculoskelet Disord 2006;7:18.
[33] Ritger PL, Peppas NA. A simple equation for description of solute release, I: Fickian and non-Fickian release from non-swellable devices in the form of slabs, spheres, cylinder or discs. J Control Release 1987;5:23–6.
[34] Siepmann J, Peppas N. Higuchi equation: derivation, applications, use and misuse. Int J Pharm 2011;418:6–12.
[35] Therapeutical prescription guide: <http://www.imedicinas.com/GPTage/>.
[36] Joosten U, Joist A, Frebel T, Brandt B, Diederichs S, von Eiff C. Evaluation of an in situ setting injectable calcium phosphate as a new carrier material for gentamicin in the treatment of chronic osteomyelitis: studies in vitro and in vivo. Biomaterials 2004;25:4287–95.
[37] Urabe K, Naruse K, Hattori H, Hirano M, Uchida K, Onuma K, et al. In vitro comparison of elution characteristics of vancomycin from calcium phosphate cement and polymethylmethacrylate. J Orthop Sci 2009;14:784–93.

## 4.4. Paper IV: Drug delivery from injectable calcium phosphate foams by tailoring the macroporosity–drug interaction

While local release of active principles provides clear benefits over systemic administration, one of its major drawbacks is, in the case of antibiotics, to increase the risk of generating antibiotic-resistant bacteria in case of long-term contact with immobilized, non-released antibiotic in the grafting material. The need for enhanced release kinetics can be achieved with improved circulation of fluids in the material to maximize the percentage of antibiotic released. This justifies the introduction of an interconnected network of macropores in CPCs by mechanical foaming to manufacture antibiotic-laden Calcium Phosphate Foams.

Additionally, the macroporosity is beneficial for bone regeneration, allowing cell colonization and nutrient circulation. Both the structural and drug loading/release patterns of doxycycline hyclate-loaded calcium phosphate foams are investigated in the following publication, as a function of antibiotic loading. Moreover, the antibacterial efficacy of the materials is tested against two common bacteria in nosocomial infections: *E.Coli* and *S. Aureus*.

Acta Biomaterialia 12 (2015) 250–259

Contents lists available at ScienceDirect

Acta Biomaterialia

journal homepage: www.elsevier.com/locate/actabiomat

# Drug delivery from injectable calcium phosphate foams by tailoring the macroporosity–drug interaction

David Pastorino, Cristina Canal, Maria-Pau Ginebra *

*Biomaterials, Biomechanics and Tissue Engineering Group, Department of Materials Science and Metallurgy, Technical University of Catalonia (UPC), Av. Diagonal 647, 08028 Barcelona, Spain*
*Centre for Research in Nanoengineering, Technical University of Catalonia (UPC), C/Pascual i Vila 15, 08028 Barcelona, Spain*
*Biomedical Research Networking Centre in Bioengineering, Biomaterials, and Nanomedicine (CIBER-BBN), Maria de Luna 11, Ed. CEEI, 50118 Zaragoza, Spain*

ARTICLE INFO

*Article history:*
Received 28 May 2014
Received in revised form 16 October 2014
Accepted 23 October 2014
Available online 29 October 2014

*Keywords:*
Calcium phosphate cement
Foam
Scaffold
Drug delivery
Controlled release

ABSTRACT

In this work, novel injectable calcium phosphate foams (CPFs) were combined with an antibiotic (doxycycline) to design an innovative dosage form for bone regeneration. The material structure, its drug release profile and antibiotic activity were investigated, while its clinical applicability was assessed through cohesion and injectability tests. Doxycycline had a clear effect on both the micro and macro structure of the CPFs, owing to its role as a nucleating agent of hydroxyapatite and to a drying effect on the paste. Doxycycline-loaded CPFs presented interconnected macroporosity, which increased drug availability compared with calcium phosphate cements, and was a critical parameter controlling the release kinetics which followed a non-Fickian diffusion model. Up to 55% (1 mg) of the drug was released progressively in 5 days, the percentage released being proportional to the macroporosity of the CPFs. All doxycycline-containing foams had immediate cohesion and were injectable. Moreover, antibacterial activity was observed against *Staphylococcus aureus* and *Escherichia coli*. Thus, in addition to enhancing osteoconduction and material resorption, macroporosity enables tuning of the local delivery of drugs from injectable calcium phosphates.



## 1. Introduction

Calcium phosphate cements (CPCs) show numerous attractive features when used as synthetic bone grafts. Their ability to set in vivo into calcium-deficient hydroxyapatite (CDHA) grants an excellent compatibility with the damaged bone and the possibility to be progressively replaced by new bone over time [1]. In addition, their use as local drug delivery systems for many drugs, mainly antibiotics, anti-inflammatories, anti-cancer or anti-osteoporosis drugs, has been widely investigated [2–6].

However, CPCs lack interconnected macroporosity. This hinders cell colonization, limits the possibility of circulation of nutrients and cell waste in the material, and impairs material resorption, thus preventing quick bone ingrowth [7]. When used as a drug delivery system, physiological fluids have reduced access to the centre of the matrix, potentially leading to an incomplete release of the active principle [8], particularly in slowly degradable CPCs, such as apatite cements [1]. On top of limiting the efficacy of the treatment, this can increase the risk of generating antibiotic resistance [9]. Different methods can be used to overcome these limitations. Specifically, drug-loaded polymeric porogens have been combined with CPCs with the purpose of generating macroporosity and releasing drugs in a controlled manner, as reviewed by Habraken et al. [10]. However, this method also has some drawbacks: (1) the macroporosity created by the porogen leaching is not available early enough to allow blood clotting in the graft; (2) leaching of the porogen might be detrimental to the regenerative process; (3) the proportion of porogen must be very high to generate an interconnected network of macropores; (4) the size of the porogen particles must be sufficient to generate macropores, and might thus be detrimental to injectability. The foaming approach used in this work presents an attractive, simple alternative to these drawbacks. Macroporous self-setting calcium phosphate foams (CPFs) can be obtained by foaming a surfactant-containing liquid and subsequently mixing with a reactive calcium phosphate powder [11–13]. This process generates an additional interconnected macroporosity to the already existing microporosity of CPCs, without losing injectability or requiring a subsequent step of porogen elimination. Thus, macroporosity is available instantaneously to

* Corresponding author at: Biomaterials, Biomechanics and Tissue Engineering Group, Department of Materials Science and Metallurgy, Technical University of Catalonia (UPC), Av. Diagonal 647, 08028 Barcelona, Spain
*E-mail address:* maria.pau.ginebra@upc.edu (M.-P. Ginebra).

http://dx.doi.org/10.1016/j.actbio.2014.10.031
1742-7061/

the release media/corporal fluids. Different additives have been studied to foam the liquid phase of CPCs: low molecular weight surfactants (Sorbitol, Tween80) [11] or proteins, such as albumen [13] or gelatin [12]. The resulting foam, its stability and structure depend strongly on the chosen foaming agent, owing to the different mechanisms of action, such as the repulsive interactions between the adsorbed layers or the confinement of aggregates within the thin films [14].

A number of antibiotics, such as aminoglycosides (gentamicin), cephalosporins (cephalexin) and glycopeptides (vancomycin) have been proposed as active principles in combination with CPCs, in applications requiring both bone regeneration and local treatment of an infection. Although the local presence of the active principle enhances its efficacy, antibiotics can have side effects. For instance: gentamicin is thought to affect cell viability, proliferation and metabolism; cephalosporins inhibit osteoblast cells function, whereas vancomycin is less aggressive at low concentrations [15]. Interestingly, Kallala et al. [16] claimed that tetracyclines present some beneficial effects when targeting bone regeneration, i.e. enhancement of bone mineralization and induction of apoptosis of osteoclasts *in vitro*, thus limiting bone resorption [17]. The tetracycline employed in this work is doxycycline hyclate (Doxy). It has been used to treat a wide variety of infections including periodontitis [18], osteomyelitis [19–21] and methicillin resistant *Staphylococcus aureus* (*S. aureus*; MRSA) [22]. Beneficial effects on bone metabolism have been reported for Doxy even at low concentrations, i.e. 2–5 $\mu g\ ml^{-1}$ [15].

In this work, for the first time, a new dosage form, intended for local treatment of infected bone defects, is proposed, based on self-setting injectable CPFs in combination with an antibiotic. Different aspects are investigated, such as: (i) the influence of the incorporation of Doxy on the porosity, macroporosity and pore interconnectivity of CPFs; (ii) the effect of the structural properties of the foam on the *in vitro* drug release kinetics; (iii) the relevance of interconnected macroporosity on the release and antimicrobial activity of the antibiotic.

## 2. Materials and methods

### 2.1. Liquid and solid phase preparation

α-TCP was used as a solid phase of CPFs and was obtained by heating in a furnace (CNR-58, Hobersal, Spain) in air a 2:1 molar mixture of calcium hydrogen phosphate ($CaHPO_4$; Sigma–Aldrich, USA) and calcium carbonate ($CaCO_3$; Sigma–Aldrich, USA) at 1400 °C for 15 h, followed by quenching in air. The α-TCP obtained was milled in an agate ball mill (Pulverisette 6, Fritsch GmbH, Germany) using 10 agate balls ($d = 30$ mm) for 15 min at 450 rpm; 2 wt.% of precipitated hydroxyapatite (HA; BP-E341, Merck, Germany) was added as a seed in the powder. The liquid phase was a solution of 1 wt.% of Polysorbate 80, herein Tween80 (Polysorbate 80, Sigma Aldrich, USA) in distilled water.

Doxycycline hyclate (Doxy; doxycycline hydrochloride hemiethanolate hemihydrate, Sigma–Aldrich, USA) in powder form was used as received. The schematic representation of the Doxy formula, i.e. $C_{22}H_{24}N_2O_8 * HCl * 0.5H_2O * 0.5C_2H_6O$, is show in Fig. 1.

### 2.2. Preparation of CPFs

Self-setting CPFs were prepared by foaming the liquid phase at 6000 rpm for 30 s using a domestic hand mixer followed by hand mixing with the solid phase. The liquid to calcium phosphate powder ratio was maintained constant and equal to 0.55 $ml\ g^{-1}$, as in previous works [11]. The amount of Doxy blended with the powder phase was a multiple of the lowest dose (D) corresponding to 0.88 wt.%. The different materials prepared, including the nomenclature used, amounts of liquid phase, calcium phosphate powder and antibiotic, and weight percentage of antibiotic in the material ($C_{doxy}$) are reported in Table 1.

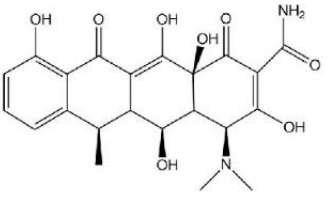


**Fig. 1.** Structural formula of doxycycline hyclate.

CPFs were then cast manually into Teflon cylindrical moulds of 6 mm in diameter and 12 mm high, and allowed to consolidate at 37 °C and 100% relative humidity for 1 h before immersion in water for 7 days for further reaction before subsequent characterization.

### 2.3. Material characterization

The surface tension of different dissolutions of Doxy in 1% of Tween 80 aqueous solution was measured. The concentrations chosen correspond to the doses of Doxy of each CPF formulation assuming total dissolution in the liquid phase, namely 0, 25, 50, 75 and 100 $mg\ ml^{-1}$. A tensiometer (K100, Krüss, Germany) with a Pt plaque was used to evaluate the surface tension.

The plastic limit of non-foamed CPC pastes containing different amounts of Doxy was evaluated via a simple technique, as described elsewhere [23]. Briefly, 1 g of powder phase was weighted and mixed with the adequate quantity of Doxy. Initially, 200 μl of distilled water was added to the powder phase and mixing was performed with a spatula until homogenization. A drop of water was then added and mixed again until homogenization. The process was repeated until the system had the consistence of a paste, and thus the plastic limit was reached. The paste was then weighted, and the liquid to powder ratio at the plastic limit was calculated.

A cohesion test was performed according to the protocol described in Montufar et al. [12]. Briefly, CPFs (0D-CPF, 1D-CPF, 2D-CPF, 3D-CPF, 4D-CPF) were freshly prepared. After 2.5 min, a small amount of the foamed material was injected into a cylindrical cavity 4 mm high and 8 mm in diameter in a commercial polyurethane sponge immersed in water at 37 °C. The integrity of the paste was evaluated visually using an arbitrary scale from 1 to 4, with 1 meaning no cohesion, i.e. paste disruption immediately after injection, and 4 meaning excellent cohesion, i.e. intact paste after injection and consolidated structure after 24 h. Three replicates were used for each composition.

To assess the effect of the addition of Doxy on injectability, CPFs were prepared and placed in a commercial syringe with a 2 mm aperture at the tip, a 13 mm cartridge and a nominal capacity of

**Table 1**
Nomenclature of the different CPFs, amounts of water, calcium phosphate (CaP) powder and antibiotic, and corresponding weight percentage of antibiotic with respect to the total weight of the CPFs ($C_{doxy}$).

| Nomenclature | Liquid phase (ml) | CaP powder (g) | Doxy (mg) | $C_{doxy}$ (wt.%) |
|---|---|---|---|---|
| 0D-CPF | 1 | 1.820 | 0 | 0 |
| 1D-CPF | 1 | 1.820 | 25 | 0.88 |
| 2D-CPF | 1 | 1.820 | 50 | 1.76 |
| 3D-CPF | 1 | 1.820 | 75 | 2.64 |
| 4D-CPF | 1 | 1.820 | 100 | 3.52 |

5 ml. The injection test was performed using a universal testing machine (BIONIX, MTS, USA) 2.5 min after preparation of the foams. The injection was performed at 15 mm $min^{-1}$ until a force of 100 N was achieved. The parameters measured were the injection force, defined as the mean value of the plateau force needed to inject the material, and the injectability, defined as the percentage of the material injected, evaluated by direct weighting of the paste [24].

X-ray diffraction analysis (XRD) of the foams after consolidation at 37 °C and 100% relative humidity for 1 h, followed by immersion in water at 37 °C for 7 days, was performed using an X'Pert powder X-ray diffractometer (PANalytical, Netherlands) to evaluate phase composition. The XRD measurements were obtained by scanning in Bragg–Brentano geometry using Cu$K_\alpha$ radiation. The experimental conditions were: 2θ scan step 0.017 between 20 and 70, counting time 50 s per step, voltage 45 kV and intensity 40 mA. The diffraction patterns were compared and phases quantified using the Joint Committee on Powder Diffraction Standards for α-TCP (JCPDS No. 00-029-0359) and HA (JCPDS No. 01-082-1943), using the EVA software (Brucker, Germany).

A field emission scanning electron microscopy (FESEM) instrument (Neon 40, Zeiss, Germany) operating at 5 kV was used to observe the internal microstructure of the CPFs. Prior to observation, samples were AuV-sputter coated (K950X, Emitech, US). The specific surface area (SSA) of Doxy-containing CPFs was evaluated by nitrogen adsorption using the Brunaueron using the t (BET) theory with an ASAP 2020 (Micromeritics, USA).

The skeletal density of non-foamed CPCs with varying amounts of Doxy was measured by helium pycnometry (AccuPyc 1330, Micromeritics, USA). The density was evaluated by mercury immersion to obtain the volume of the sample and direct weighting. The densities of both CPCs, i.e. CPFs without the foaming step, and CPFs with the same compositions were determined and enabled the total porosity, and the amount of porosity introduced by foaming, herein called total macroporosity, to be calculated [25].

Mercury intrusion porosimetry (MIP, AutoPore IV, Micromeritics, USA) was performed to determine the pore entrance size distribution (PESD) within the materials. Moreover, the open macroporosity was determined as the integral of the MIP PESD for pore diameters >10 μm. Four cylindrical samples 6 mm diameter and 12 mm high were introduced in the sample holder for the measurement, and a single measurement was performed for each composition.

A v/tome/X (Phoenix, USA) micro-computed tomography scanner was used to evaluate the three-dimensional (3-D) morphology of CPFs. The scanner was operated to obtain a voxel size of ~10 $\mu m^3$. The samples were cylinders 6 mm in diameter and 12 mm high. The 3-D volume was then reconstructed using ImageJ (US National Institutes of Health, USA).

### 2.4. Evaluation of antibiotic release

CPFs were prepared and cast manually into cylindrical moulds 8 mm in diameter and 4 mm high with only one open side, to allow contact with the release medium, and were then kept for 1 h in 100% relative humidity to allow them to have sufficient cohesion. Two controls were prepared: a 0D-CPF and a control CPC, which was prepared using the same composition and protocol as 2D-CPF, but avoiding the foaming step. A dissolution tester (Pharma Alliance, USA) was used to evaluate the release following an adaptation of the United States Pharmacopeia (USP) Paddle Dissolution Test. Each sample was put in an individual amber glass filled with 150 ml of phosphate buffer saline (PBS). Stirring conditions were set to 150 rpm, and the temperature to 37 °C according to the current USP, chapter <711> Dissolution [26]. Sampling consisted of the extraction of 1 ml aliquot and its replacement by 1 ml of fresh PBS at determined times up to 100 h. Four replicates of each type of sample were evaluated.

Doxy was quantified by UV–VIS spectrophotometry using a microplate reader (Infinite M200 Pro Microplate Reader, TECAN, Switzerland), at the maximum wavelength of Doxy $\lambda = 351$ nm. This measurement was then corrected for evaporation, sampling effect and degradation of the antibiotic, as in previous studies [8], using MATLAB software (Mathworks Inc., USA). The percentage released was plotted as a function of time. Modelling was performed using the Korsmeyer Peppas (KP) model. The variable fitted is the quantity released $M_t$, normalized by the maximum quantity released $M_\infty$ (Eq. (1)):

$$M_t/M_\infty = k.t^n \quad (1)$$

where $k$ is a constant that accounts for structural parameters of the material and characteristics of the active principle such as the effective coefficient of diffusion. The exponent $n$ allows the identification of the mechanism controlling the release. Specifically, for a given geometry of the sample it allows discerning between a release controlled by Fickian diffusion, swelling/case II transport or an Intermediate situation. The KP model is applicable only up to 60% of the quantity released. None of the CPFs reached that value after 100 h. Thus, the fitting was performed considering that $M_\infty$ is unknown and that only the constant $k$ is affected by the normalization by $M_\infty$. The exponent n describes the shape of the curve and is not affected by the normalization. The quantity released as a function of time was thus fitted with the KP equation, and both the value of the exponent $n$ and the correlation coefficient $R^2$ were reported.

### 2.5. Antibacterial activity

The antibacterial activity of the materials was tested against two bacterial strains commonly found in osteoarticular as well as in nosocomial infections: *S. aureus* and *Escherichia coli* (*E. coli*) from the Culture Collection of the University of Göteborg, Sweden. The culture media was prepared by dissolving 3.7 wt.% of brain heart infusion broth (Scharlau, Spain) in distilled water, which was sterilized by autoclaving. To determine the antibacterial activity of the materials, the agar diffusion test was used. This test determines the effectiveness of a diffusible anti-microbial agent, in the present case an antibiotic, to inhibit the bacterial growth. The test was performed by plating $10^7$ colony-forming units on agar plates, previously prepared with the appropriate culture media containing 1.5% bacteriological agar (Scharlau, Spain). Three equidistant holes 9.5 mm in diameter by 3 mm deep with a total volume of 0.23 $cm^3$ were made in each agar plate. The freshly prepared CPFs were then injected into the holes, taking special care to ensure lateral contact with the agar media. After incubation at 37 °C overnight, the diameter of inhibition for each sample was measured using images of the plates, taken with a digital camera. The inhibition zone was calculated from the diameter of the inhibition zone ($Ø_{iz}$) and the diameter of the material ($Ø_m$), according to Eq. (2) [27]. Three replicates of each formulation were used ($n = 3$).

$$\text{Inhibition zone size} = (Ø_{iz} - Ø_m)/2 \quad (2)$$

### 2.6. Statistics

Statistical differences were determined using one-way ANOVA with Tukey's post hoc tests using Minitab 16 software (Minitab, Inc., USA). Statistical significance was considered when $P < 0.05$. Data are presented as mean ± standard deviation.

## 3. Results

### 3.1. Material characterization

To evaluate the potential influence of Doxy on the preparation process and on the properties of the CPFs, the effect of antibiotic addition on the surface tension of the liquid phase was measured. Various solutions were prepared containing 1 wt.% of Tween 80 and different concentrations of Doxy. The surface tension of pure water, 72.37 ± 0.02 mN $m^{-1}$ and Tween 80 (1 wt.%), 39.66 ± 0.34 mN $m^{-1}$ was also recorded as control (Fig. 2). Although increasing Doxy concentrations significantly decreased surface tension with a total difference of 8% from 25 to 100 mg $ml^{-1}$ solutions, the differences were small compared with the large reduction induced by the surfactant.

The plastic limit of non-foamed CPCs, defined as "the minimum amount of liquid that had to be added to a powder to form a paste" [23] was evaluated as a function of the amount of Doxy added to the solid phase (Fig. 3), as an indication of the ease of producing a paste at different Doxy concentrations. No statistically significant differences ($P > 0.05$) were observed between the plastic limit of pastes with no Doxy or low quantities of Doxy, i.e. from 0D-CPF to 2D-CPF. However, the plastic limit increased significantly for 3D-CPF and 4D-CPF, $P = 0.03$ and 0.05, respectively, so these formulations required more water to form a paste. Also, at constant liquid-to-powder ratio a system containing more Doxy appeared "drier" than a mixture containing less Doxy.

All Doxy-containing formulations presented excellent cohesion, i.e. level 4. Even injecting the paste readily after preparation, the foams kept the integrity, and were intact after 24 h immersion in water, without any particle released to the surrounding medium. Only in the 0D-CPF a small fraction of particles detached from the paste, although the foam did not disintegrate, and the paste was able to consolidate after 24 h, thus recorded as level 3.

Fig. 4 shows the injectability as well as the injection force required to extrude the CPF pastes. It can be observed that all Doxy-containing foams were injectable, i.e. more than 80% of the foamed paste could be extruded, with relatively low injection force values, between 25 and 30 N.

CDHA was obtained as a result of the hydrolysis of α-TCP in all CPFs, in agreement with previous studies [4,11]. The addition of Doxy resulted in a slight increase of unreacted α-TCP, from ~1% for 0-CPF to 4–7% for 1, 2, 3 and 4D-CPF, but no clear dose-dependence was observed (Supplementary information, Fig. S1). The SSA of CPFs increased from 20 to 30 $m^2 g^{-1}$ with increasing amounts of Doxy (Table 2), until a plateau value of ~31 $m^2 g^{-1}$ for loadings >1.77 wt.%, corresponding to 2D-CPF.

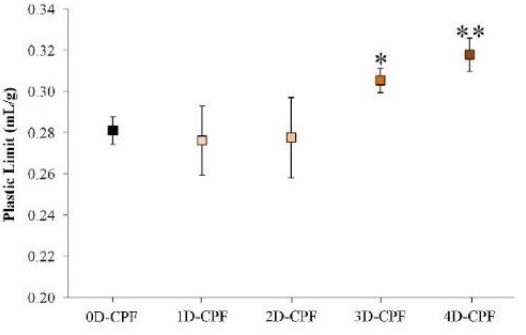


**Fig. 3.** Plastic limit of non-foamed materials for different Doxy loadings. *, ** indicate statistically significant differences between groups ($P < 0.05$).

The morphology of the foams obtained with different amounts of Doxy is shown in Fig. 5. The macrostructure of the CPFs was clearly dependent on the amount of Doxy loaded. At higher Doxy concentrations, the foam-like structure of the materials was damaged and led to its collapse in some areas, which appeared less porous in the case of the 3D-CPF and 4D-CPF.

More detailed SEM images of the fracture surfaces of the 0D-CPF and 2D-CPF samples are shown in Fig. 6, at both low and high magnifications. Macropores were spherical, and interconnections between adjacent pores were observed in the walls of most of them. Imaging of the pore walls revealed that 0D-CPF presented separate spherical aggregates of needle-like crystals resulting from the dissolution of individual α-TCP particles and precipitation of CDHA crystals. The 2D-CPF showed the same basic structure of crystalline aggregates, but with the particularity that, on the pore walls, the entangled matrix of plate-like crystals had grown flat, possibly owing to the combined presence of Doxy and Tween at the interface with air.

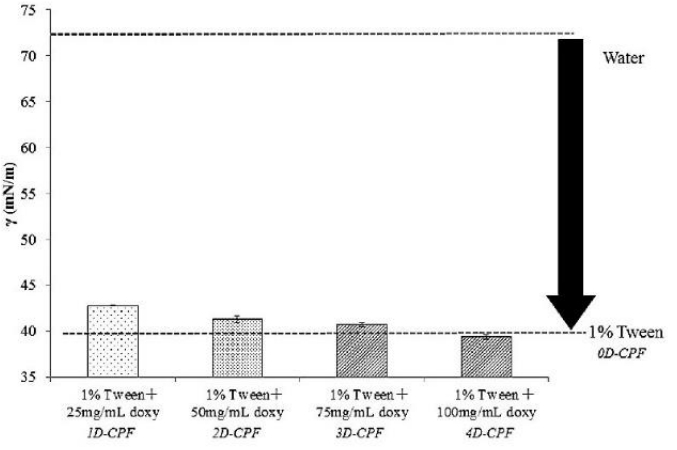


**Fig. 2.** Surface tension measurements dissolutions of Tween (1 wt.%) containing different amounts of Doxy (25, 50, 75 and 100 mg $ml^{-1}$) equivalent to 1D-CPF, 2D-CPF, 3D-CPF and 4D-CPF, respectively. Dashed lines indicate the surface tension of water and of a 1% Tween 80 solution (0D-CPF) ($n = 10$).

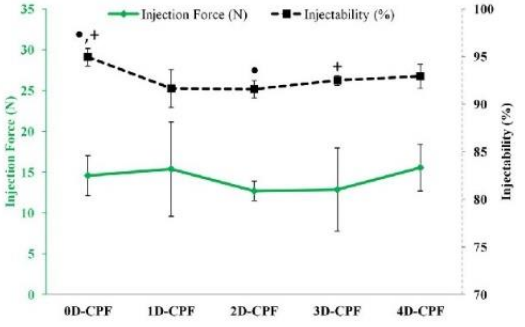


**Fig. 4.** Injection force (N) and injectability (%) of pristine and antibiotic-loaded CPFs. • and + represent statistically significant differences ($P < 0.05$) between compositions with the same symbol.

**Table 2**
Specific surface area (SSA, BET theory) of Doxy-containing CPFs.

| Composition | SSA ($m^2\ g^{-1}$) ± SD |
|---|---|
| 0D-CPF | 20.25 ± 0.03 |
| 1D-CPF | 23.47 ± 0.12 |
| 2D-CPF | 30.47 ± 0.18 |
| 3D-CPF | 31.77 ± 0.20 |
| 4D-CPF | 30.94 ± 0.19 |

The skeletal density of non-foamed CPCs determined by helium pycnometry was not affected by the addition of Doxy and was 2.75 ± 0.02 g $cm^{-3}$. The total porosity and total macroporosity of the different CPFs measured by mercury immersion, together with the interconnected porosity and interconnected macroporosity recorded by MIP are shown in Fig. 7a. The PESD in the foams containing different amounts of antibiotic is displayed in Fig. 7b. Total porosity showed minor variations, from 71.98 ± 4.94% in 0D-CPF to 65.99 ± 7.39% in 4D-CPF. The addition of antibiotic to the CPFs led to a gradual reduction in the total macroporosity from 50.2 ± 4.9% for an antibiotic-free 0D-CPF to 22.8 ± 7.4% for a 4D-CPF. Focusing on the doxy-containing CPFs, the total macroporosity decreased linearly with increasing amount of Doxy at a rate of ~10% for every 25 mg of Doxy. Moreover, more than two-thirds of the total macroporosity was interconnected, except for 4D-CPF, where the percentage of interconnected macropores was lower.

The PESD was bimodal in all formulations containing Doxy, with the peaks centred ~50 nm and 100 μm, while the 0D-CPF showed an additional peak in the micrometre range, at 3 μm. The diameter of open macropores, i.e. those >10 μm as previously defined, slightly decreased with an increasing amount of antibiotic. The intensity and position of the peak centred at 50 nm of all antibiotic-containing CPFs slightly increased with increasing amount of Doxy, while the pristine CPFs showed bigger pore entries with a mode diameter ~100 nm. The images obtained by micro-computed tomography for 0D-CPF and 2D-CPF shown in Fig. 8 provide an outlook of the morphology and macrostructure of these materials. The 2D-CPF showed smaller and less-defined macropores compared with the 0D-CPF.

### 3.2. Antibiotic release profile

The Doxy release kinetics was evaluated for all CPF formulations. The percentage released is represented as a function of time (Fig. 9a) for all CPFs and for a 2D-CPC, the non-foamed counterpart of the 2D-CPF. The initial quantity loaded, the final quantity released and the corresponding percentage released after 5 days are reported in Fig. 9b, while the relationship between final percentage released and macroporosity is represented in Fig. 9c. CPFs released a decreasing drug percentage with increasing initial amount of Doxy (Fig. 9a and b), from 54.88 ± 5.82% to 19.58 ± 2.59% from 1D-CPF to 4D-CPF, respectively. In none of the cases was a burst release observed; instead, the rate of release slowly decreased with time (Fig. 9a). The different formulations displayed potential for longer release, as the stationary state was not reached in the time-frame of this study. A maximum of 1 mg was released by 2D-CPF in 5 days. The percentage released was found to be proportional to the macroporosity of the CPFs (Fig. 9c), fitting linearly with a slope of 0.94, which suggested that macroporosity had a major influence on the percentage released. The KP model was applied to interpret the release kinetics of the CPFs. The fitting parameters are reported in Table 3.

### 3.3. Antibacterial activity

The antibacterial activity of the materials against *S. aureus* and *E. coli* is shown in Fig. 10a. All antibiotic-containing materials displayed antibacterial properties, while the pristine, 0D-CPF used as control showed no bacterial inhibition. Concerning *E. coli*, the 2D-CPC, 1D-CPF and 2D-CPF presented similar inhibition zone sizes. The 3D-CPF and 4D-CPF showed a higher value ($P < 0.05$). The diffusion test with the *S. aureus* strain did not reveal statistically significant differences between materials. When comparing the CPFs with their non-foamed counterpart 2D-CPC, no differences in the inhibition zone size were recorded. To understand this result further, the Doxy loading and the apparent density as determined by MIP of each material were used to calculate the absolute amount of antibiotic in the agar hole at the beginning of the test, reported in Table 4.

The absolute amount of Doxy present in the material at the beginning of the test was used to normalize the inhibition zone size (Fig. 10b). After normalization, it was clear that macroporous

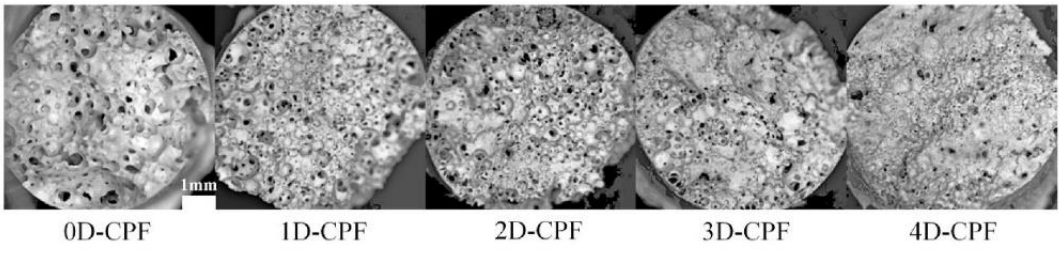


**Fig. 5.** Optical microscope images of the CPFs obtained with different concentrations of Doxy, from left to right: 0D-CPF, 1D-CPF, 2D-CPF, 3D-CPF and 4D-CPF.

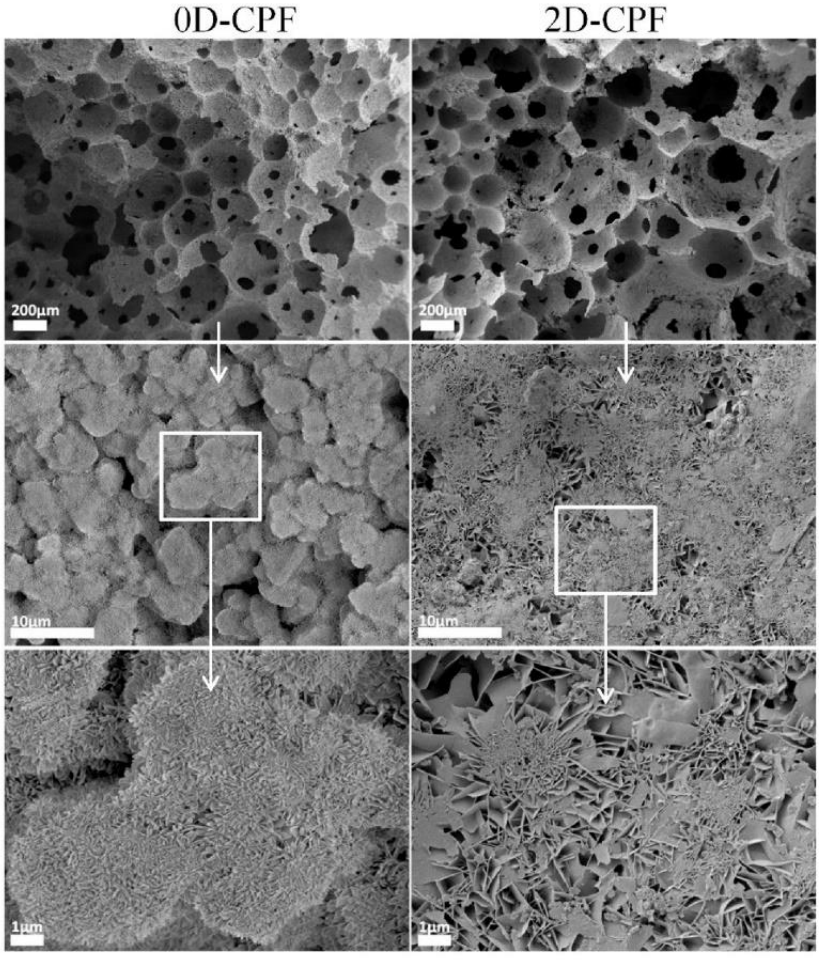


**Fig. 6.** FESEM images of the fracture surface of CPFs with detail of the macropore walls of a 0D-CPF (left) and a 2D-CPF (right) at different magnifications: 50×, 2500× and 10,000× (from top to bottom).

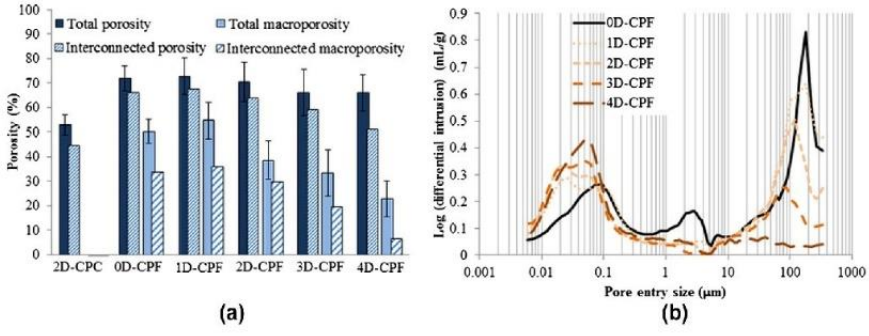


**Fig. 7.** Porosity characterization of CPFs containing different amounts of Doxy: (a) total porosity and total macroporosity as measured by immersion in Hg ($n = 12$); interconnected porosity and interconnected macroporosity as determined by MIP ($n = 4$); (b) MIP pore entry size distribution ($n = 4$).

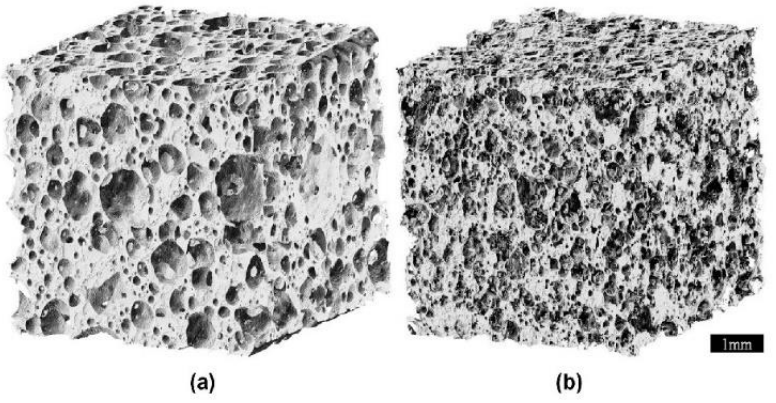


**Fig. 8.** A 3-D reconstruction of a micro-computed tomography scan of a $5 \times 5 \times 5\ mm^3$ cubic volume: (a) 0D-CPF; (b) 2D-CPF.

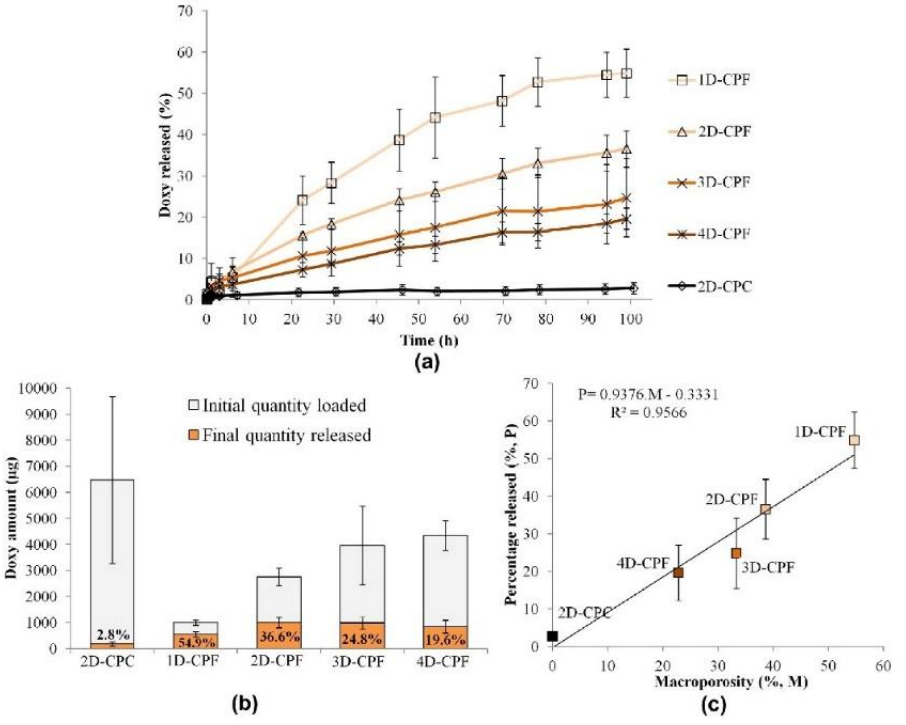


**Fig. 9.** (a) Release curves of CPFs containing different amounts of Doxy. The 2D-CPC is included for comparison. (b) Initial quantity loaded, final quantity released and final percentage released (100 h). (c) Final percentage released as a function of the macroporosity of the CPFs and CPCs.

**Table 3**
Fitted parameters of the KP model, and type of limiting transport mechanism.

| Formulation | $n$ | $R^2$ | Transport mechanism |
|---|---|---|---|
| 1D-CPF | 0.63 | 0.9866 | Non-Fickian diffusion |
| 2D-CPF | 0.60 | 0.9982 | Non-Fickian diffusion |
| 3D-CPF | 0.57 | 0.9953 | Non-Fickian diffusion |
| 4D-CPF | 0.65 | 0.9961 | Non-Fickian diffusion |

matrices were more efficient than dense matrices, regardless of the amount of active principle loaded. The bacteriostatic effect of the materials tested decreased with macroporosity.

## 4. Discussion

The CPFs developed in this work combine a number of major advantages as bone grafting materials able to deliver antibiotic locally. Together with the injectability, self-setting ability and

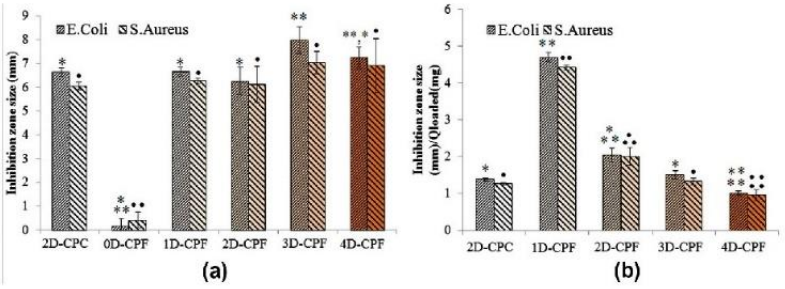


**Fig. 10.** (a) Antibacterial activity against *E. coli* and *S. aureus* of CPFs containing different amounts of Doxy and a non-foamed 2D-CPC counterpart. (b) Normalization of the antibacterial activity by the absolute amount of antibiotic in the materials. For *E. coli*, *, **, *** and **** indicate statistically significant differences ($P < 0.05$). For *S. aureus*, •, ••, ••• and •••• indicate statistically significant differences ($P < 0.05$).

**Table 4**
Calculated parameters for antibiotic-loaded CPCs and CPFs employed in the antibacterial tests: concentration of Doxy, apparent density and absolute amount of Doxy in the agar hole (0.23 $cm^3$).

| Material | $C_{doxy}$ (wt.%) | Apparent density (g $cm^{-3}$) | $Q_{doxy}$ (mg) in the agar defect |
|---|---|---|---|
| 2D-CPC | 1.76 | 1.290 | 5.22 ± 0.69 |
| 1D-CPF | 0.88 | 0.748 | 1.51 ± 0.71 |
| 2D-CPF | 1.76 | 0.808 | 3.27 ± 0.67 |
| 3D-CPF | 2.64 | 0.930 | 5.01 ± 1.41 |
| 4D-CPF | 3.52 | 0.932 | 7.55 ± 2.44 |

intrinsic nano/microporosity characteristic of CPCs, they exhibit a significant interconnected macroporosity that is known to be crucial for cell colonization, angiogenesis and, in general, for the events leading to bone regeneration [7,11,28]. This work demonstrated that the macroporosity of the injectable CPFs designed also had a significant impact in the control of the drug release kinetics of doxycycline hyclate.

To generate the macroporous structures, a 1 wt.% Tween80 solution was used as a foaming agent. Since the surface tension changes produced by antibiotic on this solution were minor (Fig. 2), they were not expected to significantly affect foamability. In contrast, a clear effect on the plastic limit was registered on the addition of high concentrations of Doxy (Fig. 3), suggesting that Doxy absorbed water, resulting in a drying effect on the unfoamed paste. An increased shear stress was thus needed to mix the powder phase with the foamed liquid phase, which can explain the partial collapse of the foamed template at high contents of Doxy, as observed in the optical microscope images (Fig. 5) and corroborated by the macroporosity results (Fig. 7a). However, this was not detrimental to their injectability which was maintained in all formulations (Fig. 4), and is an essential requirement to ensure their clinical applicability.

The general outlook of the material macrostructure obtained by micro-computed tomography reconstructions (Fig. 8) confirmed that the addition of Doxy reduced both the size of the macropores and the number of interconnections.

The addition of Doxy did not prevent the foam's setting reaction (Supplementary material Fig. S1), where the dissolution of α-TCP was followed by the precipitation of CDHA [4,11]:

$$Ca_3(PO_4)_{2(s)} + H_2O_{(l)} \rightarrow Ca_9(HPO_4)(PO_4)(OH)_{(s)}$$

However, the presence of the antibiotic was related to an increase in SSA (Table 2), which was associated with its effect on the microstructure of the CDHA crystals formed. In fact, it was suggested in a previous study [8] that, owing to its Ca-chelating ability, Doxy can act in this type of system as a nucleating agent, promoting the formation of smaller crystals and leading to a more homogeneous microstructure, as shown in Fig. 6. This is in agreement also with the disappearance (in the MIP diagram of the Doxy-containing samples (Fig. 7b)) of the peak at ~3–5 μm detected in the pristine foams.

The introduction of macroporosity in the CPCs clearly modified the drug release profile, as observed on comparing the 2D-CPF with its non-foamed counterpart 2D-CPC. The percentage released from CPFs was significantly higher in all cases compared with the 2D-CPC (Fig. 9b). However, the interdependence between Doxy concentration and macroporosity introduced additional complexity into the system. The addition of Doxy led to a progressive loss of total porosity as well as of interconnected macroporosity (Fig. 7a) and a reduction in the entrance pore size of the macropores (Fig. 7b). This was shown to be highly relevant for their drug release properties: different release kinetics were observed in the CPFs, depending on the amount of Doxy loaded; the rate of percentage released decreased with increasing Doxy concentrations, which can be related to the lower volume of macropores and their smaller size (Figs. 8 and 7b). Although CPFs were more porous than CPCs, and thus a lower amount of Doxy was present in the same volume, CPFs released a higher absolute amount of Doxy after 5 days, with a maximum of 1 mg for the 2D-CPF.

In addition, the uniform distribution of the drug in the matrix of all formulations studied was revealed by the progressive release observed, i.e. no initial burst (Fig. 9a). In general, the availability of active principles to the bone is limited and slow, compared with soft tissues or other organs, for instance. The onsite direct bioavailability of the active principle, in the present case doxycycline hyclate, maximized the efficiency of the treatment. The extended drug release profiles obtained with the present CPFs are highly desirable in controlled drug delivery matrices, as a reproducible rate and prolonged delivery are obtained, and allow a lower amount of drugs to be used [29].

For the treatment of infection, a high concentration of antibiotics is ideally needed in the first 1–2 days, and thereafter a prolonged release of a lower concentration should be maintained for another 4 weeks [30]. Although the lack of burst release may be a disadvantage when dealing with prophylactic therapy of infections, the CPFs designed here can be envisaged in this case as a complementary therapy to an initial parenteral or oral antibiotic administration, delivering Doxy onsite for the continuation of the treatment, and thus improving patient compliance. For instance, the 3D-CPF and 4D-CPF showed potential for release for 3 or 4 weeks, suitable for bone infection treatment.

The close relationship between different structural properties such as SSA, macroporosity, interconnected macroporosity, porosity and interconnected porosity was put forward by their direct

correlation with the percentage released by the CPFs using a linear fit (not shown). The quality of fit obtained, estimated through the correlation coefficient ($R^2$), was 0.842, 0.957, 0.918, 0.931 and 0.910 for SSA, macroporosity, interconnected macroporosity, porosity and interconnected porosity, respectively. The good correlation between the amount of macroporosity and the percentage of Doxy released (Fig. 9c) confirmed that macroporosity plays a key role in the drug release phenomena by enhancing fluid exchange and increasing the accessible surface, thus facilitating drug delivery and availability.

The fitting of the release profiles led to $n$ values between 0.50 and 1.00 (Table 3), which for a planar geometry corresponds to a non-Fickian diffusional release [31,32]. It is known that non-Fickian transport may be due to structural changes, temperature or saturation of the release media. As the experiments were performed in sink conditions, and following standards [26], this non-Fickian behaviour could be attributed to the self-setting nature of CPFs. Their microstructure evolving over time is responsible for the anomalous diffusion, as shown in previous works [8].

All antibiotic-containing CPFs showed bacteriostatic effect on both *E. coli* and *S. aureus* (Fig. 10a) in an agar diffusion test. *E. coli* was selected as the most commonly found bacteria in nosocomial infections, together with *S. aureus*, which is also very often responsible for osteoarticular infections. The results obtained were functions of both the matrix ability to release the active principle and the initial amount of active principle present in the material. In this type of test, where solid–solid contact, i.e. agar–material, is crucial for the diffusion of the antibiotic, the architecture of the material plays an important role: while the unfoamed CPC has optimum contact with the agar, the macroporosity of the CPFs reverts in few contact points with the agar, hampering the diffusion of the material. Additionally, no direct correlation can be sought between the release in liquid media in sink conditions with free diffusivity and the release established in agar. Nevertheless, this test has shown the antibacterial efficiency of the material.

As the same volume of material was placed in the agar, for the same weight percent of Doxy in the material the absolute quantity of antibiotic present is lower when the matrix used is more porous. The inhibition zone size was thus normalized by the absolute quantity of Doxy present in the material. The results proved that, even in the static conditions of this test and the lower amount of contact points with the agar, the interconnected macroporous structure exhibited by the CPFs was more efficient than their microporous counterpart, namely CPCs, in terms of ensuring antibiotic availability (Fig. 10b, Table 4).

Different antibiotic release profiles are reported in the literature for CPCs: from slow releasing dosage forms [8,33–36] to very fast burst release of the antibiotic [37,38]. Although some approaches successfully prevented the risk of antibiotic resistance by releasing almost all the drug loaded [39], the dosage forms did not present an adequate macrostructure to enhance bone ingrowth. The CPFs presented in this study exhibit a progressive release profile up to 1 mg in 5 days, corresponding to 55% of the quantity loaded in 2D-CPC, with potential for complete release and a simultaneous interconnected macroporosity of ~25% (Fig. 9c) that is expected to enhance, in addition, tissue colonization.

It has been proposed that tetracyclines inhibit bone resorption through different mechanisms such as decreased osteoclast activity, so incomplete release of the drug could be detrimental [40]. In the case of CPCs, it has been commonly observed that 100% release is not reached, regardless of the active principle used [6]. This aspect, which can be very significant in the case of CPCs, is expected to be minimized thanks to the macroporous structure of the foams. In fact, it has been shown that the presence of an interconnected network of macropores in the material enhances its resorption rate [41]. Thus, in case there was some unreleased residual Doxy in the material, the low quantities employed in the loading of the CPFs, and their macroporosity-enhancing fluid circulation and resorption rate would minimize the inhibiting effects of Doxy on osteoclasts, in addition to potential bacterial resistance.

## 5. Conclusion

CPFs were shown to be attractive drug delivery systems for osteoarticular applications compared with CPCs, since they overcome several of the latters' limitations. First, CPFs exhibited an interconnected macroporous structure while maintaining injectability, cohesion and self-setting ability, thus providing a template for bone ingrowth. Second, CPFs were more efficient as drug release systems, since less active principle was loaded and higher percentages and absolute amounts were released after 5 days, with potential for longer release. The therapeutic effect is expected to increase, while the risk of generating antibiotic-resistant bacteria as a result of the antibiotic still present in the matrix is reduced. Finally, the control of both macrostructure and release profile allowed the design of versatile and efficient drug delivery systems that can be adapted to different applications. While CPFs are limited to non-load-bearing applications, the combination of a prophylactic antibiotic release with a biomimetic composition and structure makes them an attractive solution to today's challenges in the fields of orthopaedics, spine and maxillofacial bone regeneration.

## Acknowledgements

Authors acknowledge the Spanish Government for financial support through Project MAT2012-38438-C03-01, co-funded by the EU through European Regional Development Funds, and Ramon y Cajal fellowship of CC. Support for the research of MPG was received through the "ICREA Academia" prize for excellence in research, funded by the Generalitat de Catalunya. The authors thank Dr. A. Navarro for kindly allowing access to his lab for surface tension determinations. The authors also acknowledge Dr. S. Meille and Prof. J. Chevalier for access to the μCT instrument at the UMR CNRS 5510 (MATEIS), Insa Lyon.

## Appendix A. Figures with essential colour discrimination

Certain figures in this article, particularly Figs. 3, 4, 7, 9, 10 are difficult to interpret in black and white. The full colour images can be found in the on-line version, at http://dx.doi.org/10.1016/j.actbio.2014.10.031

## Appendix B. Supplementary data

Supplementary data associated with this article can be found, in the online version, at http://dx.doi.org/10.1016/j.actbio.2014.10.031.

## References

[1] Dorozhkin SV. Calcium orthophosphate cements for biomedical application. J Mater Sci 2008;43:3028–57.
[2] Ginebra M-P, Traykova T, Planell JA. Calcium phosphate cements as bone drug delivery systems: a review. J Control Release 2006;113:102–10.
[3] Ginebra M-P, Traykova T, Planell JA. Calcium phosphate cements: competitive drug carriers for the musculoskeletal system? Biomaterials 2006;27:2171–7.
[4] Espanol M, Perez RA, Montufar EB, Marichal C, Sacco A, Ginebra M-P. Intrinsic porosity of calcium phosphate cements and its significance for drug delivery and tissue engineering applications. Acta Biomater 2009;5:2752–62.
[5] Verron E, Khairoun I, Guicheux J, Bouler J-M. Calcium phosphate biomaterials as bone drug delivery systems: a review. Drug Discov Today 2010;15:547–52.
[6] Ginebra M-P, Canal C, Espanol M, Pastorino D, Montufar EB. Calcium phosphate cements as drug delivery materials. Adv Drug Deliv Rev 2012;64:1090–110.

[7] Otsuki B, Takemoto M, Fujibayashi S, Neo M, Kokubo T, Nakamura T. Pore throat size and connectivity determine bone and tissue ingrowth into porous implants: three-dimensional micro-CT based structural analyses of porous bioactive titanium implants. Biomaterials 2006;27:5892–900.
[8] Canal C, Pastorino D, Mestres G, Schuler P, Ginebra M-P. Relevance of microstructure for the early antibiotic release of fresh and pre-set calcium phosphate cements. Acta Biomater 2013;9:8403–12.
[9] Tsourvakas S. Local antibiotic therapy in the treatment of bone and soft tissue infections. In: Danilla S, editor. Selected topics in plastic reconstructive surgery. InTech, Open Access; 2012. p. 17–44.
[10] Habraken WJEM, Wolke JGC, Jansen JA. Ceramic composites as matrices and scaffolds for drug delivery in tissue engineering. Adv Drug Deliv Rev 2007;59:234–48.
[11] Montufar EB, Traykova T, Gil C, Harr I, Almirall A, Aguirre A, et al. Foamed surfactant solution as a template for self-setting injectable hydroxyapatite scaffolds for bone regeneration. Acta Biomater 2010;6:876–85.
[12] Montufar EB, Traykova T, Planell JA, Ginebra M-P. Comparison of a low molecular weight and a macromolecular surfactant as foaming agents for injectable self setting hydroxyapatite foams: polysorbate 80 versus gelatine. Mater Sci Eng C 2011;31:1498–504.
[13] Ginebra M-P, Delgado J-A, Harr I, Almirall A, Del Valle S, Planell JA. Factors affecting the structure and properties of an injectable self-setting calcium phosphate foam. J Biomed Mater Res A 2007;80:351–61.
[14] Saint-Jalmes A, Peugeot M-L, Ferraz H, Langevin D. Differences between protein and surfactant foams: microscopic properties, stability and coarsening. Colloids Surf A Physicochem Eng Aspects 2005;263:219–25.
[15] Pountos I, Georgouli T, Bird H, Kontakis G, Giannoudis PV. The effect of antibiotics on bone healing: current evidence. Expert Opin Drug Saf 2011;10:935–45.
[16] Kallala R, Graham SM, Nikkhah D, Kyrkos M, Heliotis M, Mantalaris A, et al. *In vitro* and in vivo effects of antibiotics on bone cell metabolism and fracture healing. Expert Opin Drug Saf 2012;11:15–32.
[17] Ong SM, Taylor GJS. Doxycycline inhibits bone resorption by human interface membrane cells from aseptically loose hip replacements. J Bone Joint Surg Br 2003;85:456–61.
[18] Preshaw PM, Hefti AF, Jepsen S, Etienne D, Walker C, Bradshaw MH. Subantimicrobial dose doxycycline as adjunctive treatment for periodontitis. A review. J Clin Periodontol 2004;31:697–707.
[19] Job-Deslandre C, Krebs S, Kahan A. Chronic recurrent multifocal osteomyelitis: five-year outcomes in 14 pediatric cases. Joint Bone Spine 2001;68:245–51.
[20] Roeder B, Van Gils CC, Maling S. Antibiotic beads in the treatment of diabetic pedal osteomyelitis. J Foot Ankle Surg 2000;39:124–30.
[21] Bartkowski SB, Zapala J, Heczko P, Szuta M. Actinomycotic osteomyelitis of the mandible: review of 15 cases. J Cranio-Maxillo-Facial Surg 1998;26:63–7.
[22] Thompson S, Townsend R. Pharmacological agents for soft tissue and bone infected with MRSA: which agent and for how long? Injury 2011;42(Suppl. 5):S7–S10.
[23] Bohner M, Baroud G. Injectability of calcium phosphate pastes. Biomaterials 2005;26:1553–63.
[24] Montufar EB, Maazouz Y, Ginebra MP. Relevance of the setting reaction to the injectability of tricalcium phosphate pastes. Acta Biomater 2013;9:6188–98.
[25] Almirall A, Larrecq G, Delgado J. Fabrication of low temperature macroporous hydroxyapatite scaffolds by foaming and hydrolysis of an α-TCP paste. Biomaterials 2004;25:3671–80.
[26] United States Pharmacopeia and National Formulary. Dissolution <711>. Rockville, MD: US Pharmacopeial Convention; 2008. p. 267–274.
[27] Bauer AW, Kirby WM, Sherris JC, Turck M. Antibiotic susceptibility testing by a standardized single disk method. Am J Clin Pathol 1966;45:493–6.
[28] Mastrogiacomo M, Scaglione S, Martinetti R, Dolcini L, Beltrame F, Cancedda R, et al. Role of scaffold internal structure on in vivo bone formation in macroporous calcium phosphate bioceramics. Biomaterials 2006;27:3230–7.
[29] Ding X, Alani A, Robinson J. Remington. The science and practice of pharmacy. In: Hendrickson R, editor. Remington science and practice of pharmacy. Groningen: Lippincott Williams & Wilkins; 2006. p. 939–64.
[30] Geurts J, Chris Arts JJ, Walenkamp GHIM. Bone graft substitutes in active or suspected infection. Contra-indicated or not? Injury 2011;42(Suppl. 2):S82–6.
[31] Siepmann J, Peppas NA. Higuchi equation: derivation, applications, use and misuse. Int J Pharm 2011;418:6–12.
[32] Ritger PL, Peppas NA. A simple equation for description of solute release I. Fickian and non-fickian release from non-swellable devices in the form of slabs, spheres, cylinders or discs. J Control Release 1987;5:23–36.
[33] Liu W, Chang J. *In vitro* evaluation of gentamicin release from a bioactive tricalcium silicate bone cement. Mater Sci Eng C 2009;29:2486–92.
[34] Kisanuki O, Yajima H, Umeda T, Takakura Y. Experimental study of calcium phosphate cement impregnated with dideoxy-kanamycin B. J Orthop Sci 2007;12:281–8.
[35] Takechi M, Miyamoto Y, Ishikawa K, Nagayama M, Kon M, Asaoka K, et al. Effects of added antibiotics on the basic properties of anti-washout-type fast-setting calcium phosphate cement. J Biomed Mater Res 1998;39:308–16.
[36] Vorndran E, Geffers M, Ewald A, Lemm M, Nies B, Gbureck U. Ready-to-use injectable calcium phosphate bone cement paste as drug carrier. Acta Biomater 2013;9:9558–67.
[37] Alkhraisat MH, Rueda C, Cabrejos-Azama J, Lucas-Aparicio J, Mariño FT, Torres García-Denche J, et al. Loading and release of doxycycline hyclate from strontium-substituted calcium phosphate cement. Acta Biomater 2010;6:1522–8.
[38] David Chen C-H, Chen C-C, Shie M-Y, Huang C-H, Ding S-J. Controlled release of gentamicin from calcium phosphate/alginate bone cement. Mater Sci Eng C 2011;31:334–41.
[39] Schnieders J, Gbureck U, Vorndran E, Schossig M, Kissel T. The effect of porosity on drug release kinetics from vancomycin microsphere/calcium phosphate cement composites. J Biomed Mater Res B Appl Biomater 2011;99:391–8.
[40] Bettany JT, Peet NM, Wolowacz RG, Skerry TM, Grabowski PS. Tetracyclines induce apoptosis in osteoclasts. Bone 2000;27:75–80.
[41] Del Valle S, Mino N, Munoz F, Gonzalez A, Planell JA, Ginebra MP. *In vivo* evaluation of an injectable macroporous calcium phosphate cement. J Mater Sci – Mater Med 2007;18:353–61.

# 5. Discussion

## 5.1. Design of multifunctional biomaterials

Multifunctional materials are able to provide different effects by joining a number of features. The design of multifunctional biomaterials is focused on maximizing their clinical efficiency, and the general clinical procedure by facilitating the procedure, enhancing the clinical outcome or increasing its safety. Focusing on bone regeneration, the combined functions of bone regeneration and antibiotic release provide clinically relevant solutions to prevent or contribute to the treatment of bone infections.

The bioceramics used nowadays in clinics provide only limited benefits to the overall procedure when considering morbidity or effective local drug delivery, to prevent or treat certain pathologies, such as infections. Calcium phosphate cements (CPCs) present attractive properties when combining antibiotic release and bone regeneration as they are injectable biomaterials allowing minimally invasive surgeries. Additionally, different drugs, such as antibiotics may be added in the cement during preparation and its release properties can be tuned according to the composition of the CPC (**Paper III**). This is highly desirable in order to tune its release profile once implanted.

A thorough review of calcium phosphate cements used as drug delivery devices (DDS, **Paper I**) highlighted the versatility of CPCs due to their micro- nano- porous nature [79,80,47,81,72,71,82–89] allowing the loading and release of a wide range of active principles including ions, antibiotics, anti-cancer drugs or growth factors. The release profile of these drugs from CPCs depends on their physico-chemical properties while the effect of the setting reaction of CPCs on the release profile has not been investigated. The research studies performed also revealed that the link between in vitro and in vivo release profile are not straightforward and suggest further investigation should be performed [90].

Finally, to the best of our knowledge, up to now dense CPCs have been designed and studied as DDS. Macroporous CPCs are attractive scaffolds for bone regeneration but their potential as DDS has not been explored.

## 5.2. The role of material properties in the control of the performance of DDS

The design of DDS is complex due to the tight interactions between the active principle and the properties of the biomaterial. The deep understanding of the behavior of the DDS is a key-point to be able to reach a clinically relevant release profile of the active principle. Different phenomena should be taken into account including the interaction between the active principle and the matrix loaded, especially considering the setting reaction in CPCs, the loading method and the characteristics of the matrix. In the case of CPCs, porosity was identified as a key parameter of paramount interest to maximize the efficacy of CPCs for both functions:

- support of bone regeneration as porosity is a key parameter in bone regenerative processes [79,91–93].

- use as DDS, as porosity affects the active principle release profile, and thus the benefit of introducing it in the CPC matrix [79,47,88,94].

In this Thesis, a thorough characterization of the micro- and nano- porosity of CPCs was performed, highlighting the bias and differences between the techniques used up to now (Mercury intrusion porosimetry and Nitrogen sorption) [95][96–100][101,102] and adapting a technique previously used in the construction field: thermoporosimetry to CPCs (**Paper II**) [103–105]. The conclusions drawn from this study shed new light for the correct interpretation of the results extracted from these techniques, the identification of bias inherent to each of these techniques as for instance the network effect, the ink-bottle effect, the drying of the sample or the assumptions of each technique [47].

Furthermore, two phenomena are critical in order to deeply understand the characteristics of CPCs as DDS: the influence of the setting reaction and of the porosity on the release profile. Indeed, the complexity of the dissolution-precipitation process of CPCs in the early stages of implantation should be understood and linked to the evolution of porosity over time in order to study its consequences on the release profile and clinical efficacy. The effect of the microstructure and porosity on the drug release profile were recorded in drug-loaded CPCs with special focus on obtaining insights on the evolving microstructure of the cements (**Paper III**). To that aim, CPCs prepared with two different L/P ratios were prepared, adding an antibiotic (doxycycline hyclate) in the liquid phase. The drug release profile was measured either after 1 hour of setting, or 7 days in order to identify the effect of the evolving microstructure on the drug release profile, in the case of the CPCs set for 1 hour only (**Paper III**). It was shown that the addition of antibiotic significantly affected the CPCs' microstructure and, consequently, the shape of the release profile and amount released after 5 days. Porosity, regardless of the effect of the setting reaction, also affected the amount released.

Macroporosity is of paramount interest in bone regenerative processes and it can increase the fluid circulation in the material and thus affect the percentage released from the material. An incomplete release, as identified in previous works (**Paper I**) may be detrimental and even compensate the benefits brought by the local release of an active principle, and especially in the case of an antibiotic as very low local concentrations of antibiotic in the tissues during the slow degradation of the material. This phenomenon may lead to the apparition of antibiotic-resistant bacteria. The addition of interconnected macroporosity to CPCs was performed by foaming (**Paper IV**) and the effect of the addition of doxycycline hyclate on foam properties and the drug release profiles were recorded for different antibiotic loading. This work demonstrated, similarly to the conclusion of previous works (**Paper III**) that the addition of antibiotic clearly affected the structure of the foams. An important conclusion of this work is that the percentage released from CPFs was higher than the percentage released from CPCs thanks to their macroporous network. In addition, the efficiency of the matrix was enhanced when the macroporosity was higher. In other words the effect of each mg of antibiotic loaded was maximized when the matrix used presented a higher macroporosity.

The benefits brought by the addition of macroporosity in CPCs were clear, and suggested that a lower amount of antibiotic could be used, as compared to CPCs; that the bone regenerative processes should be supported by the interconnected network of macropores and that the risk of generating antibiotic-resistant bacteria was minimized. However, it should be noted that the mechanical properties of the material decreased when macroporosity was added, and that the release of antibiotic was still not complete.

## 5.3. Clinical implications

Currently, local antibiotic release combined with bone regeneration is not common in operating rooms. The conventional procedure includes prophylactic administration of antibiotic and posterior treatment systemically. The rationale of using antibiotic-loaded synthetic bone grafts is to both prevent infections potentially caused by the surgery itself and/or support the actual treatment of osteomyelitis by generating a high local antibiotic concentration.

Accurate control of the effect of the setting reaction and of the porosity from the micro to the macroscale on the release profile of antibiotic from CPCs, studied in this PhD Thesis, is highly relevant clinically as it may increase or decrease the efficacy of the antibiotic treatment.

Calcium phosphate foams respond to the definition of multifunctional biomaterials as they were shown to be able to simultaneously act as DDS and provide an adequate scaffold for bone regeneration. Moreover, the antibiotic release from CPFs was more efficient than when using CPCs, leading clinically to using lower doses with an enhanced antimicrobial effect.

The work developed in this PhD thesis opens the door to the use of different active principles in combination with the injectable CPFs such as anti-cancer, antiosteoporotic or other low molecular weight drugs or ions, or biological agents to stimulate bone repair processes. This provides a framework for potential expansion and use of CPF-based DDS in orthopedics.

# 6. Conclusions and future perspectives

## 6.1. Conclusions

This Thesis deals with the development, characterization with a special focus on porosity and optimization of calcium phosphate cements (CPCs) and foams (CPFs) as local drug delivery devices. The main finding are summarized below:

- *Regarding the characterization of porosity of CPCs:*

**1.** A new method, the thermoporosimetry, was adapted in order to characterize the micro- and nano- porosity of calcium phosphate cements. The method showed attractive features such as the evaluation of the pore entrance size and pore size distribution without needing a drying step prior to the measurement.

**2.** Three different methods to evaluate the porosity of CPCs were compared: mercury intrusion porosimetry, nitrogen sorption and thermoporosimetry. Both thermoporosimetry and nitrogen sorption showed reasonable agreement and were adapted to evaluate the micro- and nano-porosity and topography. Mercury intrusion porosimetry was able to evaluate a wider range of pore entrance sizes and, although destructive, was the most adequate method to characterize CPCs.

**3.** Thermoporosimetry, and specially nitrogen sorption, besides being non-destructive techniques, and although covering a limited size range, provided complementary information regarding pore structure associated to crystal shape at the nanoscale, recording both Pore size distribution and Pore entrance size distribution in a single experiment. Mercury intrusion porosimetry tended to register smaller sizes, especially at low Liquid/Powder ratios, due to the network effect, that has a strong influence on the outcome of this technique.

- *Regarding the use of CPCs as local drug delivery devices*

**1.** An antibiotic, Doxycycline hyclate, was successfully loaded and released from CPCs. Its addition modified the microstructure and morphology of CPCs, but did not hinder its antimicrobial activity. Doxycycline hyclate was suggested to act as nucleating agent for hydroxyapatite crystals.

**2.** The setting reaction of CPCs had an effect on the release profile of doxycycline hyclate. The fresh CPCs released following a two-step profile: fast in the first hours followed by a linear release while the set CPCs release following a mechanism controlled by Fickian diffusion.

**3.** CPCs were shown to release at best 5% of their content of Doxycycline after 5 days (100 h) in vitro. Moreover, CPCs with higher porosity released a higher proportion of antibiotic.

- *Regarding the use of CPFs as local drug delivery devices*

**1.** Doxycycline hyclate, a tetracycline antibiotic, was successfully added to CPFs, and strongly affected the network of interconnected macropores. Indeed, macroporosity decreased with addition of antibiotic due to its drying effect and role as nucleating agent of hydroxyapatite crystals.

**2.** CPFs loaded with different amounts of antibiotic released progressively a higher amount of Doxycycline than CPCs. Interestingly, CPFs could release up to 55 % of its content after 100 h, corresponding to 1 mg locally.

**3.** From an antimicrobial point of view, CPFs were shown to be more efficient matrices to release drug than CPCs, as less active principle was necessary to reach similar antimicrobial results in vitro, due to the superior release profile recorded.

## **6.2.** Future perspectives

**1.** The long-term release profiles of CPCs and CPFs is a parameter of interest that shoud be assessed in order to evaluate the viability of these biomaterials to be used clinically as local drug delivery devices, replacing totally the systemic administration of antibiotic and providing adequate antibiotic administration over at least three weeks.

**2.** The *in vivo* antimicrobial efficacy and bone regenerative properties of antibiotic-loaded CPCs and CPFs should be carefully evaluated, as a first pre-clinical assessment of their potential as drug delivery devices.

**3.** The optimization of the mechanical properties of calcium phosphate foams would represent an additional functionality together with the additional clinical advantages, including the regenerative potential and antimicrobial functions.

# References


[1] Bronner F, Farach-Carson MC, Mikos AG. Engineering of functional skeletal tissues. October 2007.

[2] McCarthy EF, Khurana JS, Zhang PJ. Essentials in Bone and Soft-Tissue Pathology. Springer Verlag; 2009.

[3] Dorozhkin S V. Calcium Orthophosphates in Nature, Biology and Medicine. Materials (Basel) 2009;2:399–498.

[4] Wang X, Nyman JS, Dong X, Leng H, Reyes M. Fundamental Biomechanics in Bone Tissue Engineering. Synth Lect Tissue Eng 2010;2:1–225.

[5] Stamatoukou AG, Grimer RJ. Malignant primary tumours of bone. Surg 2006;24:392–6.

[6] Kanis JA. Bone and cancer: Pathophysiology and treatment of metastases. Bone, vol. 17, 1995, p. 101S – 105S.

[7] Buijs JT, van der Pluijm G. Osteotropic cancers: from primary tumor to bone. Cancer Lett 2009;273:177–93.

[8] Colvin L, Fallon M. Challenges in cancer pain management--bone pain. Eur J Cancer 2008;44:1083–90.

[9] Juárez P, Guise TA. TGF-β in cancer and bone: Implications for treatment of bone metastases. Bone 2011;48:23–9.

[10] Sterling JA, Edwards JR, Martin TJ, Mundy GR. Advances in the biology of bone metastasis: How the skeleton affects tumor behavior. Bone 2011;48:6–15.

[11] Lin P, Frink S. Intralesional treatment of bone tumors. Oper Tech Orthop 2004;14:251–8.

[12] Silva ACV, da Rosa MI, Fernandes B, Lumertz S, Diniz RM, dos Reis Damiani MEF. Factors associated with osteopenia and osteoporosis in women undergoing bone mineral density test. Rev Bras Reumatol (English Ed 2014:6–11.

[13] Tanriover MD, Oz SG, Tanriover A, Kilicarslan A, Turkmen E, Guven GS, et al. Hip fractures in a developing country: osteoporosis frequency, predisposing factors and treatment costs. Arch Gerontol Geriatr 2010;50:e13–8.

[14] Klein-Nulend J, van Oers RFM, Bakker AD, Bacabac RG. Bone cell mechanosensitivity, estrogen deficiency, and osteoporosis. J Biomech 2014;48:855–65.

[15] Bauer NB, Khassawna T El, Goldmann F, Stirn M, Ledieu D, Schlewitz G, et al. Characterization of bone turnover and energy metabolism in a rat model of primary and secondary osteoporosis. Exp Toxicol Pathol 2015;67:287–96.

[16] Garnero P. New developments in biological markers of bone metabolism in osteoporosis. Bone 2014;66:46–55.

[17] Brown JP, Albert C, Nassar B a., Adachi JD, Cole D, Davison KS, et al. Bone turnover markers in the management of postmenopausal osteoporosis. Clin Biochem 2009;42:929–42.

[18] Marie PJ. The calcium-sensing receptor in bone cells: A potential therapeutic target in osteoporosis. Bone 2010;46:571–6.

[19] Ochsner PE, Hailemariam S. Histology of osteosynthesis associated bone infection. Injury 2006;37 Suppl 2:S49–58.

[20] Axford JS. Joint and bone infections. Medicine (Baltimore) 2010;38:194–201.

[21] Thompson S, Townsend R. Pharmacological agents for soft tissue and bone infected with MRSA: which agent and for how long? Injury 2011;42 Suppl 5:S7–10.

[22] Brown WE, Chow LC. A new calcium phosphate setting cement. J Dent Res 1983;62:672.

[23] LeGeros RZ, Chohayeb A, Shulman A. Apatitic calcium phosphates: possible dental restorative materials. J Dent Res 1982;61:343.

[24] Friedman CD, Costantino PD, Takagi S, Chow LC. Bonesource hydroxyapatite cement: A novel biomaterial for craniofacial skeletal tissue engineering and reconstruction. J Biomed Mater Res 1998;43:428–32.

[25] Kamerer DB, Hirsch BE, Snyderman CH, Costantino P, Friedman CD. Hydroxyapatite cement: a new method for achieving watertight closure in transtemporal surgery. Am J Otol 1994;15:47–9.

[26] Constantz BR, Ison IC, Fulmer MT, Poser RD, Smith ST, VanWagoner M, et al. Skeletal repair by in situ formation of the mineral phase of bone. Science (80- ) 1995;267:1796–9.

[27] Horstmann WG, Verheyen CCPM, Leemans R. An injectable calcium phosphate cement as a bone-graft substitute in the treatment of displaced lateral tibial plateau fractures. Injury 2003;34:141–4.

[28] Strauss EJ, Egol KA. The management of ankle fractures in the elderly. Injury 2007;38 Suppl 3:S2–9.

[29] Liverneaux PA. Osteoporotic distal radius curettage - filling with an injectable calcium phosphate cement. A cadaveric study. Eur J Orthop Surg Traumatol 2004;15:1–6.

[30] Welch RD, Zhang H, Bronson DG. Experimental tibial plateau fractures augmented with calcium phosphate cement or autologous bone graft. J Bone Joint Surg Am 2003;85:222.

[31] Aral A, Yalçin S, Karabuda ZC, Anil A, Jansen JA, Mutlu Z. Injectable calcium phosphate cement as a graft material for maxillary sinus augmentation: an experimental pilot study. Clin Oral Implants Res 2008;19:612–7.

[32] Bai B, Jazrawi LM, Kummer FJ, Spivak JM. The use of an injectable, biodegradable calcium phosphate bone substitute for the prophylactic augmentation of osteoporotic vertebrae and the management of vertebral compression fractures. Spine (Phila Pa 1976) 1999;24:1521–6.

[33] Schildhauer T, Bennett A, Wright T, Lane J, O'Leary P. Intravertebral body reconstruction with an injectable in situ-setting carbonated apatite: Biomechanical evaluation of a minimally invasive technique. J Orthop Res 1999;17:67–72.

[34] Maestretti G, Cremer C, Otten P, Jakob RP. Prospective study of standalone balloon kyphoplasty with calcium phosphate cement augmentation in traumatic fractures. Eur Spine J 2007;16:601–10.

[35] Libicher M, Hillmeier J, Liegibel U, Sommer U, Pyerin W, Vetter M, et al. Osseous integration of calcium phosphate in osteoporotic vertebral fractures after kyphoplasty: initial results from a clinical and experimental pilot study. Osteoporos Int 2006;17:1208–15.

[36] Mermelstein LE, Chow LC, Friedman CD, Crisco JJ. The reinforcement of cancellous bone screws with calcium phosphate cement. J Orthop Trauma 1996;10:15–20.

[37] Moore DC, Maitra RS, Farjo LA, Graziano GP, Goldstein SA. Restoration of pedicle screw fixation with an in situ setting calcium phosphate cement. Spine (Phila Pa 1976) 1997;22:1696–705.

[38] Ooms E, Wolke J, Van der Waerden J, Jansen J. Use of injectable calcium-phosphate cement for the fixation of titanium implants: An experimental study in goats. J Biomed Mater Res Part B Appl Biomater 2003;66:447–56.

[39] Takemasa R, Kiyasu K, Tani T, Inoue S. Validity of Calcium Phosphate Cement Vertebroplasty for Vertebral Non-Union after Osteoporotic Fracture with Middle Column Involvement. Spine J 2007;7:148S – 148S.

[40] Tomita S, Kin A, Yazu M, Abe M. Biomechanical evaluation of kyphoplasty and vertebroplasty with calcium phosphate cement in a simulated osteoporotic compression fracture. J Orthop Sci 2003;8:192–7.

[41] Lewis G. Injectable bone cements for use in vertebroplasty and kyphoplasty: State-of-the-art review. J Biomed Mater Res Part B Appl Biomater 2006;76:456–68.

[42] Montufar EB, Traykova T, Schacht E, Ambrosio L, Santin M, Planell J a, et al. Self-hardening calcium deficient hydroxyapatite/gelatine foams for bone regeneration. J Mater Sci Mater Med 2010;21:863–9.

[43] Morgan E, Yetkinler D, Constantz B, Dauskardt R. Mechanical properties of carbonated apatite bone mineral substitute: strength, fracture and fatigue behaviour. J Mater Sci Mater Med 1997;8:559–70.

[44] Ginebra MP, Fernandez E, De Maeyer E a. PA, Verbeeck RMHM, Boltong MGG, Ginebra J, et al. Setting Reaction and Hardening of an Apatitic Calcium Phosphate Cement. J Dent Res 1997;76:905–12.

[45] Ginebra MP, Fernandez E, Driessens FCM, Planell JA. Modeling of the hydrolysis of alpha-tricalcium phosphate. J Am Ceram Soc 1999;82:2808–12.

[46] Chen WC, Lin JHC, Ju CP. Transmission electron microscopic study on setting mechanism of tetracalcium phosphate/dicalcium phosphate anhydrous-based calcium phosphate cement. J Biomed Mater Res Part A 2003;64:664–71.

[47] Espanol M, Perez RA, Montufar EB, Marichal C, Sacco A, Ginebra MP. Intrinsic porosity of calcium phosphate cements and its significance for drug delivery and tissue engineering applications. Acta Biomater 2009;5:2752–62.

[48] Ginebra MP, Driessens FCM, Planell JA. Effect of the particle size on the micro and nanostructural features of a calcium phosphate cement: A kinetic analysis. Biomaterials 2004;25:3453–62.

[49] Bohner M, Gbureck U. Technological issues for the development of more efficient calcium phosphate bone cements: a critical assessment. Biomaterials 2005;26:6423–9.

[50] Chow LC. Next generation calcium phosphate-based biomaterials. Dent Mater J 2009;28:1–10.

[51] Ginebra MP, Espanol M, Montufar EB, Perez R a, Mestres G. New processing approaches in calcium phosphate cements and their applications in regenerative medicine. Acta Biomater 2010;6:2863–73.

[52] Gauthier O, Bouler J-M, Aguado E, Pilet P, Daculsi G. Macroporous biphasic calcium phosphate ceramics: influence of macropore diameter and macroporosity percentage on bone ingrowth. Biomaterials 1998;19:133–9.

[53] Von Doernberg MC, von Rechenberg B, Bohner M, Grünenfelder S, van Lenthe GH, Müller R, et al. In vivo behavior of calcium phosphate scaffolds with four different pore sizes. Biomaterials 2006;27:5186–98.

[54] Frayssinet P, Rouquet N. High compressive strength macroporous calcium phosphate ceramics for bone repair. J Biomech 1998:31100.

[55] Xu HHK, Quinn JB. Calcium phosphate cement containing resorbable fibers for short-term reinforcement and macroporosity. Biomaterials 2002;23:193–202.

[56] Lopez-Heredia MA, Sariibrahimoglu K, Yang W, Bohner M, Yamashita D, Kunstar A, et al. Influence of the pore generator on the evolution of the mechanical properties and the porosity and interconnectivity of a calcium phosphate cement. Acta Biomater 2012;8:404–14.

[57] Xue Z, Zhang H, Jin A, Ye J, Ren L, Ao J, et al. Correlation between degradation and compressive strength of an injectable macroporous calcium phosphate cement. J Alloys Compd 2012;520:220–5.

[58] Chen W, Zhou H, Tang M, Weir MD, Bao C, Xu H. Gas-foaming calcium phosphate cement scaffold encapsulating human umbilical cord stem cells. Tissue Eng Part A 2011;21201:1–38.

[59] Montufar EB, Traykova T, Gil C, Harr I, Almirall A, Aguirre A, et al. Foamed surfactant solution as a template for self-setting injectable hydroxyapatite scaffolds for bone regeneration. Acta Biomater 2010;6:876–85.

[60] Perut F, Montufar EB, Ciapetti G, Santin M, Salvage J, Traykova T, et al. Novel soybean/gelatine-based bioactive and injectable hydroxyapatite foam: material properties and cell response. Acta Biomater 2010;7:1780–7.

[61] Almirall A, Larrecq G, Delgado JA, Martínez S, Planell JA, Ginebra MP. Fabrication of low temperature macroporous hydroxyapatite scaffolds by foaming and hydrolysis of an α-TCP paste. Biomaterials 2004;25:3671–80.

[62] Geurts J, Chris Arts JJ, Walenkamp GHIM. Bone graft substitutes in active or suspected infection. Contra-indicated or not? Injury 2011;42 Suppl 2:S82–6.

[63] Montufar EB, Traykova T, Planell JA, Ginebra MP. Comparison of a low molecular weight and a macromolecular surfactant as foaming agents for injectable self setting hydroxyapatite foams: Polysorbate 80 versus gelatine. Mater Sci Eng C 2011;31:1498–504.

[64] Navarro M, del Valle S, Martínez S, Zeppetelli S, Ambrosio L, Planell JA, et al. New macroporous calcium phosphate glass ceramic for guided bone regeneration. Biomaterials 2004;25:4233–41.

[65] Miño-Fariña N, Muñoz-Guzón F, López-Peña M, Ginebra MP, Del Valle-Fresno S, Ayala D, et al. Quantitative analysis of the resorption and osteoconduction of a macroporous calcium phosphate bone cement for the repair of a critical size defect in the femoral condyle. Vet J 2009;179:264–72.

[66] Jain KK. Drug delivery systems - An overview. Methods Mol Biol 2008;437:1–50.

[67] Cheng EY, Nimphius N, Hennen CR. Antibiotic therapy and the anesthesiologist. J Clin Anesth 1995;7:425–39.

[68] Praveen S, Rohaizak M. Local antibiotics are equivalent to intravenous antibiotics in the prevention of superficial wound infection in inguinal hernioplasty. Asian J Surg 2009;32:59–63.

[69] Schwach-Abdellaoui K, Vivien-Castioni N, Gurny R. Local delivery of antimicrobial agents for the treatment of periodontal diseases. Eur J Pharm Biopharm 2000;50:83–99.

[70] Nandi SK, Mukherjee P, Roy S, Kundu B, De DK, Basu D. Local antibiotic delivery systems for the treatment of osteomyelitis – A review. Mater Sci Eng C 2009;29:2478–85.

[71] Ginebra MP, Traykova T, Planell JA. Calcium phosphate cements: Competitive drug carriers for the musculoskeletal system? Biomaterials 2006;27:2171–7.

[72] Ginebra MP, Canal C, Espanol M, Pastorino D, Montufar EB. Calcium phosphate cements as drug delivery materials. Adv Drug Deliv Rev 2012;64:1090–110.

[73] Mestres G, Kugiejko K, Pastorino D, Unosson J, Öhman C, Karlsson Ott M, et al. Changes in the drug release pattern of fresh and set simvastatin-loaded brushite cement. Mater Sci Eng C 2016;58:88–96.

[74] Loca D, Sokolova M, Locs J, Smirnova A, Irbe Z. Calcium phosphate bone cements for local vancomycin delivery. Mater Sci Eng C Mater Biol Appl 2015;49:106–13.

[75] Van de Watering FCJ, Molkenboer-Kuenen JDM, Boerman OC, van den Beucken JJJP, Jansen JA. Differential loading methods for BMP-2 within injectable calcium phosphate cement. J Control Release 2012;164:283–90.

[76] Akkineni AR, Luo Y, Schumacher M, Nies B, Lode A, Gelinsky M. 3D plotting of growth factor loaded calcium phosphate cement scaffolds. Acta Biomater 2015.

[77] Irbe Z, Loca D, Vempere D, Berzina-Cimdina L. Controlled release of local anesthetic from calcium phosphate bone cements. Mater Sci Eng C Mater Biol Appl 2012;32:1690–4.

[78] Verron E, Pissonnier M-L, Lesoeur J, Schnitzler V, Fellah BH, Pascal-Moussellard H, et al. Vertebroplasty using bisphosphonate-loaded calcium phosphate cement in a standardized vertebral body bone defect in an osteoporotic sheep model. Acta Biomater 2014;10:4887–95.

[79] Ginebra MP, Traykova T, Planell JA. Calcium phosphate cements as bone drug delivery systems: A review. J Control Release 2006;113:102–10.

[80] Verron E, Khairoun I, Guicheux J, Bouler J-M. Calcium phosphate biomaterials as bone drug delivery systems: a review. Drug Discov Today 2010;15:547–52.

[81] Bose S, Tarafder S. Calcium phosphate ceramic systems in growth factor and drug delivery for bone tissue engineering: A review. Acta Biomater 2012;8:1401–21.

[82] Otsuka M, Otsuka K. Bone Regeneration by Using Drug Delivery System Technology and Apatite Intelligent Materials. J Hard Tissue Biol 2005;14:261–2.

[83] Habraken WJEM, Wolke JGC, Jansen J a. Ceramic composites as matrices and scaffolds for drug delivery in tissue engineering. Adv Drug Deliv Rev 2007;59:234–48.

[84] Patel S. Optimising calcium phosphate cement formulations to widen clinical application . n.d.

[85] Wu P, Grainger DW. Drug/device combinations for local drug therapies and infection prophylaxis. Biomaterials 2006;27:2450–67.

[86] Vo T, Kasper F, Mikos A. Strategies for controlled delivery of growth factors and cells for bone regeneration. Adv Drug Deliv Rev 2012;64:1292–309.

[87] Schussele A. Drug delivery to the bone-implant interface: Functional hydroxyapatite surfaces and particles 2007.

[88] Pastorino D, Canal C, Ginebra M-P. Drug delivery from injectable calcium phosphate foams by tailoring the macroporosity–drug interaction. Acta Biomater 2014.

[89] Zilberman M, Elsner JJ. Antibiotic-eluting medical devices for various applications. J Control Release 2008;130:202–15.

[90] Joosten U, Joist a, Frebel T, Brandt B, Diederichs S, von Eiff C. Evaluation of an in situ setting injectable calcium phosphate as a new carrier material for gentamicin in the treatment of chronic osteomyelitis: studies in vitro and in vivo. Biomaterials 2004;25:4287–95.

[91] Amini AR, Laurencin CT, Nukavarapu SP. Bone tissue engineering: recent advances and challenges. Crit Rev Biomed Eng 2012;40:363–408.

[92] Hannink G, Arts JJC. Bioresorbability, porosity and mechanical strength of bone substitutes: what is optimal for bone regeneration? Injury 2011;42 Suppl 2:S22–5.

[93] Petrochenko P, Narayan R. Novel approaches to bone grafting: porosity, bone morphogenetic proteins, stem cells, and the periosteum. J Long-Term Eff … 2010;20:303–15.

[94] Canal C, Pastorino D, Mestres G, Schuler P, Ginebra MP. Relevance of microstructure for the early antibiotic release of fresh and pre-set calcium phosphate cements. Acta Biomater 2013;9:8403–12.

[95] Diamond S. Mercury porosimetry An inappropriate method for the measurement of pore size distributions in cement-based materials. Cem Concr Res 2000;30:1517–25.

[96] Galle C. Effect of drying on cement-based materials pore structure as identified by mercury intrusion porosimetry A comparative study between oven- , vacuum- , and freeze-drying. Water 2001;31:1467–77.

[97] Galle C. Reply to the discussion by S . Diamond of the paper " Effect of drying on cement-based materials pore structure as identified by mercury intrusion porosimetry : a comparative. Cem Concr Res 2003;33:171–2.

[98] Leon CA. New perspectives in mercury porosimetry 1998.

[99] Chatterji S. A discussion of the paper ‴ Mercury porosimetry — an inappropriate method for the measurement of pore size distributions in cement-based materials ‴ by S . Diamond $. Mercury 2001;31:1657–8.

[100] Galle C, Diamond S. A discussion of the paper " Effect of drying on cement-based materials pore structure as identified by mercury porosimetry — a comparative study. Vacuum 2003;33:169–70.

[101] Dombrowski R. The Horvath–Kawazoe method revisited. Colloids Surfaces A Physicochem Eng Asp 2001;187-188:23–39.

[102] Moro F, Böhni H. Ink-bottle effect in mercury intrusion porosimetry of cement-based materials. J Colloid Interface Sci 2002;246:135–49.

[103] Sun Z, Scherer G. Cement and Concrete Research Pore size and shape in mortar by thermoporometry. Cem Concr Res 2010;40:740–51.

[104] Landry M. Thermoporometry by differential scanning calorimetry: experimental considerations and applications. Thermochim Acta 2005;433:27–50.

[105] Riikonen J, Salonen J, Lehto V-P. Utilising thermoporometry to obtain new insights into nanostructured materials. J Therm Anal Calorim 2010;105:811–21.